Naval Research Laboratory
Stennis Space Center, MS 39529-5004

NRL/MR/7322--97-8054

Interim Report on Validation of the Navy Surf Model

Y. Larry Hsu

Ocean Dynamics and Prediction Branch
Oceanography Division

Theodore Mettlach
Eileen Kennelly
Marshall Earle

Neptune Sciences Inc.
Slidell, LA 70458

October 14, 1997

Approved for public release; distribution unlimited.

REPORT DOCUMENTATION PAGE

Form Approved
OBM No. 0704-0188

1. AGENCY USE ONLY *(Leave blank)*	2. REPORT DATE	3. REPORT TYPE AND DATES COVERED
	October 14, 1997	Final

4. TITLE AND SUBTITLE

Interim Report on Validation of the Navy Surf Model

5. FUNDING NUMBERS

Job Order No. 573-5952-08
Program Element No. 0603207N
Project No. X2008
Task No.
Accession No. DN258048

6. AUTHOR(S)

Y. Larry Hsu, Theodore Mettlach*, Eileen Kennelly*, and Marshall Earle*

7. PERFORMING ORGANIZATION NAME(S) AND ADDRESS(ES)

Naval Research Laboratory
Marine Geosciences Division
Stennis Space Center, MS 39529-5004

8. PERFORMING ORGANIZATION REPORT NUMBER

NRL/MR/7322--97-8054

9. SPONSORING/MONITORING AGENCY NAME(S) AND ADDRESS(ES)

Commander, Space and Naval Warfare Systems Command
PMW 185-3B, 2451 Crystal Drive
Arlington, VA 22245-5200

10. SPONSORING/MONITORING AGENCY REPORT NUMBER

11. SUPPLEMENTARY NOTES

*Neptune Sciences Inc., 150 Cleveland, Slidell, LA 70458

12a. DISTRIBUTION/AVAILABILITY STATEMENT

Approved for public release; distribution unlimited.

12b. DISTRIBUTION CODE

13. ABSTRACT *(Maximum 200 words)*

The upgraded Navy Surf Model is described and extensively validated using data acquired during the National Sediment Transport Study (NSTS), Leadbetter Beach, California, in February 1980 and during the Duck Experiment on Low-Frequency and Incident-band Longshore and Across-shore Hydrodynamics (DELILAH), Duck, North Carolina in October 1990. The accuracy of the model is characterized by root-mean-square errors and linear correlation and regression analyses of wave height, longshore current, and modified surf index.

14. SUBJECT TERMS

ocean models, military oceanography, data assimilation

15. NUMBER OF PAGES

233

16. PRICE CODE

17. SECURITY CLASSIFICATION OF REPORT	18. SECURITY CLASSIFICATION OF THIS PAGE	19. SECURITY CLASSIFICATION OF ABSTRACT	20. LIMITATION OF ABSTRACT
Unclassified	Unclassified	Unclassified	SAR

TABLE OF CONTENTS

1. INTRODUCTION

This report documents and describes a validation study of various versions of the Navy Surf Model. The model has evolved steadily since its was introduced to the Fleet in 1988, but this is the first extensive validation of the model using a set of comprehensive surf zone measurements.

1.1 Requirements

Today's Operational Maneuver from the Sea Strategy requires detailed knowledge of the complex littoral battle space. Expeditionary forces must be prepared to breach varying layers of coastal mines and other obstacles, especially in the surf zone. The importance of surf conditions to naval and military operations are explicitly stated in several recent publications by the Joint Chiefs of Staff (1989, 1991, 1992, 1993).

An essential element in the success of amphibious operations is a series of accurate surf forecasts covering the period of time from initial planning until logistics over the shore is completed. The surf zone can be a dangerous place; in view of the tremendous number of people and equipment entering this zone during an operation, it is critical that the on-scene commander know its natural hazards. If conditions are forecast to be lower than encountered, lives and equipment may be put in jeopardy; forecasting conditions too high may limit a commander's options.

For naval and military operations, the surf is described by five different, but related, properties (*Joint Surf Manual* [Commander, Naval Surface Force, Pacific and Commander Naval Surface Force, Atlantic, 1987]): height of the highest one-third of breaking waves; the time period between successive breaking waves; the angle between breaking waves and the beach; the type of breaking waves; the longshore (littoral) current. A single, dimensionless number called the modified surf index (MSI) provides a measure of overall surf conditions. Other characteristics with varying influences on operations are the surf zone width, wave length in the surf zone, the average depth of water at the point of breaking, the direction from which sea or swell approaches the coast, speed of breakers, the steepness of breakers, the amount of spray, variability in the height of breaking waves, and the expected change in breaker height (U.S. Naval Oceanographic Office, 1969). In this study, wave height, longshore current, and surf zone width are evaluated.

1.2 Overview of the Navy Surf Model

The navy surf model software has been used extensively throughout the Fleet since it was introduced. It is contained in the Geophysical Fleet Mission Program Library (GFMPL), the Tactical Environmental Support System (TESS), and the Mobile Oceanographic Support System (MOSS), and was developed because previous surf forecasting techniques were mainly manual techniques based on methods dating to the 1950's which did not adequately consider local shallow water effects. The model is the primary software for operational surf forecasting. The model is also used for systems development and surf climate descriptions. For example, Dowling *et al* (1993) and Salsman *et al* (1993) used the model to make surf characterizations for the development of the EATD Explosive Neutralization System and Nichols *et al* (1996) used the

model to establish engineering requirements for the Advanced Amphibious Assault Vehicle (AAAV).

The surf model software is comprised of a surf zone model program, a wave refraction program, and a number of utility programs. In this study, only the surf zone model program is validated, and the term *the surf model* or *the model* will be used to describe only the surf zone model program. References to different versions of the model are made by name, as described below. A description of the model and recent improvements is given in Section 2.0. It is important to stress the difference between the surf model and the refraction program. The refraction program calculates refraction and shoaling of deep water wave energy shoreward to a point outside the surf zone. The existing refraction model, which is based on the RCPWAVE model (Ebersole *et al*, 1986), is now being replaced by REFDIF1 (Kirby and Dalrymple, 1994).

Surf model inputs are the following: (1) wind speed and direction; (2) wave conditions, either in the form of the wave parameters of height, period and direction, or a complete directional wave spectrum; (3) a nearshore depth profile that extends to a depth of about 15 to 25 feet. The input wave conditions and the nearshore depth profile are the more important of the three inputs. The depth profile used in the model is computed from the user-provided depth profile and tide level. Model outputs are the following: (1) a forecast in the SURFCST format from the *Joint Surf Manual*; (2) MSI; and (3) an optional listing of distances offshore, depths, wave heights, wavelengths, percent breaking waves, and longshore currents at regularly spaced intervals throughout the surf zone.

The following are versions of the model that have been developed:

1.2.1. NAVSURF

The original version of the model, here called NAVSURF, is described extensively in Earle (1988, 1989). The model has evolved steadily, but the basic program structure has remained unchanged.

1.2.2. NCSCSURF

The first improvements to the model were delivered to the Naval Oceanographic and Atmospheric Research Laboratory in July 1991. Four improvements were made: (1) horizontal mixing was added to provide better longshore current forecasts for beaches with offshore bars; (2) wind generation of longshore currents was added; (3) a better specification of swell direction inputs was added; (4) numerical calculations of the percentages of different breaker types was added. These improvements are described in Earle (1991).

The following year, the newly improved model was further modified to operate on a Navy desk top computer (DTC-2) for the Naval Coastal Systems Command (NCSC), which was a Sun workstation with the Sun UNIX operating system. NAVSURF operates on a Hewlett-Packard 9020A with the HP-UX operating system. The NCSC version, designated NCSCSURF, incorporated the 1991 changes and was also made more portable than NAVSURF because HP-

specific features, especially graphics, were abandoned for simple ASCII text input and output files. The NCSC modifications are described in Earle (1992).

1.2.3. SPE_SURF

When NAVSURF was developed, there was no capability to input directional wave spectra for automated model input. Thus, the model was designed to internally generate a directional wave spectrum by superimposing a modified Pierson-Moskowitz wind wave directional spectrum derived from input parameters of wind wave height, period and direction and a narrow banded swell wave directional spectrum derived from input parameters of swell wave height, period, and direction. In anticipation of automated spectrum input, NAVSURF internally utilized wave frequency and directional bands that were identical to those in the Global Spectral Ocean Wave Model (GSOWM), the Navy's operational global wave forecasting model at the time. Since NCSCSURF contained this original limitation, it was modified by Mettlach *et al* (1996) to allow direct input of directional wave spectra. The modified version, designated SPE_SURF, allows input of directional wave spectrum files from the global and regional Navy wind driven WAve Model (WAM) and the Endeco/YSI Type 1156 Wave Track Buoy.

Later versions of SPE_SURF include options for the input of directional wave spectra collected from the directional wave array at the Coastal Engineering Research Center's (CERC) Waterways Experiment Station (WES) Field Research Facility (FRC) at Duck, North Carolina and directional wave spectrum output files from the wave model STWAVE (Resio and Perrie, 1994).

1.2.4 EXPSURF

The first major overhaul of the model was done by Marshall Earle and Eileen Kennelly of Neptune Sciences Inc. (NSI) in the summer of 1996 under the project *Surf Model Improvements* funded by ONR. Many model improvements including some that had been considered by NSI in various applications of the model since 1988 were incorporated into a comprehensive revision of the software, which was streamlined, modularized, and made portable for a range of operating systems and machines. Additionally, the roller theory of Lippmann *et al* (1996) was incorporated as a model option. Both ONR and the SPAWAR-funded project *Surf Model Upgrade* jointly contributed to the roller implementation effort.

EXPSURF was an interim step in the ongoing development of SURF96. In this validation study, EXPSURF was used, under certain options, to simulate NCSCSURF and SPE_SURF; it was tested extensively against standard input and output cases from NCSCSURF and SPE_SURF and exact agreement was found.

1.2.5. SURF96

The modularity of EXPSURF provided a framework for greatly expanding the range of options available to the model user while keeping the original structure of the model. The most recent version of the model, designated SURF96, grew out of EXPSURF and incorporates several

theoretical and numerical improvements. A detailed description of the model and its recent improvements is given in Section 2.0. There are situations, including several that are not demonstrated by these validations, where SURF96 provides significantly better results than NAVSURF. Plans have been made to document SURF96 as an upgrade to NAVSURF while further improvements are being made. Specifically, improved longshore current calculations are being examined in ongoing work. In addition, options incorporated into SURF96 for testing and validation are being evaluated more fully to select a standard option suite for Navy operational use.

1.3 Validation Method

This study uses two versions of the model–EXPSURF and SURF96, two sets of options for each version, and field measurements from two surf zone experiments. The first experiment is the National Sediment Transport Study (NSTS) experiment on Leadbetter Beach, Santa Barbara, California, conducted during January and February 1980. Gable (1981), Wu *et al* (1985), and Thornton and Guza (1986, 1989) have described this experiment. The second experiment is the Duck Experiment on Low-frequency and Incident-band Longshore and Across-shore Hydrodynamics (DELILAH) conducted at FRF in October 1990. Birkemeier et al (1991), Church and Thornton (1993), Thornton and Kim (1993), and Smith *et al* (1993) have provided information about this experiment. Most of the directional wave and tide data were downloaded from the FRF through *http://frf.wes.army.mil*. Professor Edward Thornton provided depth survey data and processed nearshore wave height and current data. The validation data reduction methods used to prepare model inputs and verification data are described in Section 3.0.

A total of 4 model runs were made using four NSTS cases and 79 DELILAH cases. Model options and other details are explained in section 4.0. Each model run was made using concurrently acquired, available wind and wave data. Input depth profiles are from surveys conducted on the same, or previous, day as the wind and wave data. Measurements of wave height and longshore current in the surf zone are used to validate model output. The model outputs were compared to measurements and the intercomparisons are presented in Section 5.0. The accuracy of model-derived surf zone width and modified surf index for 19 DELILAH cases are also presented in Section 5.0.

2. SURF MODEL DESCRIPTION

This section briefly describes the surf model, including SURF96. The first subsection gives an overview of the model and subsequent subsections describe specific model representations or calculations with an emphasis on recent changes incorporated in SURF96.

2.1 Overview

The model is parametric and one-dimensional and is largely based on Thornton and Guza (1983, 1986). The assumptions include: (1) approximately straight and parallel bottom contours within the surf zone; (2) a directional wave spectrum that is narrow banded in frequency and direction; (3) a Rayleigh wave height distribution; (4) linear wave theory. The directional wave spectrum used for model initialization can be obtained from a wave model or measurements. If an offshore directional wave spectrum is used, it must be properly refracted, shoaled and diffracted to a user-selected starting depth *dstart,* which should lie seaward of the breaker line. At *dstart*, the directional wave energy distribution is reduced to three representative physical values: (1) the direction of the vertically-averaged wave momentum flux, (2) the incident root-mean-square wave height H_0 and (3) the dominant wave frequency f_p. The direction of the wave momentum flux is computed by the method of Higgin *et al* (1981) with the important assumption that the directional wave spectrum at *dstart* is narrow banded in both direction and frequency. From *dstart*, the model incrementally calculates the root-mean-square wave height H_{rms} along a transect normal to the beach to very near the beach at the still water level. As waves move through the surf zone, the average rate of energy dissipation due to wave breaking and frictional dissipation balances the gradient of shoreward energy flux. Energy is extracted using the energy dissipation of a propagating bore modeled after a weighted Rayleigh-distribution of wave heights. Longshore current calculations at each increment are based on longshore current theory using radiation stress (Longuet-Higgins, 1970a,b).

The width of the surf zone is based on either (1) the percentage of breaking waves or (2) the percentage of breaking waves and the location of maximum energy dissipation. In NCSCSURF, the surf zone is based on the more offshore of two points: either the most seaward point at which more than 33 percent of the waves are breaking or the point at which there is a maximum in energy dissipation. For MSI calculations, the significant breaker height $H_{sig} = \sqrt{2} \cdot H_{rms}$ and the longshore current V are the highest calculated in the surf zone. The percentage of each breaker type–spilling, plunging or surging–is found from a widely accepted paramaterization of wave period, wave height, and bottom slope and considers the model-determined breaking wave probability distribution. Breaker angle is found from the direction of the vertically averaged wave momentum flux at *dstart*. MSI is calculated using the criteria given in the *Joint Surf Manual*.

2.2 Wave and Roller Energy

One of the important changes to EXPSURF and SURF96 is the incorporation of wave rollers.

The flows of spilling breakers can be separated into two layers, an upper layer of energy causing turbulent wave breaking which rides over a lower layer of energy corresponding to organized wave motion. The turbulent water above the wave is termed a surface roller. The original idea of such a two-layer system was introduced by Longuet-Higgins and Turner (1974). The refinements of Svendsen (1984a,b) were applied by Schäffer *et al* (1993) to a Bousinesq model for waves breaking in shallow water. EXPSURF and SURF96 incorporate the model of Lippman *et al* (1995, 1996) which produced results consistent with measurements from both a planar and a barred beach.

Calculations of wave height and longshore current in the surf zone use the wave energy present at a point offshore. The energy per unit surface area in a wave is calculated as

$$E_w = \frac{1}{8}\rho g H_{rms}^2 \tag{1}$$

where ρ is water density and g is the acceleration due to gravity. H_{rms} is the root-mean-square wave height. When a wave breaks, the turbulent water spilling off the front of the wave is defined as a wave roller. The energy per unit area associated with a roller is given as

$$E_r = \frac{1}{8}\rho c f \frac{H_b^3}{h \tan\sigma} \tag{2}$$

where c is the phase speed of the wave, f is the zero crossing frequency, H_b is the height of the wave at breaking, h is water depth, and σ is the angle the roller makes with the body of the wave. A value σ equal to 5 degrees was used in SURF96. It is important to note that by definition a wave roller is a spilling wave.

2.3 Energy Dissipation in the Surf Zone

As a wave propagates into the surf zone, some of its energy is dissipated. If wave roller energy is not considered, as in NAVSURF, the energy flux balance equation is written as

$$\frac{\partial(E_w c_g \cos\theta)}{\partial x} = -\langle \epsilon_b \rangle \tag{3}$$

where E_w is the wave energy, c_g is the wave group velocity, θ is the wave direction relative to shore normal x, positive seaward, and H is root-mean-square wave height. ϵ_b is the ensemble averaged dissipation function, modeled after a breaking wave distribution function. It has the form

$$<\epsilon_b>=\frac{1}{4}\rho g f\frac{B^3}{h}\int H^3 p_b(H)dH \tag{4}$$

where B is an empirical coefficient, and $p_b(H)$ is the probability distribution for breaking waves described as

$$p_b(H)=W(H)p(H) \tag{5}$$

The distribution is a weighted Rayleigh distribution. Weighting functions $W(H)$ have been described by Whitford (1992b) and Thornton and Guza (1983). See Section 2.4 for a complete description of the available weighting functions in SURF96.

If wave roller energy is considered, the energy flux balance becomes

$$\frac{\partial(E_w c_g\cos\theta)}{\partial x}+\frac{\partial(E_r c\cos\theta)}{\partial x}=-<\epsilon_r> \tag{6}$$

where the dissipation term now becomes a function of the roller term and is written as

$$<\epsilon_r>=\frac{1}{4}\rho g f\frac{H_b^3}{h}\cos\sigma\int H^3 p_b(H)dH \tag{7}$$

2.4 Breaking Wave Probability Distribution Weighting Functions

The solutions of equations (4) and (7) involve integrating a weighted Rayleigh distribution,

$$\int p_b(H)=\int W(H)p(H)dH \tag{8}$$

A number of weighting functions, $W(H)$, have been described in the literature. $W(H)$ must range from zero to unity. Five weighting functions have been incorporated in SURF96:

$$W_1(H)=\left[\frac{H_{rms}}{\gamma h}\right]^2 \tag{9a}$$

$$W_2(H)=\left[\frac{H_{rms}}{\gamma h}\right]^4 \tag{9b}$$

$$W_3(H)=\left[\frac{H_{rms}}{\gamma h}\right]^2\left(1-e^{-\left[\frac{H}{\gamma h}\right]^2}\right) \tag{9c}$$

$$W_4(H)=\left[\frac{H_{rms}}{\gamma h}\right]^4\left(1-e^{-\left[\frac{H}{\gamma h}\right]^2}\right) \tag{9d}$$

$$W_5(H)=\tanh\left[8\left[\frac{H_{rms}}{\gamma h}-1\right]\right]\left(1-e^{-\left[\frac{H}{\gamma h}\right]^2}\right) \tag{9e}$$

where γ is an empirical value of 0.42, and h is water depth.

The user can select which weighting function to use throughout the model. Note that in NCSCSURF and SPE_SURF, equation (9d) was used as the weighting function for the energy dissipation function, $<\epsilon_b>$.

2.5 Solution to Wave Height in the Surf Zone

Equation (6) is solved using a numerical forward stepping and convergence scheme to determine wave, and possibly roller, energy along with H_{rms} values at each point. This stepping scheme takes the form

$$(E_w c_g \cos\theta)_{i-1}+(E_r c\cos\theta)_{i-1}=-<\epsilon>\Delta x+(E_w c_g\cos\theta)_i+(E_r c\cos\theta)_i \tag{10}$$

If wave rollers are considered, $<\epsilon> = <\epsilon_r>$. Otherwise, $<\epsilon> = <\epsilon_b>$ and $E_r = 0.0$.

The above equation is solved at each consecutive point stepping through the surf zone toward the beach from *dstart*. The right-hand-side (RHS) of equation (10) at *dstart*, the *i*th point, is determined from radiation stress parameters calculated from the initial energy spectra (Earle, 1989). To solve for the wave and roller energy components, E_w and E_r at the i+1 point, a convergence routine is used until the left-hand-side (LHS) of equation (10) becomes equal to the RHS. To do so, an initial shooting value of H_{rms} at point i+1 is set equal to H_{rms} at point i (given by the radiation stress calculations). H_{rms} at point i +1 is iterated until the LHS equals the RHS within a given tolerance. Values of H_{rms} at consecutive points, moving toward the coast, are calculated in this way. At each point, the incident wave angle is refracted using Snell's Law.

2.6 Longshore Current Calculations

There are two options in SURF96 for calculating longshore current in the surf zone. The first option in based on radiation stress longshore current theory (Longuest-Higgins, 1970a, 1970b) using the balance of momentum equation in the longshore direction given by

$$\tau_y^h + \frac{d}{dx}\left(\mu h \frac{dv}{dx}\right) - \langle\tau_y^b\rangle + \tau_y^w = 0 \qquad (11)$$

where h is the water depth and v is the longshore current in the cross shore x direction. The first term on the left hand side is the horizontal stess in the along shore direction exerted by waves on the water and is given by

$$\tau_y^h = \langle\epsilon_b\rangle \frac{\sin\theta}{c} \qquad (12)$$

where c is wave phase speed and θ is the angle of wave apporach with respect to x. The second term represents horizontal mixing. In SURF96, μ the horizontal eddy viscosity is given by

$$\mu = 2\rho h^2 \left(\frac{\langle\epsilon_b\rangle}{\rho}\right)^{1/3} \qquad (13)$$

where the factor 2 is an empirical constant. The third term is the mean stress due to bottom friction given by

$$\langle\tau_y^b\rangle = c_d \rho |\bar{U}| v \qquad (14)$$

where c_d is the bottom drag coefficient and $|\bar{U}|$ is the magnitude of the near bottom horizontal wave orbital velocity. Following Thornton and Guza (1986) and Thornton and Whitford (1991)

$|\bar{U}|$ is given by

$$|\bar{U}| = \frac{\sqrt{\pi}\, f\, H}{\sinh(kh)} \tag{15}$$

where f is wave frequency, H is root-mean-square wave height and k is the radian wave number. The fourth term is the wind stress in the longshore direction given by

$$<\tau_y^w> = c_a\, \rho_a\, |\bar{W}| W_y \tag{16}$$

where c_a is the wind drag coefficient, ρ_a is the air density, $|\bar{W}|$ is the total wind speed, and W_y is the along shore component of $\bar{W}$.

Longshore current is solved using a finite difference approach after wave dissipation and wave height are found for each grid point, i in the the surf zone using the following

$$V_i = E_i\, V_{i-1} + F_i \tag{17}$$

where

$$E_i = \frac{-A_i}{-(B_{i+1} + A_i + A_{i+1}) + (A_{i+1}\, E_{i+1})} \tag{18}$$

and

$$F_i = \frac{\left(\frac{A_{i+1}F_{i+1}}{\Delta x^2} + C_{i+1}\right)\Delta x^2}{-(B_{i+1} + A_i + A_{i-1}) + (A_{i+1} + E_{i+1})} \tag{19}$$

The terms A_i, B_i and C_i are given as follows:

$$A_i = 2\rho h_i^2 \left(\frac{<e_b>_i}{\rho}\right)^{1/3} \tag{20}$$

$$B_i = \frac{c_d \rho f \sqrt{\pi} H_i}{\sinh(k_i h_i)} \tag{21}$$

$$C_i = \frac{-\langle e_b \rangle_i \sin\theta}{c_i} - \rho_a c_a |\bar{W}|^2 \sin\theta_w \tag{22}$$

where θ_w is the direction of the wind with respect to shore normal. In the above solution, the wave dissipation function depends on the weighting function $W(H)$ selected. This solution for longshore current is employed in SPE_SURF and NCSCSURF. The original surf model NAVSURF does not contain the horizontal mixing term.

The second method for calculating longshore current employs the momentum balance equation without horizontal mixing. Instantaneous stress exerted by the waves on the water is balanced by bottom stress, which is a nonlinear quadratic term of the form

$$\tau_y^b = \rho c_d U_y |\bar{U}| \tag{23}$$

where ρ is the density of water, c_d is the bottom drag coefficient and U_y is the instantaneous longshore current. $|\bar{U}|$ is the magnitude of the instantaneous, near bottom, horizontal current speed, which is given by

$$|\bar{U}|^2 = U_x^2 + U_y^2. \tag{24}$$

The components of $\bar{U}$ can be decomposed into the time averaged current speed and the near bottom wave orbital speed such that

$$U_x = u + u_b \tag{25}$$

and

$$U_y = v + v_b \tag{26}$$

In (25) and (26) the subscript b denotes near bottom wave orbital motion, which can be written

$$u_b = u_w \cos\theta, \quad v_b = u_w \sin\theta \tag{27}$$

where

$$u_w = \sqrt{u_b^2 + v_b^2} \tag{28}$$

It is noted that in this derivation the mean current speed in (25) and (26) is assumed to be the vertically averaged current speed.

Expanding (24) using (27) yields

$$|\bar{U}| = (U_x^2 + 2U_x u_w \cos\theta + U_y^2 + 2U_y u_w \sin\theta + u_w^2)^{1/2} = D_1^{1/2} \tag{29}$$

The time average of (23) over several wave periods assuming stationary wave and current conditions is written

$$\langle \tau_y^b \rangle = D_2 \langle U_y |\bar{U}| \rangle = \frac{\langle \epsilon_b \rangle \sin\theta}{c} \tag{30}$$

where $D_2 = \rho c_d$ = constant. After rearranging (30) to make the variable Q

$$Q = \langle (v + u_w \sin\theta) D_1^{1/2} \rangle \tag{31}$$

the equation for the time- and vertically averaged longshore current $\langle v \rangle$ can be written,

$$\langle v \rangle = \frac{Q - \langle D_1^{1/2} u_w \sin\theta \rangle}{\langle D_1^{1/2} \rangle} \tag{32}$$

Linear wave theory provides relationships for u_w,

$$u_w = \frac{g\,H\,T}{2L\,\cosh\left(\frac{2\pi h}{L}\right)} \tag{33}$$

where

$$T = \left(\frac{gk\,\tanh(kh)}{4\pi^2}\right)^{-1/2} \tag{34}$$

and $L = 2\pi/k$ and k is the radian wave number.

The undertow term of Dally and Dean (1986)

$$U_x = \frac{3}{16}\sqrt{gh}\left(\frac{H}{h}\right)^3 \tag{35}$$

is included in SURF96 and has been tested; however, for this study, U_x was set to zero. Equation (32) is solved iteratively using a shooting method such that at each grid point where H, h and $<\epsilon_b>$ are known, $<v>$ is initially set to zero, then the difference between the left and right hand side of the equation is compared to a small tolerance. The iterative value of $<v>$ is repeatedly put back in (32) as U_y until the tolerance is met. Note that $<U_y>$ in $<D_1>$ is $<v>$.

2.7 Determination of Breaker Types: Spilling, Plunging, Surging

In the old version, the calculation of the percentage of spilling, plunging and surging waves is based on a single point at the maximum breaker height location. In SURF96, averaged percentage values are used. Inside the surf zone, where the bottom slope is positive, i.e., where depths increase with increasing distance from shore, H_{rms} and the percent breaking types determined from H_{rms} are ranked from highest to lowest. For the highest one-tenth of H_{rms} values, the average of each associated breaker percentages is determined and the corresponding values of percent of spilling, plunging and surging waves are averaged. The averages make up the final output of the percentage of breaker types found in the surf model output file.

Earle (1989, 1991) describe how probability distributions of breaker type are calculated at locations in the surf zone as a function of the probability distribution for breaking waves, wave period, and local bottom slope. Comparisons of analytic and numerical solutions to equations (4), (7), and (8) revealed close agreement at depths greater than a few feet; but in shallower water, the two solution types differed; the analytic solution sometimes yielded values of W(H) greater than

unity. Thus, in SURF96, numerical integration is used.

2.8 Self Starting Routine

Since wave parameters are determined from the wave energy at all points in the surf zone, it is imperative that energy transformation be accurately modeled, especially in the outer edge of the surf zone where few waves are breaking. When no waves are breaking, the roller terms and the dissipation in equation (6) should be zero. It has been found that where the bottom slope is small and *dstart* is a depth where the percentage of breaking waves is less than five percent, the model gradually dissipates energy seaward of the actual breaker line causing the waves that enter the surf zone to have too little energy. In other words, starting the model too far offshore can cause excess energy loss.

A routine was introduced into SURF96 which prevents excessive energy dissipation outside the surf zone. If selected, this *Self Start* routine calculates wave energy and the percent of breaking waves at each point offshore without dissipating energy until the percent of breaking waves exceeds five percent. The user may select this routine as an option. The algorithm for *SelfStart* is the following:

1. Initial wave parameters at *dstart* are determined.

2. Wave velocity and angle are calculated at point $i = 2$. Wave angle includes refraction.

3. Wave energy and subsequently H_{rms} are calculated at point $i = 2$ using

$$(E_w)_{i+1} = \frac{(E_w c_g \cos\theta)_i}{(c_g \cos\theta)_{i+1}} \tag{36}$$

4. Given H_{rms} at point $i = 2$, the percent of breaking waves is calculated. If it does not exceed 5 percent, repeat steps 2, 3, and 4 until the percent of breaking waves does exceed 5 percent.

5. Once the percent of breaking waves to exceed 5 percent, continue calculating wave energies (along with roller energies if so selected) using equation (10).

2.9 Directional Energy Spectra

SURF96 allows users to generate surf forecasts with seven different energy spectra types. The user can choose from the following: (1) internally generated spectra; (2) DELILAH spectra; (3) regional WAM spectra; (4) global WAM spectra; (5) Endeco buoy spectra; (6) REFDIF1 spectra;

(7) STWAVE spectra.

If option 1 (internally generated spectra) is selected, a modified Pierson-Moskowitz spectrum is calculated based on sea and swell conditions defined in the surf model input file. This is exactly analogous to NCSCSURF.

2.10 Surf Zone Width

Surf zone width in SURF96 is defined as the distance offshore to where 10 percent of the waves have broken whereas previous versions of the model use the more offshore of two points: the most seaward point at which more than 33 percent of the waves are breaking or the point at which there is a maximum in energy dissipation. In SURF96, if the percentage of breaking waves never exceeds 10 percent, a warning message is displayed to alert the user. The change to a 10 percent threshold is based on an investigation jointly funded by ONR and SPAWAR described in Section 3.2.7.

2.11 Internal Gridding

Prior versions of the model calculate depths, distances offshore, and surf zone parameters at a user-specified gridding interval. It has been found that wide intervals may not always resolve important features in the depth profile. Such aliasing may have a deleterious effect on subsequent calculations, especially percent breaker calculations, which are dependent on local bottom slope. To preclude this potential problem, SURF96 uses an internal grid with an initial 2 feet horizontal spacing. If the horizontal extent of the profile is so great that array sizes cannot accommodate a 2 feet spacing, the model automatically regrids to a greater interval (3 or more feet). All calculations of surf zone parameters are done at this internal interval, but output is displayed according to the user- specified output interval. A linear interpolation scheme is used to interpolate from the internally gridded values to the user defined output interval.

3. VALIDATION DATA REDUCTION

The NSTS and DELILAH data sets provide input to the model as well as measurements for verifying model output. This section describes the data sets used. The NSTS data set, constituting four cases without wind or directional wave spectra, is very small compared to the extensive DELILAH data set.

3.1 NSTS Data Description

The NSTS depth profiles used were generously provided by Professor E.B. Thornton. A comprehensive listing of the NSTS wave and current data is given in Kraus and Larson (1991, pp. 107, B5-B9) and Thornton and Guza (1989, p. 368). All measurements were 68 minute averages.

3.1.1. Offshore Waves.

Directional wave spectra were unavailable; therefore, swell wave parameters from Kraus and Larson (1991) were used for wave input. The depths at which wave parameters were collected are given in Kraus and Larson (1991).

3.1.2. Wind

No wind data were obtained; wind speed was set to zero for all NSTS runs.

3.1.3. Longshore Current in the Surf Zone.

These data were taken directly from Kraus and Larson (1991, pp. B6-B9).

3.1.4. Wave Height in the Surf Zone.

These data were taken directly from Kraus and Larson (1991, pp. B6-B9).

3.1.5. Depth Profiles

Nearshore depth profiles from Professor Thornton were used without modification. Personal communication with Mary Bristow at the Naval Postgraduate School confirmed that the depth profiles contained tide level.

3.2. DELILAH Data Description

The DELILAH experiment deployed 87 instruments from the shoreline out to the 3 meter (10 feet) depth contour, and collected a vast amount of data. The data collected make it possible to rigorously evaluate the performance of the surf model. The following subsections give details of the DELILAH measurements used in this study.

3.2.1. Offshore Directional Wave Spectra

Directional wave spectra used as input to the surf model were acquired at a nine-element linear array of bottom-mounted pressure gauges located on the 8-meter (26 feet) contour about 900 meters (0.5 nautical miles) offshore. Table 1 gives information on the data acquisition and processing of the directional wave spectra; the data were processed by FRF. The basic analysis algorithm is the iterative maximum likelihood estimator derived and described by Pawka (1983).

Table 1. DELILAH directional wave spectrum information.

Length of time series processed	8192 seconds
Data sampling frequency of time series	4 hertz
Number of data points in a data segment	4096 points
Number of frequency bands averaged	15 bands
Number of half-lapped segments analyzed	10 segments
Degrees of freedom of spectral estimates	160 dof
Number of output frequency bands	29 bands
Width of an output frequency band	0.00977 hertz
Number of output direction bins (arcs)	91 directional arcs
Width of an output direction bin	2 degrees
Depth of measuring array	25.8 feet (7.86 meters)

3.2.2. Wind Measurements

Mean vector wind direction and mean wind speed were obtained from time series of wind direction and wind speed measurements acquired concurrently with the directional array data from

an anemometer 19.4 meters (63.7 feet) above mean sea level on the beach. Since Earle (1991) states that the optimum height of wind measurements used for model input should be 10 meters (32.8 feet), a comparison was made between the DELILAH wind speed measurements at 19.4 meters and those same wind speeds reduced to the 10 meter level using a logarithmic wind profile, assuming neutral stability. For the 79 cases, a fractional error of 8 percent or less was found between the 19.4 meter, and the derived, 10 meter, wind speeds. Thus, the uncorrected 19.4 meter wind speed was used for all runs.

3.2.3. Longshore Current in the Surf Zone

Longshore current measurements were acquired from an array of nine current meters located along a transect normal to the shore line and extending from near the water line to approximately 800 feet (245 meters) offshore. Five-minute mean measurements covering the same time period as the directional array acquisition period were averaged and used to validate model estimates.

3.2.4. Wave Height in the Surf Zone

Mean values of H_{rms} were obtained from pressure sensors located in the same horizontal location as the current meters. Five-minute mean measurements covering the same time period as the directional array acquisition period were averaged and used to validate model estimates.

3.2.5. Depth Profiles

Two series of depth surveys were used to construct the nearshore depth profiles used with the model. The first series of surveys were the Deep Sled surveys which encompassed an area 1600 meters (5250 feet) along shore from near 100 meters (328 feet) shoreward of the beach to 1800 meters (5900 feet) offshore. Contours from the 8-meter directional array to the surf zone sensors are largely straight and parallel to the beach; however, there is a deep trough under the FRF pier.

The second series of depth surveys, covering an area approximately 600 meters (1967 feet) along shore and 375 meters (1230 feet) offshore to near the 4 meter (13 feet) contour are called the Minigrid surveys. The minigrid surveys were made daily during the course of DELILAH, however the survey of 13 October 1990 is incomplete because of high waves on that day, thus the 12 October profile was used for 13 October runs. Figure 1 is a contour plot of one survey.

The origin of the FRF coordinate system is the intersection of a shore-parallel baseline with the southern boundary of FRF property. Positive directions are toward 340 degrees North along shore and toward 070 degrees North cross shore. Elevation data are referenced to the 1929 National Geodetic Vertical Datum.

The sensors that acquired wave height and longshore current in this study are located along a

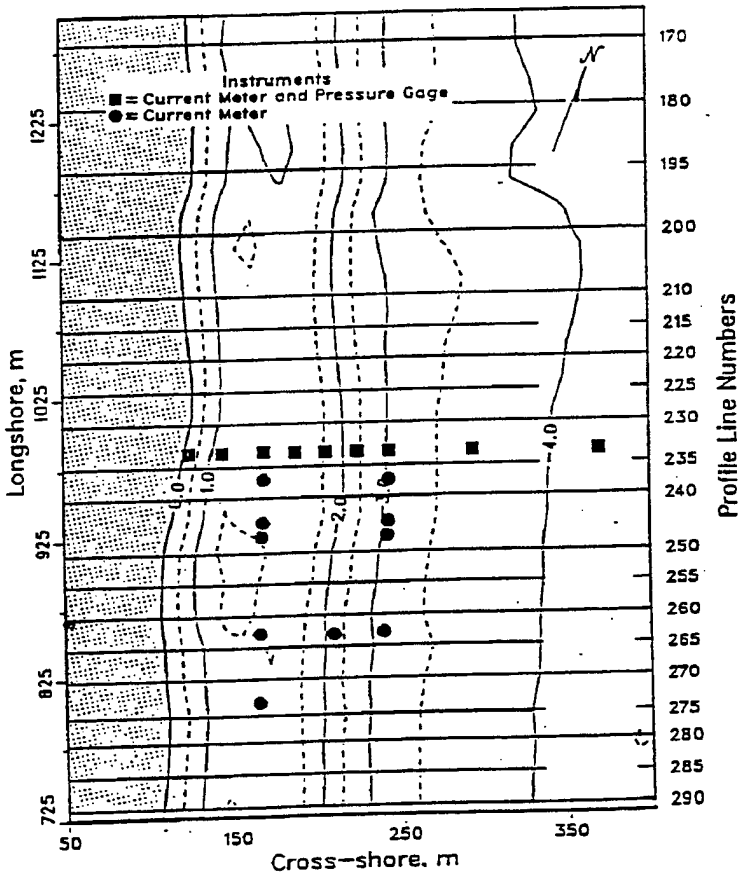

DELILAH mini-grid profile lines

Figure 2.

Figure 1 DELILAH mini-grid profile lines (from FRF, 1991).

cross shore transect at 985 meters along shore, shown as the square marks on Figure 1.

A single depth profile cross shore of the 985-meter line was constructed by taking all Deep Sled measurements within 25 meters either side of the 985-meter line. Daily depth profiles were constructed by taking measurements 10 meters either side of the 978-meter line of the minigrid surveys, which was closest to the surf zone sensors. The single Deep Sled line was merged with each of the minigrid lines by replacing all Deep Sled measurements over the range of minigrid measurements with minigrid measurements. Figure 2, which gives the depth profiles used, is shown to illustrate the dynamic evolution of the nearshore depth profiles during DELILAH. The nearshore is terraced until 9 October, after which a pronounced bar is formed. Thornton *et al* (1996) have explored the generation of this bar using an energetics-based sediment transport model.

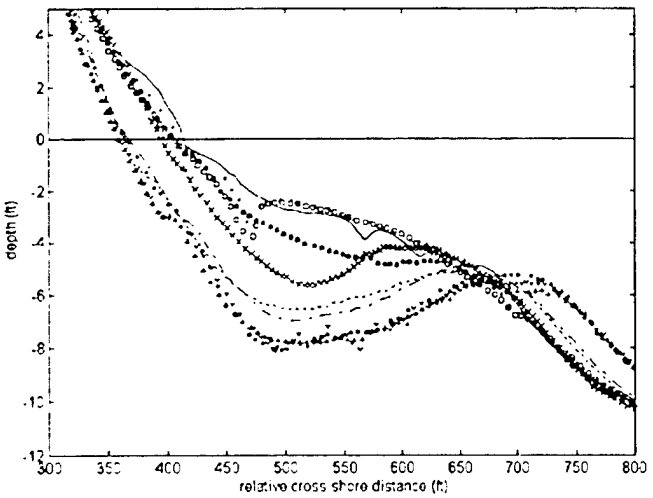

Figure 2 DELILAH nearshore depth profiles for ten days: 6 Oct (large o); 7 Oct (small +); 8 Oct (solid line); 9 Oct (•); 10 Oct (large x); 11 Oct (dotted line); 12 Oct (dash dot line); 14 Oct (large +); 15 Oct (small x); 16 Oct (small o).

3.2.6. Tide Level

Mean tide level over the acquisition time was obtained from a pressure gauge at the 8-meter array. Tide level is used in the model to determine the still water level. All versions of the surf model permit tide level variation for each model run so that, for a given input depth profile, different surf conditions may be produced for different tide levels. A simple example is that waves may break over an offshore bar at low tide, but may break closer to the beach at high tide.

3.2.7 Surf Zone Width

Surf zone width is an important parameter for Navy applications. MSI calculations also indirectly depend on the surf zone width, which must be determined for MSI validation. The surf model provides a realistic representation that larger waves break further offshore than do smaller waves. There is not a single location where all waves break. Thus, the distance to the offshore position where an appropriate percentage of waves are breaking is used to determine surf zone width. This percentage was refined using available DELILAH video imagery. Lippmann and Holman (1991) and Holman *et al* (1993) have shown several applications of video image processing to the study of nearshore processes during DELILAH. FRF (1991, Appendices B and C) gives detailed information on the location of cameras and ground coordinate points. Several 10-minute averaged video image files in .jpg format and software for displaying and rectifying the images were provided by Professor Rob Holman, Oregon State University through Dr. Todd Holland of the

Naval Research Laboratory, Stennis Space Center.

Images acquired at, or sufficiently near, the same time as model run times were analyzed by identifying the locations of maximum contrast between the offshore area of little or no breaking waves, represented by a dark area, and the offshoremost area of breaking waves, represented by an area of relatively high brightness. The distance between the still water point and the point of maximum contrast is defined to be the width of the surf zone.

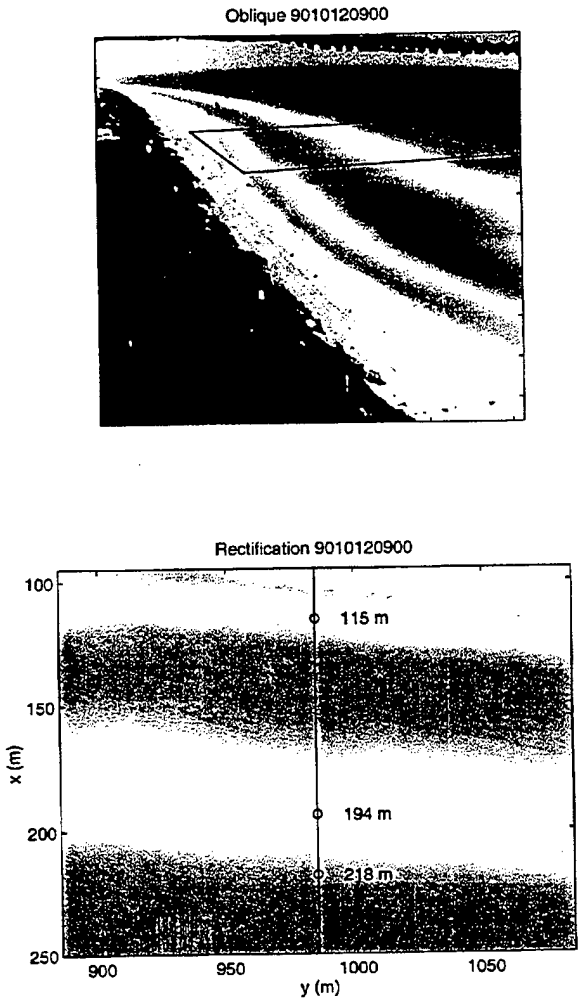

Figure 3 is a facsimile of one the video images used. The upper image shows the camera view; the box drawn on the upper image is rectified to a horizontal plane in FRF coordinates and shown in the lower image. The 985-meter line, the still water point at 115 meters, the point of maximum brightness at 194 meters, and the point of maximum contrast at 218 meters are denoted. The high brightness either side of the still water point shows surf run-up in the swash zone. It is noted that the bar feature as illustrated in Figure 2 started around 200 m offshore just inside the white area consistent with the breaking image.

Figure 3 10-minute averaged video image from 0900 EST 12 October 1990 (top) and rectified image (bottom). See text for details.

For those periods without adequate video imagery, daily, early morning visual surf zone observations reported by FRF were used for surf zone width. The visual observations are not referenced to a particular transect, but rather the distance offshore at which the first breaking waves appear from the FRF pier. The video images are therefore considered to be more accurate validation measurements than the visual observations.

3.2.8 General Wave Conditons

Sample plots of the DELILAH data are shown in Figure 4 (Birkemeier et al, 1991). Wave condition were low at the beginning of the experiment but increased after 9 October and then peaked on 13 October. Waves generally aproached from the southeast. Except on 16 October, most of the waves can be described as having one dominant peak.

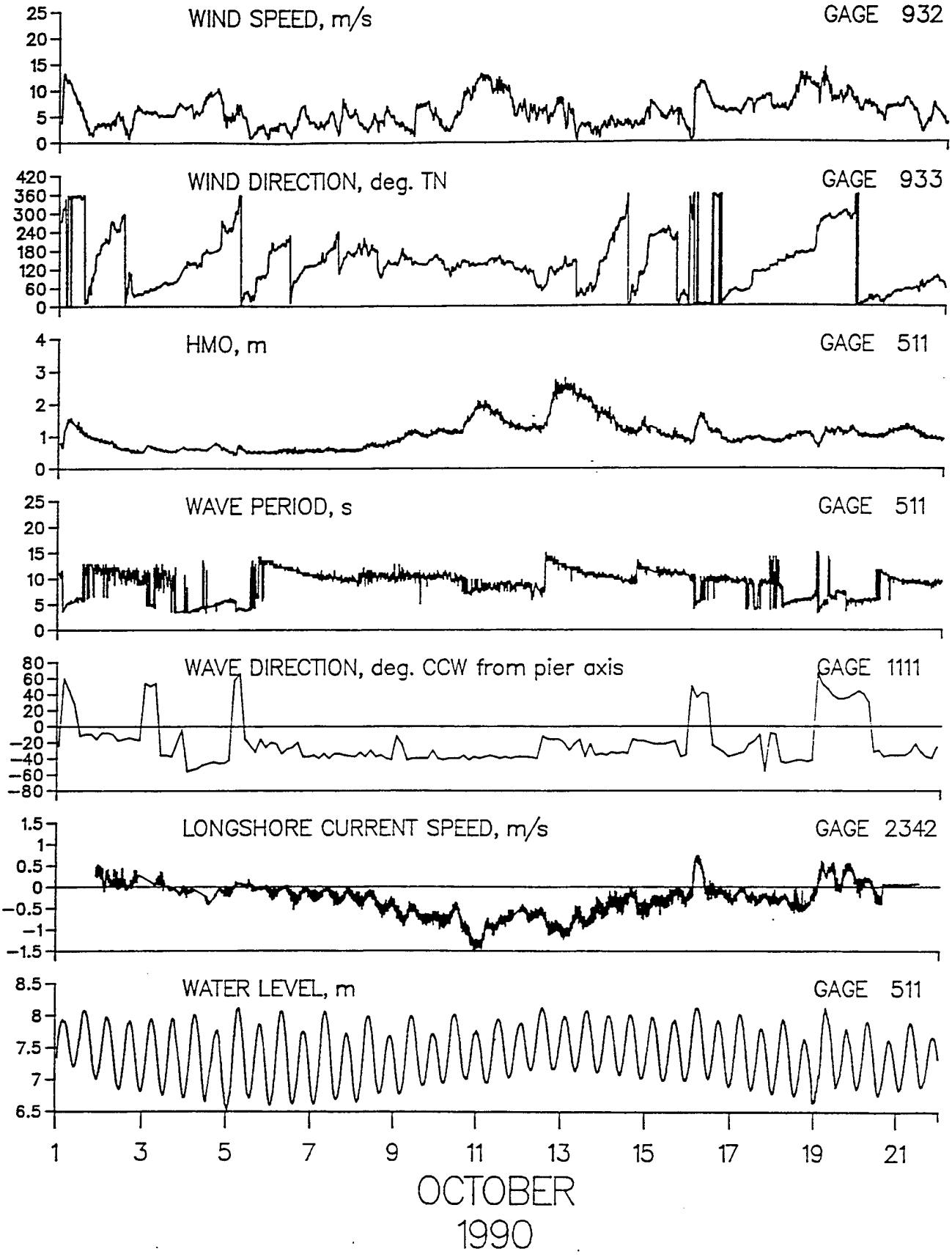

Figure 4. Sample plots for DELILAH Data

4. MODEL RUNS

Eight sets of model runs, summarized in Table 2, are made to build a basis for comparison between the older versions of the model and recent improvements. EKPSURF has the following options:

1. Rollers or not
2. Directional wave spectrum or wave parameters

SURF96 has the following options:

1. Rollers or not
2. Directional wave spectrum or wave parameters
3. One of five weighting functions
4. Self start or not
5 Linear or nonlinear bottom friction

Each option for EXPSURF and SURF96 was tested, but only 4 combinations from both versions of the model are used in this study. The main objectives are: (1) to compare roller with no roller runs and (2) to compare the effects of linear and nonlinear bottom friction on longshore current. The run options used are identified as follows:

1st letter	S = Wave parameters. (NSTS data) D= Directional wave spectra. (DELILAH data)
2nd letter	S = EXPSURF without rollers E = EXPSURF with rollers L = SURF96 with rollers, linear bottom friction, self start, and TG83 9 = SURF96 with rollers, nonlinear bottom friction, self start, and TG83.

The SS and DS runs provide a baseline for evaluating model improvements. The SE and DE runs were the same as the SS and DS runs, respectively, except that the roller term of Lippmann *et al* (1996) was used in the latter. The S9 and D9 runs are the same as the SL and DL runs, respectively, except that nonlinear bottom friction is used in the latter. SURF96 has five different weighting functions, but all runs are made using the Thornton and Guza (1983) weighting function given in equation (9c), which is the only one available in earlier versions of the model.

Table 2. Summary of preliminary validation runs. *NSTS* denotes data collected at Leadbetter Beach, Santa Barbara 1980; *FRF* denotes DELILAH data; *EXP* denotes model EXPSURF; *SURF* denotes model SURF96; *N runs* denotes the number of runs made; *Waves* denotes wave input, where h_o, T_p, θ_p are swell parameters and $S(f,\theta)$ is a complete directional wave spectrum; *d_start* denotes the depth at which model surf zone calculations were selected to begin; *wind* denotes wind speed and direction inputs to the model; *Δx in* denotes internal model grid spacing; *Δx out* denotes output interval; *roller* denotes use of roller term; *W(H)* is the breaking wave probability distribution weighting function used, where TG83 is the *W(H)* from Thornton and Guza (1983), equation (9c); *selfstart* denotes use of the self start option; *b_frctn* indicates linear or nonlinear bottom friction; and *ID* indicates an identifier for the set of runs.

Summary of Runs								
Data	NSTS	NSTS	NSTS	NSTS	FRF	FRF	FRF	FRF
Model	EXP	EXP	SURF	SURF	EXP	EXP	SURF	SURF
N runs	4	4	4	4	79	79	79	79
Waves	h_o, T_p, θ_p	h_o, T_p, θ_p	h_o, T_p, θ_p	h_o, T_p, θ_p	$S(f,\theta)$	$S(f,\theta)$	$S(f,\theta)$	$S(f,\theta)$
dstart	11-13ft.	11-13ft	11-13ft	11-13ft	20 ft	20 ft	20 ft	20 ft
wind	no	no	no	no	yes	yes	yes	yes
Δx in	4 ft	4 ft	4 ft	4 ft	2 ft	2 ft	2 ft	2 ft
Δx out	4 ft	4 ft	4 ft	4 ft	4 ft	4 ft	4 ft	4 ft
roller	no	yes	yes	yes	no	yes	yes	yes
W(H)	TG83	TG83	TG83	TG83	TG83	TG83	TG83	TG83
selfstart	no	no	yes	yes	no	no	yes	yes
b_frctn	linear	linear	linear	non	linear	linear	linear	non
ID	SS	SE	SL	S9	DS	DE	DL	D9

5. RESULTS AND DISCUSSIONS

The results of the model runs of Table 2 are presented in this section and in the plots in Appendices A and B. The subplots in these figures are the depth, H_{rms}, percent breaking waves and the longshore current V, respectively. Each figure shows the results of two model runs. The positions of the DELILAH pressure gauges are shown "o" and the positions of the DELILAH current meters are shown as "+". The horizontal position of the sensors are relative to the still water level. The following sections describe the results of the model in estimating wave height, longshore current, surf zone width, and modified surf index.

Note in Appendices A and B that the wave height output from the SL and S9 runs, and from the DL and D9 runs are identical. This is expected because the difference in bottom friction only affects the longshore current computation. For the SL, S9, DL, and D9 runs, using *Self Start*, the surf zone width encompasses that length for which the model estimates more than 5 percent of the waves to be breaking or broken. For the SS, SE, DS, and DE runs, model output is given for the entire cross shore length from *dstart* to the edge of the water. The summary scatter diagrams of model output are shown in Appendix C.

5.1. NSTS Results

5.1.1 Wave Height

The NSTS beach has a rather flat beach profile without any bar features. From Appendix A, the model does a reasonable job in wave height prediction showing the first shoaling effect and then the decay due to breaking. Columns 3 through 6 of Table 3 show the accuracy of the various model runs in describing wave height throughout the surf zone at Leadbetter Beach. Column 3 is the Pearson product-moment coefficient of correlation between model wave height and the corresponding wave height measurement. The correlations from among the four sets of runs agree to within .089 showing little significant difference among model runs.

The fourth column of Table 3 gives the slope, and the fifth column 4 gives the y-intercept, of the linear regression curve through the N (x = measurement, y = model) pairs (See Appendix C). The SS runs yield the best slope value, and the SL and S9 runs yield the best bias value. The root-mean-square of the fractional error of wave height is lowest from the SS runs and highest from the SL and S9 runs.

5.1.2 Longshore Current

The cross shore profiles of longshore current measurements contain a peak between 100 feet offshore and the water's edge, but except for the 3 February case, the model produces a current profile that increases monotonically from offshore to the water's edge. This problem can be traced

to the formulation of the longshore current which employs, for all options, the wave dissipation function $<\epsilon_b>$. A detailed investigation of the complete equations for $<\epsilon_b>$ has revealed that for all $W(H)$, the ratio of wave height to depth is the controlling factor for wave dissipation and thus longshore current. For all five $W(H)$ in SURF96 and the single $W(H)$ in previous versions of the model, it can be shown that

$$<\epsilon_b> \leq K\frac{H^p}{h^q} \tag{37}$$

where K is a constant which includes all constant factors in (4) and (9) and where $p > q$. The inequality (37) suggests that in very shallow water the rate of wave dissipation may be too large, thus causing too large longshore currents. The problem is unimportant to naval operations in that it only occurs in depths of less than 0.5 meters, except when spurious longshore currents at these depths are so large that that they mask the more important, more accurately modelled currents at deeper depths. The problem may overcome by simply ending surf zone calculations at shallow depths. This deficiency will be evaluated and eliminated in the near future.

The overall accuracy of the model at NSTS was highest from the SS (non-roller) runs as shown in Table 3 by having the highest correlation between measurement and model and the lowest rms error.

Table 3. NSTS Wave Height and Longshore Current Verification. Model runs and data of 3-6 February 1980. M is the model version. N is the number of model output-measurement pairs for all days and all measurements in the surf zone for which there is a corresponding model output value. R denotes the correlation coefficient between N pairs. *slope* is the slope of a best fit linear regression through the N pairs and *bias* is the y-intercept of the best fit linear regression curve through the N pairs. ϵ is the root-mean-square of the fractional error for N pairs. Subscripts H denote rms wave height and subscripts V denote longshore current. Units of $bias_H$ are feet and units of $bias_V$ are knots.

M	N	R_H	$slope_H$	$bias_H$	ϵ_H	R_V	$slope_V$	$bias_V$	ϵ_V
SS	45	0.8721	0.9083	0.1797	0.2827	0.7479	0.6257	0.0975	0.4719
SE	45	0.8789	0.9055	0.1806	0.3042	0.6968	0.7844	0.1041	0.6008
SL	42	0.8700	0.7664	0.1755	0.4976	0.5841	0.5524	0.1095	0.5867
S9	42	0.8700	0.7664	0.1755	0.4976	0.5270	0.4431	0.0954	0.6502

5.2 DELILAH Results

At the beginning of the experiment, the beach profile at Duck has a small bar feature nearshore. The increasing wave conditions from 9 October built a large bar feature further offshore.

5.2.1 Wave Height

In general, the model gives good wave height prediction for both roller and non-roller runs. The number of DELILAH runs makes a more detailed comparison of the model output and measurements possible than with the limited NSTS runs. Table 4 gives the correlation coefficient, slope, and bias of the model for N measurement pairs, but at *each* sensor for the DS, DE, and DL and D9 runs. The sensors were in fixed positions throughout the course of DELILAH and due to the changing water level the model output nearest the measurement was found and used in the statistics. In Table 4, sensor $S = 1$ is closest to the edge of the water and $S = 9$ is the most seaward (See Figure 1).

The SURF96 runs, i.e. the DL and D9 runs yielded the highest overall correlation and a slope near unity from sensor $S = 2$ located in relatively shallow water where there was often a trough shoreward of the bar. The DE runs produced high correlations and slopes near unity seaward of the bar.

Scatter diagrams of measured and model wave heights from the 79 DELILAH runs for all measurements taken together and all measurements by sensor are given in Appendix C.

Table 4. DELILAH Wave Height Verification. Correlation and simple linear regression statistics of DS, DE, DL, and D9 model versus measured wave height throughout the surf zone. *S* is the sensor location. *N* is the number of model output-measurement pairs, *R* is the correlation coefficient for the *N* pairs, *slope* is the slope of the best fit linear regression curve through the pairs, and *bias* is the y-intercept (in feet). DL and D9 results are identical. The smaller number of pairs from the DL and D9 runs is due to the self start option used which restricted model output to those locations with 5 of more percent breaking waves. Highest correlation coefficient shown in **bold**.

	DS				*DE*				*DL & D9*			
S	*N*	*R*	*slope*	*bias*	*N*	*R*	*slope*	*bias*	*N*	*R*	*slope*	*bias*
1	62	**0.7843**	0.8377	0.8087	62	0.7742	1.0334	0.8225	59	0.7600	0.9242	0.9347
2	79	0.9629	0.9431	0.2482	79	0.9786	1.3697	0.1373	79	**0.9894**	1.1777	0.3236
3	74	0.8716	0.8986	0.5488	74	0.9012	1.3307	0.4198	74	**0.9281**	1.2558	0.4495
4	79	0.9356	0.8623	0.6916	79	0.9564	1.2170	0.5390	79	**0.9707**	1.1207	0.6249
5	79	0.9329	0.6269	1.2507	79	**0.9664**	0.9130	1.0411	78	0.9566	0.8154	1.1432
6	39	0.9011	0.5394	1.3459	39	**0.9537**	0.9633	0.9116	31	0.8883	0.7237	1.3407
7	79	0.9163	0.6360	1.3011	79	**0.9741**	1.1210	0.8028	78	0.9382	0.8500	1.3055
8	79	0.9180	0.5938	1.3899	79	**0.9701**	1.0390	0.8921	67	0.9341	0.7713	1.4505
9	79	0.9517	0.7584	1.3080	79	**0.9833**	1.2163	0.7855	65	0.9634	0.9228	1.4090

5.2.2 Longshore Current

Compared to measurements, the model tends to underpredict the peak of the longshore current, which is generally shoreward of the bar, and, as with the NSTS runs, to give inaccurate, monotonically increasing currents close to the water's edge. However, the model did, at times, provide remarkably good current profiles, as, for example, the 1300 EST 6 October and 1300 EST 7 October cases. Close examination reveals that all versions of the model produce the best longshore current profiles when the tide is low. The more common monotonic increase in longshore current near the water's edge on each of the NSTS runs and on the DELILAH runs at higher tide does not exist on the DELILAH runs at low tide. The physical reason for better model performance at low tide appears associated with the greater loss of wave energy when the top of the bar is very shallow and thus a greater dissipative influence. The disscussion of poorly modelled wave dissipation due to the ratio of wave height to water depth in Section 5.1.2, which describes NSTS longshore current results, is also relevant to the DELILAH runs. From the general tendency for the modelled peak of longshore current to be too low at all, but the most shallow, depths, except when wave dissipation has previously occurred at a shoreward, shallow location, it is confidently inferred that wave dissipation is controlled by more than the ratio of wave height to water depth.

Table 5 summarizes the correlation, slope, and bias of all DELILAH measurement-model output pairs by sensor for all model runs. The correlation coefficient is consistently highest for the DE runs; however, the lowest rms errors are from the DS runs. Scatter diagrams of the longshore current measurements and model output are given in Appendix C.

Table 5. DELILAH Longshore Current Verification. Correlation and simple linear regression statistics of DS, DE, DL, and D9 model versus measured longshore current throughout the surf zone. *S* is the sensor location. *N* is the number of model output-measurement pairs, *R* is the correlation coefficient for the *N* pairs, *slope* is the slope of the best fit linear regression curve through the pairs, and *bias* is the y-intercept (in feet). DL and D9 results are identical. The smaller number of pairs from the DL and D9 runs is due to the self start option used which restricted model output to those locations with 5 of more percent breaking waves. Highest correlation shown in **bold**.

	DS				DE			
S	*N*	*R*	*slope*	*bias*	*N*	*R*	*slope*	*bias*
1	66	0.5758	0.7738	0.2051	66	**0.7935**	1.1019	0.3173
2	79	0.7803	0.3374	0.0679	79	**0.8488**	0.5184	0.0523
3	74	0.6511	0.1554	0.2203	74	**0.7858**	0.2764	0.1778
4	79	0.8529	0.3125	0.1404	79	**0.9278**	0.5198	0.0779
5	79	0.8872	0.3889	0.1397	79	**0.9383**	0.6608	0.0510
6	39	0.9476	0.5586	0.1385	39	**0.9701**	0.9858	-0.0535
7	59	0.7857	0.3761	0.1506	59	**0.8317**	0.5563	0.1011
8	79	0.7891	0.3621	0.1166	79	**0.8799**	0.4650	0.0337
9	79	0.7862	0.4106	0.1462	79	**0.8531**	0.3969	0.0657

	DL				D9			
S	*N*	*R*	*slope*	*bias*	*N*	*R*	*slope*	*bias*
1	63	0.7845	0.9185	0.2967	63	0.7093	0.5682	0.2789
2	79	0.8413	0.4516	0.0837	79	0.5600	0.1322	0.0622
3	74	0.7737	0.2449	0.2062	74	0.1336	0.0255	0.2371
4	79	0.9009	0.4460	0.0953	79	0.7662	0.2477	0.1692
5	78	0.9071	0.5439	0.0605	78	0.8977	0.4776	0.1576
6	31	0.9165	0.8229	-0.0488	31	0.8745	0.4769	0.0474
7	59	0.8036	0.5063	0.0747	59	0.8112	0.2958	0.0823
8	67	0.8421	0.4575	0.0336	67	0.8511	0.2259	0.0693
9	65	0.8178	0.4508	0.0811	65	0.8492	0.2586	0.1144

5.2.3 Surf Zone Width

It is not possible to validate the surf zone width from the limited NSTS data set, however both visual observations and video imagery from DELILAH have made it possible to validate model estimates of surf zone width. Table 6 gives the model surf zone width for 21 model runs. The simpler definition of surf zone width in SURF96 produced improved surf zone estimates in some cases, especially those in which there were extremely narrow widths from the DS and DE runs.

Table 6. Verification of surf zone width in feet from 22 DELILAH cases. Columns *DAY* and *TIME* denote model run time in October 1990 (EST). *DS* denotes surf zone width from surf model runs using EXPSURF simulating SPE_SURF. *DE* denotes runs using EXPSURF with rollers. *DL* denotes runs using SURF96 with linear bottom friction. *D9* denotes runs using SURF96 with nonlinear bottom friction. Column pairs *time-pier* and *time-video* denote FRF surf zone width observations (in bold) from pier and surf zone width (in bold) determined from 10 minute averaged video imagery.

DAY	*TIME*	*DS*	*DE*	*DL*	*D9*	*time*	*pier*	*time*	*video*	*time*	*video*	*time*	*video*
6	0700	57	69	237	237	0832	**131**						
6	1600	188	208	274	274			1656	**197**				
7	0700	58	74	260	260	0846	**203**	0651	**174**				
7	1300	216	224	276	276			1531	**180**				
8	0700	61	81	299	299	0650	**220**						
8	1300	247	255	303	303			1316	**233**				
8	1600	231	239	299	299			1626	**272**				
9	0700	61	293	377	377	0700	**299**	0856	**279**				
9	1000	69	97	376	376			1106	**262**				
9	1300	57	285	369	369			1236	**308**	1316	**285**	1406	**289**
9	1900	276	296	386	386			1516	**285**	1721	**285**		
10	0700	44	312	400	400	0745	**308**						
11	0700	330	370	485	485		**1050**						
12	0700	47	359	443	443	0655	**345**	0857	**338**				

DAY	*TIME*	*DS*	*DE*	*DL*	*D9*	*time*	*pier*	*time*	*video*	*time*	*video*	*time*	*video*
13	0700	1763	391	1752	1752		**1316**	0804	**374**	0904	**400**		
13	1000	329	389	1590	1590			1004	**384**				
14	0700	55	403	503	503	0748	**381**						
14	1000	374	402	502	502			1004	**420**	1203	**358**		
15	0700	61	381	471	471	0724	**351**	0703	**308**				
15	1000	370	390	482	482			1003	**348**				
16	0700	47	71	--	475	0810	**390**						

5.2.4 Modified Surf Index

Although the MSI cannot be validated, a consistency check can be made. The formula for MSI given in the *Joint Surf Manual* uses the maximum wave height in the surf zone, maximum longshore current speed in the surf zone, breaker angle, wave period, and breaker type. The method used to check MSI is to replace the contribution of wave height and longshore current from the model with the respective contribution from measurement, while keeping the model contributions of wave angle, wave period, and breaker type. Wave angle and period are from actual directional wave spectra and there are no objective measurements of breaker type. In view of the fact that the four versions of the model for each case will give varying estimates of breaker type, MSI was checked for each version of the model.

The 19 cases used for MSI comparisons are given in Table 7, which lists values of wave height and longshore current for the measured, and four model versions. The measured values are the highest values in the surf zone as determined from the greatest zone width for each run in Table 6. Table 7 reveals a general tendency for the model to provide slightly higher wave heights than observed and to provide longshore current estimates that are lower than observed.

The results of Table 7 are used to compute the MSI values of Table 8, which shows that approximately one-third of the model estimates of MSI were higher than the model-measurement calculation of MSI. Some of the larger difference can be contributed to the larger longshore current from the model. For instance, the 0700 EST 8 October case in Table 7 shows a lonshore current of 2.4 knots as against the measured value of 0.99. Since the contribution of longshore current to MSI is 3 times the longshore current in knots, the model current contributed 7.2 and while measurement contributed 2.97, which results in a difference in MSI of 4.23. The rms error of wave height, longshore current speed, and MSI for the 19 cases are given in Table 9. Further discussion is not useful unless significant improvement of longshore current prediction can be made.

5.3 Discussions

Several improvements incorporated into EXPSURF and SURF96 are not evaluated directly by these validation data sets. Although the *Self Start* option is not explicitly evaluated, surf model runs at other beaches show that starting the model too far from the breaker line causes underestimation of wave energy. Also, it has been found that using an excessively large calculation interval has, at times, provided unrealistic results. Inappropriate gridding is avoided in SURF96 with the added feature of automatic internal gridding. Breaker type has not been evaluated owing to the lack of precise measurements, but it is known from visual observations that the model realistically estimates spilling and plunging breakers. Model estimates of surging breakers have not been evaluated because such breakers rarely occur. Previous model versions calculated the percentage of breaker types only at the point of maximum occurrence, which made these versions excessively sensitive to local bottom slope. In SURF96, the use of average breaker type over the entire surf zone yields estimates that are less affected by small changes in depth.

The main objectives of this validation report have been to validate and test the robustness of SURF96 under a wide range of wind, tide, and wave conditions at both barred and straight beaches. In practice, some of the cases should not have been included because the conditions at the time violate a basic assumption in the model—some DELILAH directional wave spectra contain two energy peaks, which violates the assumption that wave energy be narrow banded in frequency and direction in the Thornton and Guza formulation. However, they are included to evaluate how badly the model will perform under such a situation. The present longshore current model is not supposed to work well for barred beaches. But the results for barred beaches are included for evaluation purpose.

Table 7. DELILAH wave height and longshore current verification: 19 Cases. *DD* is the day in October 1990. *HH* is the hour (EST). *H_meas* is the highest measured wave height in the surf zone where the width of the surf zone is defined by either video or direct observation. *H_DS*, *H_DE*, *H_DL*, and *H_D9* are the respective model outputs from the versions noted. Measurements and model output of longshore current *V* are defined in the same way as *H*. Wave heights are in units of feet and longshore currents are in units of knots. Model output higher than measured is shown in **bold**.

DD	*HH*	*H_meas*	*H_DS*	*H_DE*	*H_DL*	*H_D9*	*V_meas*	*V_DS*	*V_DE*	*V_DL*	*V_D9*
6	7	1.33	**1.8**	**2.1**	**2.2**	**2.2**	0.42	**0.7**	**1.1**	**1.1**	**0.9**
6	16	1.24	**1.8**	**2.1**	**2.1**	**2.1**	0.97	0.6	0.6	0.6	0.6
7	7	1.60	**1.7**	**2.1**	**2.4**	**2.4**	0.54	**0.8**	**1.3**	**1.2**	**1.0**
7	13	0.98	**2.0**	**2.2**	**2.2**	**2.2**	1.02	0.6	0.8	0.7	0.7
8	7	1.76	1.7	**2.1**	**2.8**	**2.8**	0.99	**2.4**	**1.4**	**1.4**	**1.1**
8	13	1.74	**2.4**	**2.7**	**2.7**	**2.7**	1.24	0.6	0.7	0.7	0.7
8	16	1.70	**2.4**	**2.7**	**2.7**	**2.7**	1.58	0.6	0.8	0.8	0.9
9	7	2.52	1.8	**3.6**	**3.7**	**3.7**	1.89	0.8	1.3	1.2	1.0
9	10	2.46	2.2	**2.8**	**4.0**	**4.0**	1.67	1.0	**1.8**	**1.8**	1.1
9	13	2.46	1.6	**3.4**	**3.6**	**3.6**	1.93	0.8	1.3	1.2	1.0
9	19	2.46	**2.8**	**3.5**	**3.6**	**3.6**	1.99	0.7	1.1	1.1	0.9
10	7	2.50	1.6	**3.6**	**3.7**	**3.7**	1.92	0.7	1.2	1.2	1.0
11	7	4.10	2.6	3.8	3.8	3.8	2.70	1.1	1.7	1.4	1.2
12	7	2.33	1.7	**3.6**	**3.6**	**3.6**	1.69	0.6	1.6	1.1	1.0
13	7	4.52	**7.1**	4.3	**7.1**	**7.1**	2.19	1.3	**2.3**	1.2	1.1
13	10	2.81	**3.2**	**4.5**	**6.8**	**6.8**	2.24	0.7	1.8	1.2	1.1
14	7	2.45	2.2	**3.8**	**3.9**	**3.9**	1.03	0.3	0.8	0.5	0.6
14	10	2.13	**3.0**	**3.8**	**3.8**	**3.8**	1.04	0.3	0.8	0.6	0.6
15	7	2.29	**2.4**	**3.6**	**3.7**	**3.7**	0.99	0.8	**1.8**	**1.7**	**1.3**

Table 8. DELILAH Modified Surf Index. Verification of MSI using observed surf zone width and maximum measured wave height and maximum absolute value of measured longshore current. The respective contributions of model wave height and current to MSI have been replaced by the respective contribution of measured wave height and current. Model contributions to MSI from other factors left unchanged. Capital *M* denote best MSI estimates from model and measurements; small *m* denote model derived MSI. Model MSI that is higher than model-measurement MSI is shown in **bold**.

DD	*HH*	*M_DS*	*M_DE*	*M_DL*	*M_D9*	*m_DS*	*m_DE*	*m_DL*	*m_D9*
6	7	3.19	3.09	2.09	2.19	**4.5**	5.9	**5.0**	**4.5**
6	16	4.55	4.95	4.95	4.85	4.0	4.7	4.7	4.6
7	7	4.62	4.92	3.62	3.52	**5.5**	**7.7**	**6.4**	**5.7**
7	13	4.44	4.44	4.44	4.44	4.2	**5.0**	**4.7**	**4.7**
8	7	5.43	5.03	5.03	5.23	**9.6**	**6.6**	**7.3**	**6.6**
8	13	5.66	6.56	6.16	6.26	4.4	5.9	5.5	5.6
8	16	8.64	8.34	7.24	7.24	6.4	7.0	5.9	6.2
9	7	8.59	7.09	8.49	8.39	4.6	6.4	7.6	6.9
9	10	9.67	8.47	8.97	9.27	7.4	**9.2**	**10.9**	9.1
9	13	9.75	7.35	9.55	9.45	5.5	6.4	8.5	7.8
9	19	9.33	10.93	8.33	8.43	5.8	9.3	6.8	6.3
10	7	8.86	9.06	6.66	6.86	4.3	8.0	5.7	5.3
11	7	13.70	14.80	11.90	11.80	7.4	11.5	7.7	7.0
12	7	7.90	8.40	6.80	6.80	4.0	**9.4**	6.3	6.0
13	7	6.79	11.69	6.89	6.69	6.7	**11.8**	6.5	6.0
13	10	9.83	10.13	5.33	5.43	5.6	**10.5**	6.2	**6.0**
14	7	6.74	6.74	4.44	4.64	4.3	**7.4**	4.3	**4.8**
14	10	4.55	6.95	4.75	4.75	3.2	**7.9**	**5.1**	**5.1**
15	7	6.26	5.26	5.56	5.46	5.8	**9.0**	**9.1**	**7.8**

Table 9. Root-mean-square of the fractional error in the longshore current ϵ_v and wave height ϵ_H in the surf zone, and MSI ϵ_{MSI} for 19 DELILAH cases using four versions of the surf model.

	DS	*DE*	*DL*	*D9*
ϵ_V	.640	.603	.621	.523
ϵ_H	.386	.552	.687	.687
ϵ_{MSI}	.374	.322	.428	.338

6. CONCLUSIONS

In general, the surf model accurately estimates wave height throughout the surf zone. Compared to older versions, the roller option provides better results for higher wave conditions; however, criteria for automatically choosing the roller option must be developed for an operational version of the model. The validation tests have shown that the upgraded model is computationally robust and provides reasonable surf zone estimates. The major deficiency of the model is in its longshore current computation, which underpredicts the maximum value, and tends to give values that are too high in very shallow water. This deficiency is closely associated with the basic formulation of the wave energy dissipation function. The implementation of nonlinear linear bottom stress formulation of longshore current does not provide significant improvement over the older formulation. The longshore current model will be the focus for future ONR and SPAWAR projects.

The wide range of options in the model produce largely similar results for wave height and longshore current; however, the best set of options for given conditions must be determined. A decision tree approach should be developed to assist users in choosing these options.

The NSTS and DELILAH data set are a valuable resource for further testing of the surf model, and the DELILAH set has been used for wave refraction model verification. However, a deficiency in this study has been a lack of observations of breaker type. Future validation data sets should include these important observations owing their importance in surf zone descriptions.

ACKNOWLEDGMENTS

The authors thank Prof. Edward Thornton of the Naval Postgraduate School, Professor Robert Guza of the Scripps Institution of Oceanography and Dr. Chuck Long of the Field Research Facility for providing the DELILAH data set. Professor Rob Holman of Oregon State University and Dr. Todd Holland of the Naval Research Laboratory, Stennis Space Center (NRL-SSC) provided the video imagery and assistance in analysis. This work was sponsored by the Space and Naval Warfare Systems Command under program element 603207N–Surf Model Upgrade Project and by the Office of Naval Research (ONR) through NRL-SSC under task entitled Surf Model Improvements under U.S. Navy contract N00014-94-C-6024. CDR Tim Sheridan is the program manager for the SPAWAR-sponsored effort and Mr. Ed Chaika (ONR) and Mr. Jack McDermid (NRL-SSC) are the program managers for the ONR-sponsored effort. LCDR Casey Church provided helpful criticism and assistance in obtaining the data sets, which have become available since the Navy Surf Model was first developed.

REFERENCES

Birkemeier el al, 1991: *DELILAH Experiment: Investigator's Summary Report*, Field Research Facility, Waterways Experiment Station, Coastal Engineering Research Center, U.S. Army Corps of Engineers.

Church, J.C. and E.B. Thornton, 1993: Effects of breaking wave induced turbulence within a longshore current model, *Coastal Engineering*, **20**, 1-28.

Commander, Naval Surface Force, Pacific and Commander, Naval Surface Force, Atlantic,1987: *Joint Surf Manual*, COMNAVSURFPAC/COMNAVSURFLANTINST 3840.1B, 02 January 1987, 13 chap., 1 appendix.

Dally, W.R. and R.G. Dean, 1986: Mass flux and undertow in a surf zone, by I.A. Svendsen–discussion, *Coastal Engineering*, **10**, 289-307.

Dowling, G.B., G.G Salsman, M.D. Earle, and E.P. Kennelly, 1993: Surf Zone Characterization for the EATD Explosive Neutralization System, A&T Technical Report No. 93-505, Contract N61331-92-D-0042/0047, Analysis and Technology, Inc., 124 Gwyn Drive, Panama City Beach, Fl 32408, September, 1993, 45 pp.

Earle, M.D., 1988: *Surf Forecasting Software User's Manual*, NORDA Technical Note 352, 194 pp., Naval Research Laboratory, Stennis Space Center, MS.

Earle, M.D., 1989: *Surf Forecasting Software Scientific Reference Manual*, NORDA Technical Note 351, 261 pp., Naval Research Laboratory, Stennis Space Center, MS.

Earle, M.D., 1991: *Surf Forecasting Software Improvements*, Neptune Sciences, Inc., Report for Naval Research Laboratory, Stennis Space Center, MS, 31 pp.

Earle, M.D., 1992: *Amphibious Warfare Tactical Decision Aid: Surf Model for Use on DTC-2 Computers*, Neptune Sciences, Inc., Report for Naval Coastal Systems Center, 24 pp., February 1992.

Ebersole A.E., M.A. Cialone and M.D. Parker, 1986: Regional Coastal Processes Numerical Modeling System, Tech. Report, CERC-86-4, Waterways Exp. Staion., Vicksburg, MS,160 pp.

Gable, C.G., Ed., 1981: Report on data from the Nearshore Sediment Transport Study Experiment on Leadbetter Beach Santa Barbara, California, January-February 1980, IMR Ref 80-5, Institute of Marine Resources, University of California.

Higgins, A.L., R.J. Seymour and S.S. Pawka, 1981: A compact representation of ocean wave directionality, *Applied Ocean Research*, **3**(3), 105-112.

Holman, R.A., A.H. Sallenger, Jr., T.C. Lippmann and J.W. Haines, 1993: The Application of Video Image Processing to the Study of Nearshore Processes, *Oceanography*, **6**(3), 78-85.

Joint Chiefs of Staff, 1989: *Joint Doctrine for Landing Force Operations*, 1 November 1989.

Joint Chiefs of Staff, 1991: *Joint Tactics, Techniques, and Procedures for Joint Logistics over the Shore*, 22 August 1991.

Joint Chiefs of Staff, 1992: *Doctrine for Joint Special Operations*, 28 October 1992.

Joint Chiefs of Staff, 1993a: *Joint Doctrine for Amphibious Embarkation*, 16 April 1993.

Kirby, J.T. and R.A. Dalrymple, 1994: *Combined Refraction/Diffraction Model, REF/DIF 1, Version 2.5, Documentation and User's Manual*, CACR Report No. 94-22, Center for Applied Coastal Research, Department of Civil Engineering, University of Delaware, Newark, DE, 171 pp.

Kraus, N.C. and M. Larson, 1991: *NMLONG: Numerical model for simulating the longshore current: Report 1: Model Development and Tests*, Dredging Research Program Technical Report DRP-91-1, Coastal Engineering Research Center, US Army Corps of Engineer, 166 pp.

Larson, M., 1995: Model for Decay of Random Waves in Surf Zone, *J. Waterway, Port, Coastal, and Ocean Engineering*, **121** (1), 1-12.

Larson, M. and N.C. Kraus, 1991: Numerical Model of Longshore Current for Bar and Trough Beaches, *J. Waterway, Port, Coastal, and Ocean Engineering*, **117** (4), 326-347.

Lippmann, T.C. and R.A. Holman, 1991: Phase speed and angle of breaking waves measured with video techniques, *Proceedings of Coastal Sediments '91 Specialty Conference*, American Society of Civil Engineers, New York, 542-556

Lippmann, T.C., E.B. Thornton and A.J.H.M. Reniers, 1995: Wave Stress and Longshore Current on Barred Profiles, *Proc. Of the International Conference on Coastal Research in Terms of Large Scale Experiments*, Gdansk Poland, 401-412.

Lippmann, T.C., A.H. Brookins, and E.B. Thornton, 1996: Wave energy transformation on natural profiles, *Coastal Engineering*, **27**, 1-20.

Longuet-Higgins, M.S., 1970a: Longshore Currents Generated by Obliquely Incident Sea Waves, 1, *Journal of Geophysical Research*, **75**(33), 6678-6789.

Longuet-Higgins, M.S., 1970b: Longshore Currents Generated by Obliquely Incident Sea Waves, 2, *Journal of Geophysical Research*, **75**(33), 6790--6801.

Longuet-Higgins, M.S. and J.S. Turner, 1974: An 'entraining plume' model of a spilling breaker, *J. Fluid Mech,*. **63**(1), 1-20.

Mettlach, T. R., E.P. Kennelly and D.A. May, 1996: *Surf Forecasting Using Directional Wave Spectra with the Navy Standard Surf Model*, NRL Technical Memorandum NRL/MR/7240--96-8019, Naval Research Laboratory, Stennis Space Center, MS, 23 pp.

Nichols, C.R., M.D. Earle, D.C. Herringshaw, S.M. Mayfield, 1996: *METOC conditions affecting AAAV ship-to-objective maneuver: A detailed analysis of power projection points sited along Iranian and Korean coasts,* Neptune Sciences Inc. Report to Naval Research Laboratory, Stennis Space Center, MS, 105 pp.

Pawka, S.S., 1983: Island shadows in directional wave spectra, *Journal of Geophysical Research*, **88** (4), 2579-2591.

Resio, D.T. and W. Perrie, 1991. A numerical study of nonlinear energy fluxes due to wave-wave interactions, Part 1. Methodology and basic results. *J. Fluid Mech.*, **223**, 1603-629.

Salsman, G.G., G.B. Dowling, E.P. Kennelly, and M.D. Earle, 1993: Characterization of Surf Generated Longshore Currents for the EATD Explosive Neutralization System, A&T Technical Report No. 93-505, Contract N61331-92-D-0042/0047, Analysis and Technology, Inc., 124 Gwyn Drive, Panama City Beach, Fl 32408, August, 1993, 59 pp.

Schäffer, H.A., P.A. Madsen and R. Diegaard, 1993: A Boussinesq model for waves breaking in shallow water, *Coastal Engineering*, **20**, 185-202.

Smith, J.M., M. Larson and N.C. Kraus, 1993: Longshore Current on a Barred Beach: Field Measurement and Calculation, *Journal of Geophysical Research*, **89** (C12), 22,717-22,731.

Svendsen, I.A., 1984: Wave Heights and Set-Up in a Surf Zone, *Coastal Engineering*, **8**, 303-329.

Svendsen, I.A., 1984: Mass Flux and UnderTow In A Surf Zone, *Coastal Engineering*, **8**, 347-364.

Thornton, E.B and R.T. Guza, 1983: Transformation of Wave Height Distribution, *Journal of Geophysical Research*, **88** (C10),5925-5938.

Thornton, E.B and R.T. Guza, 1986: Surf zone longshore currents and random waves, *Journal of Physical Oceanography*, **16**, 1165-1178.

Thornton, E.B and R.T. Guza, 1989: Models for surf zone dynamics, *Nearshore Sediment Transport*, **R.**J. Seymour, ed., Plenum Press, New York, pp 337-369.

Thornton, E.B. and C.S. Kim, 1993: Longshore Current and Wave Height Modulation at Tidal Frequency Inside the Surf Zone, *Journal of Geophysical Research,* **98** (C9), 16,509-16,519.

Thornton, E.B., R.T. Humiston and W. Birkemeier, 1996: Bar/trough generation on a natural beach, *J. Geophys. Res.*, **101** (C5), 12,097-12,119.

U.S. Naval Oceanographic Office, 1969: *Breakers and Surf, Principles in Forecasting*, H.O. Pub. No. 234, 56 pp.

Whitford, D.J. and E.B. Thornton, 1992a: Longshore Currents over a Barred Beach, I: Field Experiment, *J. Physical Oceanography,*. submitted for publication.

Whitford, D.J. and E.B. Thornton, 1992b: Longshore Currents over a Barred Beach, II: Model, *J. Physical Oceanography.*, submitted for publication.

Wu, C.S., E.B. Thornton and R.T. Guza, 1985: Waves and Longshore Currents: Comparison of a Numerical Model with Field Data, *Journal of Geophysical Research,* **90** (C3), 4951-4958.

Appendix A
Model and Data Comparison for NSTS

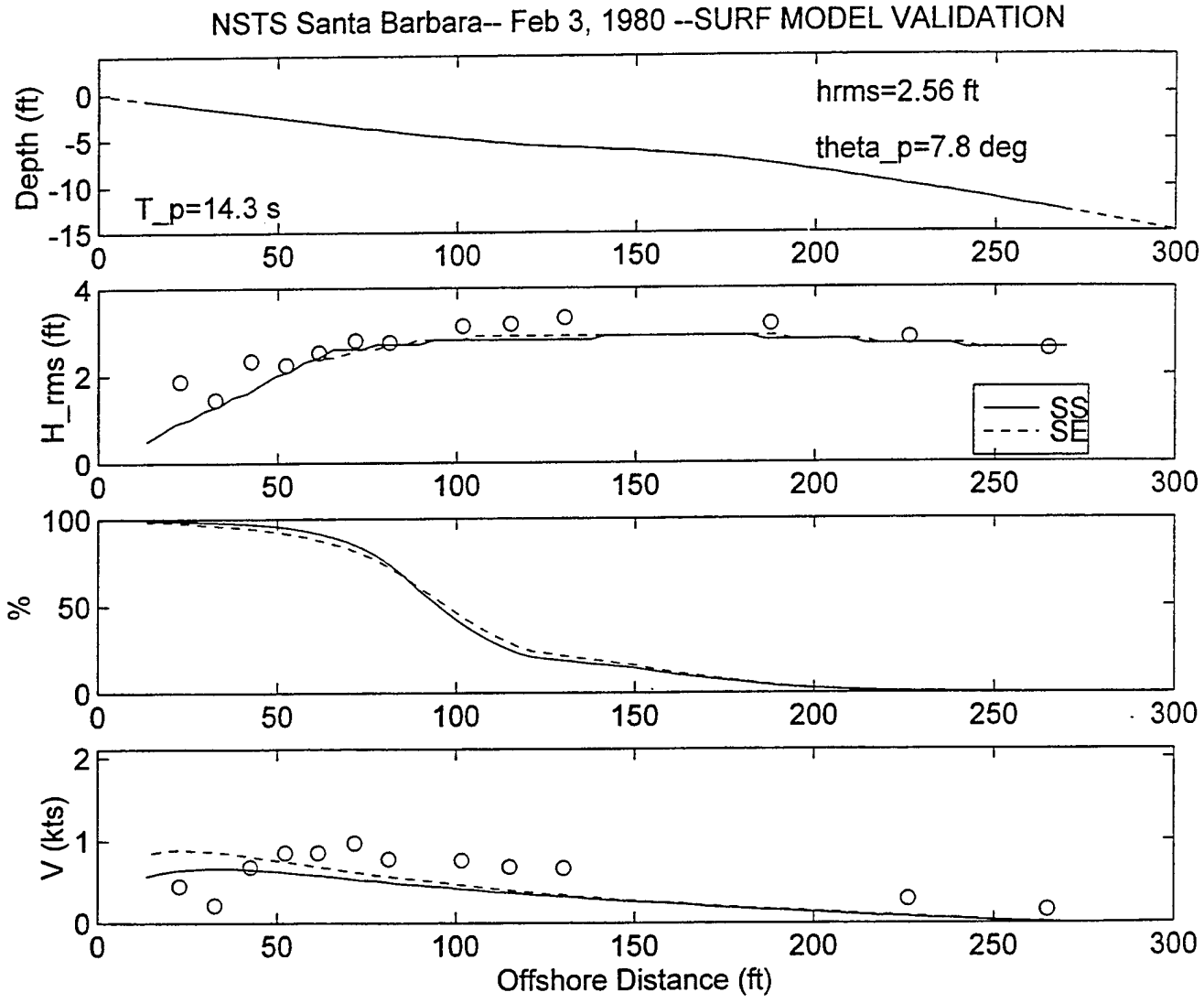
NSTS Santa Barbara-- Feb 3, 1980 --SURF MODEL VALIDATION
Depth (ft)
hrms=2.56 ft
theta_p=7.8 deg
T_p=14.3 s
H_rms (ft)
SS
SE
%
V (kts)
Offshore Distance (ft)

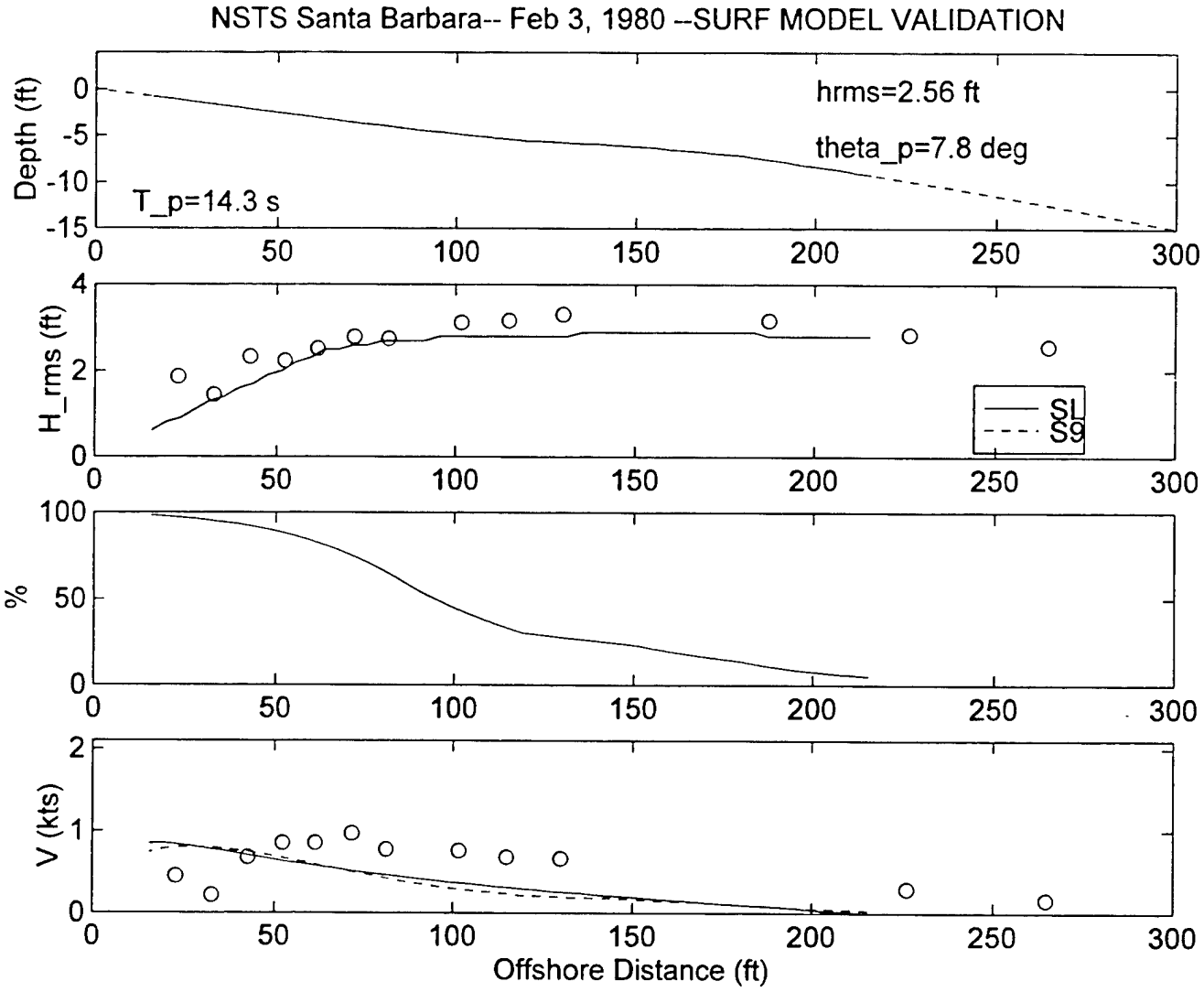
NSTS Santa Barbara-- Feb 3, 1980 --SURF MODEL VALIDATION
Depth (ft)
hrms=2.56 ft
theta_p=7.8 deg
T_p=14.3 s
H_rms (ft)
SL
S9
%
V (kts)
Offshore Distance (ft)

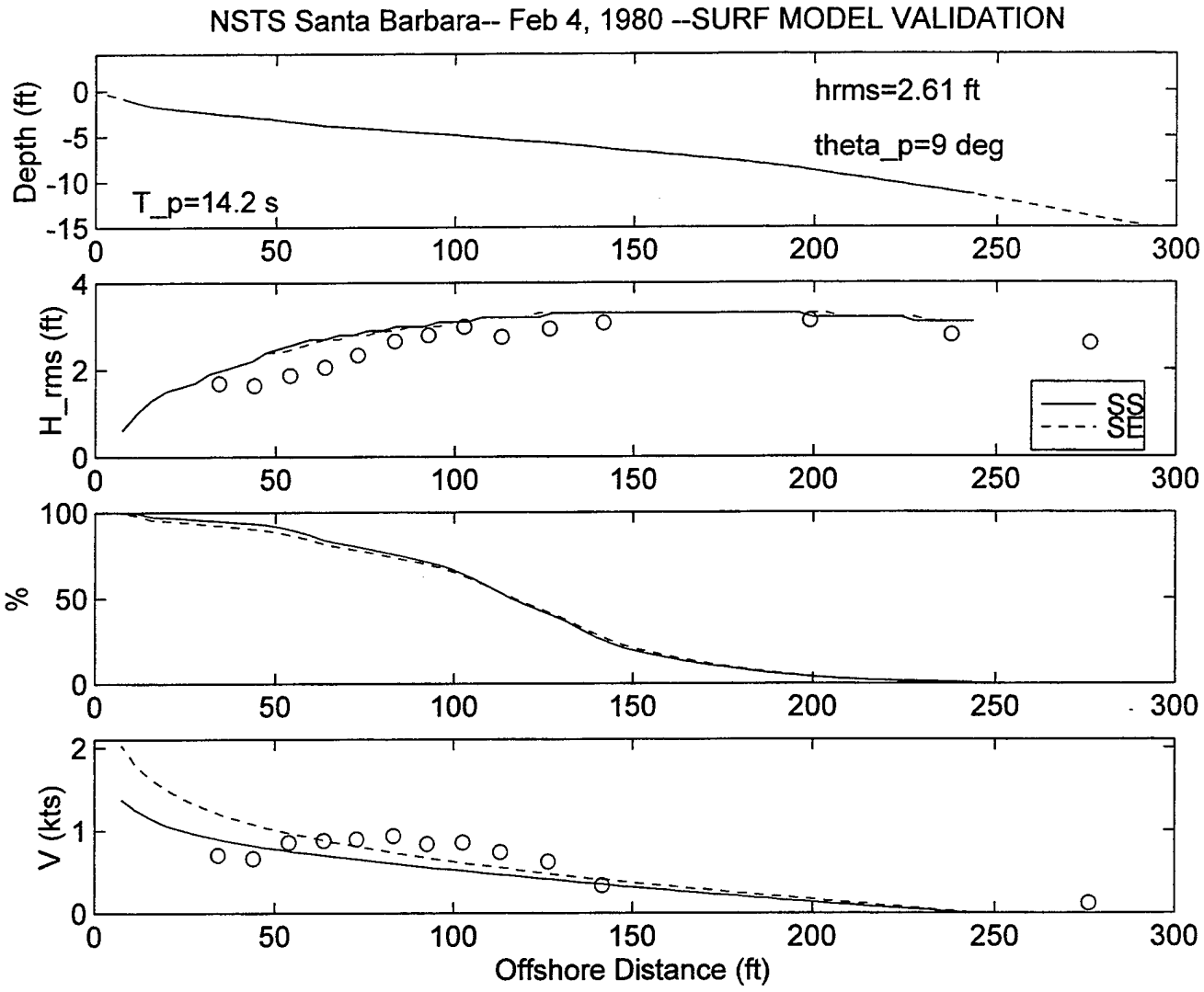
NSTS Santa Barbara-- Feb 4, 1980 --SURF MODEL VALIDATION
Depth (ft)
hrms=2.61 ft
theta_p=9 deg
T_p=14.2 s
H_rms (ft)
SS
SE
%
V (kts)
Offshore Distance (ft)

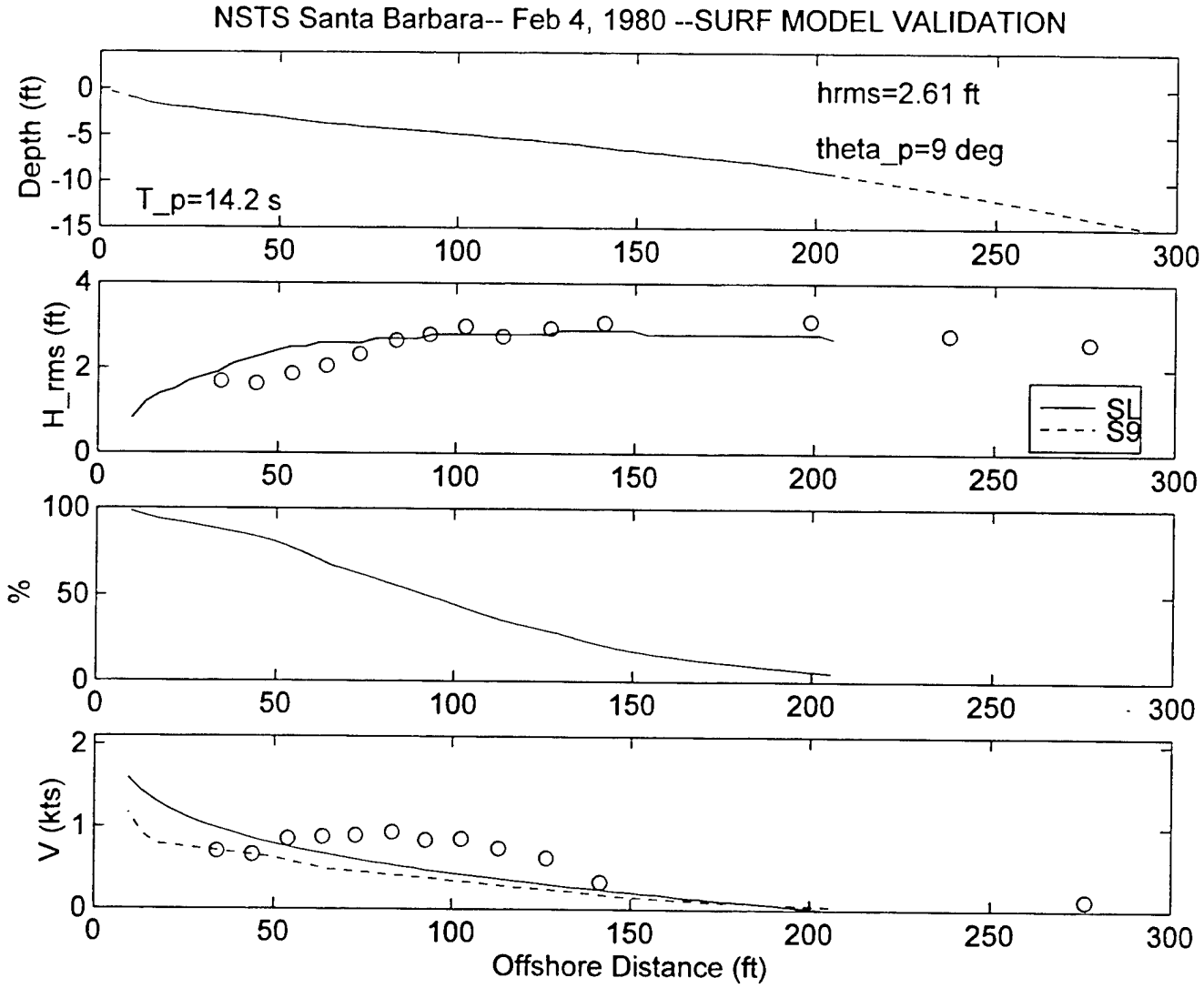
NSTS Santa Barbara-- Feb 4, 1980 --SURF MODEL VALIDATION
Depth (ft)
hrms=2.61 ft
theta_p=9 deg
T_p=14.2 s
H_rms (ft)
SL
S9
%
V (kts)
Offshore Distance (ft)

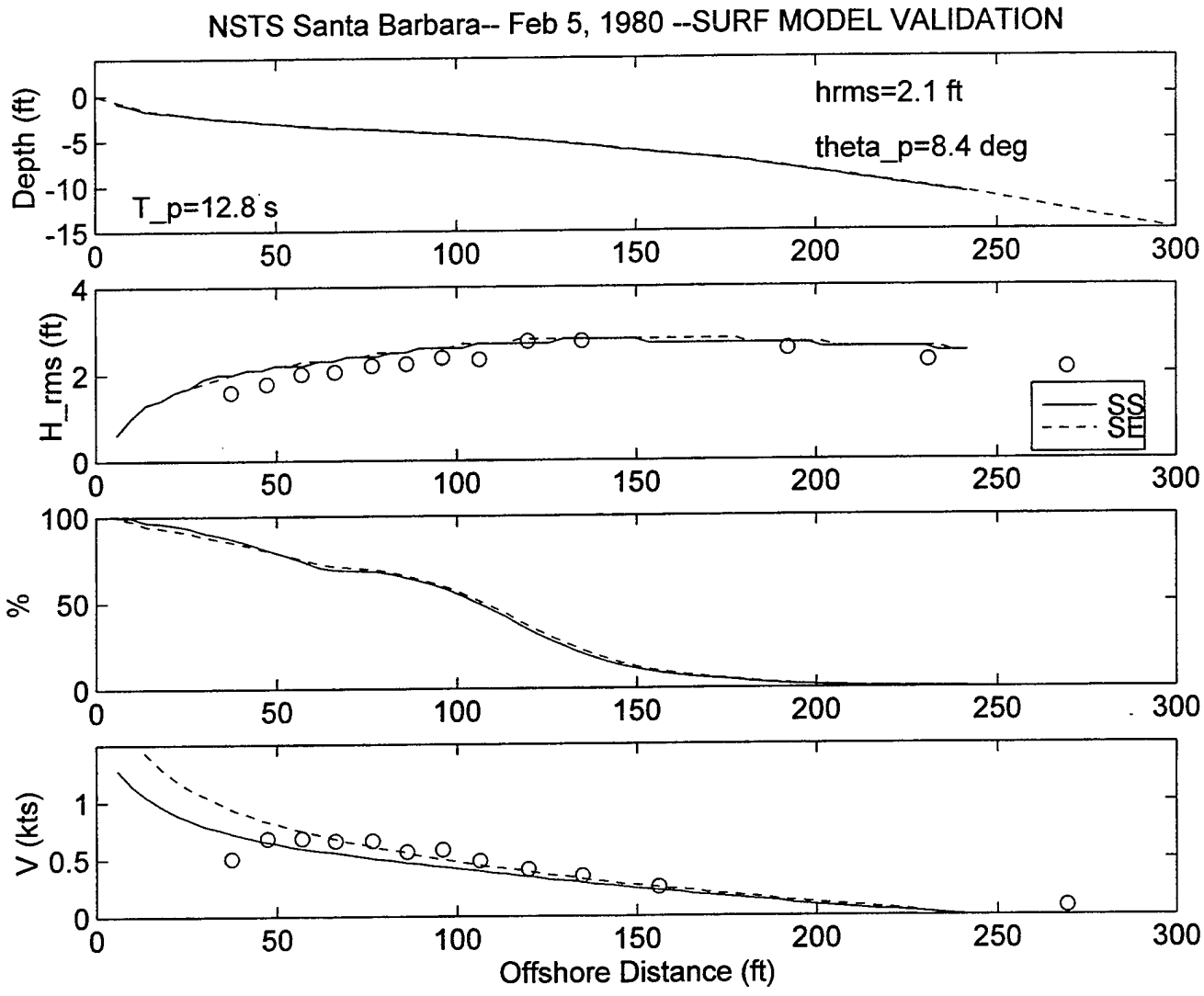
NSTS Santa Barbara-- Feb 5, 1980 --SURF MODEL VALIDATION
Depth (ft)
hrms=2.1 ft
theta_p=8.4 deg
T_p=12.8 s
H_rms (ft)
%
V (kts)
Offshore Distance (ft)

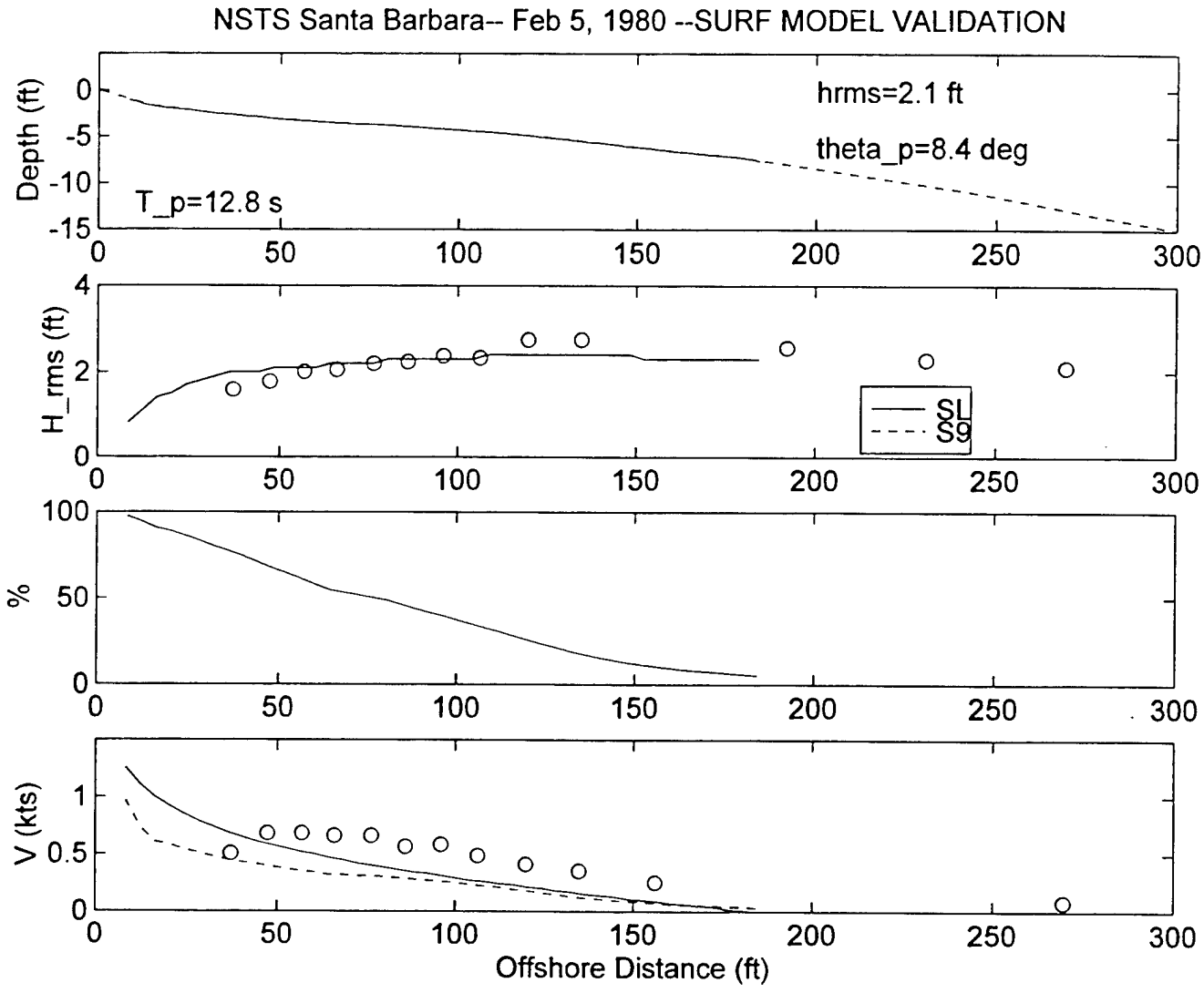
NSTS Santa Barbara-- Feb 5, 1980 --SURF MODEL VALIDATION
Depth (ft)
hrms=2.1 ft
theta_p=8.4 deg
T_p=12.8 s
H_rms (ft)
SL
S9
%
V (kts)
Offshore Distance (ft)

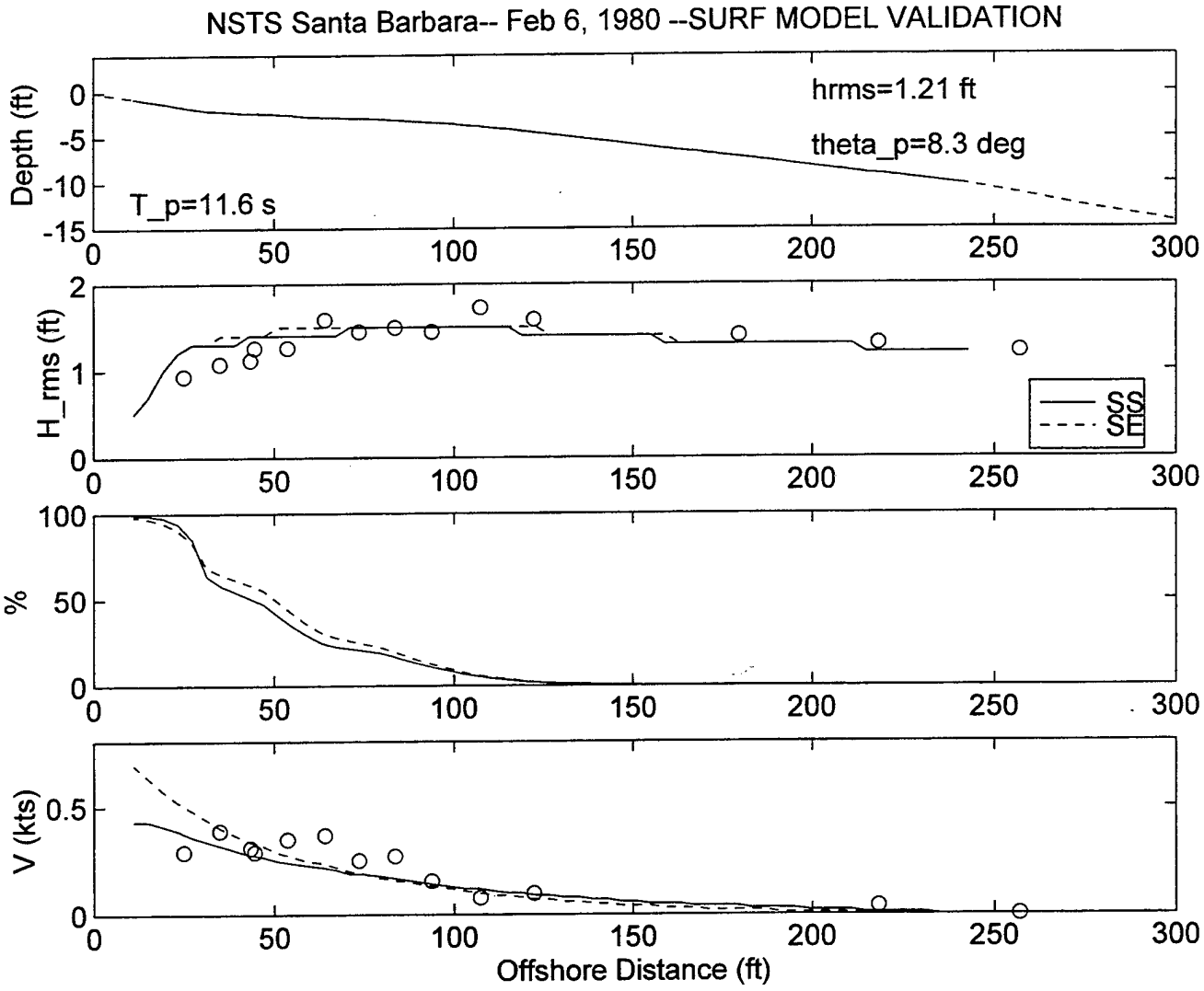
NSTS Santa Barbara-- Feb 6, 1980 --SURF MODEL VALIDATION
Depth (ft)
0
-5
-10
-15
hrms=1.21 ft
theta_p=8.3 deg
T_p=11.6 s
0
50
100
150
200
250
300
H_rms (ft)
2
1
0
SS
SE
%
100
50
0
V (kts)
0.5
0
Offshore Distance (ft)

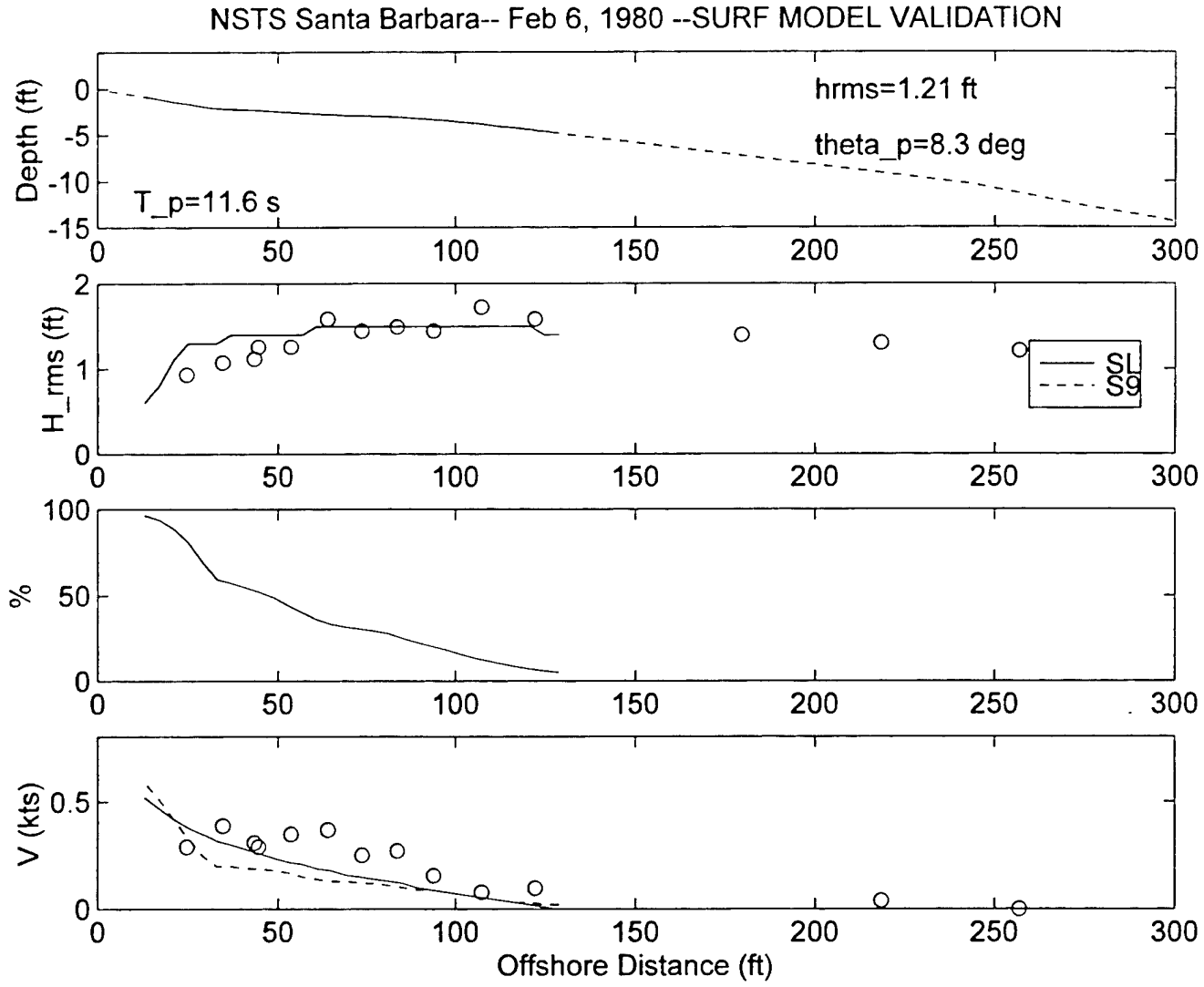
NSTS Santa Barbara-- Feb 6, 1980 --SURF MODEL VALIDATION
Depth (ft)
hrms=1.21 ft
theta_p=8.3 deg
T_p=11.6 s
H_rms (ft)
SL
SS
%
V (kts)
Offshore Distance (ft)

Appendix B
Model and Data Comparison for DELILAH

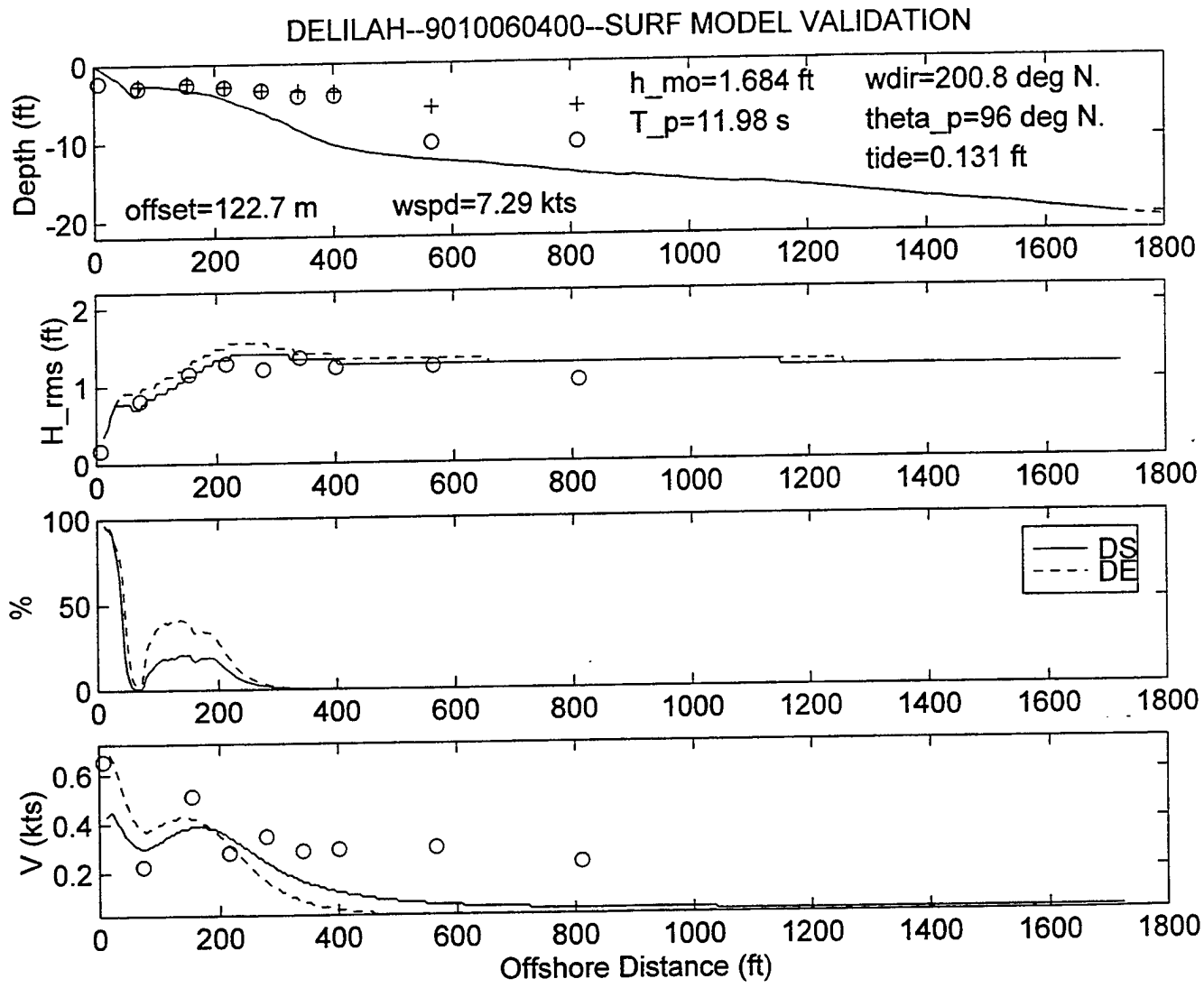
DELILAH--9010060400--SURF MODEL VALIDATION
Depth (ft)
h_mo=1.684 ft
T_p=11.98 s
wdir=200.8 deg N.
theta_p=96 deg N.
tide=0.131 ft
offset=122.7 m
wspd=7.29 kts
H_rms (ft)
%
DS
DE
V (kts)
Offshore Distance (ft)

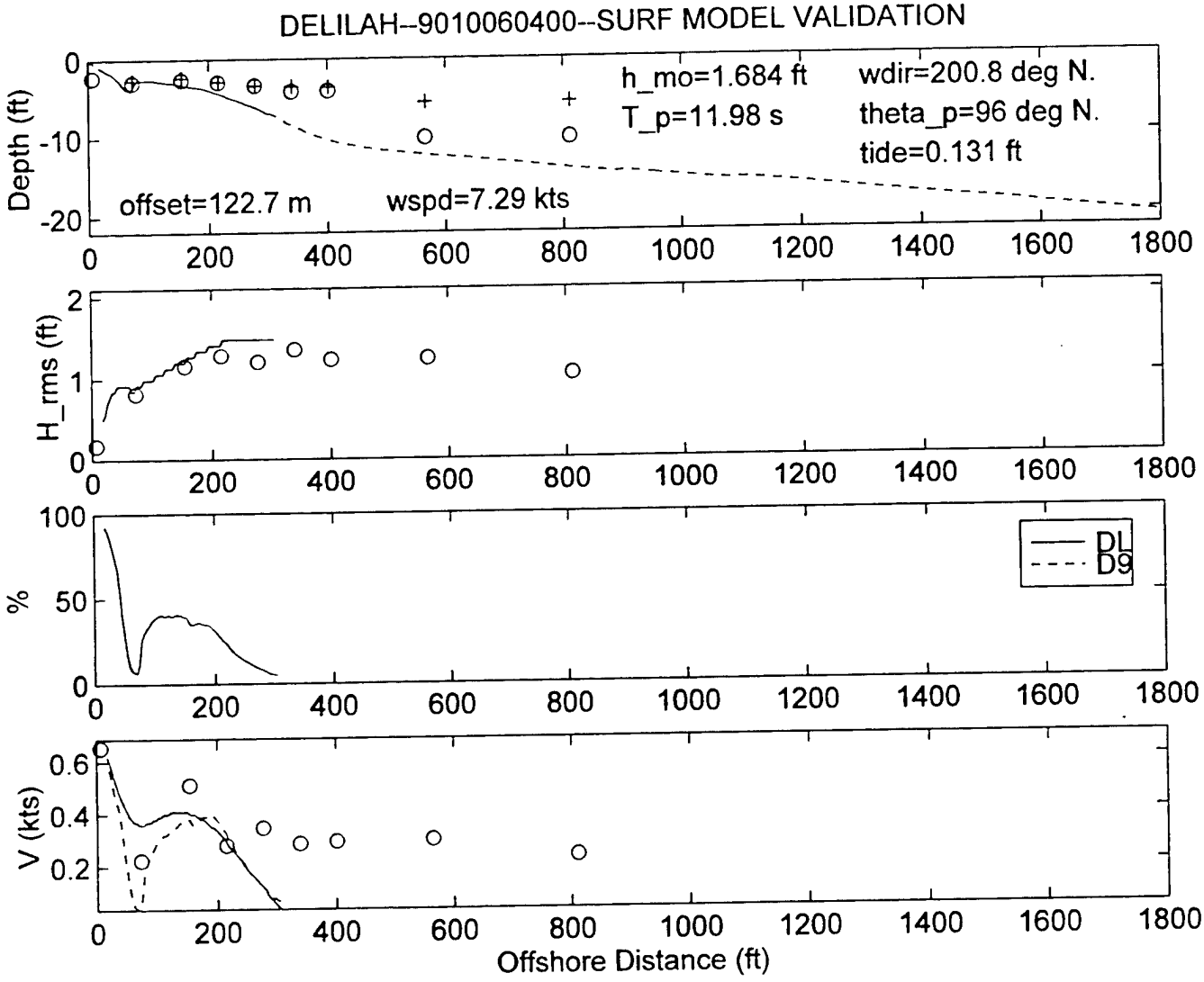
DELILAH--9010060400--SURF MODEL VALIDATION
Depth (ft)
h_mo=1.684 ft
T_p=11.98 s
wdir=200.8 deg N.
theta_p=96 deg N.
tide=0.131 ft
offset=122.7 m
wspd=7.29 kts
H_rms (ft)
%
DL
D9
V (kts)
Offshore Distance (ft)

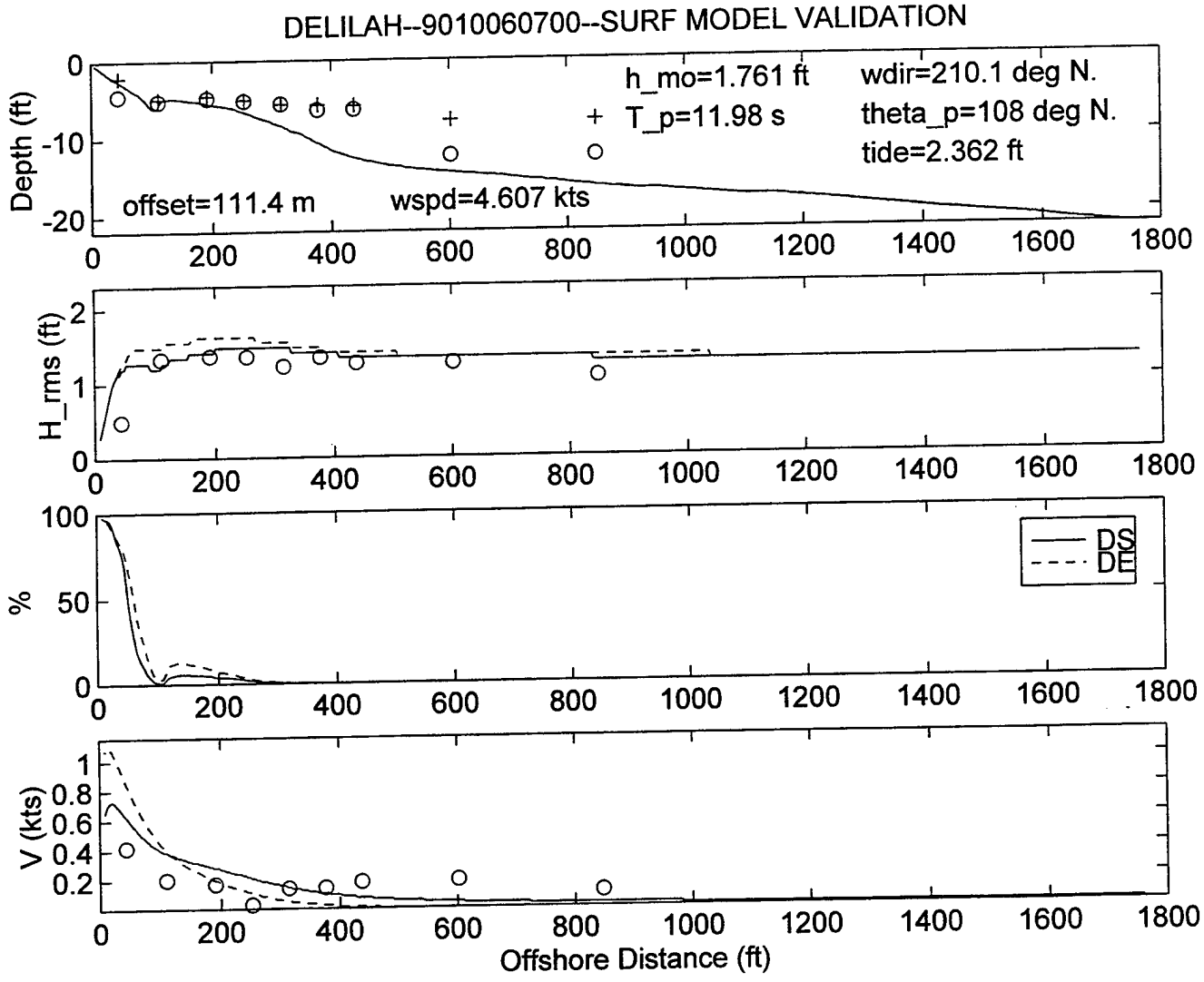
DELILAH--9010060700--SURF MODEL VALIDATION
Depth (ft)
h_mo=1.761 ft
T_p=11.98 s
wdir=210.1 deg N.
theta_p=108 deg N.
tide=2.362 ft
offset=111.4 m
wspd=4.607 kts
H_rms (ft)
%
DS
DE
V (kts)
Offshore Distance (ft)

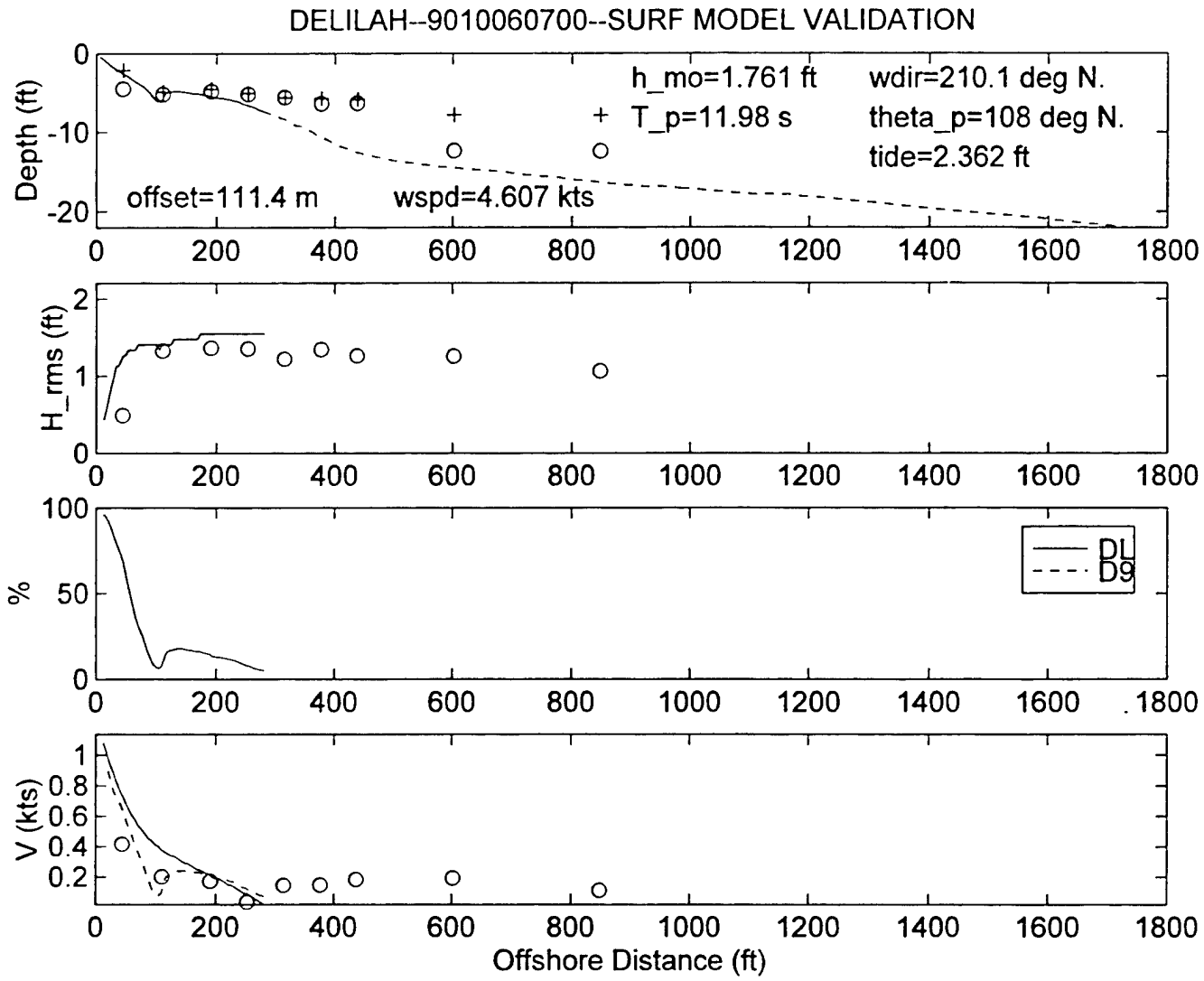
DELILAH--9010060700--SURF MODEL VALIDATION
Depth (ft)
h_mo=1.761 ft
T_p=11.98 s
wdir=210.1 deg N.
theta_p=108 deg N.
tide=2.362 ft
offset=111.4 m
wspd=4.607 kts
H_rms (ft)
%
DL
D9
V (kts)
Offshore Distance (ft)

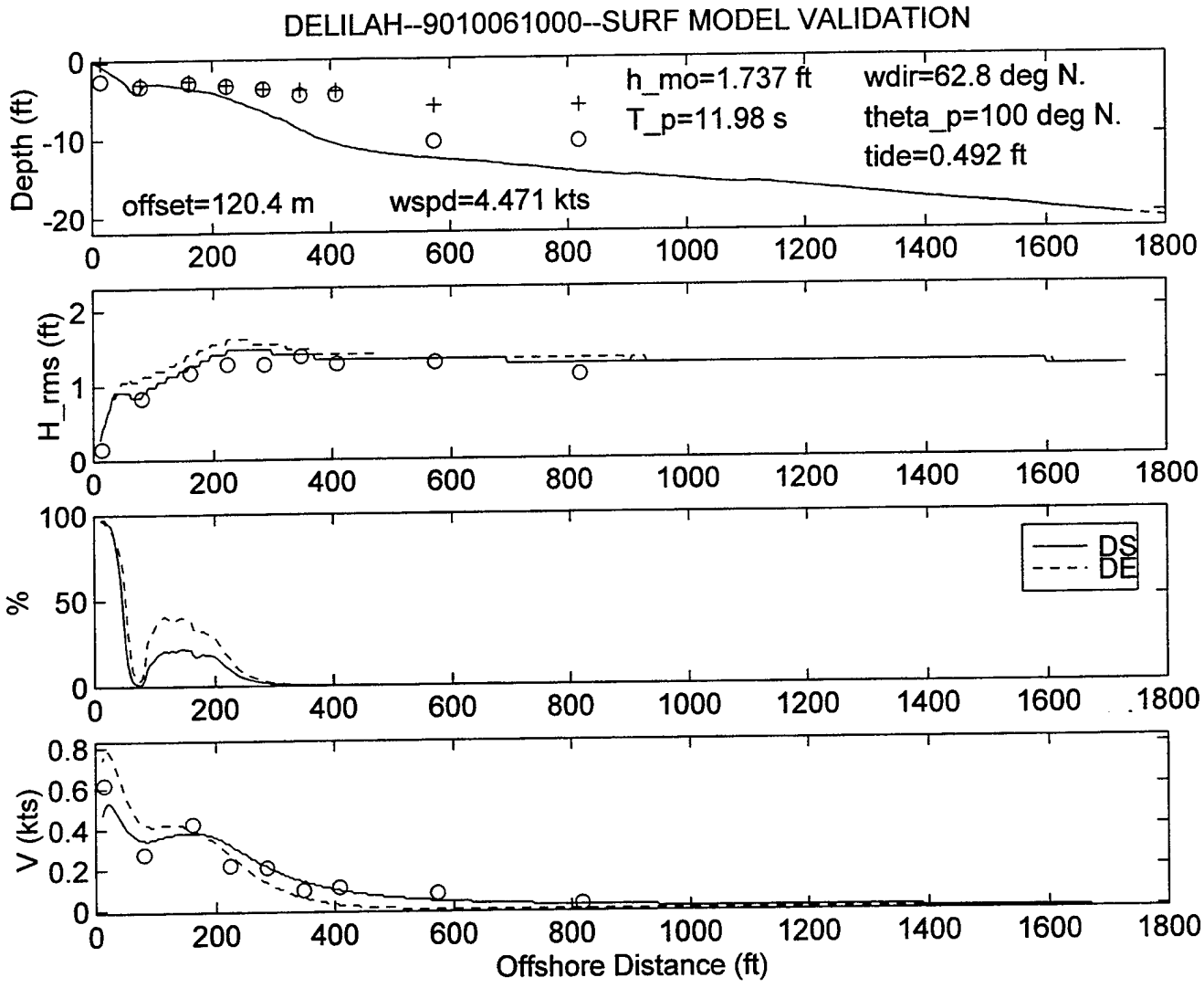
DELILAH--9010061000--SURF MODEL VALIDATION
Depth (ft)
h_mo=1.737 ft
T_p=11.98 s
wdir=62.8 deg N.
theta_p=100 deg N.
tide=0.492 ft
offset=120.4 m
wspd=4.471 kts
H_rms (ft)
%
DS
DE
V (kts)
Offshore Distance (ft)

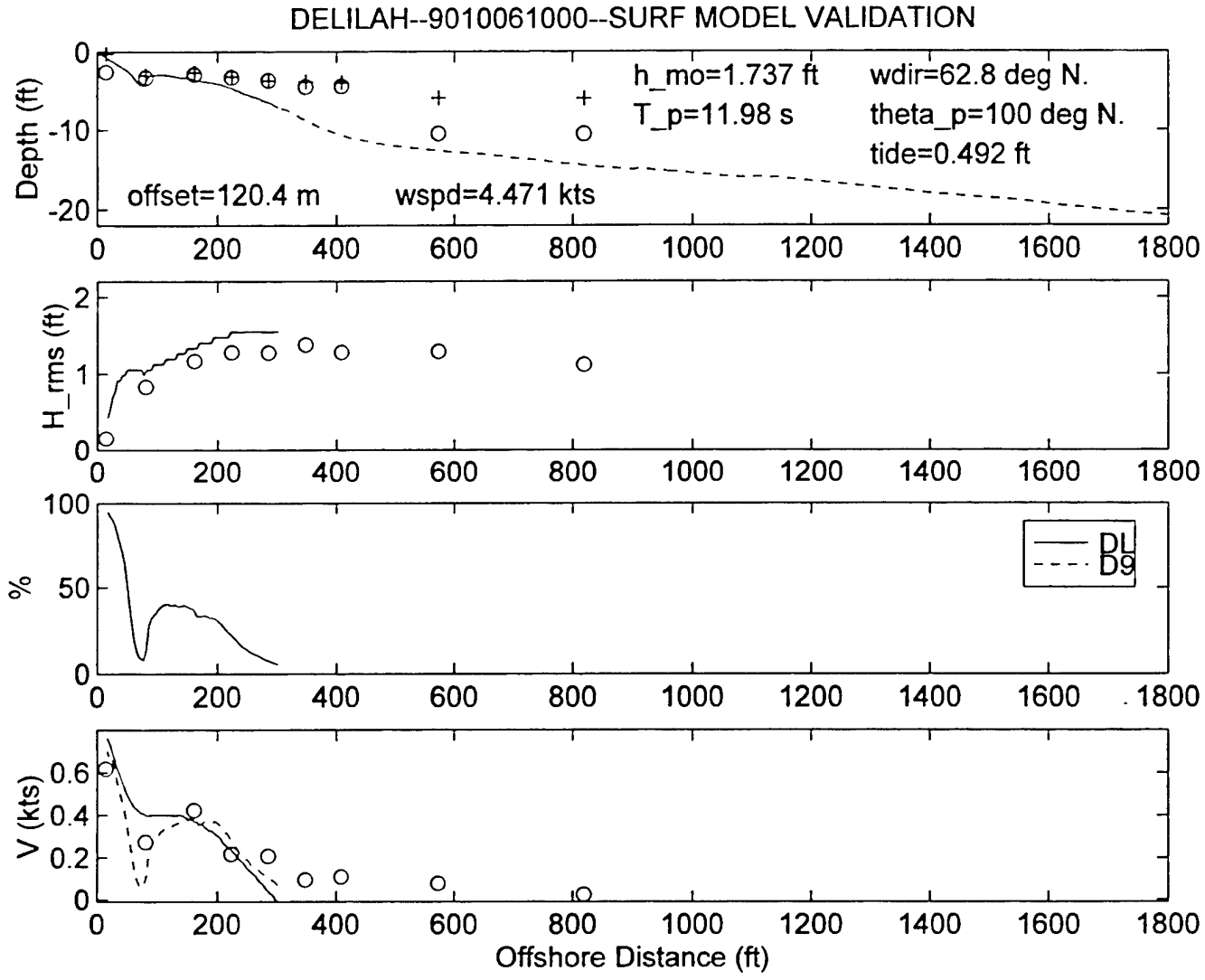
DELILAH--9010061000--SURF MODEL VALIDATION
Depth (ft)
h_mo=1.737 ft
T_p=11.98 s
wdir=62.8 deg N.
theta_p=100 deg N.
tide=0.492 ft
offset=120.4 m
wspd=4.471 kts
H_rms (ft)
%
DL
D9
V (kts)
Offshore Distance (ft)

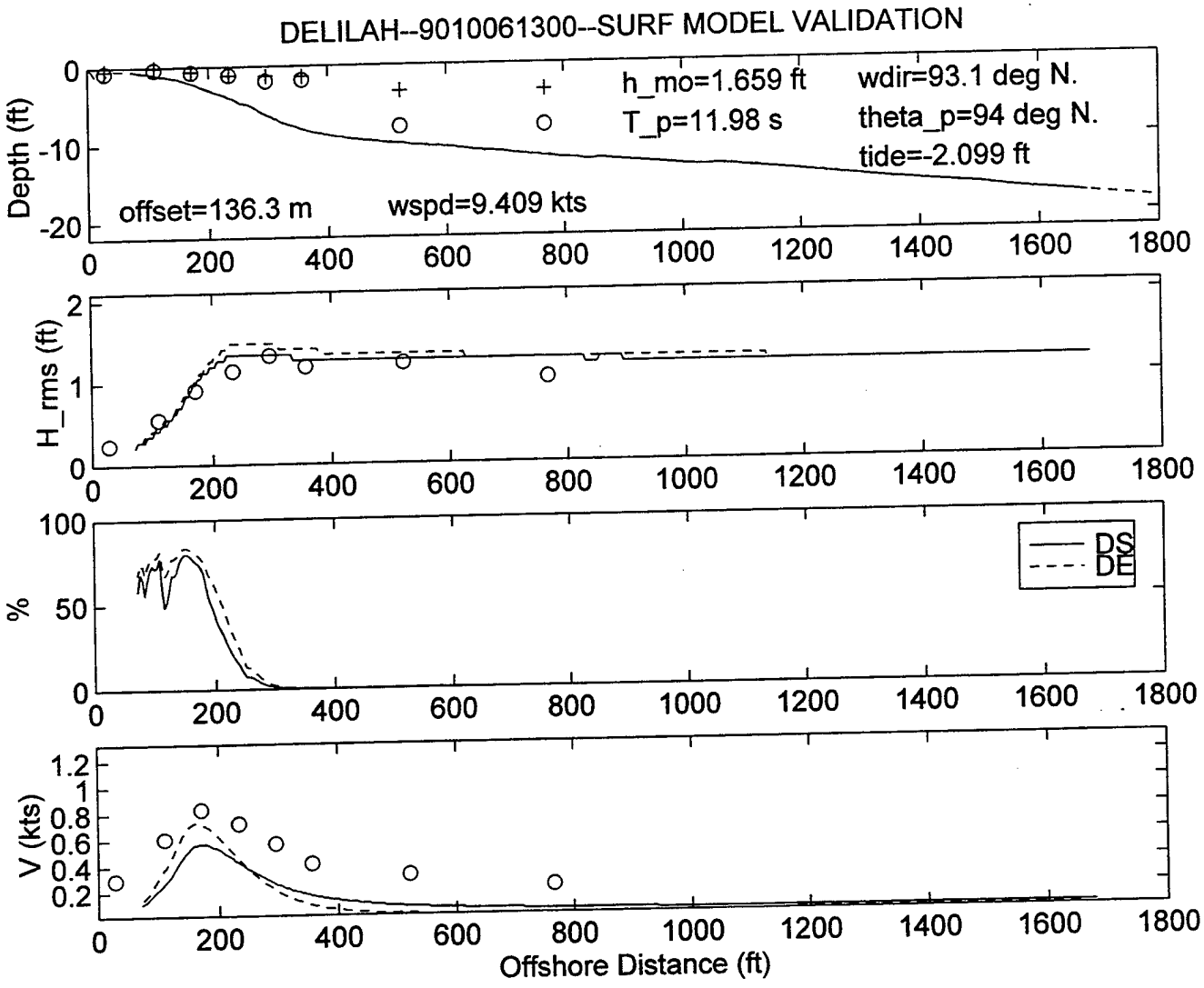
DELILAH--9010061300--SURF MODEL VALIDATION
Depth (ft)
h_mo=1.659 ft
T_p=11.98 s
wdir=93.1 deg N.
theta_p=94 deg N.
tide=-2.099 ft
offset=136.3 m
wspd=9.409 kts
H_rms (ft)
%
DS
DE
V (kts)
Offshore Distance (ft)

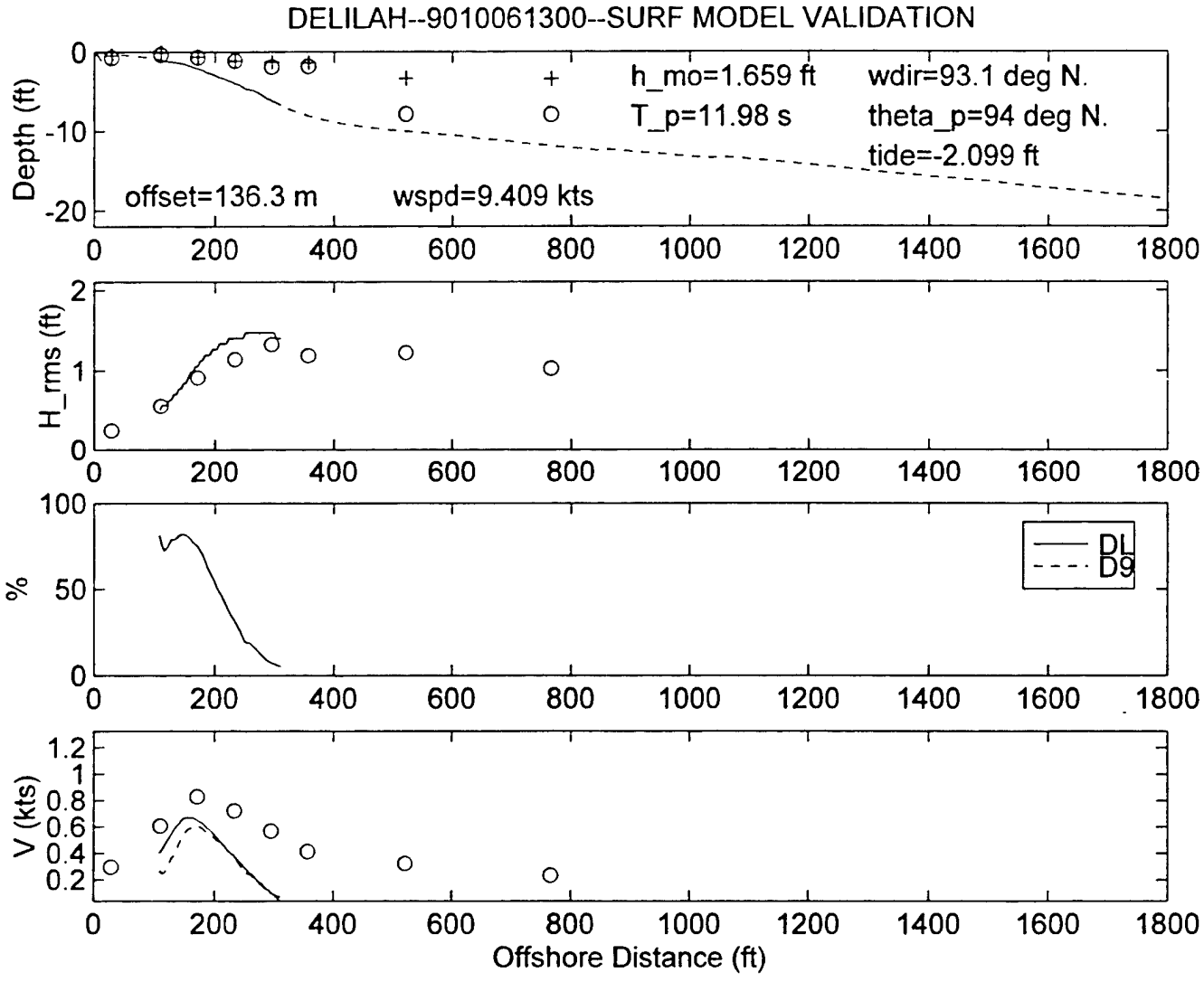
DELILAH--9010061300--SURF MODEL VALIDATION
Depth (ft)
h_mo=1.659 ft
T_p=11.98 s
wdir=93.1 deg N.
theta_p=94 deg N.
tide=-2.099 ft
offset=136.3 m
wspd=9.409 kts
H_rms (ft)
%
DL
D9
V (kts)
Offshore Distance (ft)

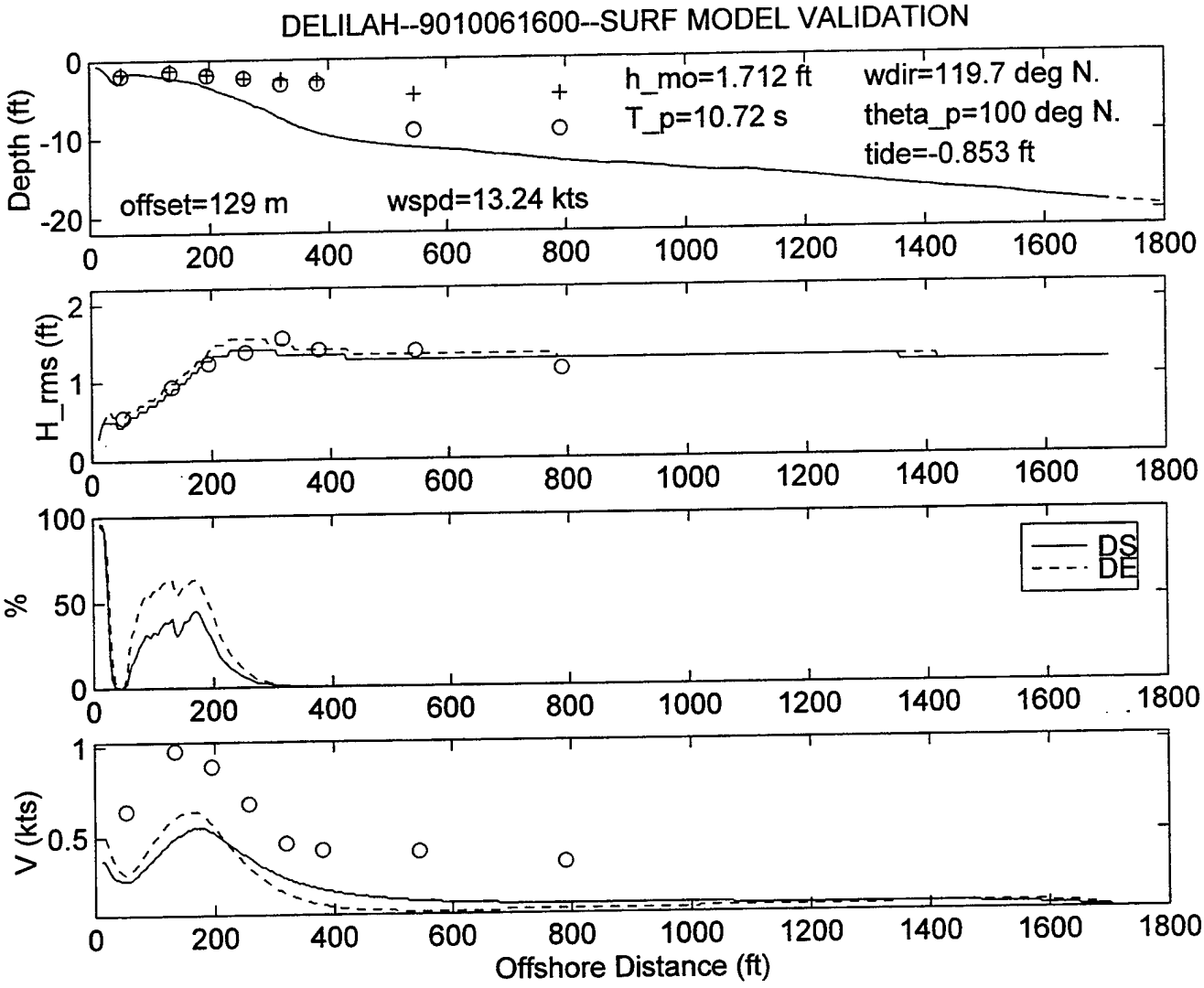
DELILAH--9010061600--SURF MODEL VALIDATION
Depth (ft)
h_mo=1.712 ft
T_p=10.72 s
wdir=119.7 deg N.
theta_p=100 deg N.
tide=-0.853 ft
offset=129 m
wspd=13.24 kts
H_rms (ft)
%
DS
DE
V (kts)
Offshore Distance (ft)

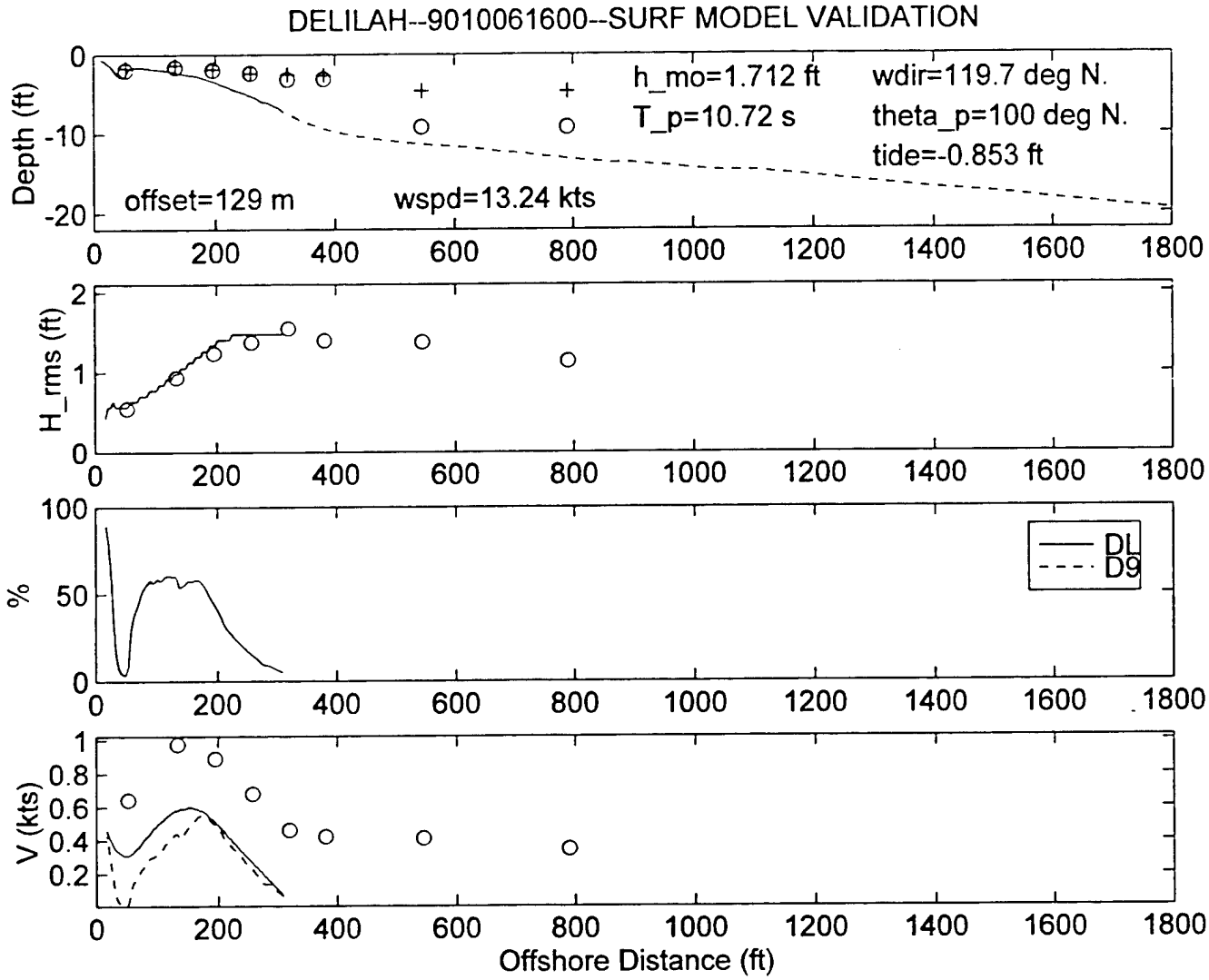
DELILAH--9010061600--SURF MODEL VALIDATION
Depth (ft)
h_mo=1.712 ft
T_p=10.72 s
wdir=119.7 deg N.
theta_p=100 deg N.
tide=-0.853 ft
offset=129 m
wspd=13.24 kts
H_rms (ft)
%
DL
D9
V (kts)
Offshore Distance (ft)

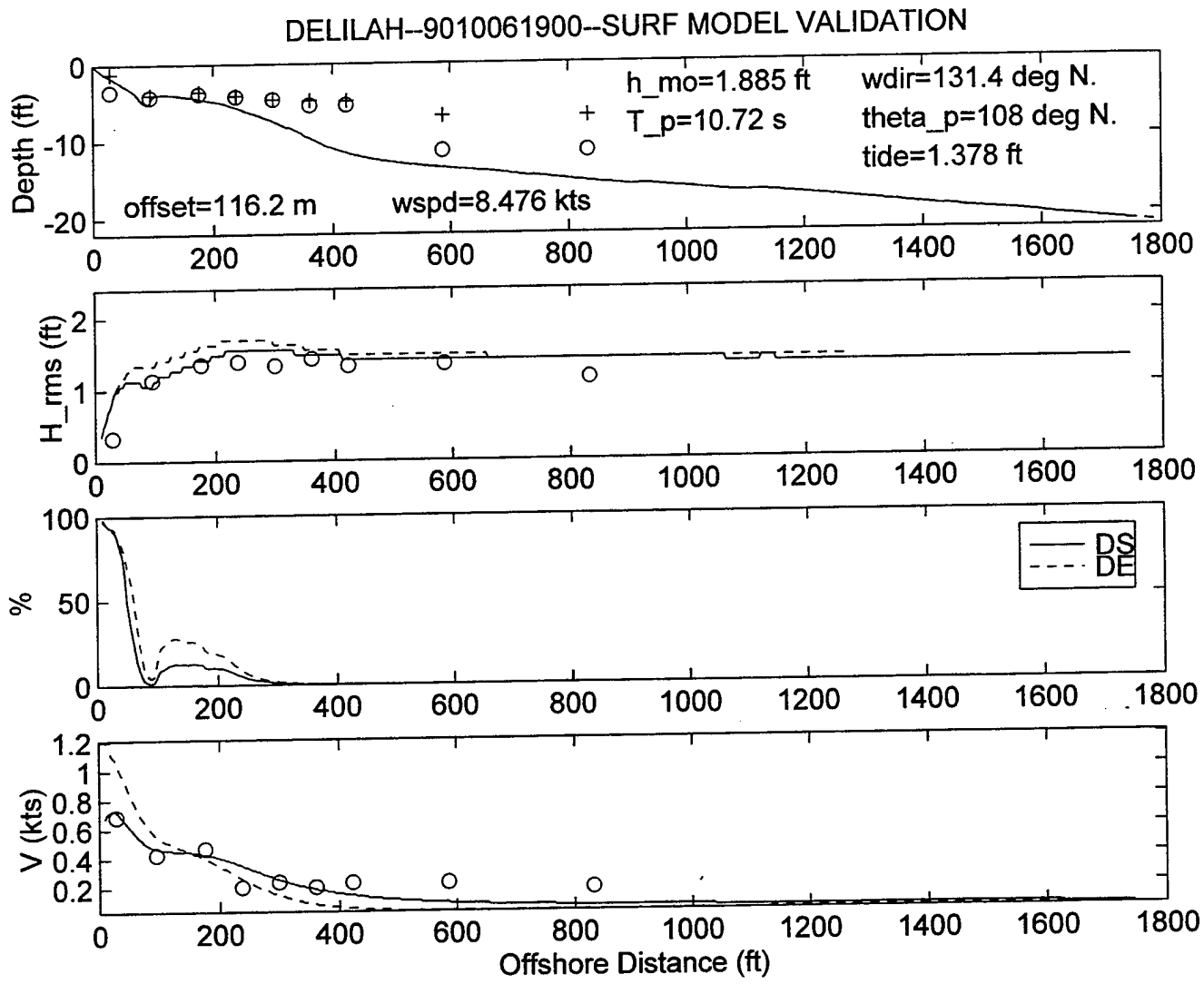
DELILAH--9010061900--SURF MODEL VALIDATION
Depth (ft)
h_mo=1.885 ft
T_p=10.72 s
wdir=131.4 deg N.
theta_p=108 deg N.
tide=1.378 ft
offset=116.2 m
wspd=8.476 kts
H_rms (ft)
%
DS
DE
V (kts)
Offshore Distance (ft)

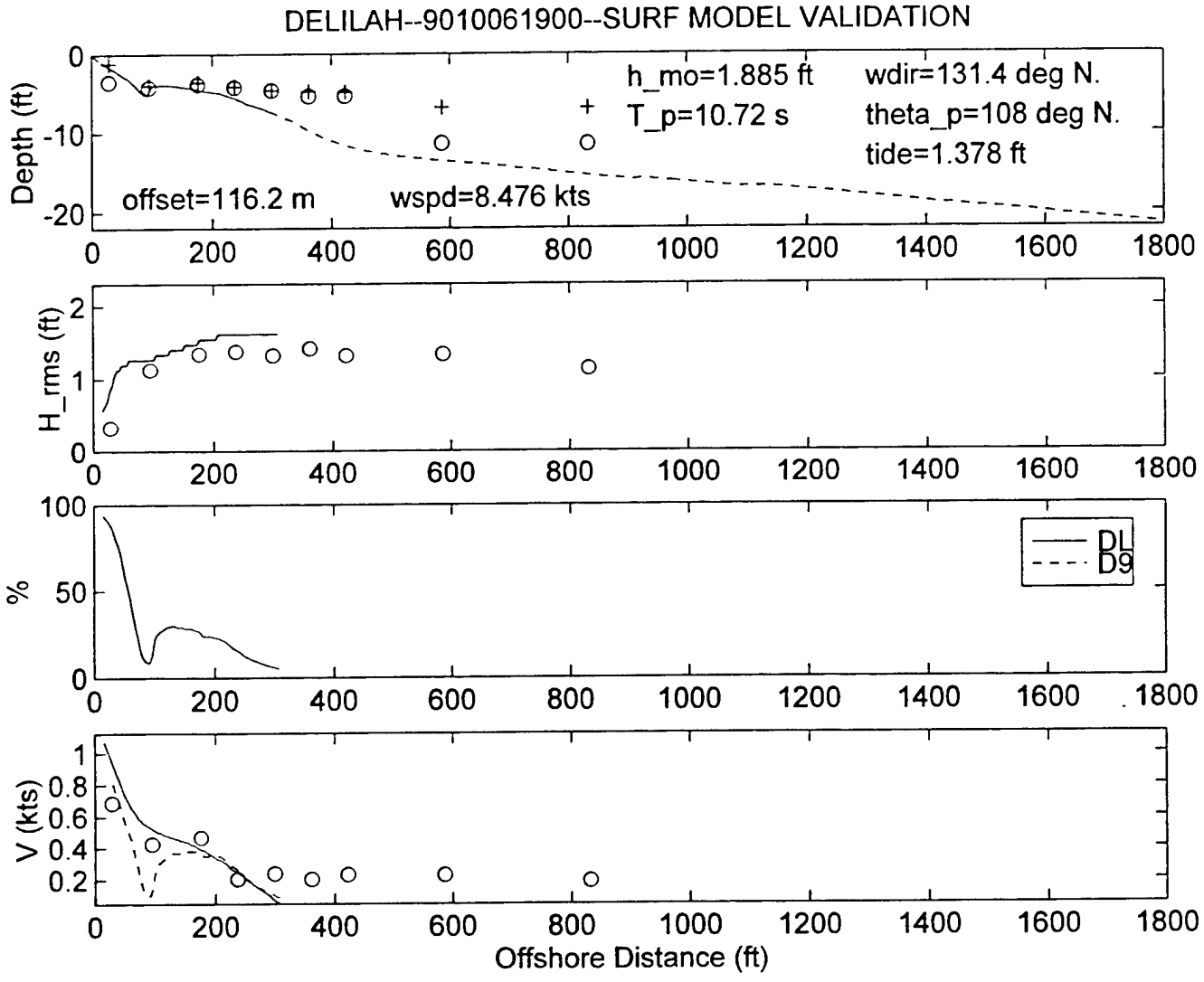
DELILAH--9010061900--SURF MODEL VALIDATION
Depth (ft)
h_mo=1.885 ft
T_p=10.72 s
wdir=131.4 deg N.
theta_p=108 deg N.
tide=1.378 ft
offset=116.2 m
wspd=8.476 kts
H_rms (ft)
%
DL
D9
V (kts)
Offshore Distance (ft)

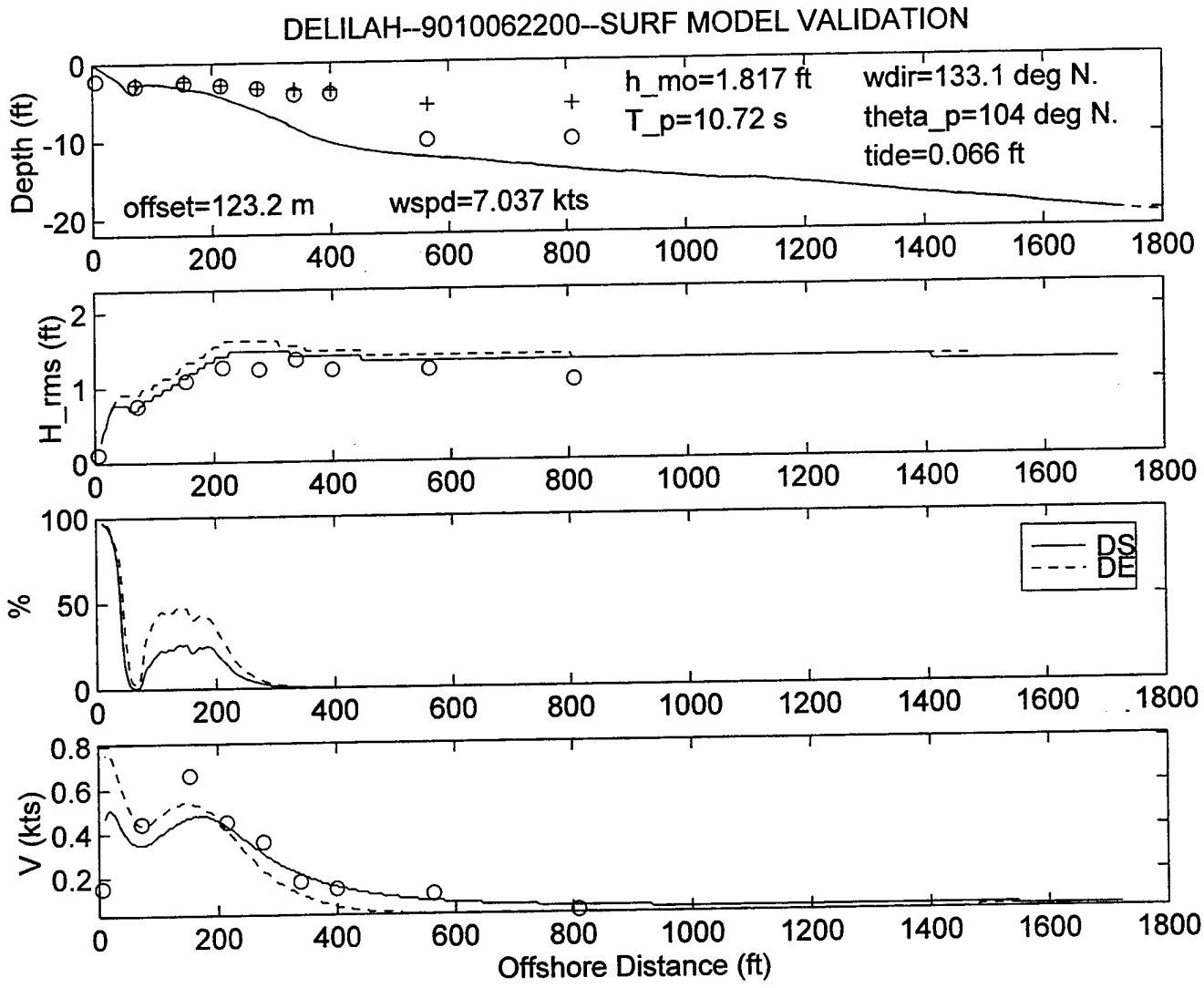
DELILAH--9010062200--SURF MODEL VALIDATION
Depth (ft)
h_mo=1.817 ft
T_p=10.72 s
wdir=133.1 deg N.
theta_p=104 deg N.
tide=0.066 ft
offset=123.2 m
wspd=7.037 kts
H_rms (ft)
%
DS
DE
V (kts)
Offshore Distance (ft)

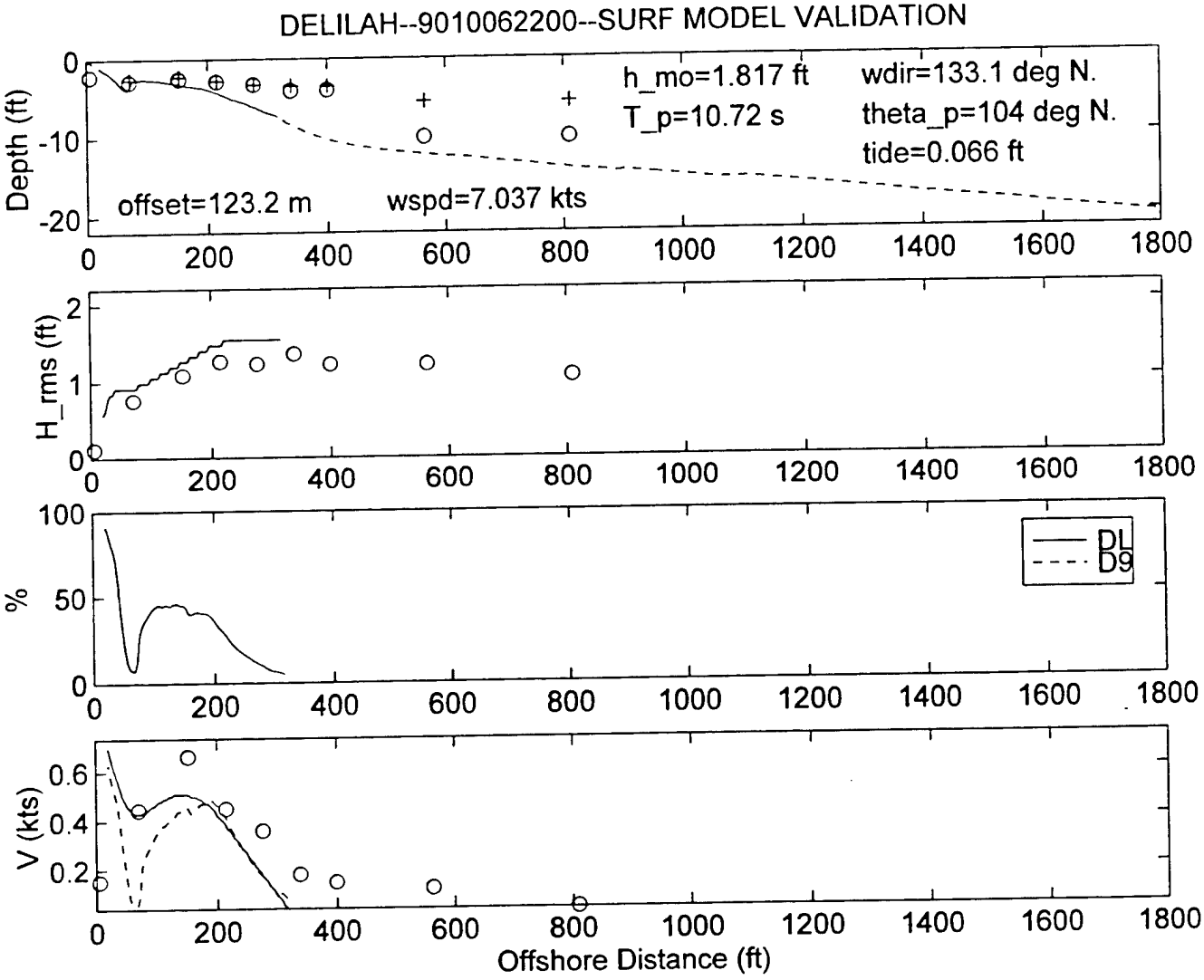
DELILAH--9010062200--SURF MODEL VALIDATION
Depth (ft)
h_mo=1.817 ft
T_p=10.72 s
wdir=133.1 deg N.
theta_p=104 deg N.
tide=0.066 ft
offset=123.2 m
wspd=7.037 kts
H_rms (ft)
%
DL
D9
V (kts)
Offshore Distance (ft)

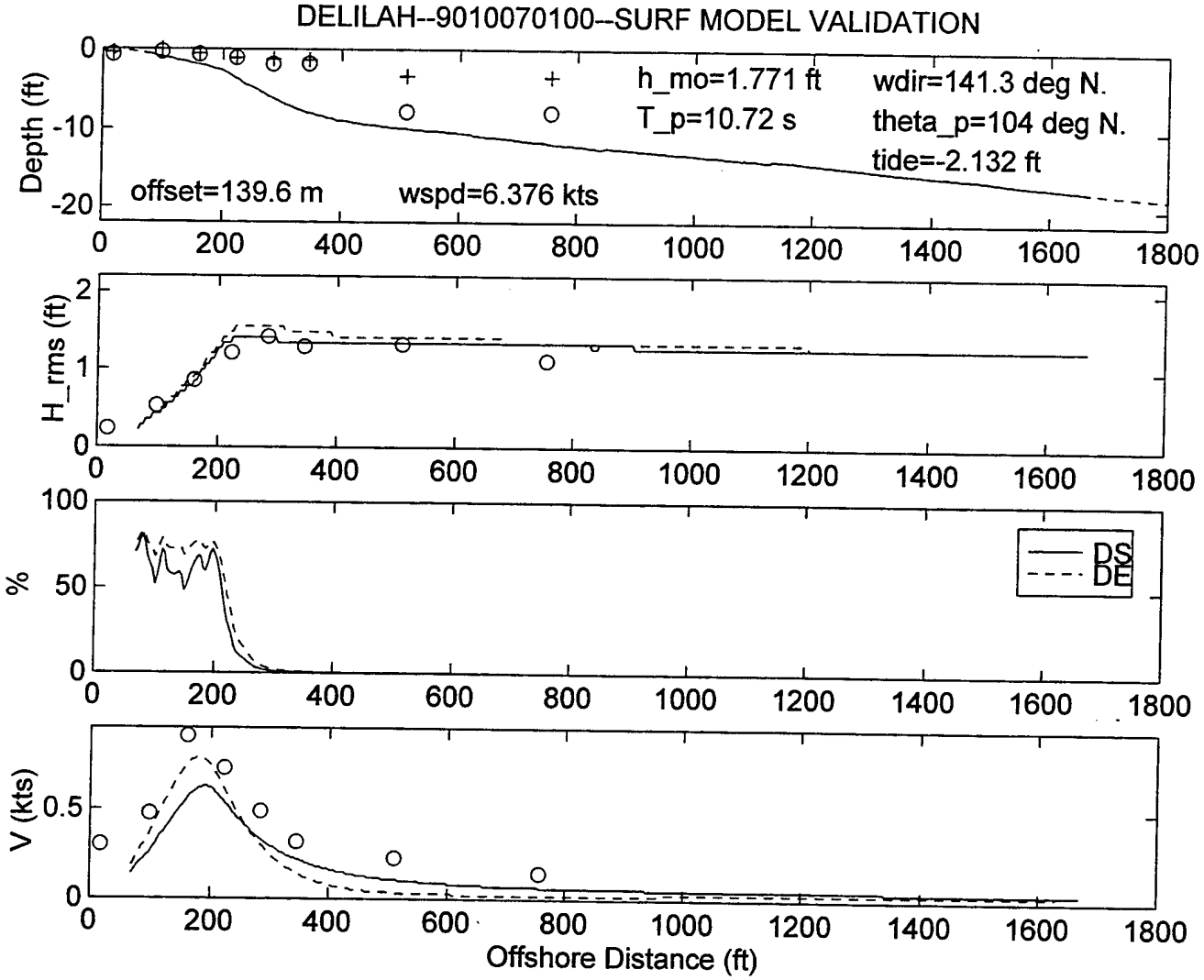
DELILAH--9010070100--SURF MODEL VALIDATION
Depth (ft)
h_mo=1.771 ft
T_p=10.72 s
wdir=141.3 deg N.
theta_p=104 deg N.
tide=-2.132 ft
offset=139.6 m
wspd=6.376 kts
H_rms (ft)
%
DS
DE
V (kts)
Offshore Distance (ft)

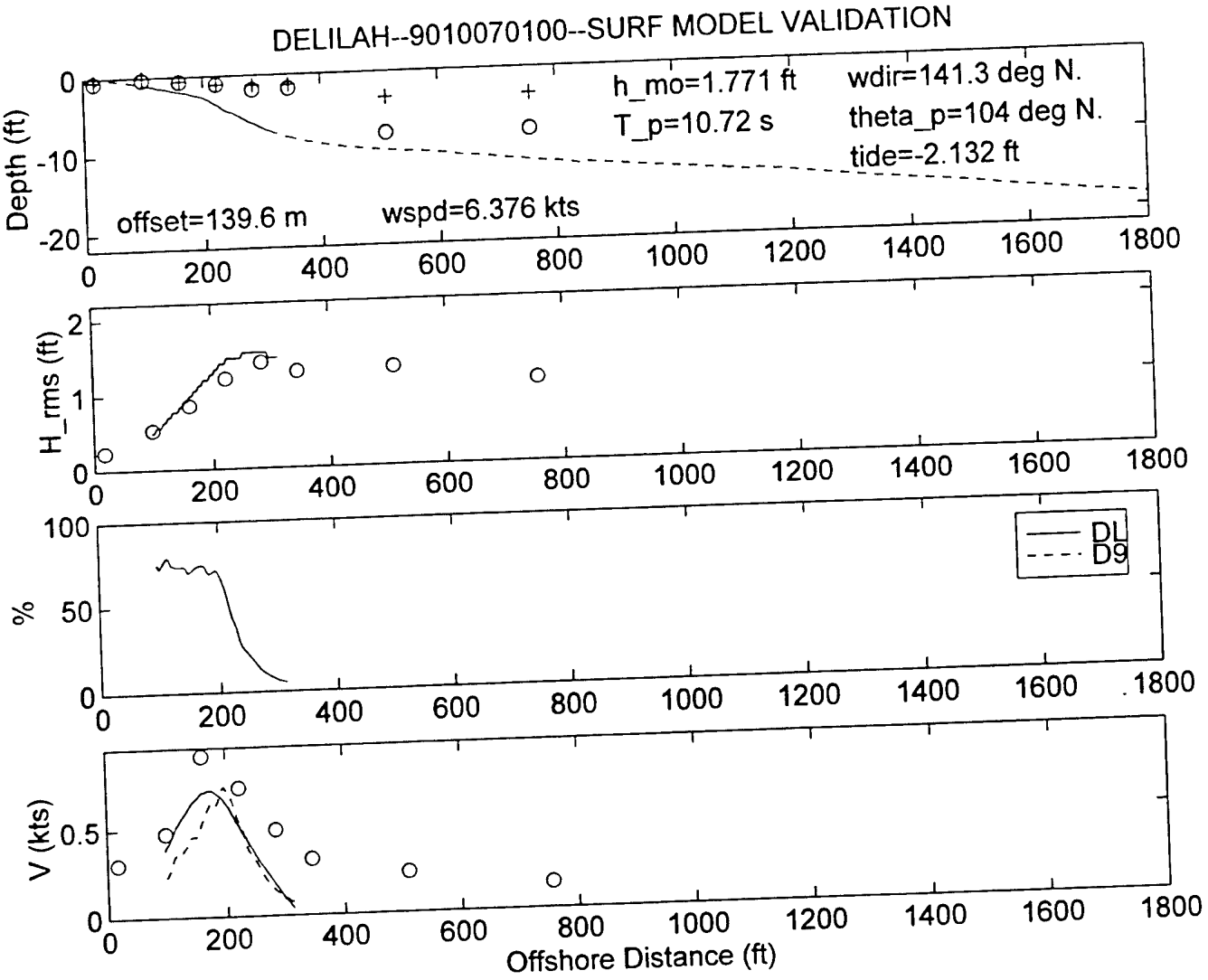
DELILAH--9010070100--SURF MODEL VALIDATION
Depth (ft)
h_mo=1.771 ft
wdir=141.3 deg N.
T_p=10.72 s
theta_p=104 deg N.
tide=-2.132 ft
offset=139.6 m
wspd=6.376 kts
H_rms (ft)
%
DL
D9
V (kts)
Offshore Distance (ft)

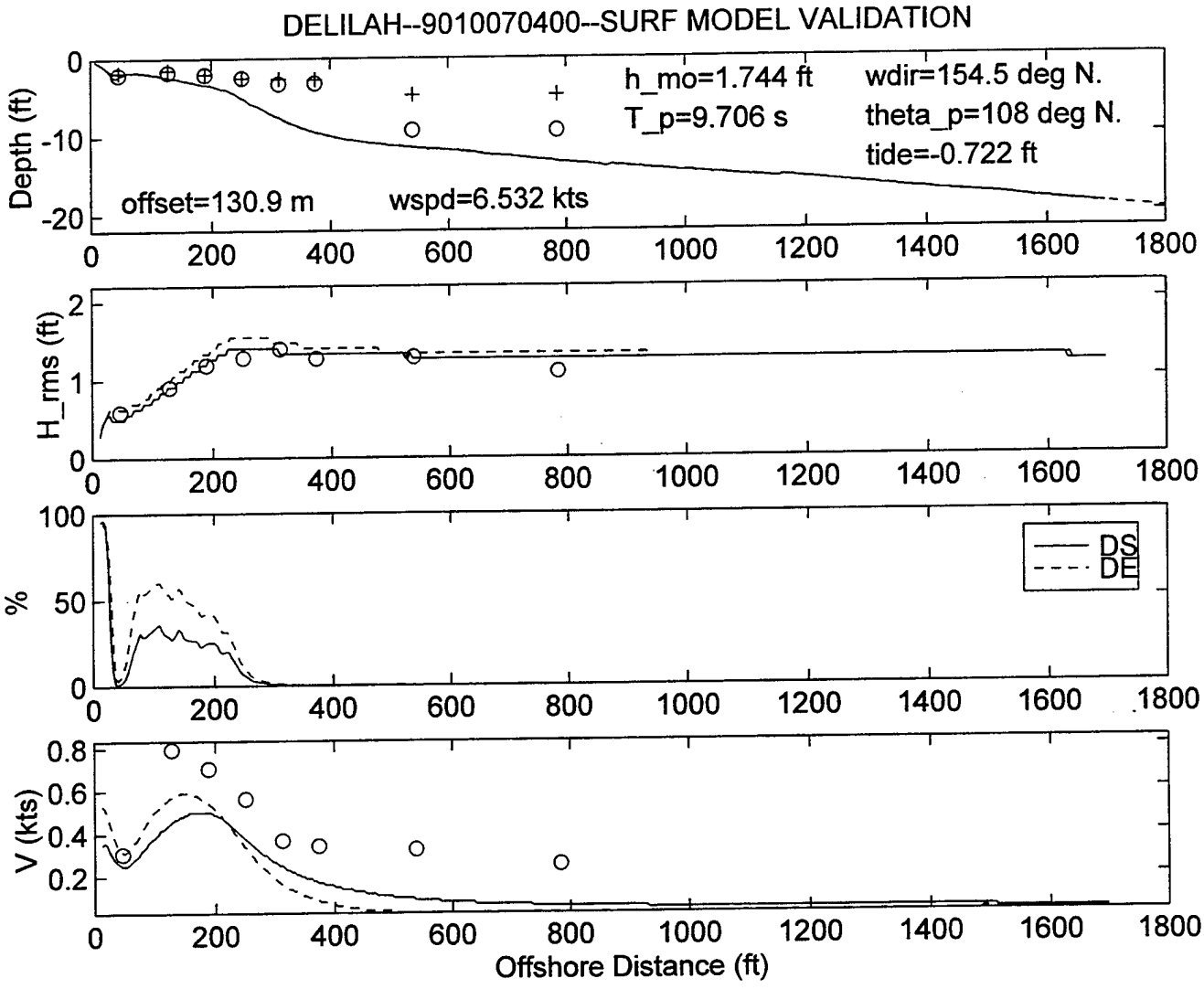
DELILAH--9010070400--SURF MODEL VALIDATION
Depth (ft)
h_mo=1.744 ft
T_p=9.706 s
wdir=154.5 deg N.
theta_p=108 deg N.
tide=-0.722 ft
offset=130.9 m
wspd=6.532 kts
H_rms (ft)
%
DS
DE
V (kts)
Offshore Distance (ft)

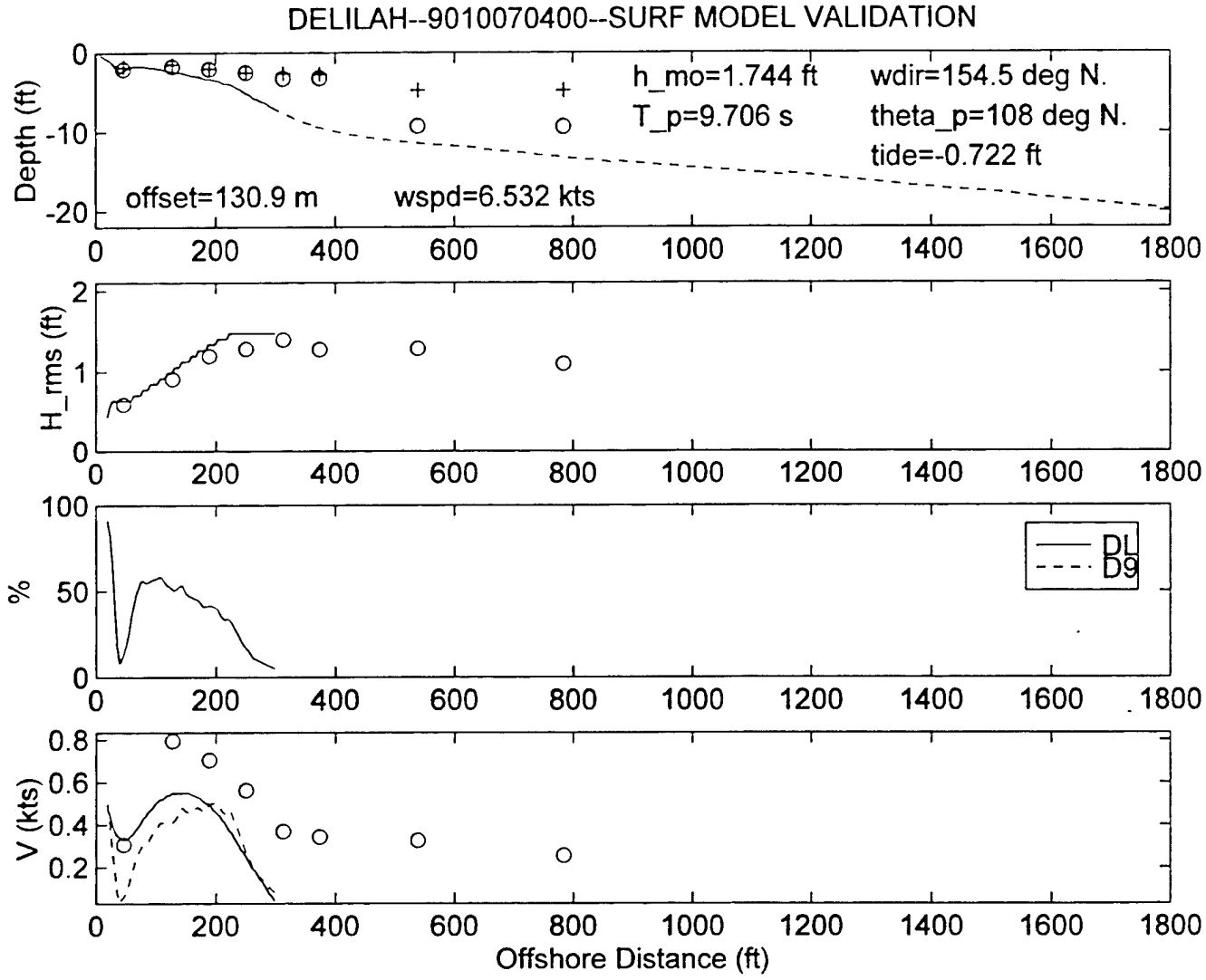
DELILAH--9010070400--SURF MODEL VALIDATION
Depth (ft)
h_mo=1.744 ft
T_p=9.706 s
wdir=154.5 deg N.
theta_p=108 deg N.
tide=-0.722 ft
offset=130.9 m
wspd=6.532 kts
H_rms (ft)
%
DL
D9
V (kts)
Offshore Distance (ft)

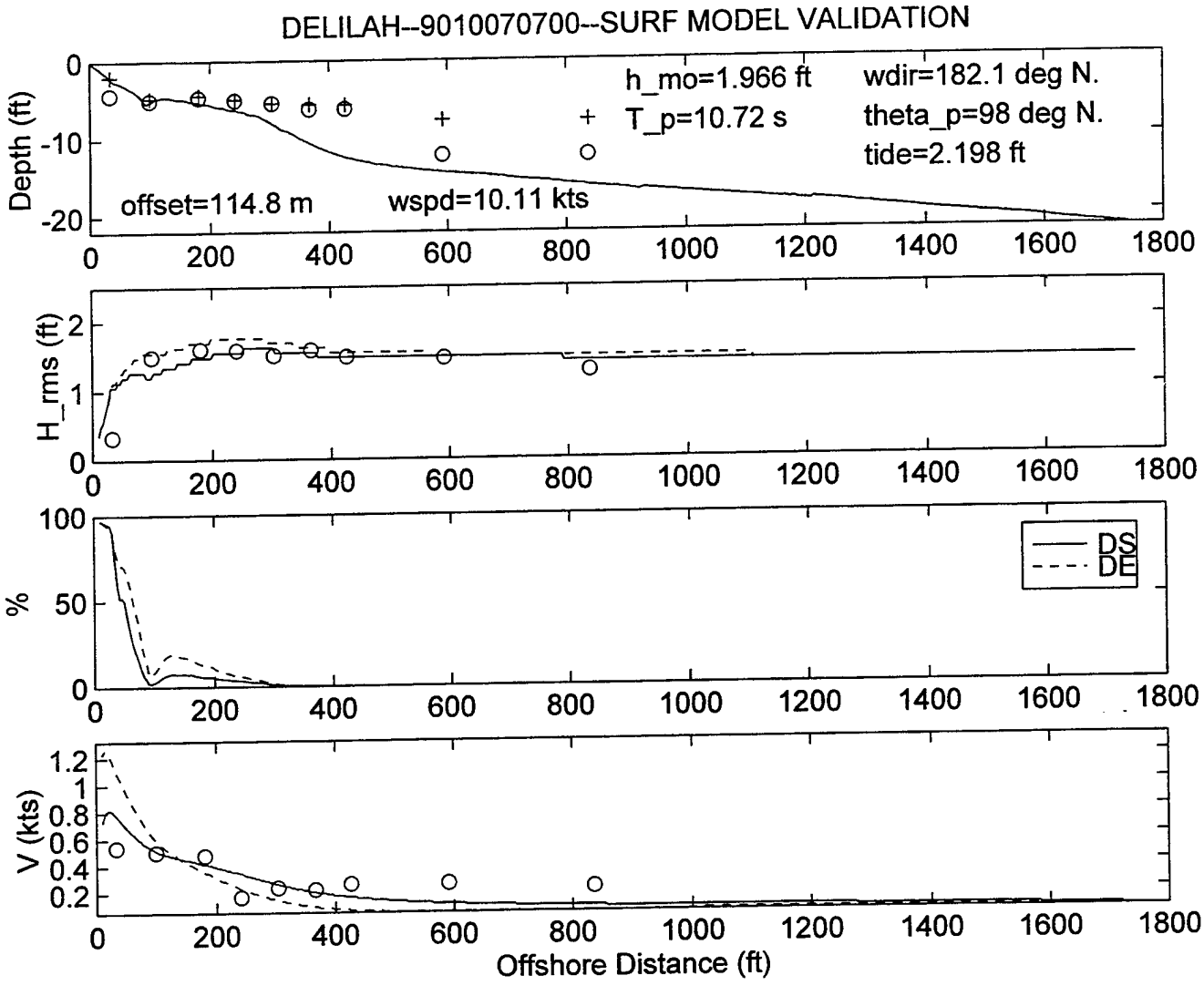
DELILAH--9010070700--SURF MODEL VALIDATION
Depth (ft)
h_mo=1.966 ft
T_p=10.72 s
wdir=182.1 deg N.
theta_p=98 deg N.
tide=2.198 ft
offset=114.8 m
wspd=10.11 kts
H_rms (ft)
%
DS
DE
V (kts)
Offshore Distance (ft)

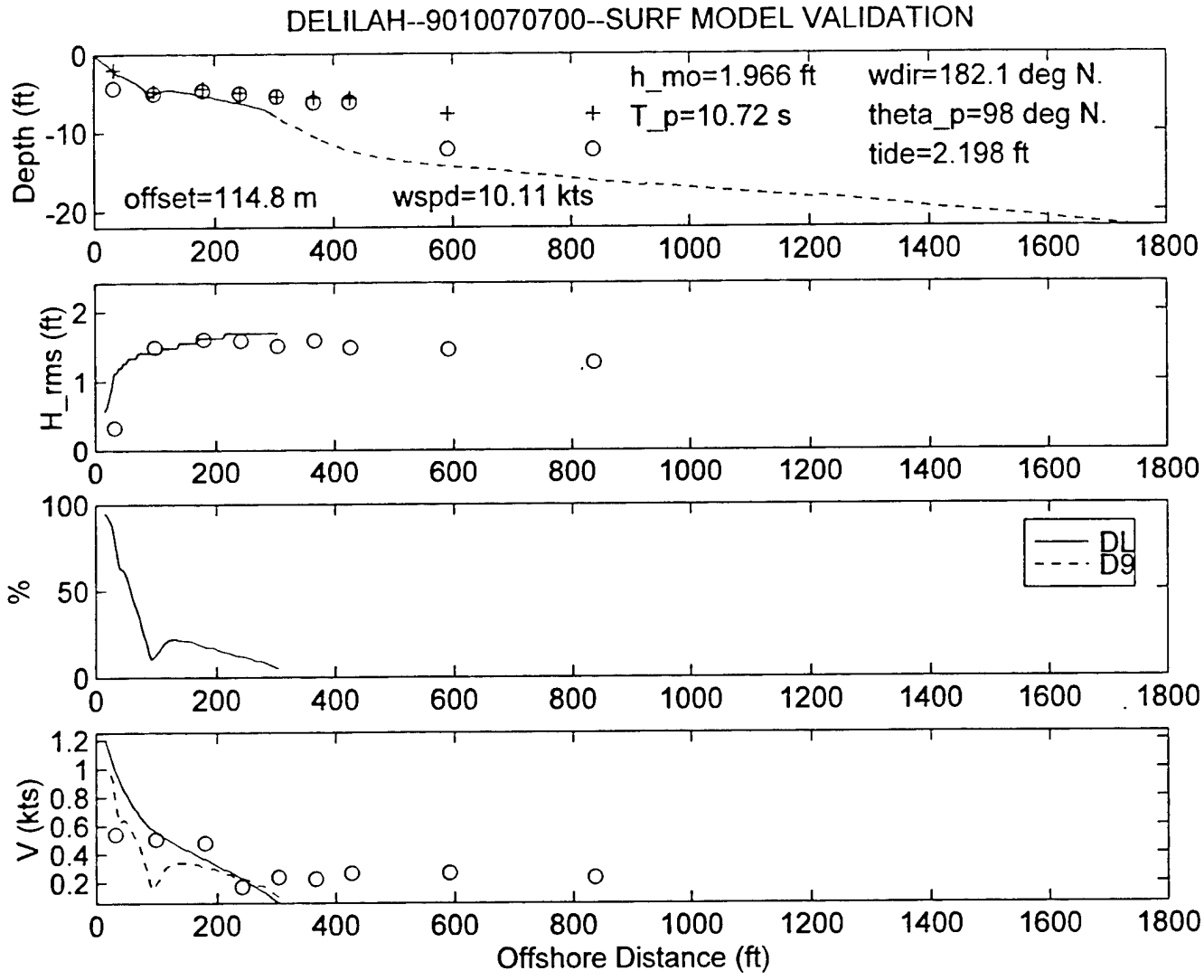
DELILAH--9010070700--SURF MODEL VALIDATION
Depth (ft)
h_mo=1.966 ft
T_p=10.72 s
wdir=182.1 deg N.
theta_p=98 deg N.
tide=2.198 ft
offset=114.8 m
wspd=10.11 kts
H_rms (ft)
%
DL
D9
V (kts)
Offshore Distance (ft)

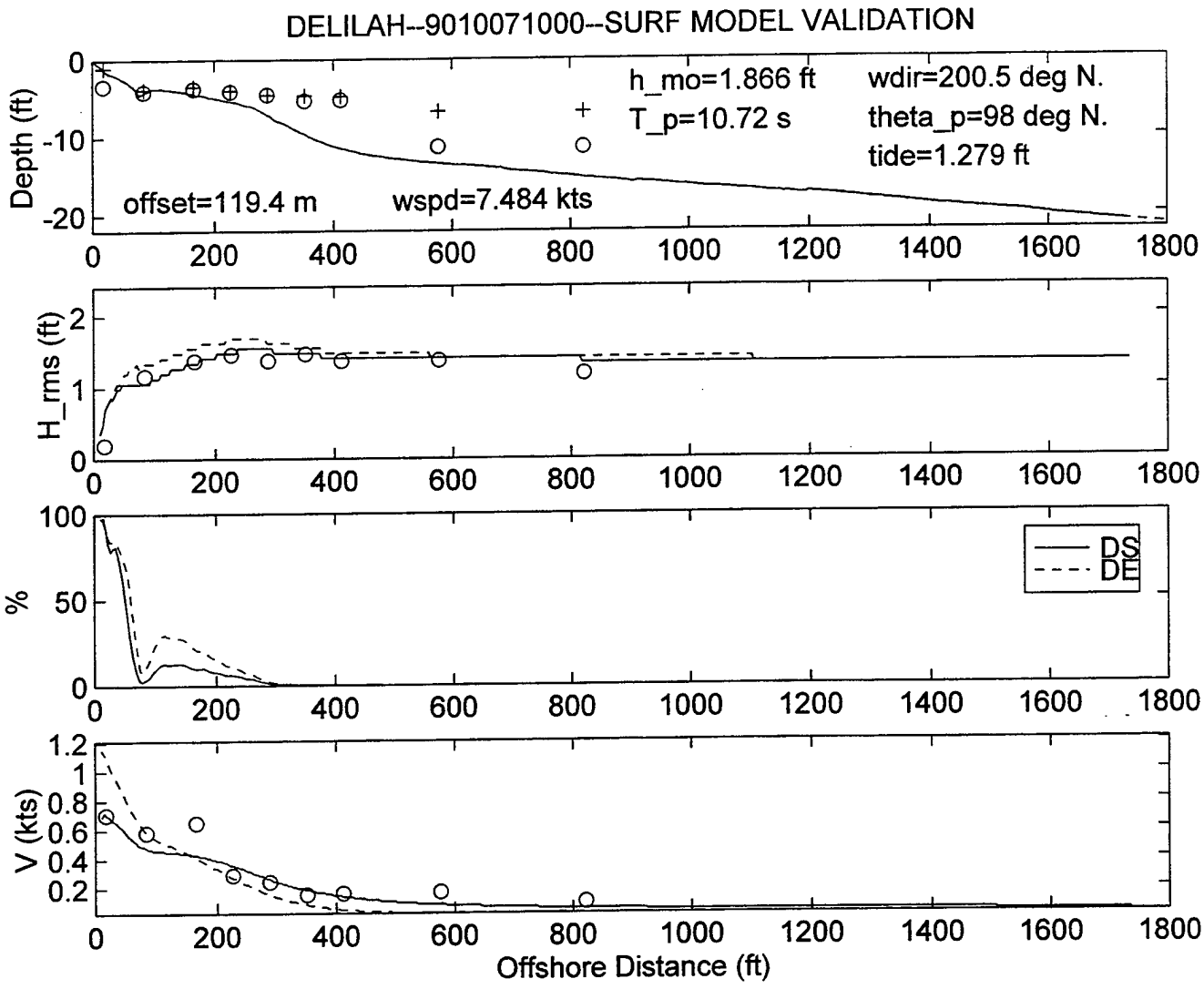
DELILAH--9010071000--SURF MODEL VALIDATION
Depth (ft)
h_mo=1.866 ft
T_p=10.72 s
wdir=200.5 deg N.
theta_p=98 deg N.
tide=1.279 ft
offset=119.4 m
wspd=7.484 kts
H_rms (ft)
%
DS
DE
V (kts)
Offshore Distance (ft)

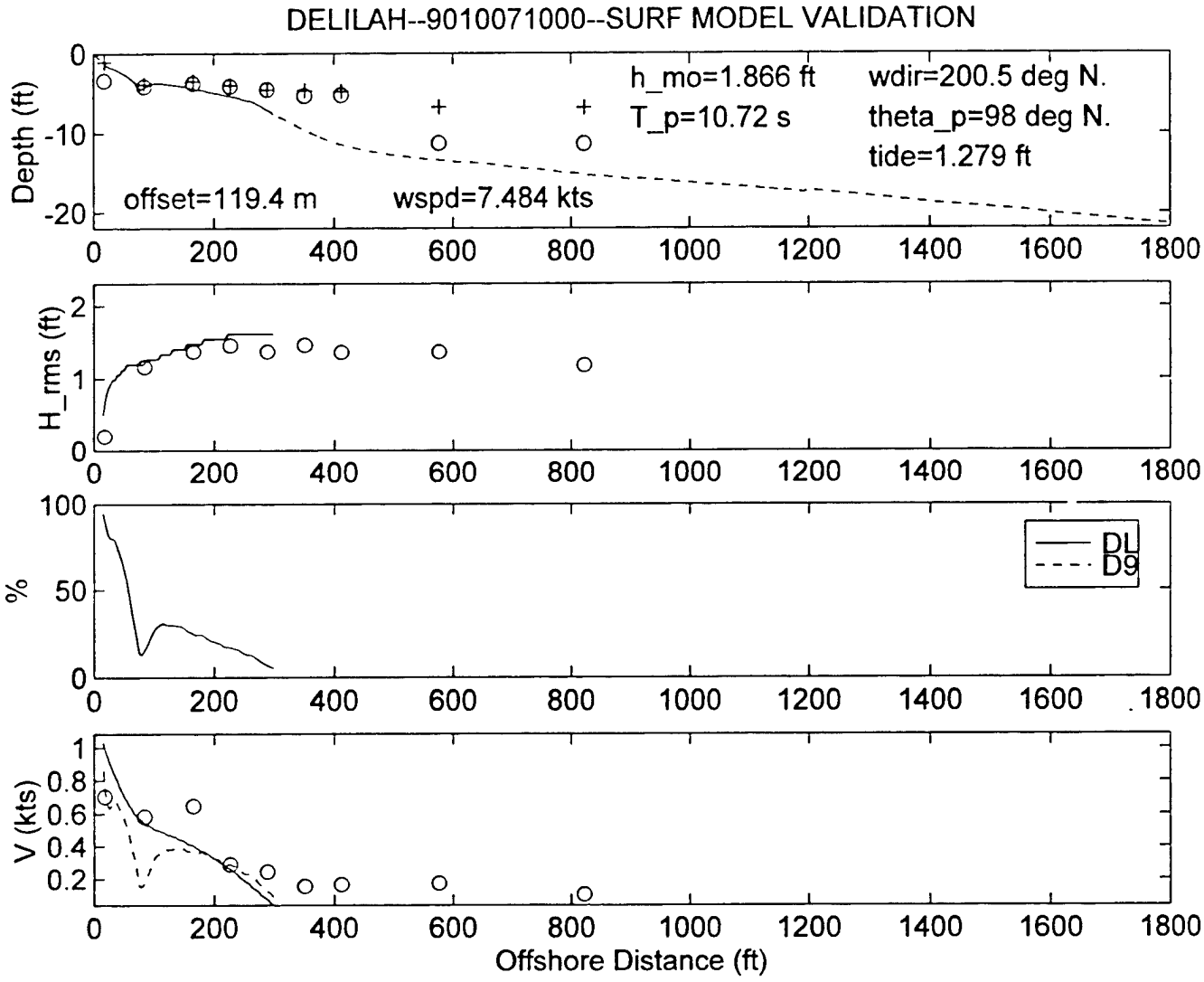
DELILAH--9010071000--SURF MODEL VALIDATION
Depth (ft)
h_mo=1.866 ft
T_p=10.72 s
wdir=200.5 deg N.
theta_p=98 deg N.
tide=1.279 ft
offset=119.4 m
wspd=7.484 kts
H_rms (ft)
%
DL
D9
V (kts)
Offshore Distance (ft)

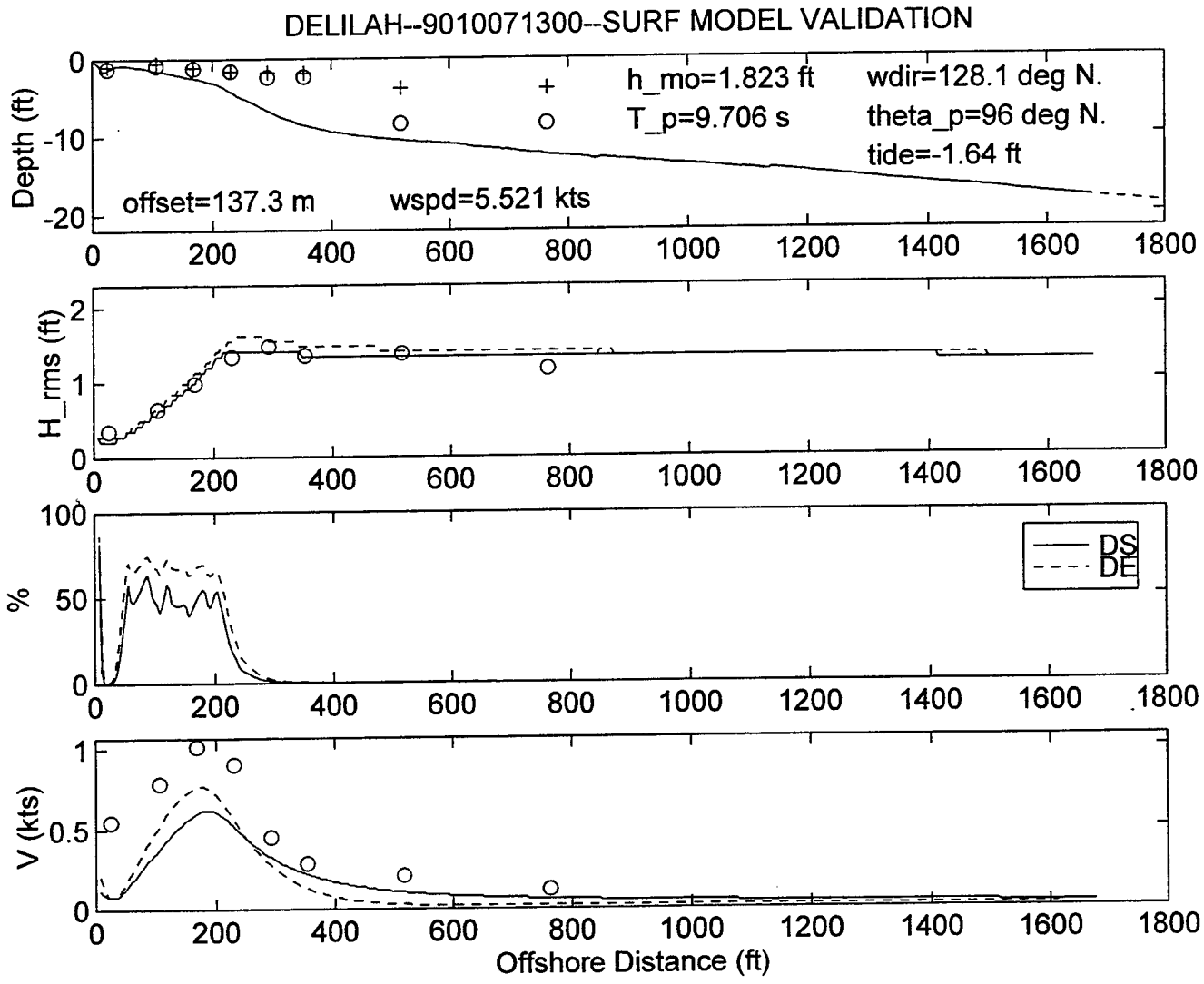
DELILAH--9010071300--SURF MODEL VALIDATION
Depth (ft)
h_mo=1.823 ft
T_p=9.706 s
wdir=128.1 deg N.
theta_p=96 deg N.
tide=-1.64 ft
offset=137.3 m
wspd=5.521 kts
H_rms (ft)
%
DS
DE
V (kts)
Offshore Distance (ft)

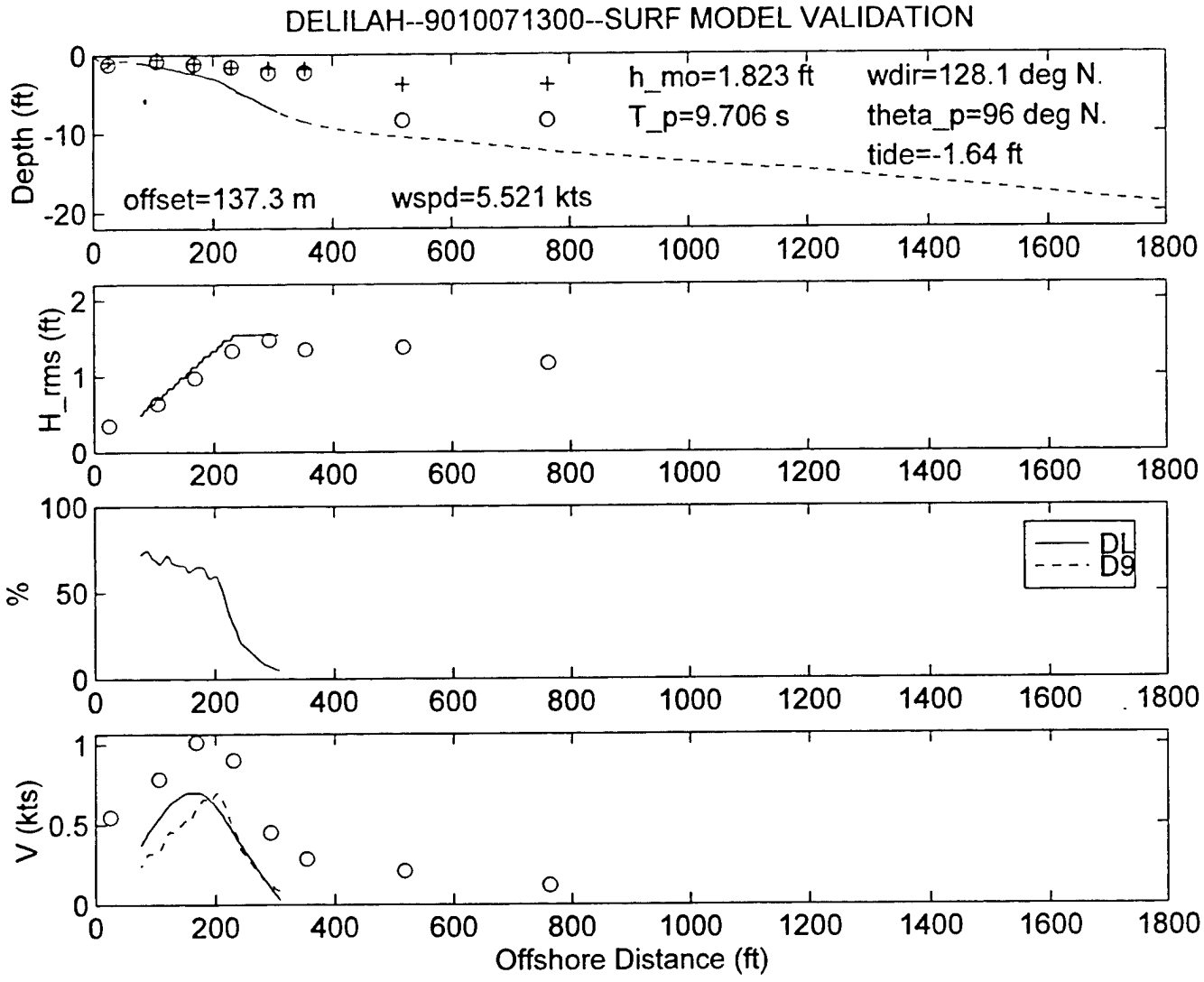
DELILAH--9010071300--SURF MODEL VALIDATION
Depth (ft)
h_mo=1.823 ft
T_p=9.706 s
wdir=128.1 deg N.
theta_p=96 deg N.
tide=-1.64 ft
offset=137.3 m
wspd=5.521 kts
H_rms (ft)
%
DL
D9
V (kts)
Offshore Distance (ft)

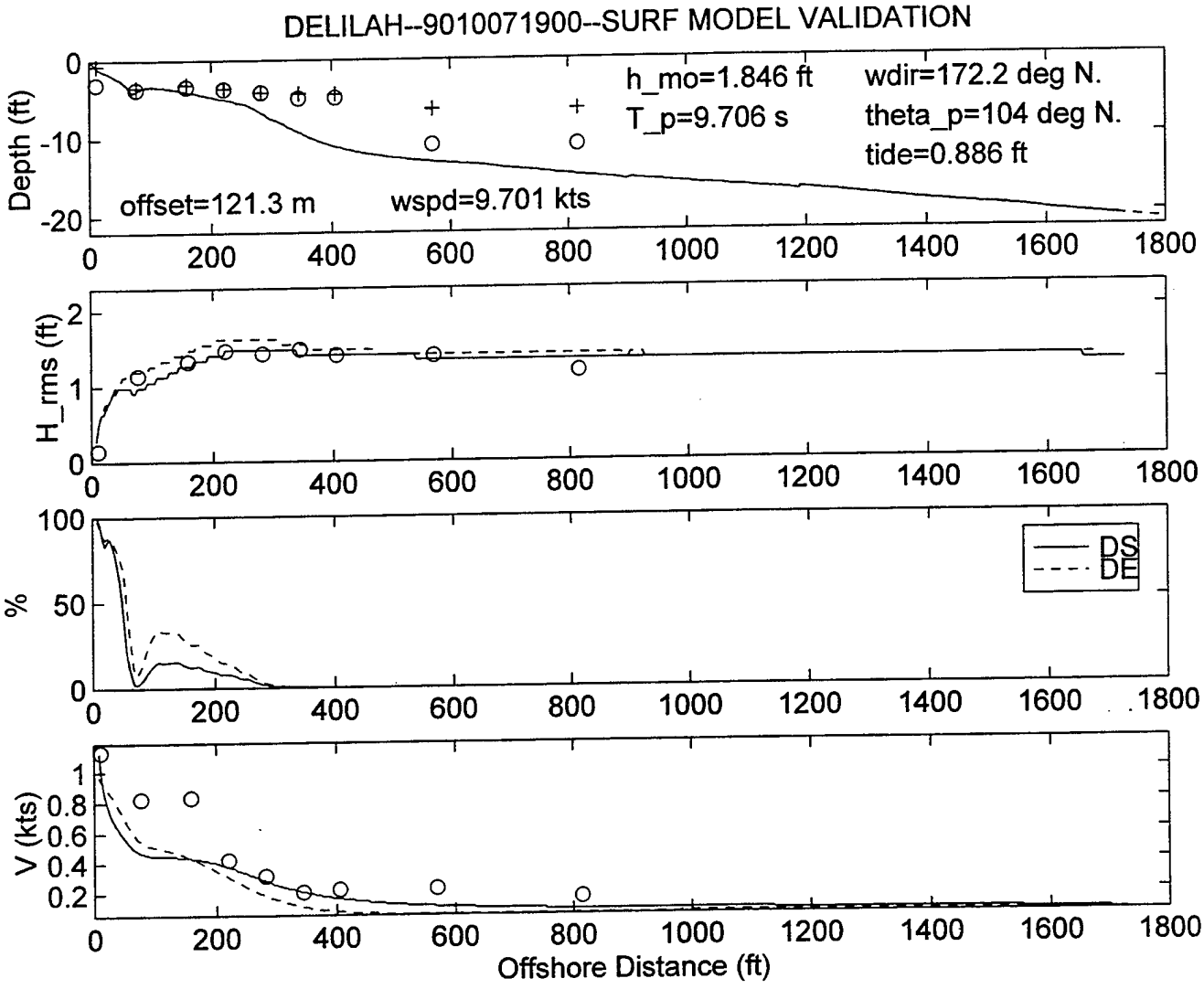
DELILAH--9010071900--SURF MODEL VALIDATION
Depth (ft)
h_mo=1.846 ft
T_p=9.706 s
wdir=172.2 deg N.
theta_p=104 deg N.
tide=0.886 ft
offset=121.3 m
wspd=9.701 kts
H_rms (ft)
%
DS
DE
V (kts)
Offshore Distance (ft)

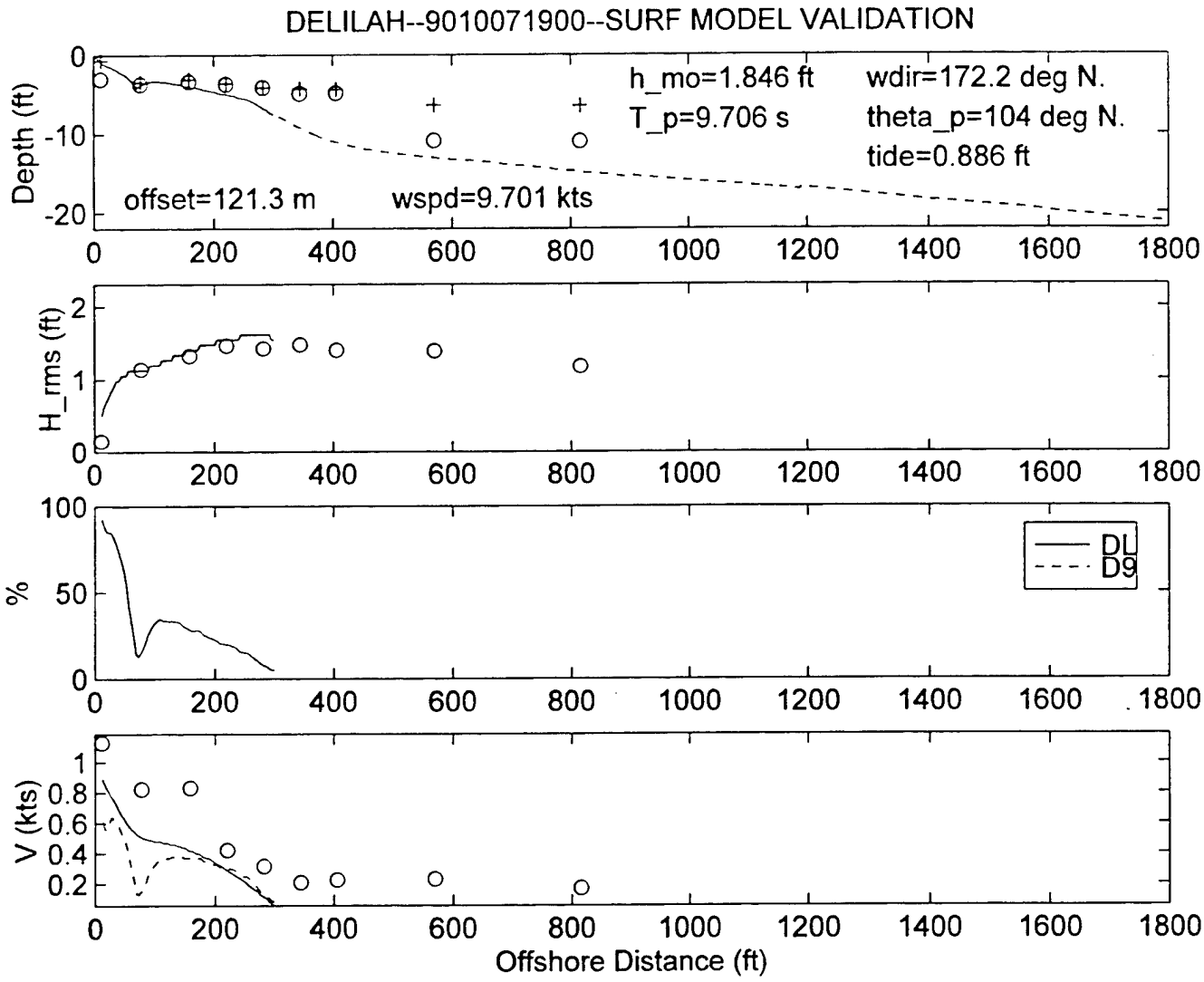
DELILAH--9010071900--SURF MODEL VALIDATION
Depth (ft)
h_mo=1.846 ft
T_p=9.706 s
wdir=172.2 deg N.
theta_p=104 deg N.
tide=0.886 ft
offset=121.3 m
wspd=9.701 kts
H_rms (ft)
%
DL
D9
V (kts)
Offshore Distance (ft)

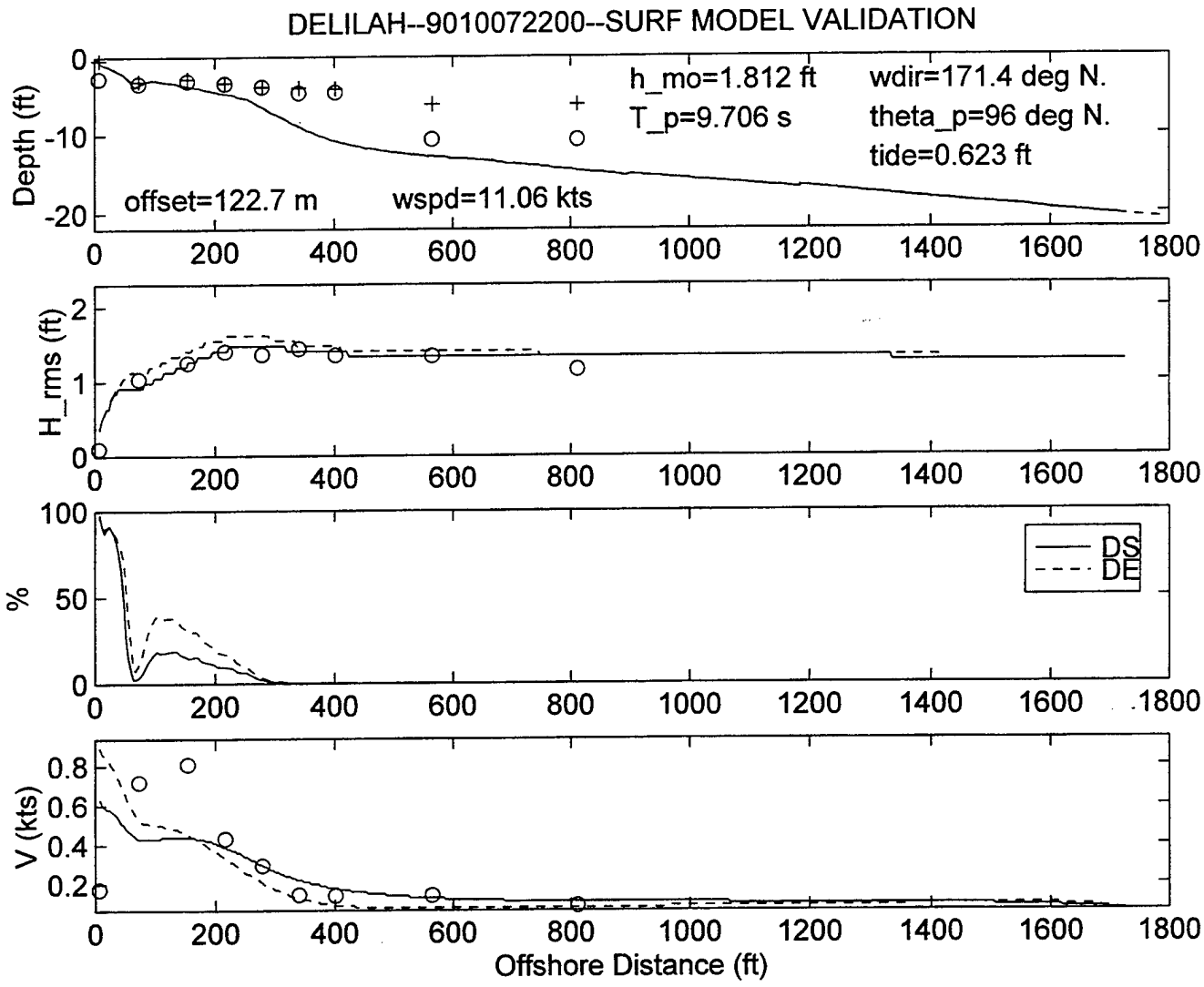
DELILAH--9010072200--SURF MODEL VALIDATION
Depth (ft)
h_mo=1.812 ft
T_p=9.706 s
wdir=171.4 deg N.
theta_p=96 deg N.
tide=0.623 ft
offset=122.7 m
wspd=11.06 kts
H_rms (ft)
%
DS
DE
V (kts)
Offshore Distance (ft)

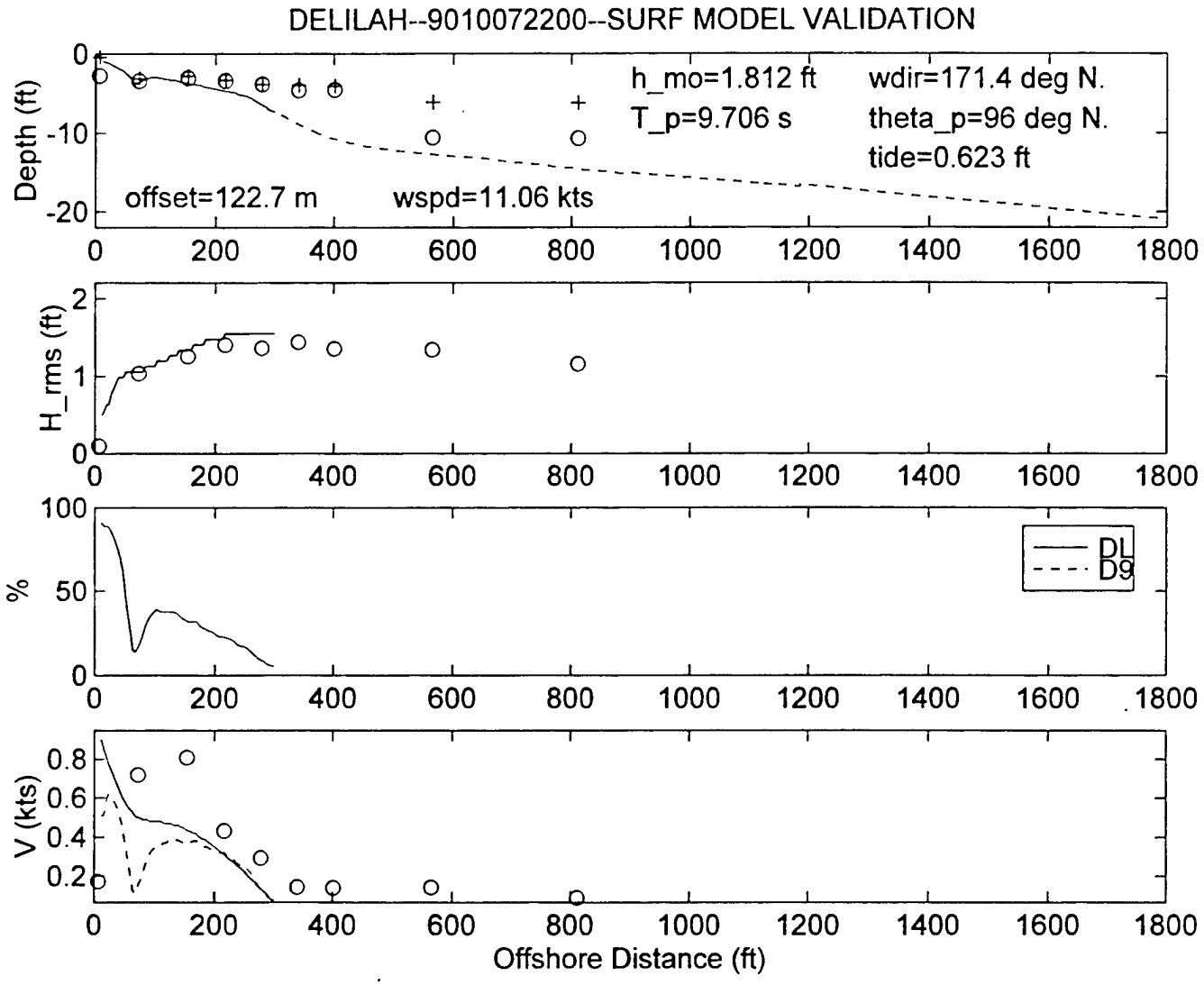
DELILAH--9010072200--SURF MODEL VALIDATION
Depth (ft)
h_mo=1.812 ft
T_p=9.706 s
wdir=171.4 deg N.
theta_p=96 deg N.
tide=0.623 ft
offset=122.7 m
wspd=11.06 kts
H_rms (ft)
%
DL
D9
V (kts)
Offshore Distance (ft)

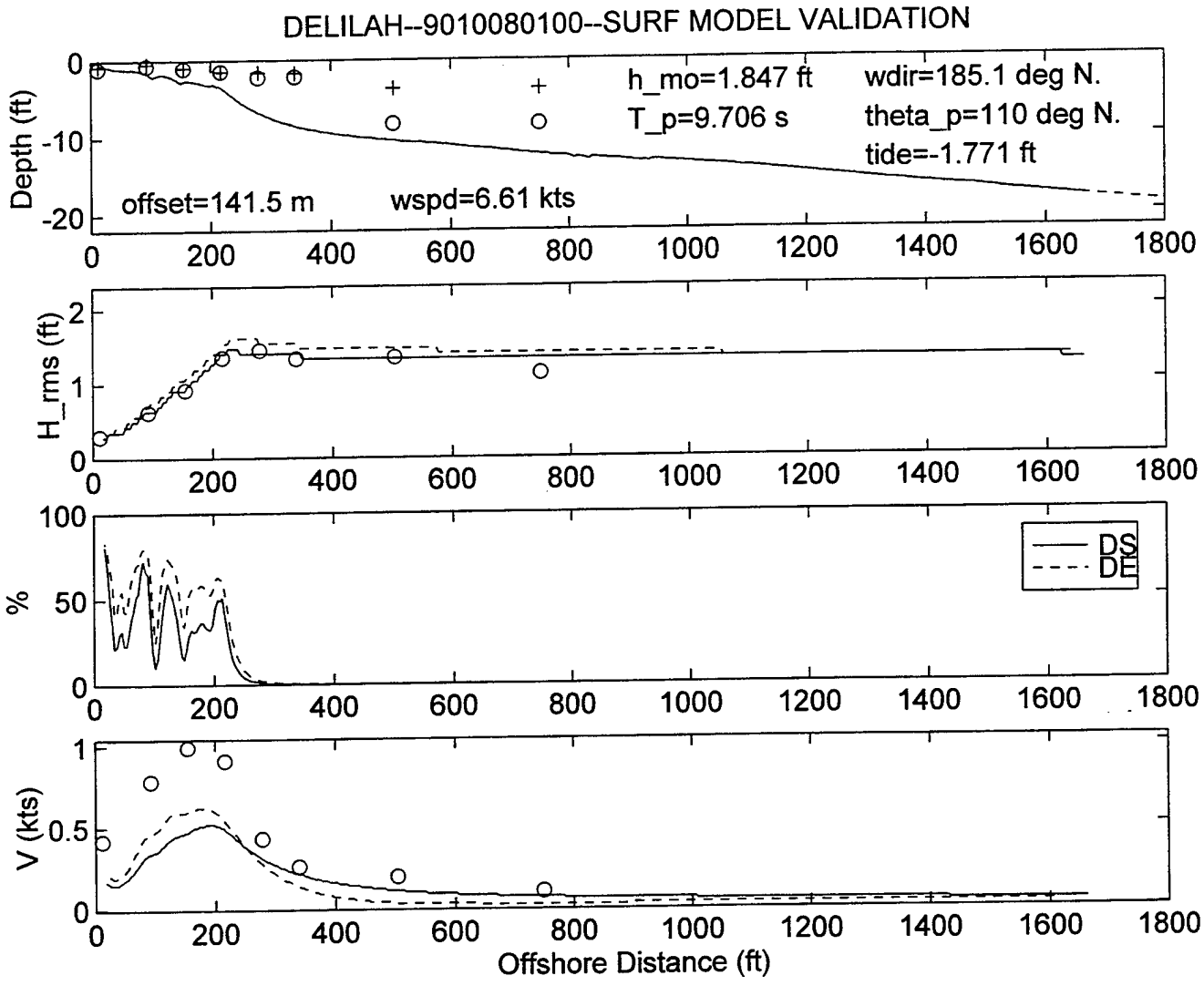
DELILAH--9010080100--SURF MODEL VALIDATION
Depth (ft)
h_mo=1.847 ft
T_p=9.706 s
wdir=185.1 deg N.
theta_p=110 deg N.
tide=-1.771 ft
offset=141.5 m
wspd=6.61 kts
H_rms (ft)
%
DS
DE
V (kts)
Offshore Distance (ft)

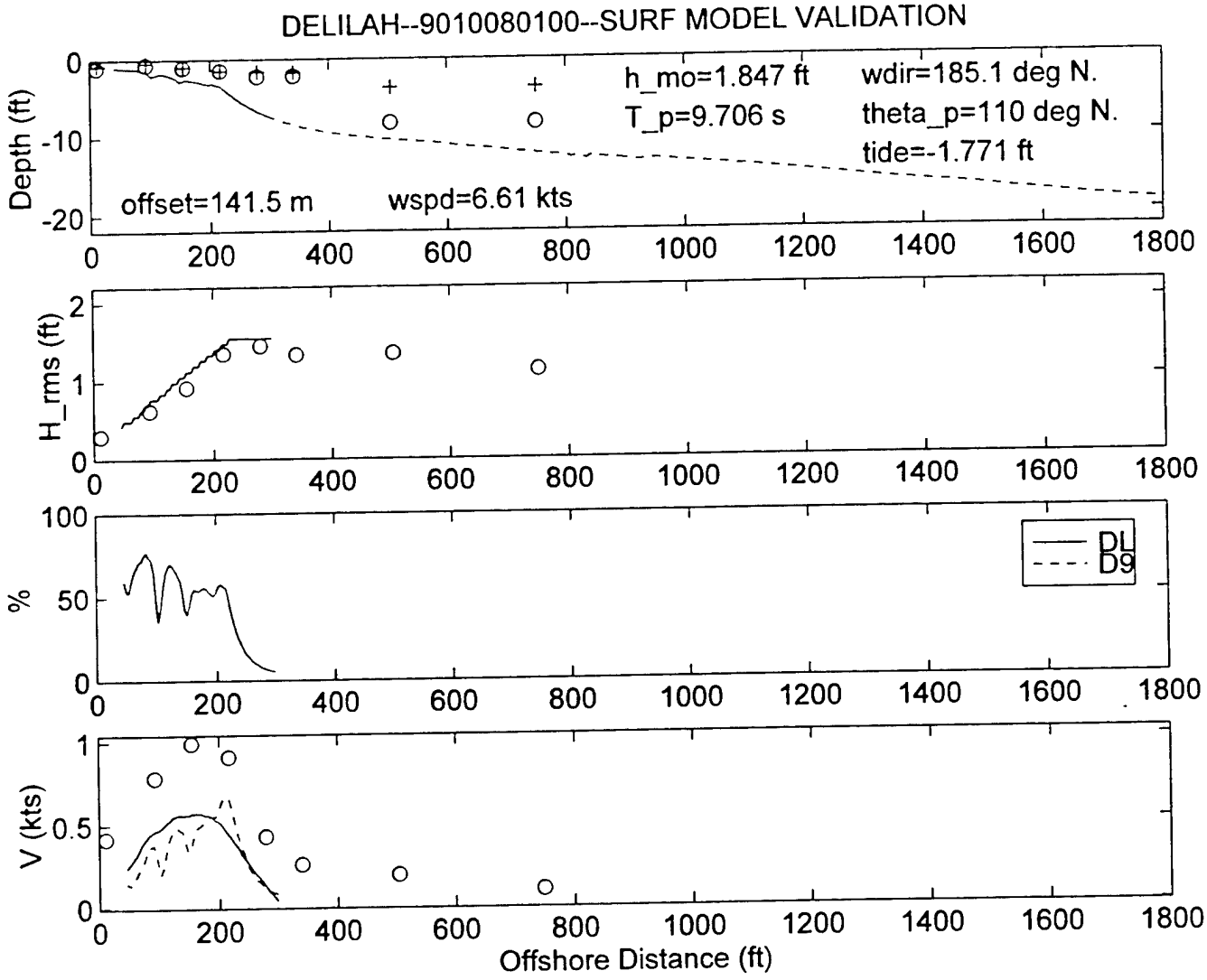
DELILAH--9010080100--SURF MODEL VALIDATION
Depth (ft)
h_mo=1.847 ft
T_p=9.706 s
wdir=185.1 deg N.
theta_p=110 deg N.
tide=-1.771 ft
offset=141.5 m
wspd=6.61 kts
H_rms (ft)
%
D1
D9
V (kts)
Offshore Distance (ft)

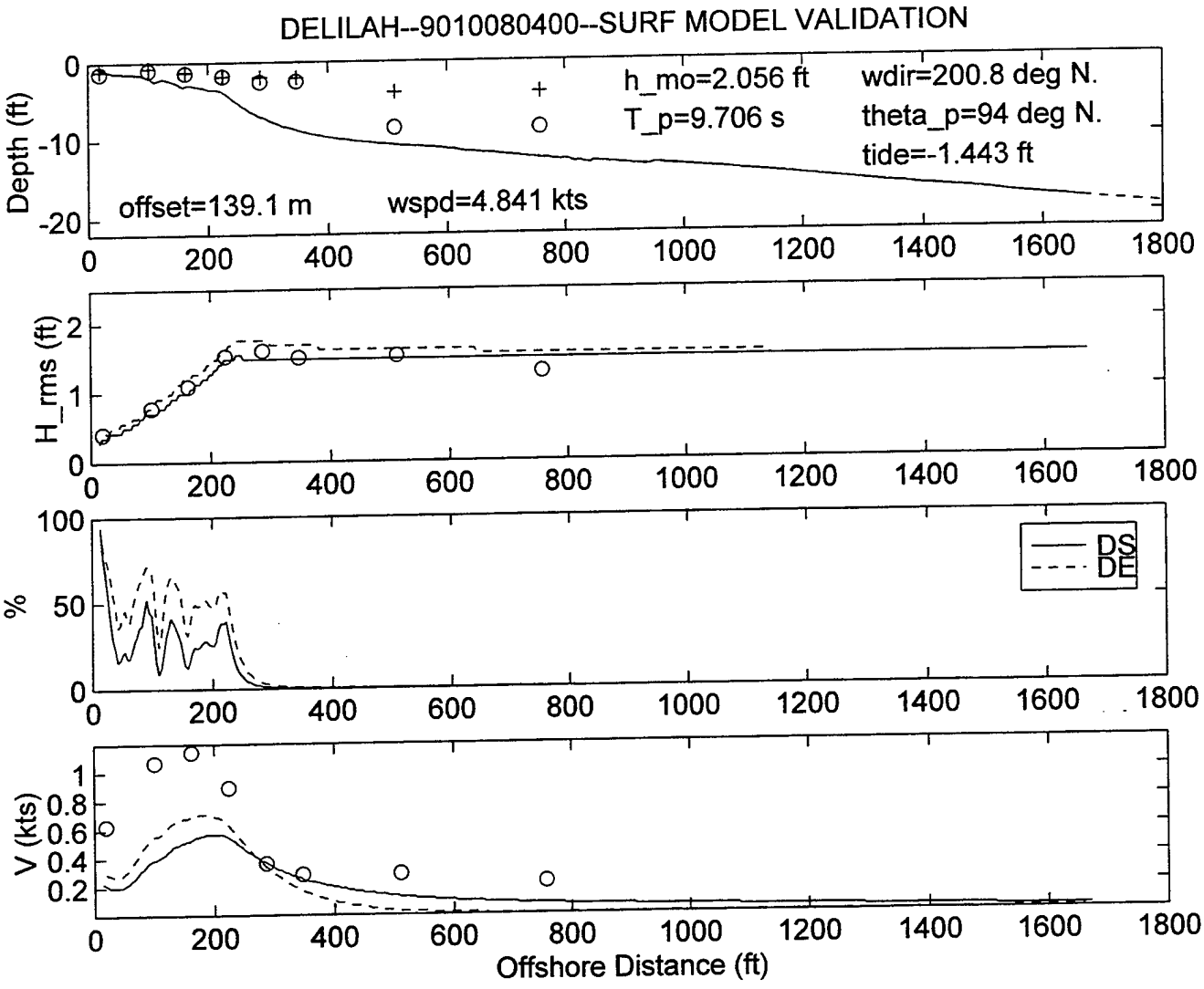
DELILAH--9010080400--SURF MODEL VALIDATION
Depth (ft)
h_mo=2.056 ft
T_p=9.706 s
wdir=200.8 deg N.
theta_p=94 deg N.
tide=-1.443 ft
offset=139.1 m
wspd=4.841 kts
H_rms (ft)
%
DS
DE
V (kts)
Offshore Distance (ft)

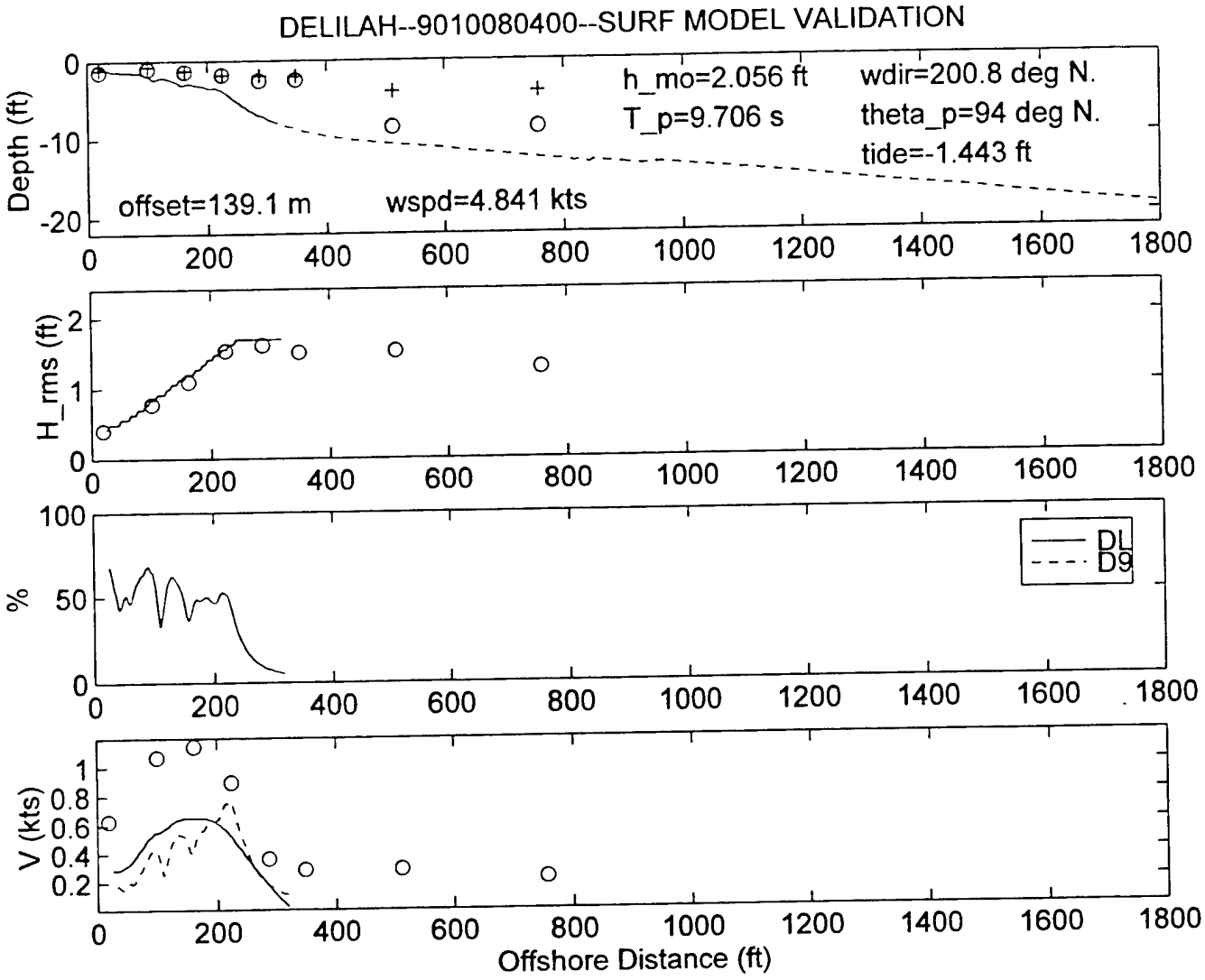
DELILAH--9010080400--SURF MODEL VALIDATION
Depth (ft)
h_mo=2.056 ft
T_p=9.706 s
wdir=200.8 deg N.
theta_p=94 deg N.
tide=-1.443 ft
offset=139.1 m
wspd=4.841 kts
H_rms (ft)
%
DL
D9
V (kts)
Offshore Distance (ft)

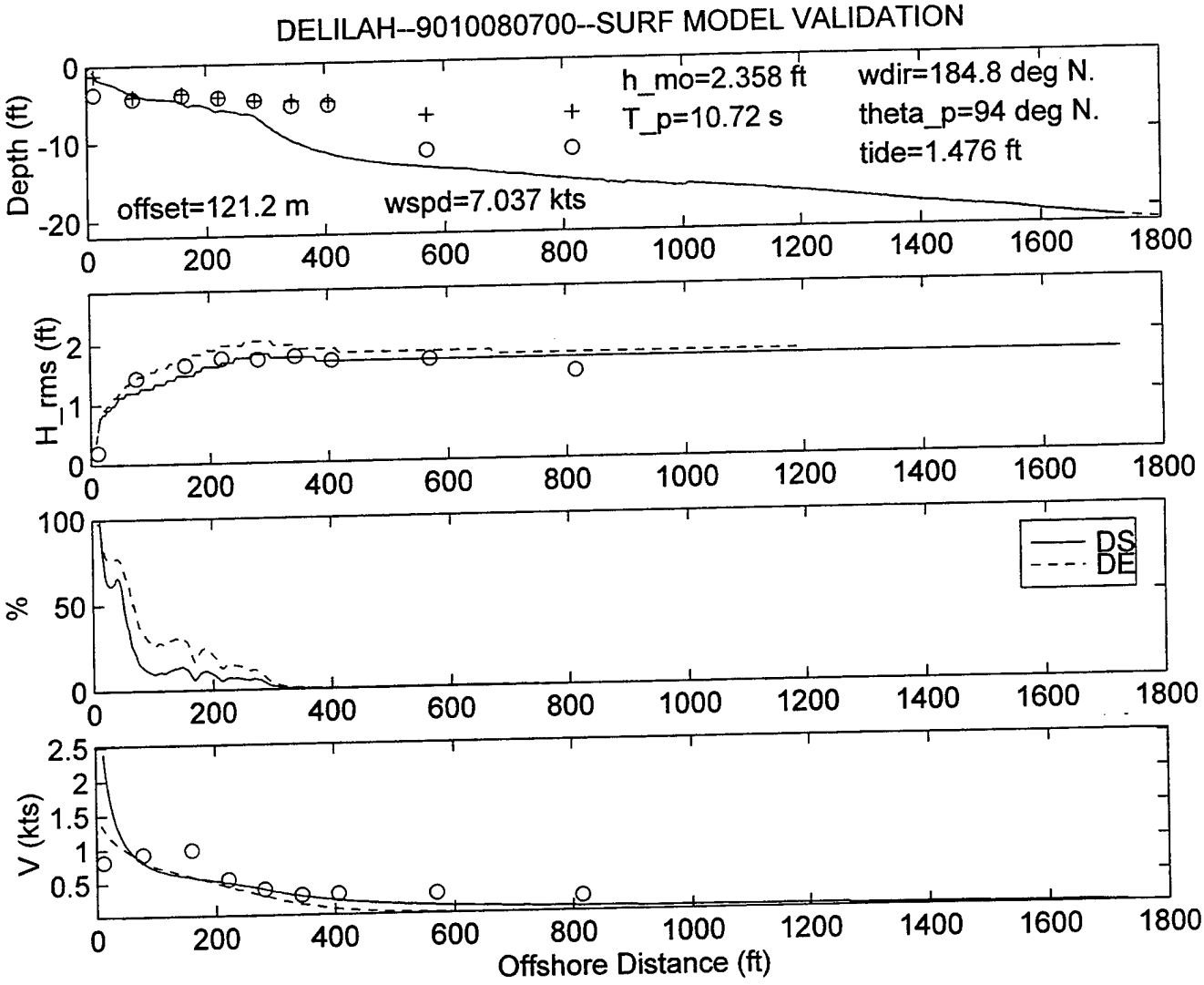
DELILAH--9010080700--SURF MODEL VALIDATION
Depth (ft)
h_mo=2.358 ft
T_p=10.72 s
wdir=184.8 deg N.
theta_p=94 deg N.
tide=1.476 ft
offset=121.2 m
wspd=7.037 kts
H_rms (ft)
%
DS
DE
V (kts)
Offshore Distance (ft)

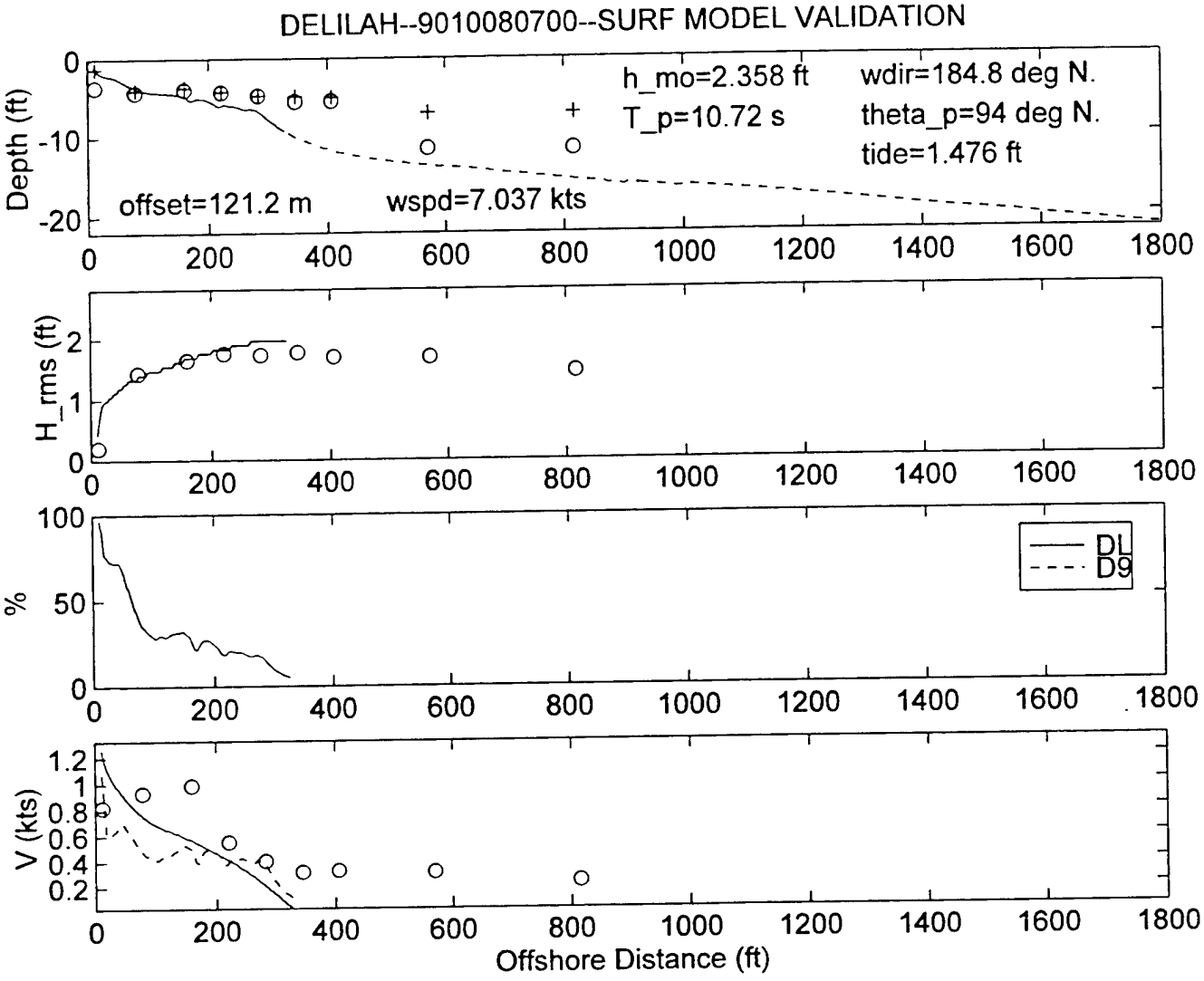
DELILAH--9010080700--SURF MODEL VALIDATION
Depth (ft)
h_mo=2.358 ft
T_p=10.72 s
wdir=184.8 deg N.
theta_p=94 deg N.
tide=1.476 ft
offset=121.2 m
wspd=7.037 kts
H_rms (ft)
%
DL
D9
V (kts)
Offshore Distance (ft)

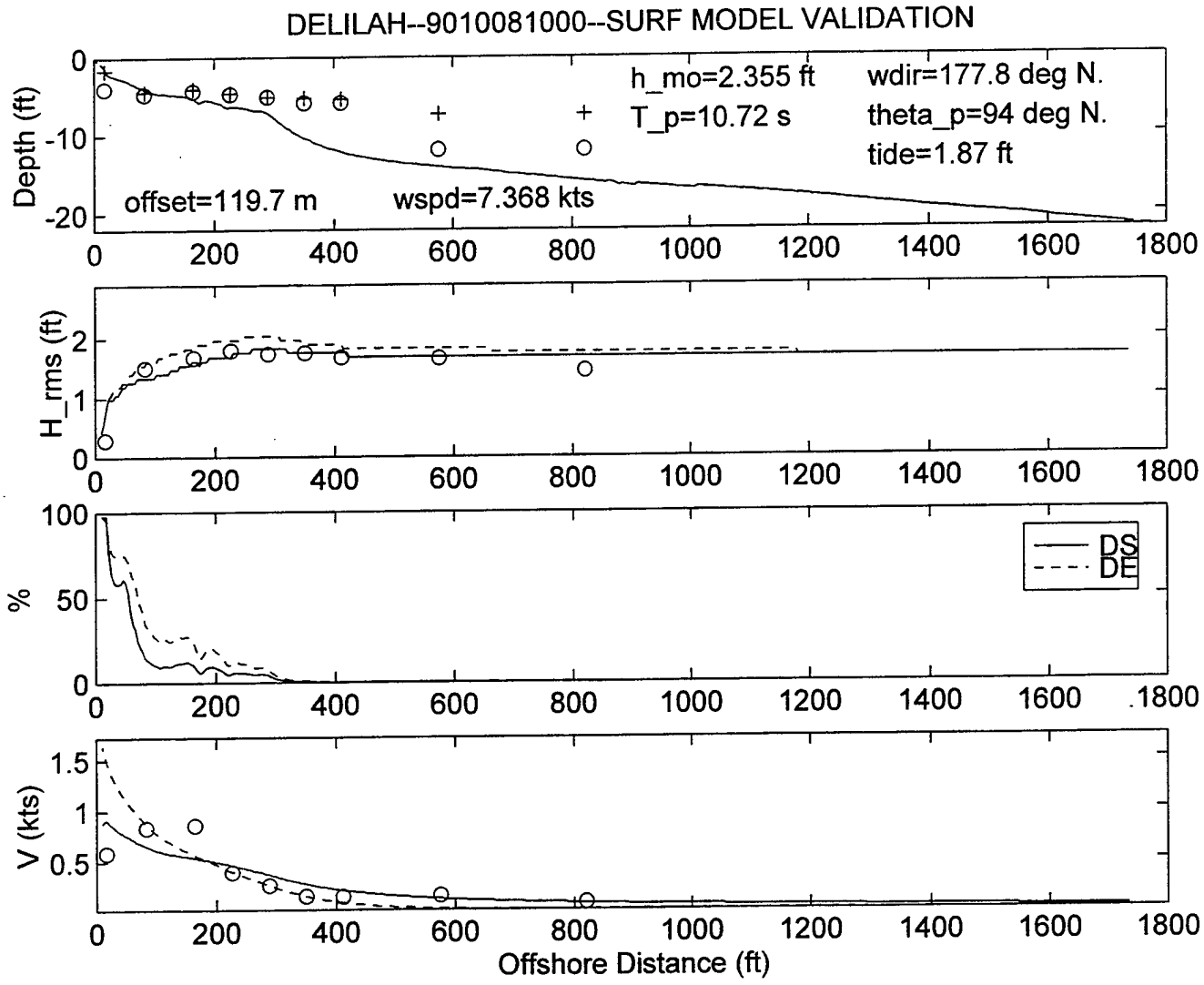
DELILAH--9010081000--SURF MODEL VALIDATION
Depth (ft)
h_mo=2.355 ft
T_p=10.72 s
wdir=177.8 deg N.
theta_p=94 deg N.
tide=1.87 ft
offset=119.7 m
wspd=7.368 kts
H_rms (ft)
%
DS
DE
V (kts)
Offshore Distance (ft)

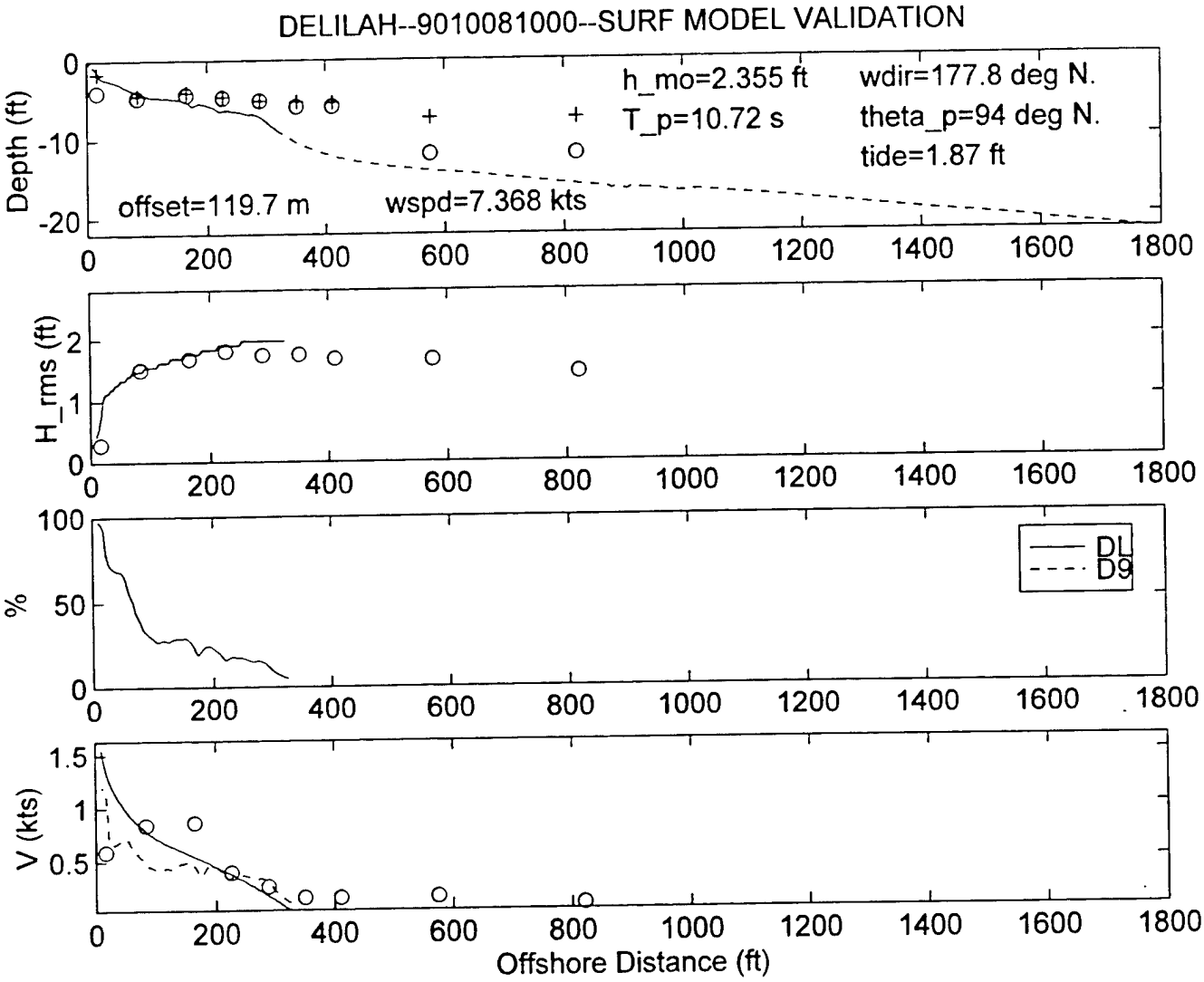
DELILAH--9010081000--SURF MODEL VALIDATION
Depth (ft)
h_mo=2.355 ft
T_p=10.72 s
wdir=177.8 deg N.
theta_p=94 deg N.
tide=1.87 ft
offset=119.7 m
wspd=7.368 kts
H_rms (ft)
%
DL
D9
V (kts)
Offshore Distance (ft)

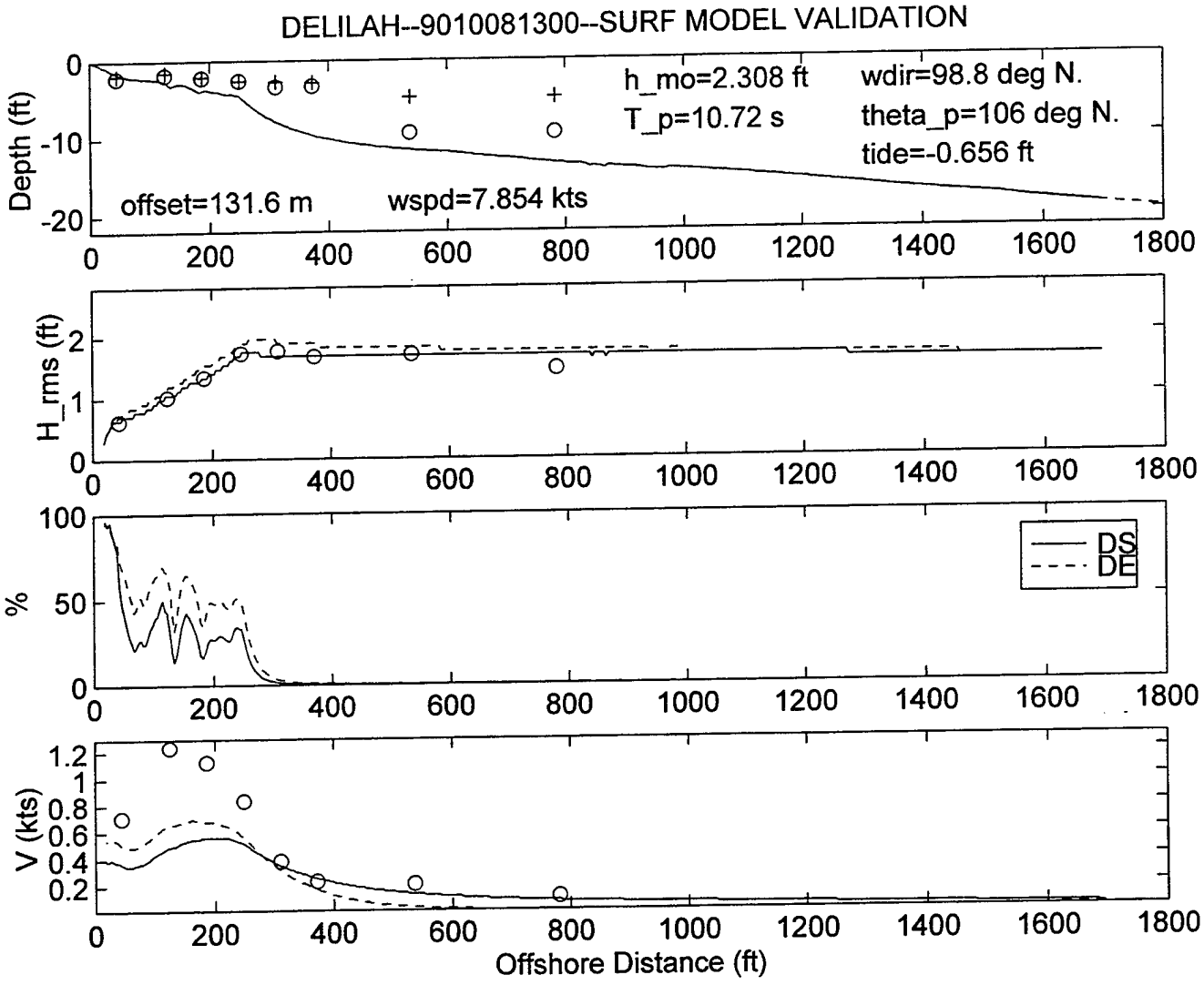
DELILAH--9010081300--SURF MODEL VALIDATION
Depth (ft)
h_mo=2.308 ft
T_p=10.72 s
wdir=98.8 deg N.
theta_p=106 deg N.
tide=-0.656 ft
offset=131.6 m
wspd=7.854 kts
H_rms (ft)
%
DS
DE
V (kts)
Offshore Distance (ft)

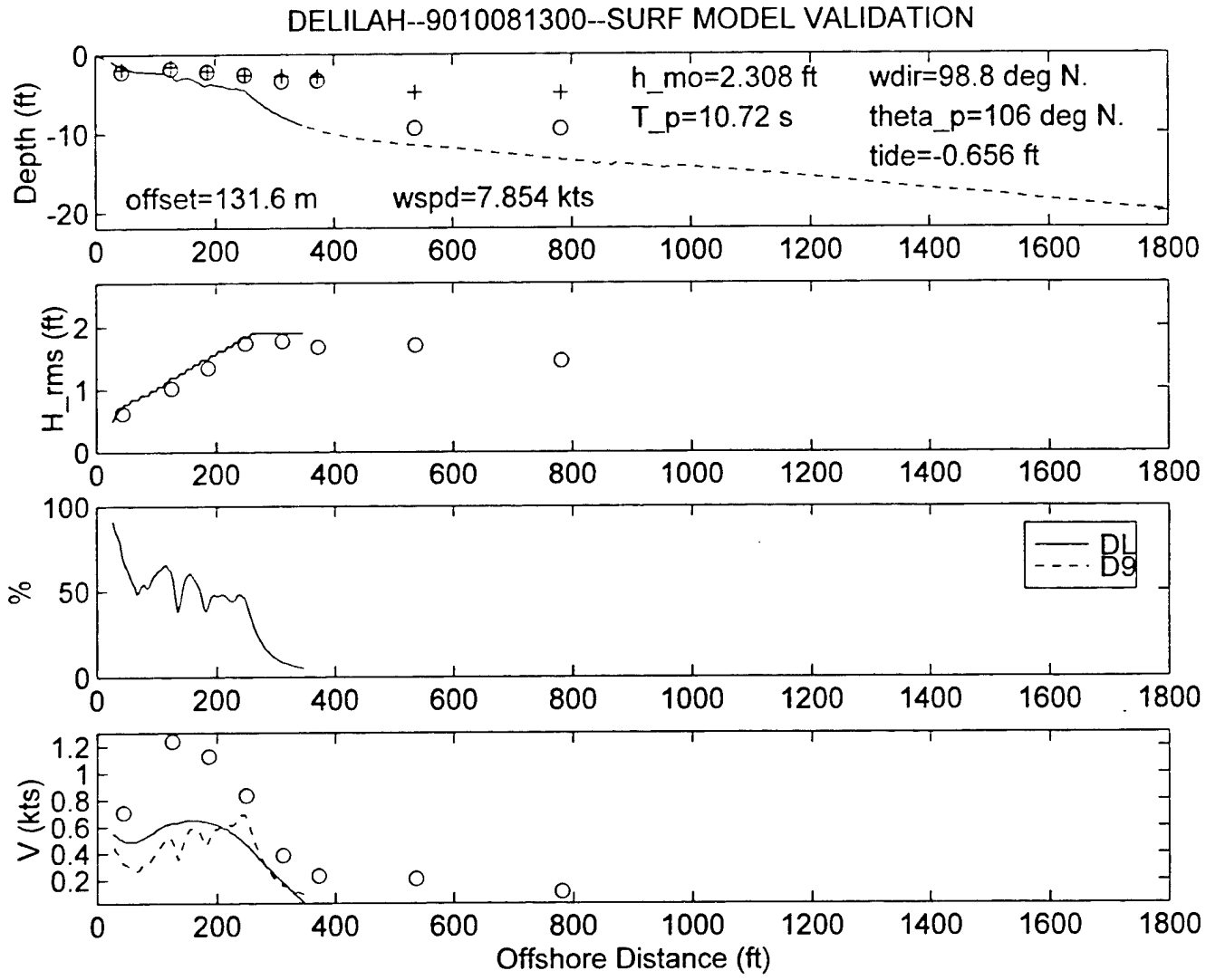
DELILAH--9010081300--SURF MODEL VALIDATION
Depth (ft)
h_mo=2.308 ft
T_p=10.72 s
wdir=98.8 deg N.
theta_p=106 deg N.
tide=-0.656 ft
offset=131.6 m
wspd=7.854 kts
H_rms (ft)
%
DL
D9
V (kts)
Offshore Distance (ft)

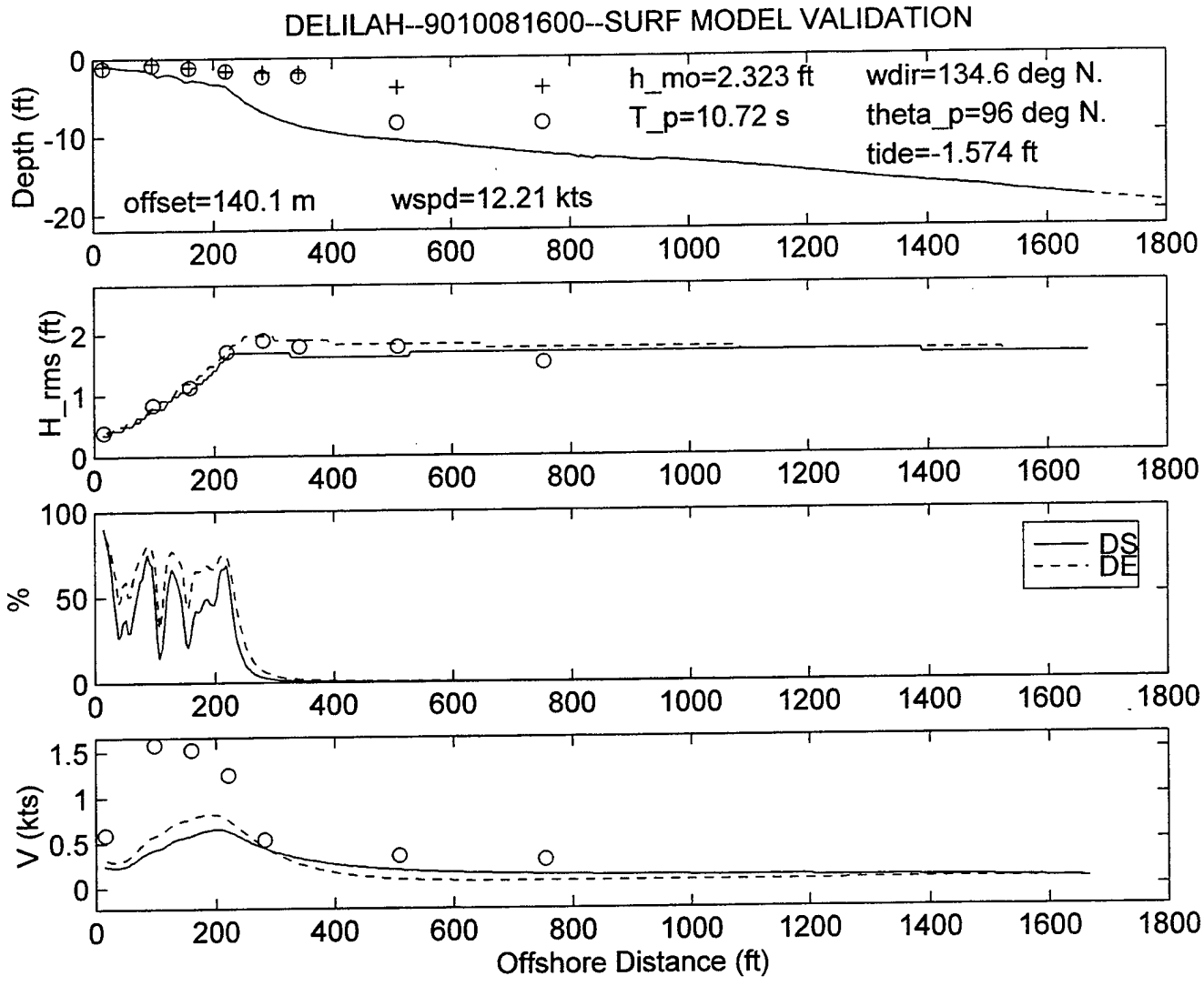
DELILAH--9010081600--SURF MODEL VALIDATION
Depth (ft)
h_mo=2.323 ft
T_p=10.72 s
wdir=134.6 deg N.
theta_p=96 deg N.
tide=-1.574 ft
offset=140.1 m
wspd=12.21 kts
H_rms (ft)
%
DS
DE
V (kts)
Offshore Distance (ft)

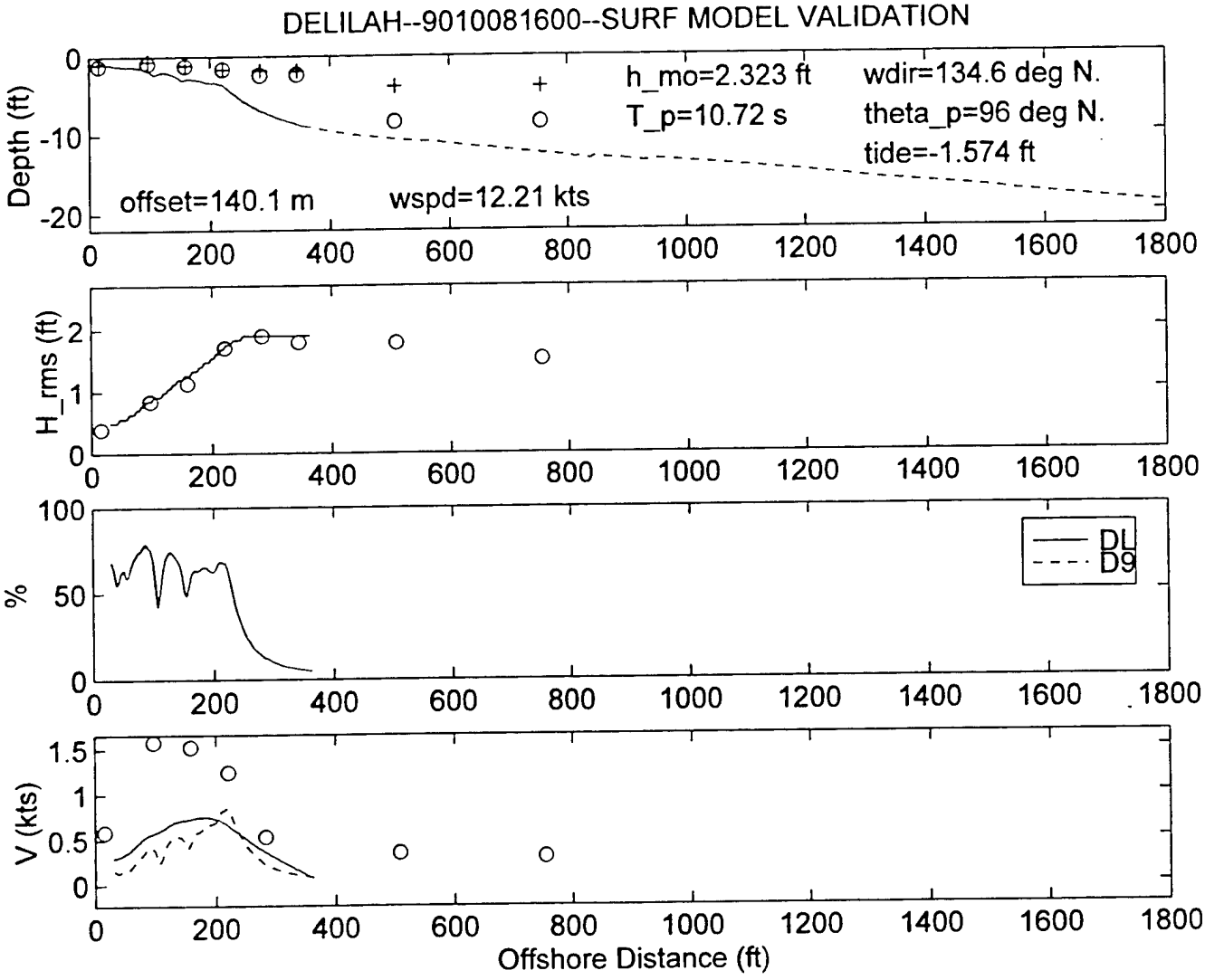
DELILAH--9010081600--SURF MODEL VALIDATION
Depth (ft)
h_mo=2.323 ft
T_p=10.72 s
wdir=134.6 deg N.
theta_p=96 deg N.
tide=-1.574 ft
offset=140.1 m
wspd=12.21 kts
H_rms (ft)
%
DL
D9
V (kts)
Offshore Distance (ft)

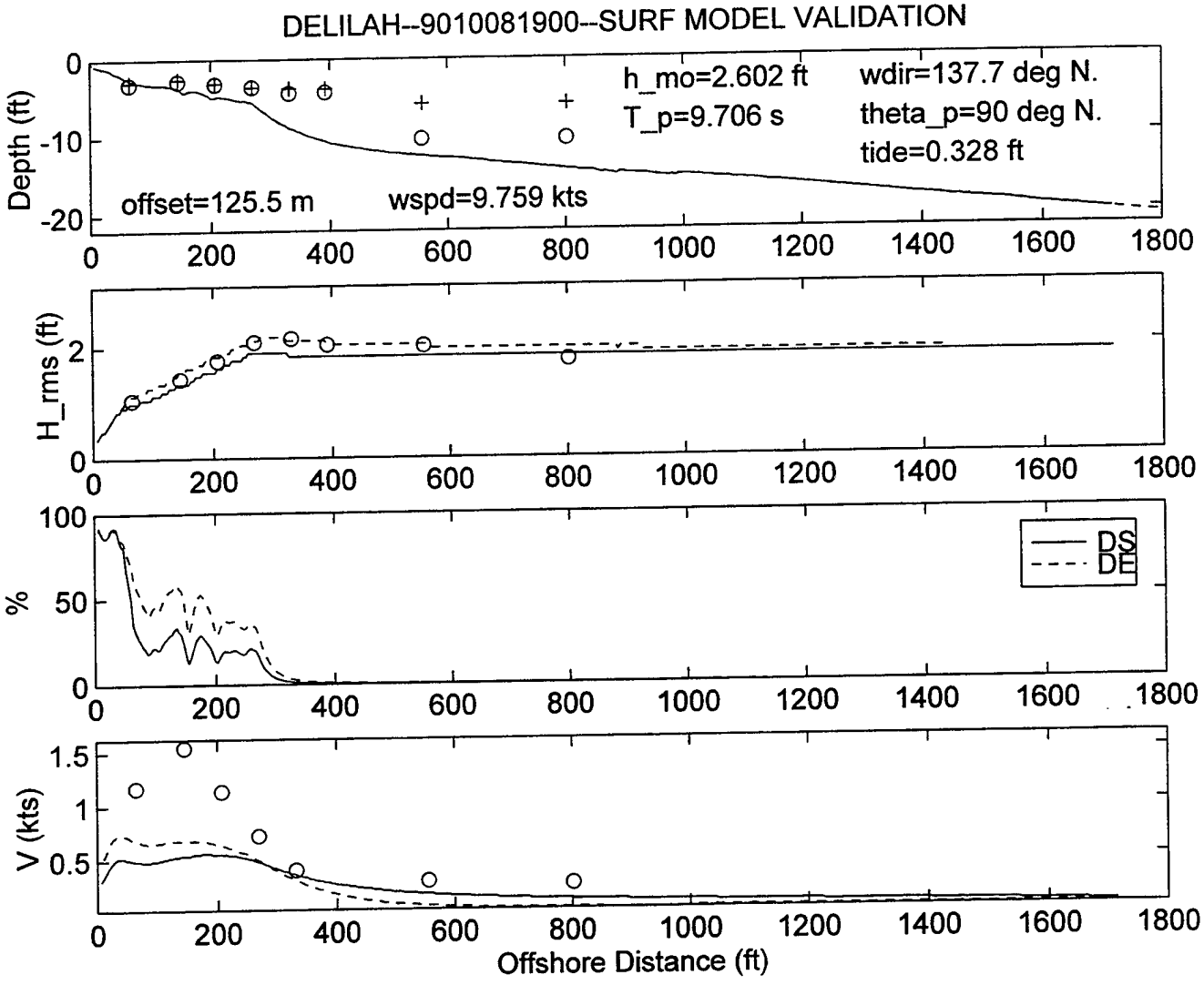
DELILAH--9010081900--SURF MODEL VALIDATION
Depth (ft)
h_mo=2.602 ft
T_p=9.706 s
wdir=137.7 deg N.
theta_p=90 deg N.
tide=0.328 ft
offset=125.5 m
wspd=9.759 kts
H_rms (ft)
%
DS
DE
V (kts)
Offshore Distance (ft)

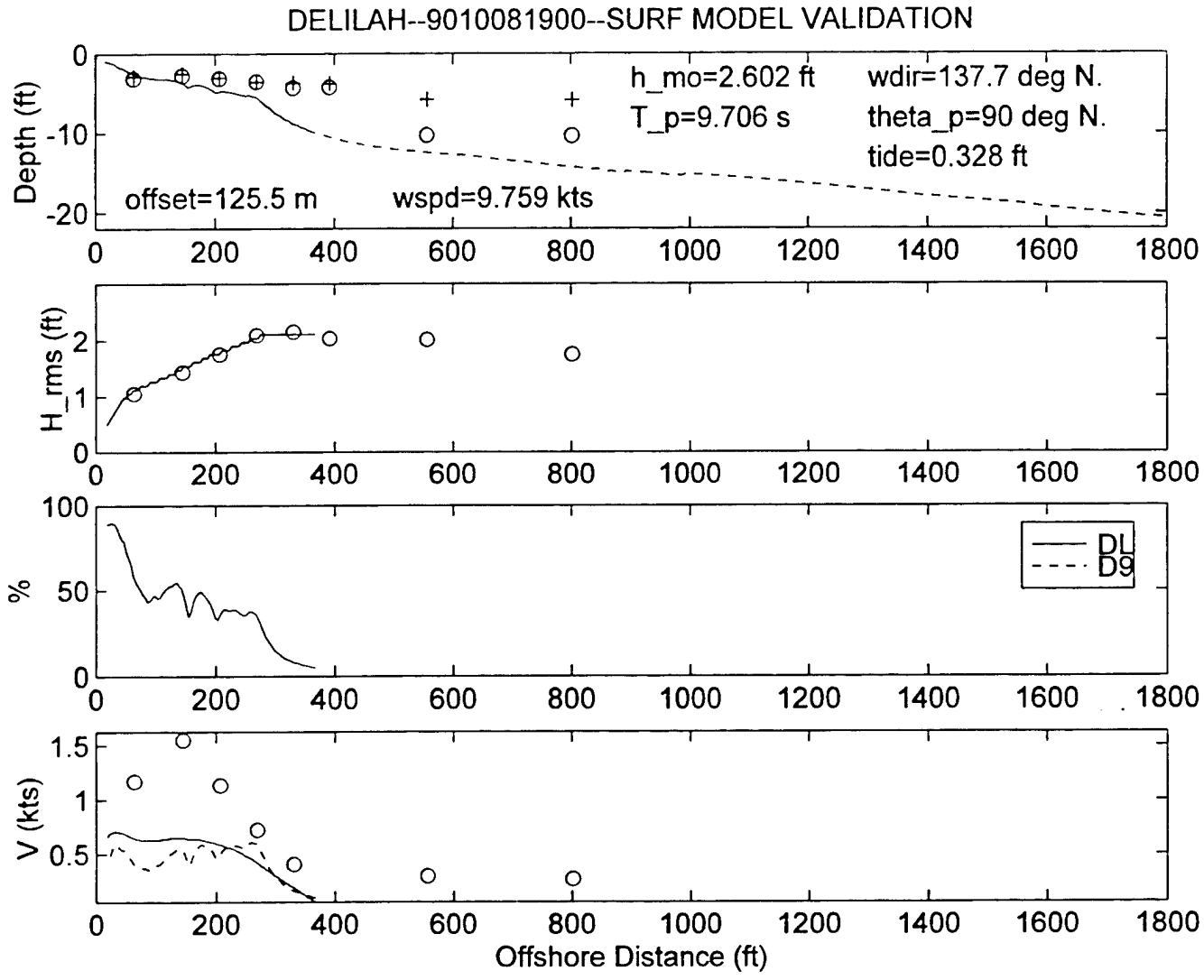
DELILAH--9010081900--SURF MODEL VALIDATION
Depth (ft)
h_mo=2.602 ft
T_p=9.706 s
wdir=137.7 deg N.
theta_p=90 deg N.
tide=0.328 ft
offset=125.5 m
wspd=9.759 kts
H_rms (ft)
%
DL
D9
V (kts)
Offshore Distance (ft)

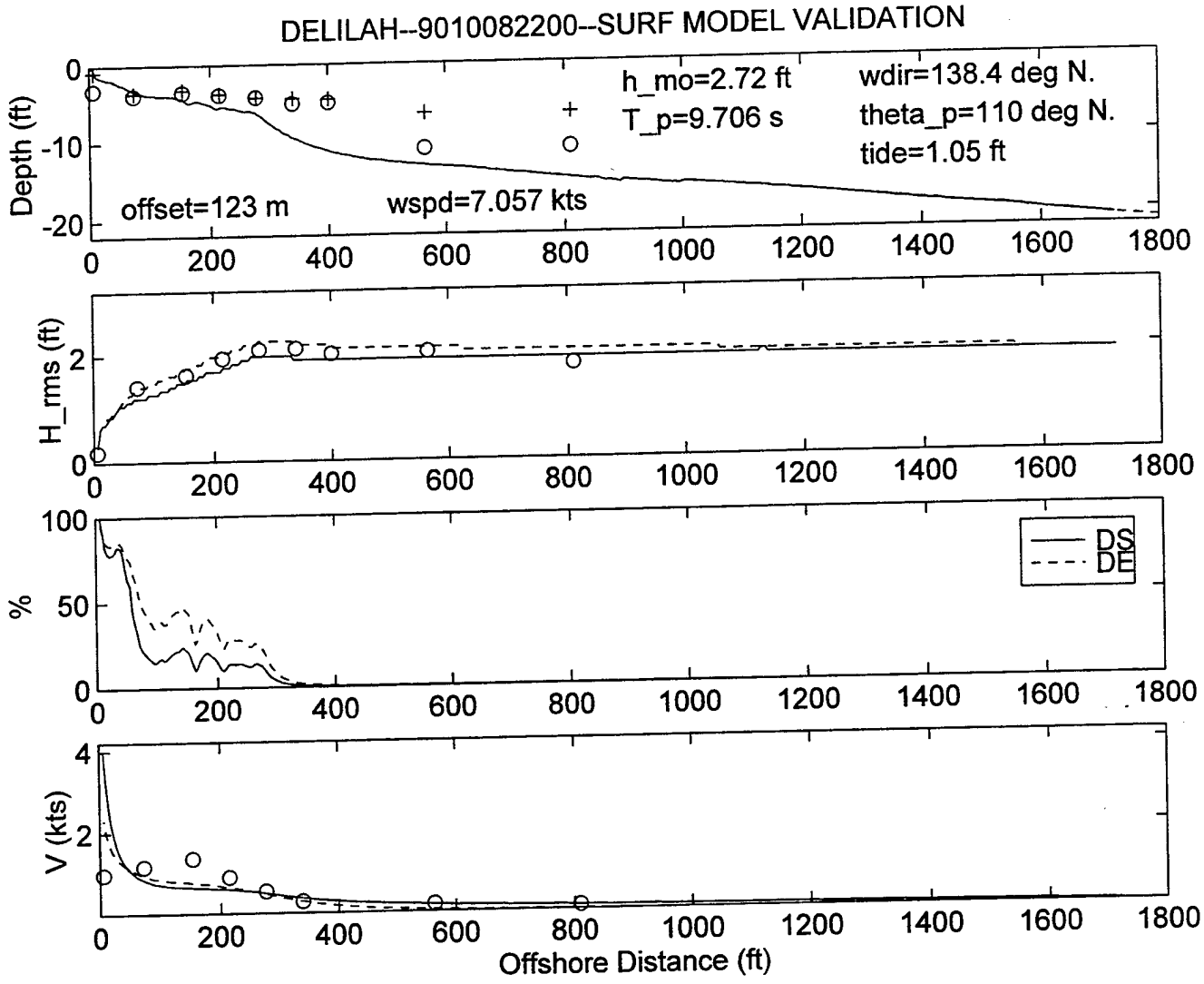
DELILAH--9010082200--SURF MODEL VALIDATION
Depth (ft)
h_mo=2.72 ft
T_p=9.706 s
wdir=138.4 deg N.
theta_p=110 deg N.
tide=1.05 ft
offset=123 m
wspd=7.057 kts
H_rms (ft)
%
DS
DE
V (kts)
Offshore Distance (ft)

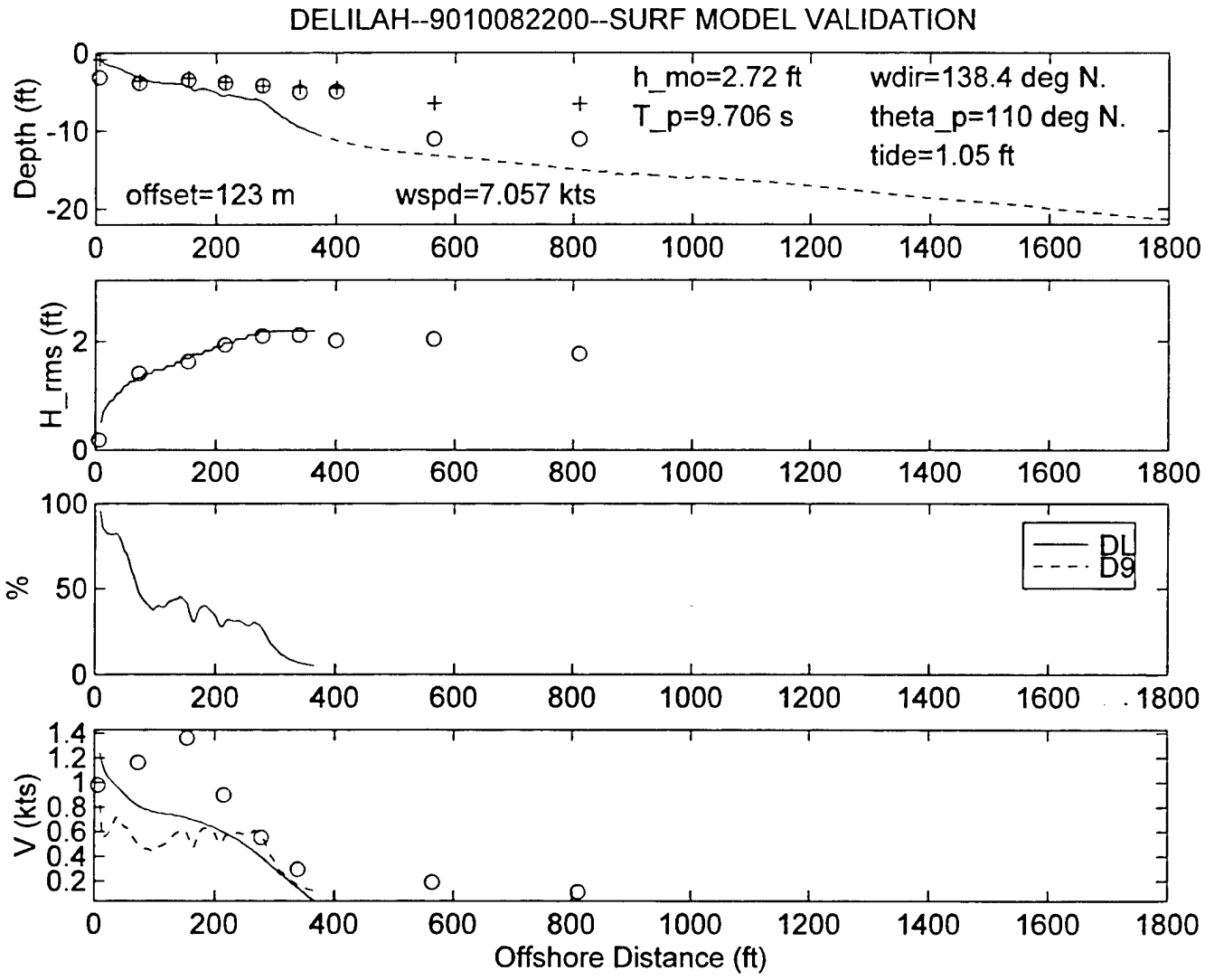
DELILAH--9010082200--SURF MODEL VALIDATION
Depth (ft)
h_mo=2.72 ft
T_p=9.706 s
wdir=138.4 deg N.
theta_p=110 deg N.
tide=1.05 ft
offset=123 m
wspd=7.057 kts
H_rms (ft)
%
DL
D9
V (kts)
Offshore Distance (ft)

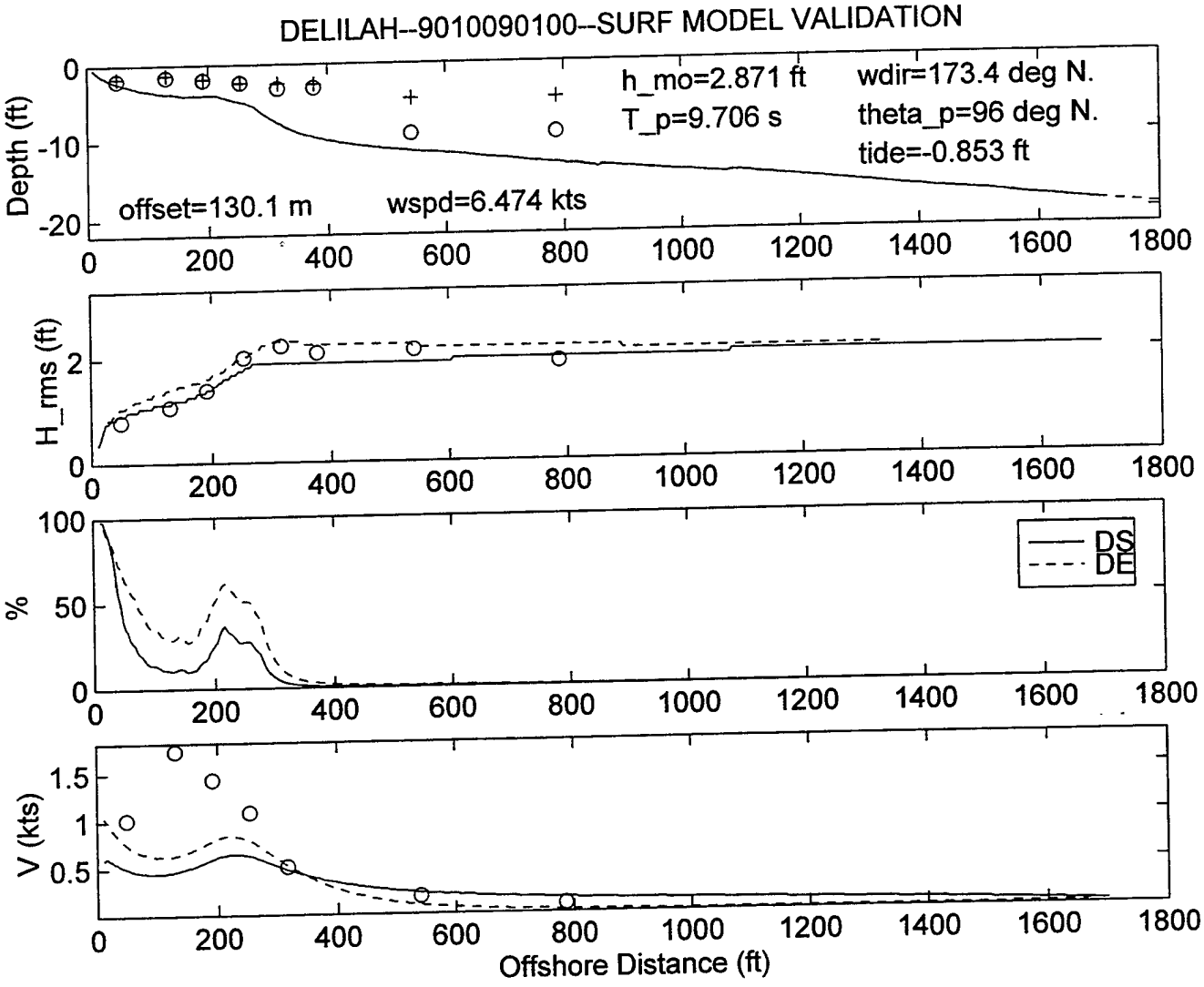
DELILAH--9010090100--SURF MODEL VALIDATION
Depth (ft)
h_mo=2.871 ft
T_p=9.706 s
wdir=173.4 deg N.
theta_p=96 deg N.
tide=-0.853 ft
offset=130.1 m
wspd=6.474 kts
H_rms (ft)
%
DS
DE
V (kts)
Offshore Distance (ft)

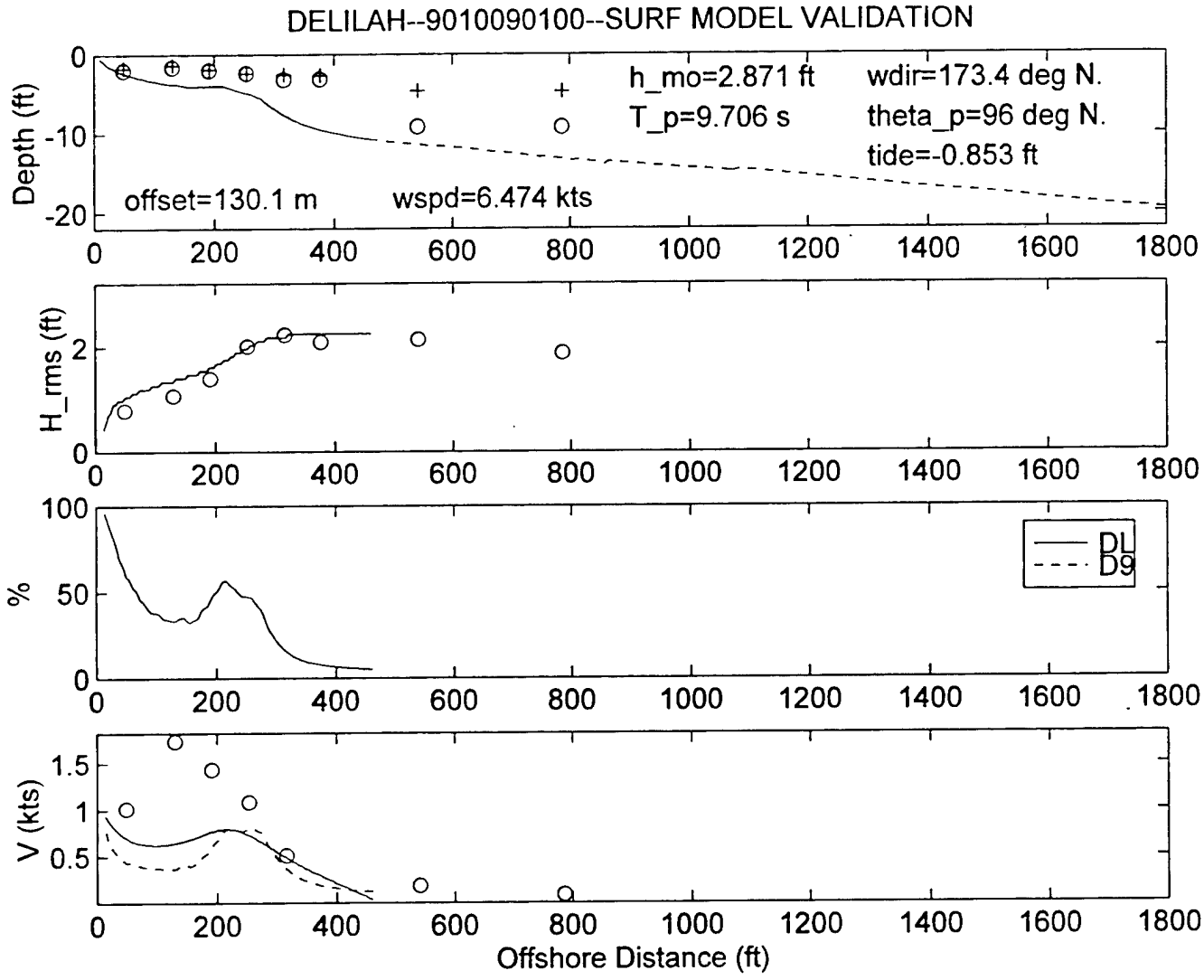
DELILAH--9010090100--SURF MODEL VALIDATION
Depth (ft)
h_mo=2.871 ft
T_p=9.706 s
wdir=173.4 deg N.
theta_p=96 deg N.
tide=-0.853 ft
offset=130.1 m
wspd=6.474 kts
H_rms (ft)
%
DL
D9
V (kts)
Offshore Distance (ft)

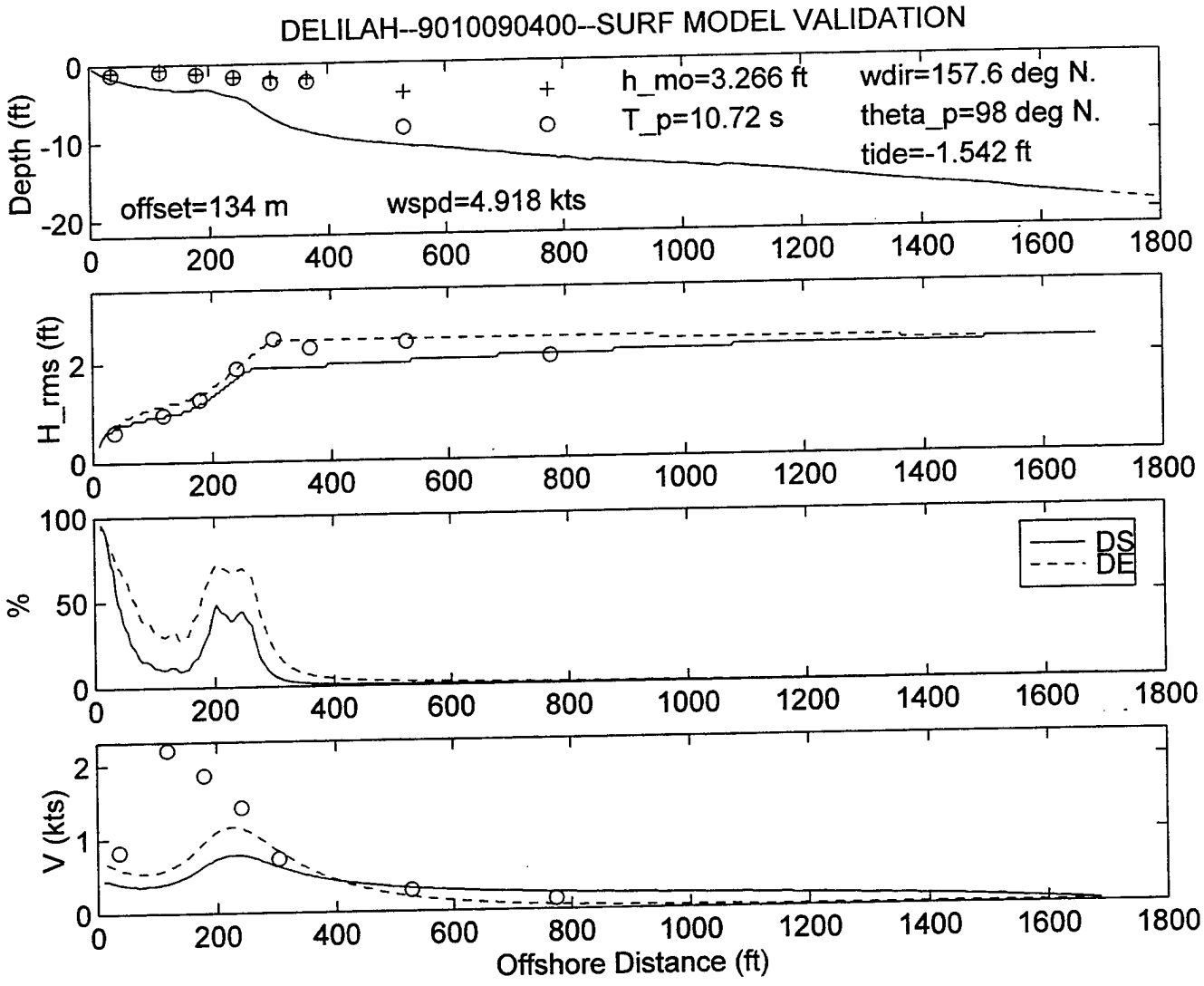
DELILAH--9010090400--SURF MODEL VALIDATION
Depth (ft)
h_mo=3.266 ft
T_p=10.72 s
wdir=157.6 deg N.
theta_p=98 deg N.
tide=-1.542 ft
offset=134 m
wspd=4.918 kts
H_rms (ft)
%
DS
DE
V (kts)
Offshore Distance (ft)

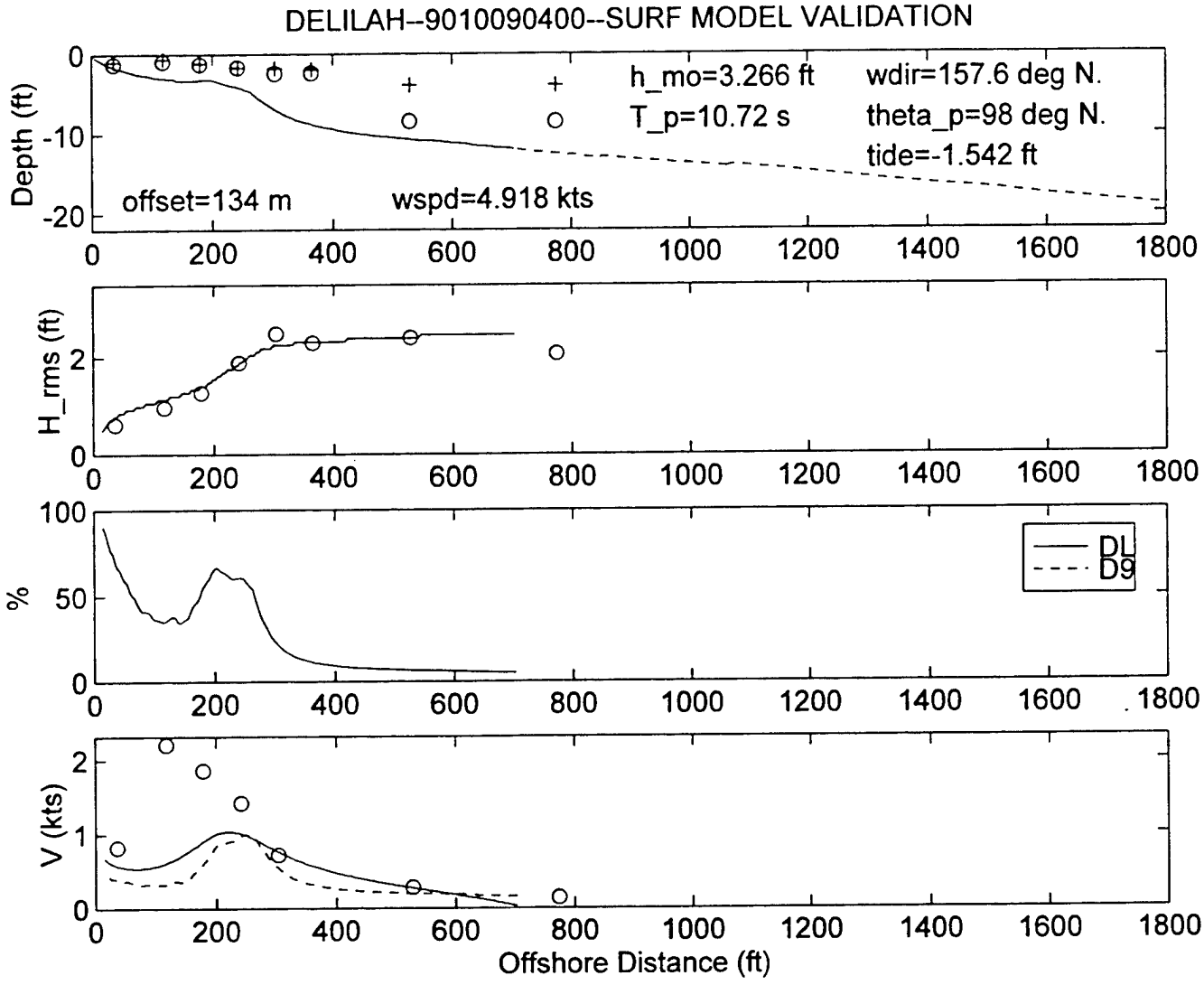
DELILAH--9010090400--SURF MODEL VALIDATION
Depth (ft)
h_mo=3.266 ft
T_p=10.72 s
wdir=157.6 deg N.
theta_p=98 deg N.
tide=-1.542 ft
offset=134 m
wspd=4.918 kts
H_rms (ft)
%
DL
D9
V (kts)
Offshore Distance (ft)

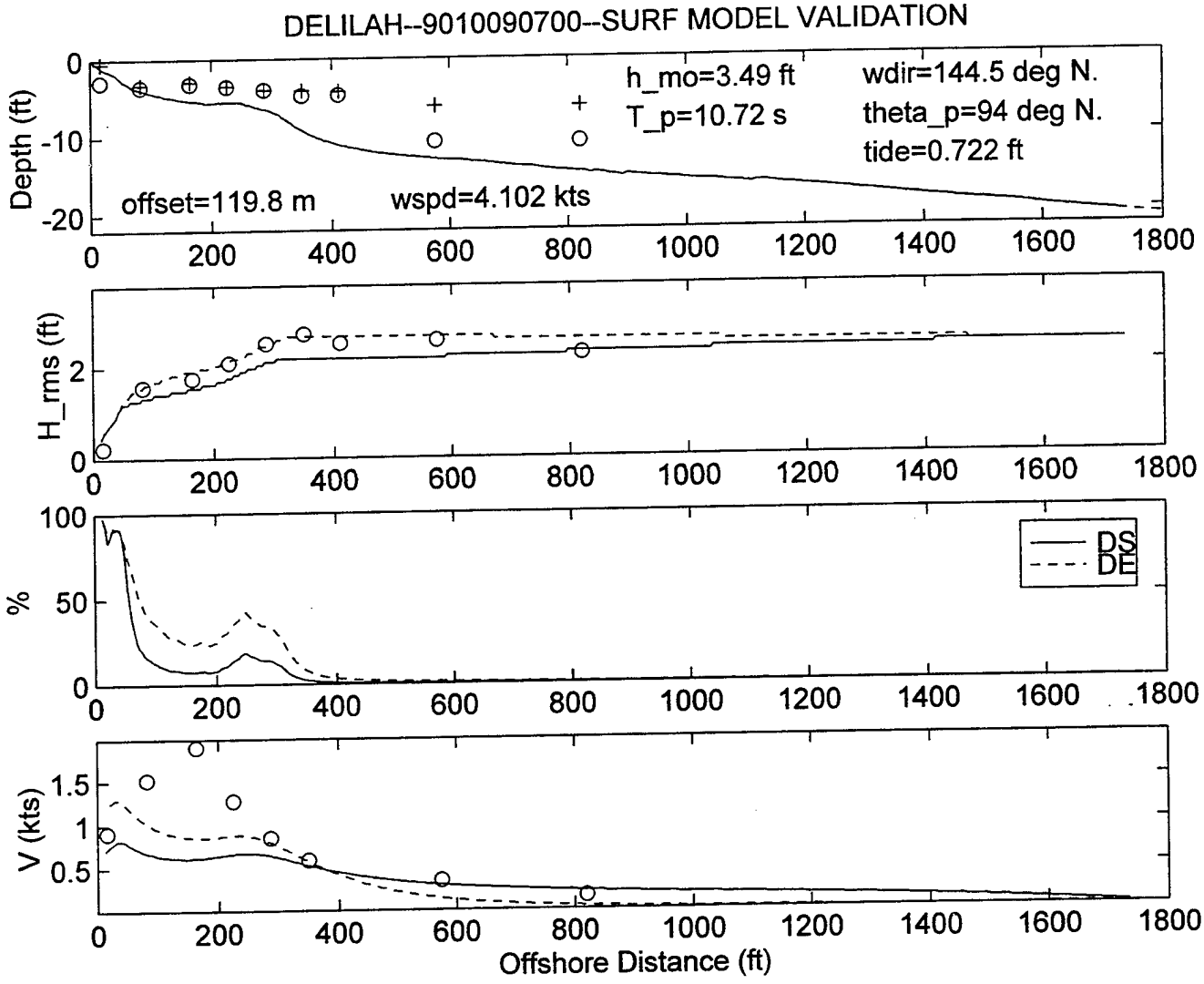
DELILAH--9010090700--SURF MODEL VALIDATION
Depth (ft)
h_mo=3.49 ft
T_p=10.72 s
wdir=144.5 deg N.
theta_p=94 deg N.
tide=0.722 ft
offset=119.8 m
wspd=4.102 kts
H_rms (ft)
%
DS
DE
V (kts)
Offshore Distance (ft)

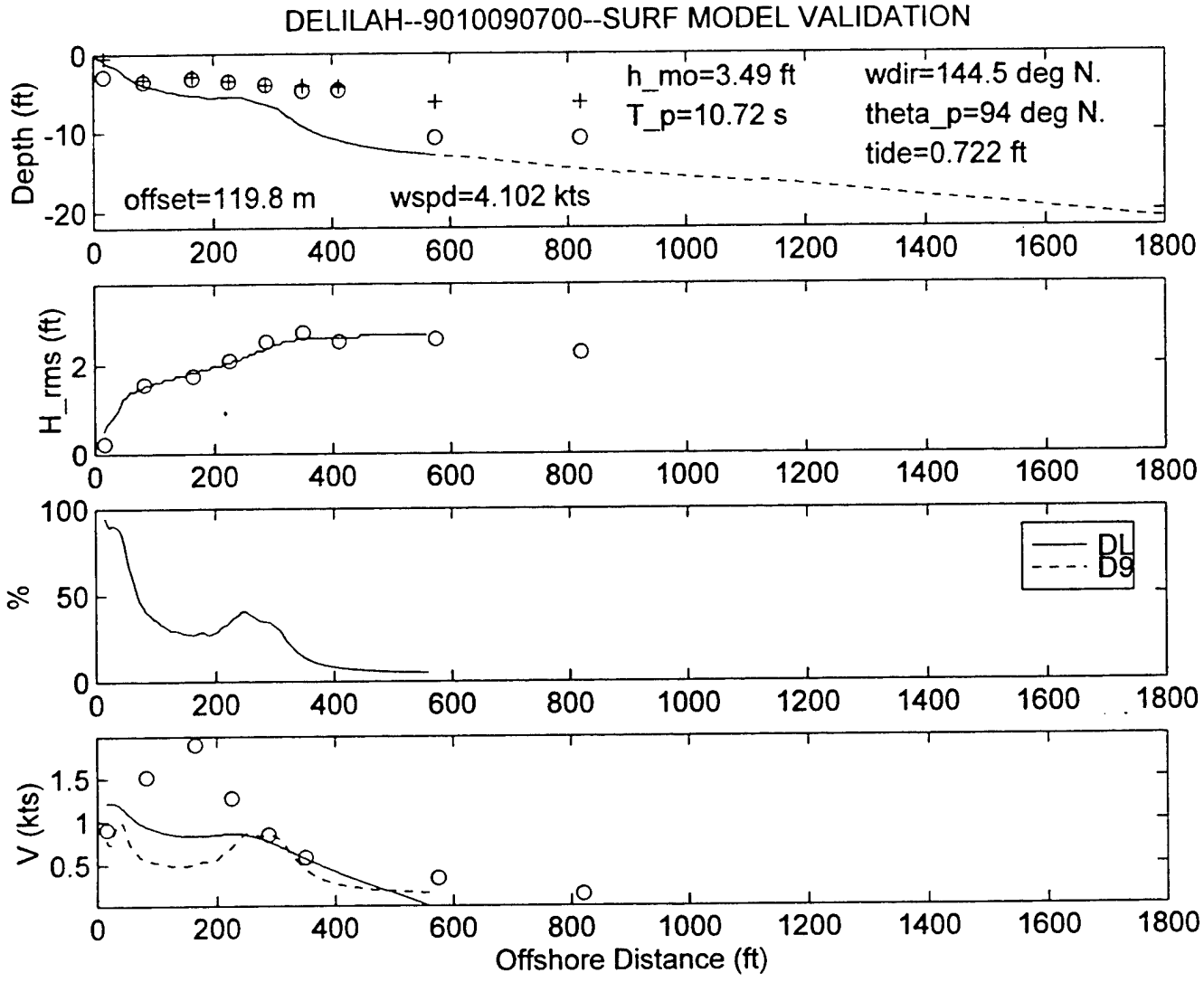
DELILAH--9010090700--SURF MODEL VALIDATION
Depth (ft)
h_mo=3.49 ft
T_p=10.72 s
wdir=144.5 deg N.
theta_p=94 deg N.
tide=0.722 ft
offset=119.8 m
wspd=4.102 kts
H_rms (ft)
%
DL
D9
V (kts)
Offshore Distance (ft)

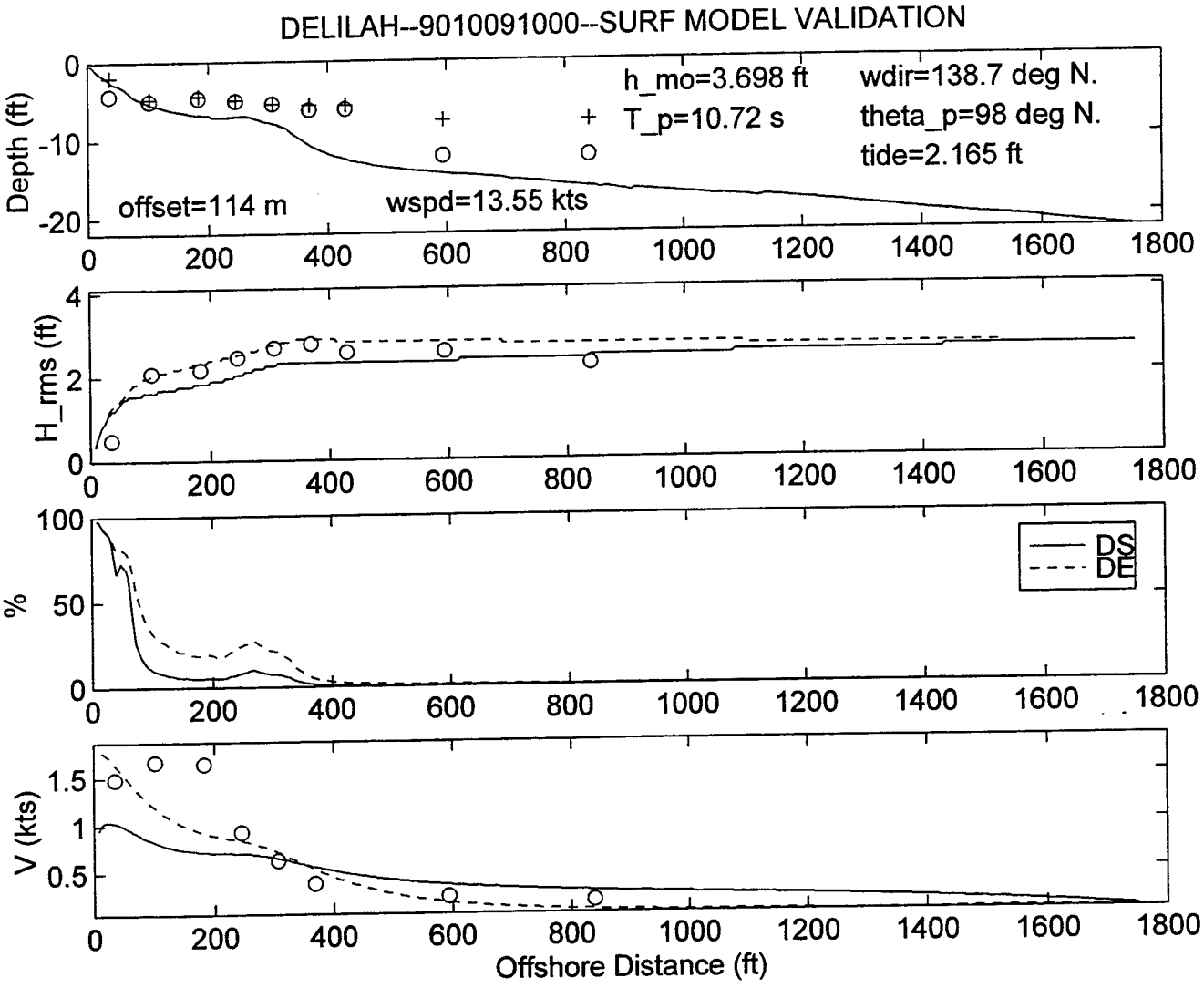
DELILAH--9010091000--SURF MODEL VALIDATION
Depth (ft)
h_mo=3.698 ft
T_p=10.72 s
wdir=138.7 deg N.
theta_p=98 deg N.
tide=2.165 ft
offset=114 m
wspd=13.55 kts
H_rms (ft)
%
DS
DE
V (kts)
Offshore Distance (ft)

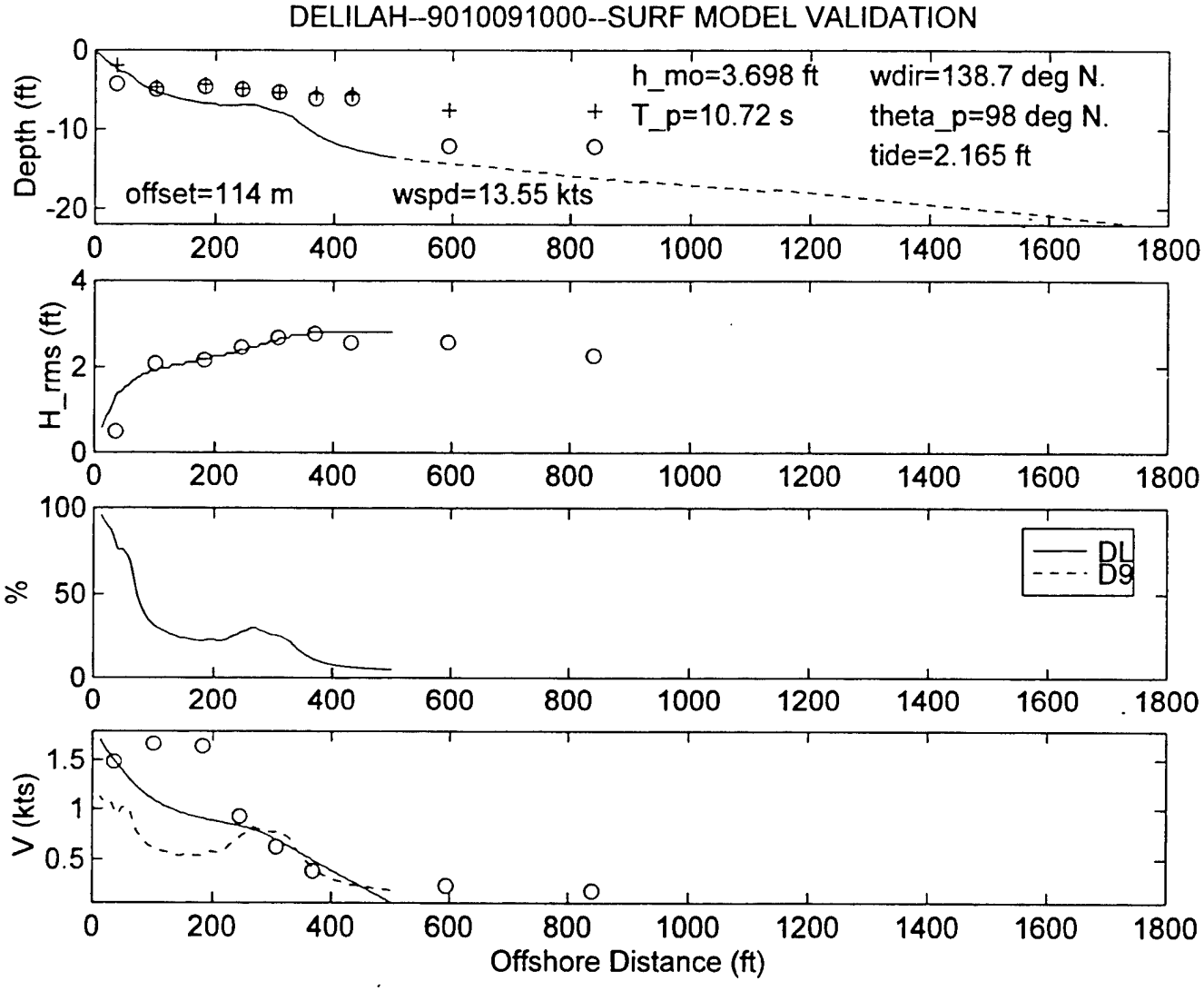
DELILAH--9010091000--SURF MODEL VALIDATION
Depth (ft)
h_mo=3.698 ft
T_p=10.72 s
wdir=138.7 deg N.
theta_p=98 deg N.
tide=2.165 ft
offset=114 m
wspd=13.55 kts
H_rms (ft)
%
DL
D9
V (kts)
Offshore Distance (ft)

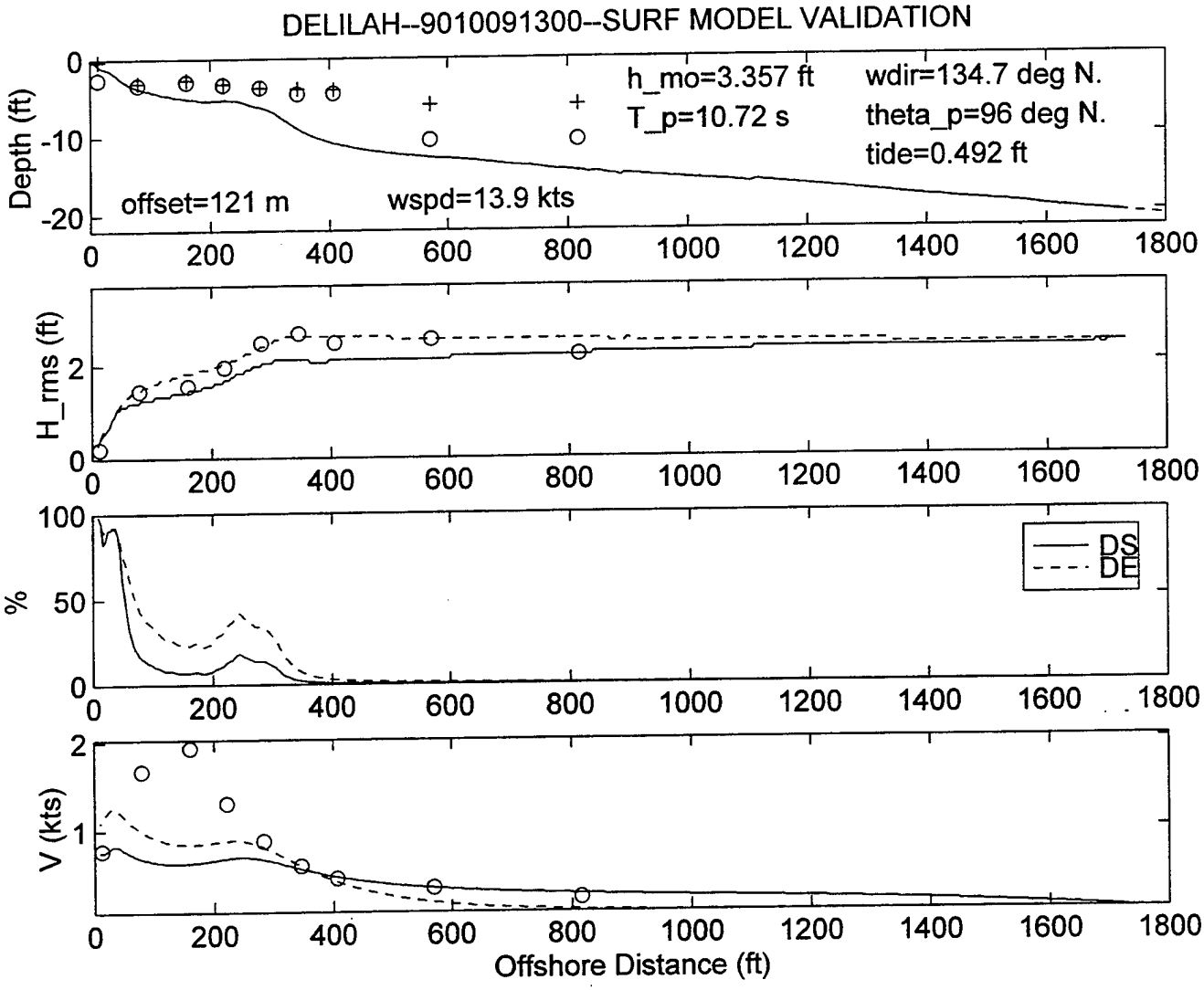
DELILAH--9010091300--SURF MODEL VALIDATION
Depth (ft)
h_mo=3.357 ft
T_p=10.72 s
wdir=134.7 deg N.
theta_p=96 deg N.
tide=0.492 ft
offset=121 m
wspd=13.9 kts
H_rms (ft)
%
DS
DE
V (kts)
Offshore Distance (ft)

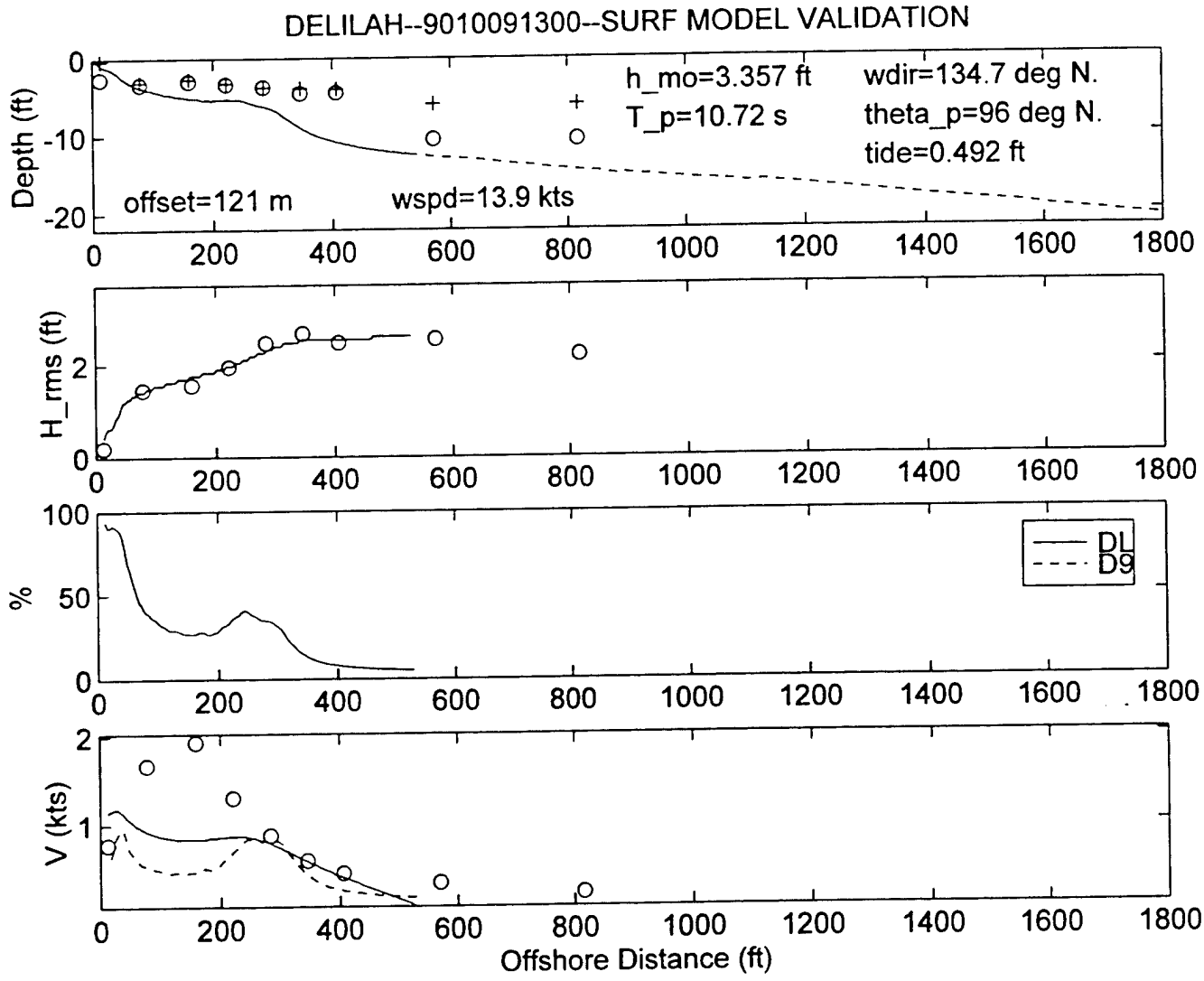
DELILAH--9010091300--SURF MODEL VALIDATION
Depth (ft)
h_mo=3.357 ft
T_p=10.72 s
wdir=134.7 deg N.
theta_p=96 deg N.
tide=0.492 ft
offset=121 m
wspd=13.9 kts
H_rms (ft)
%
DL
D9
V (kts)
Offshore Distance (ft)

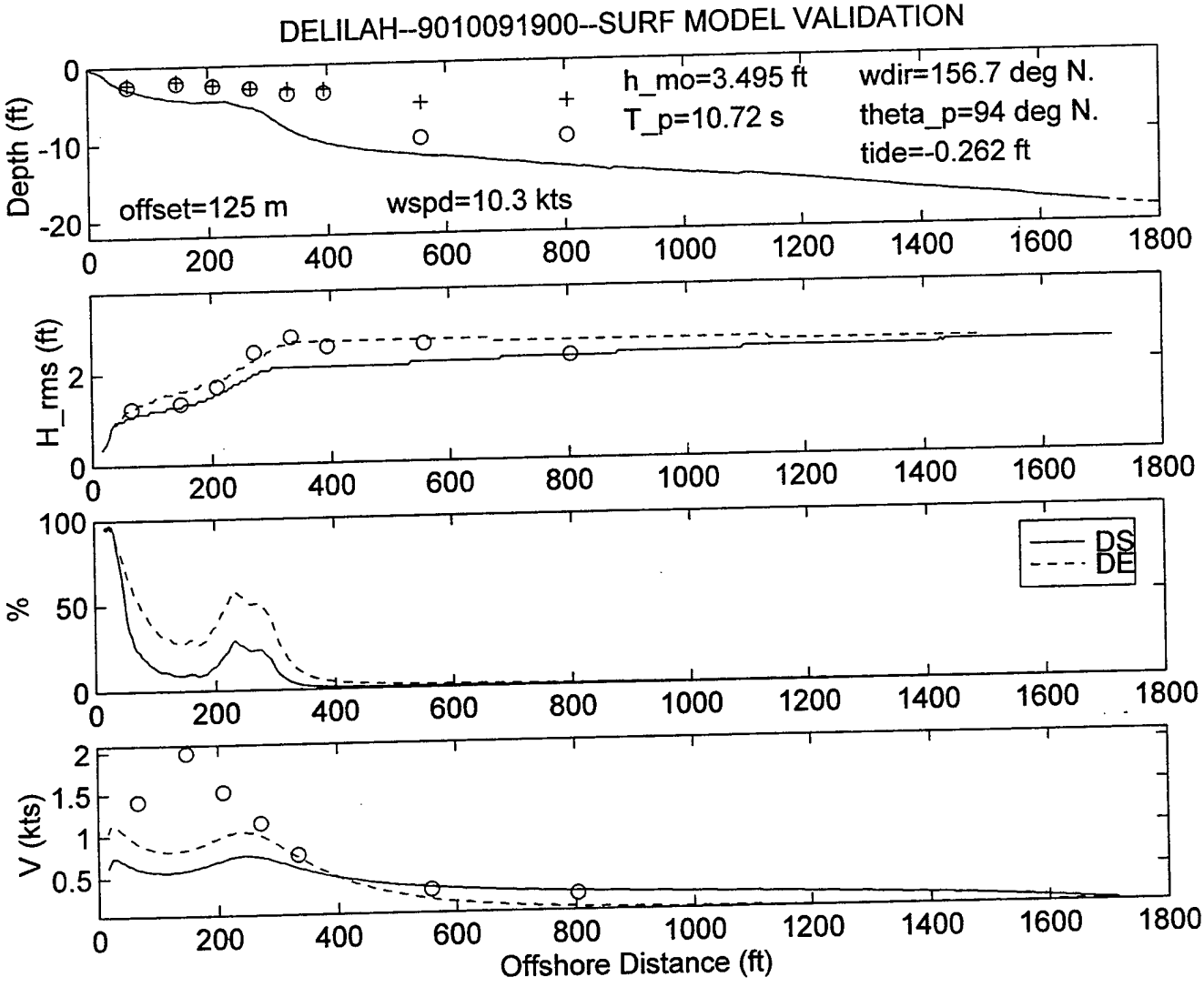
DELILAH--9010091900--SURF MODEL VALIDATION
Depth (ft)
h_mo=3.495 ft
T_p=10.72 s
wdir=156.7 deg N.
theta_p=94 deg N.
tide=-0.262 ft
offset=125 m
wspd=10.3 kts
H_rms (ft)
%
DS
DE
V (kts)
Offshore Distance (ft)

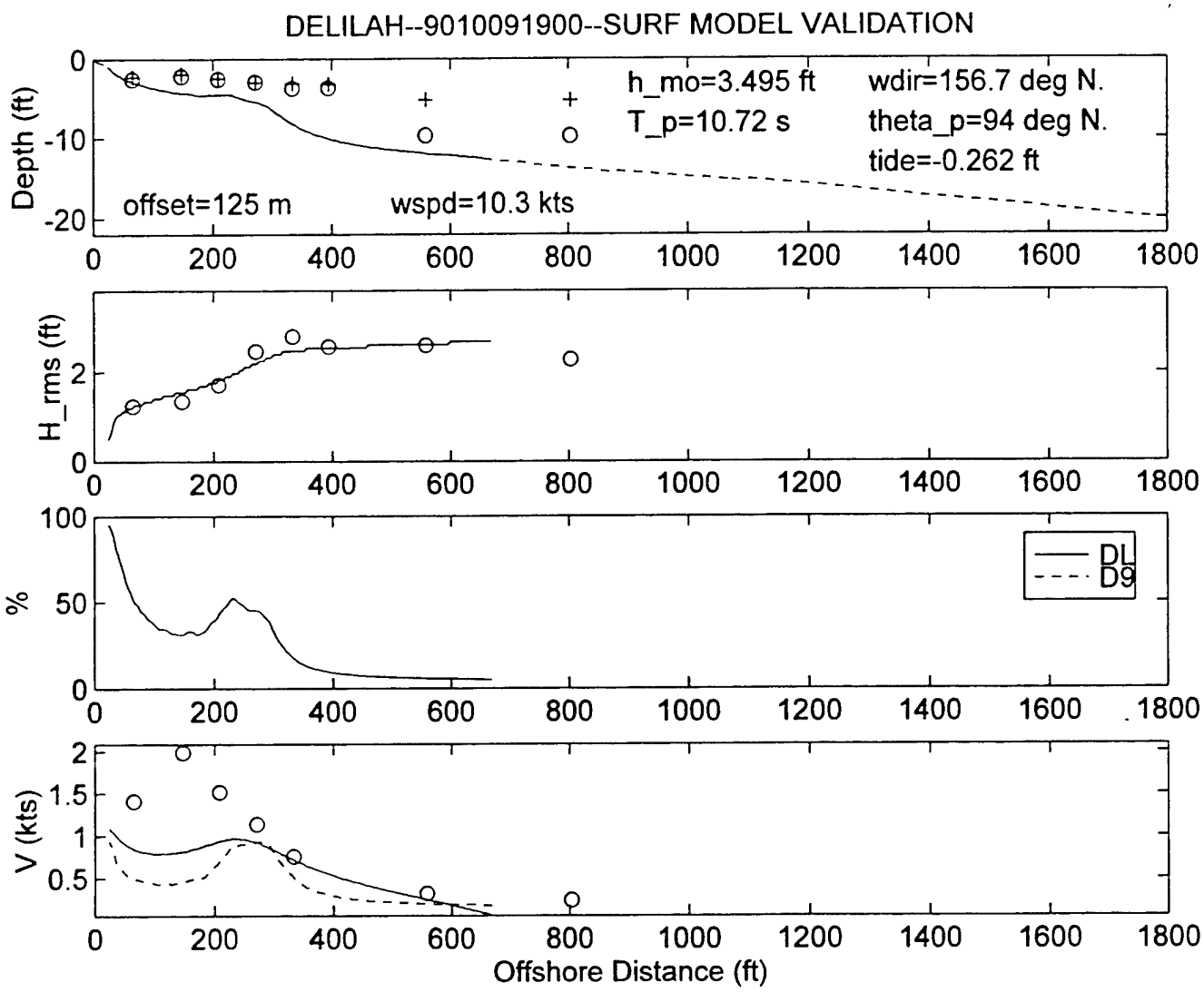
DELILAH--9010091900--SURF MODEL VALIDATION
Depth (ft)
h_mo=3.495 ft
T_p=10.72 s
wdir=156.7 deg N.
theta_p=94 deg N.
tide=-0.262 ft
offset=125 m
wspd=10.3 kts
H_rms (ft)
%
DL
D9
V (kts)
Offshore Distance (ft)

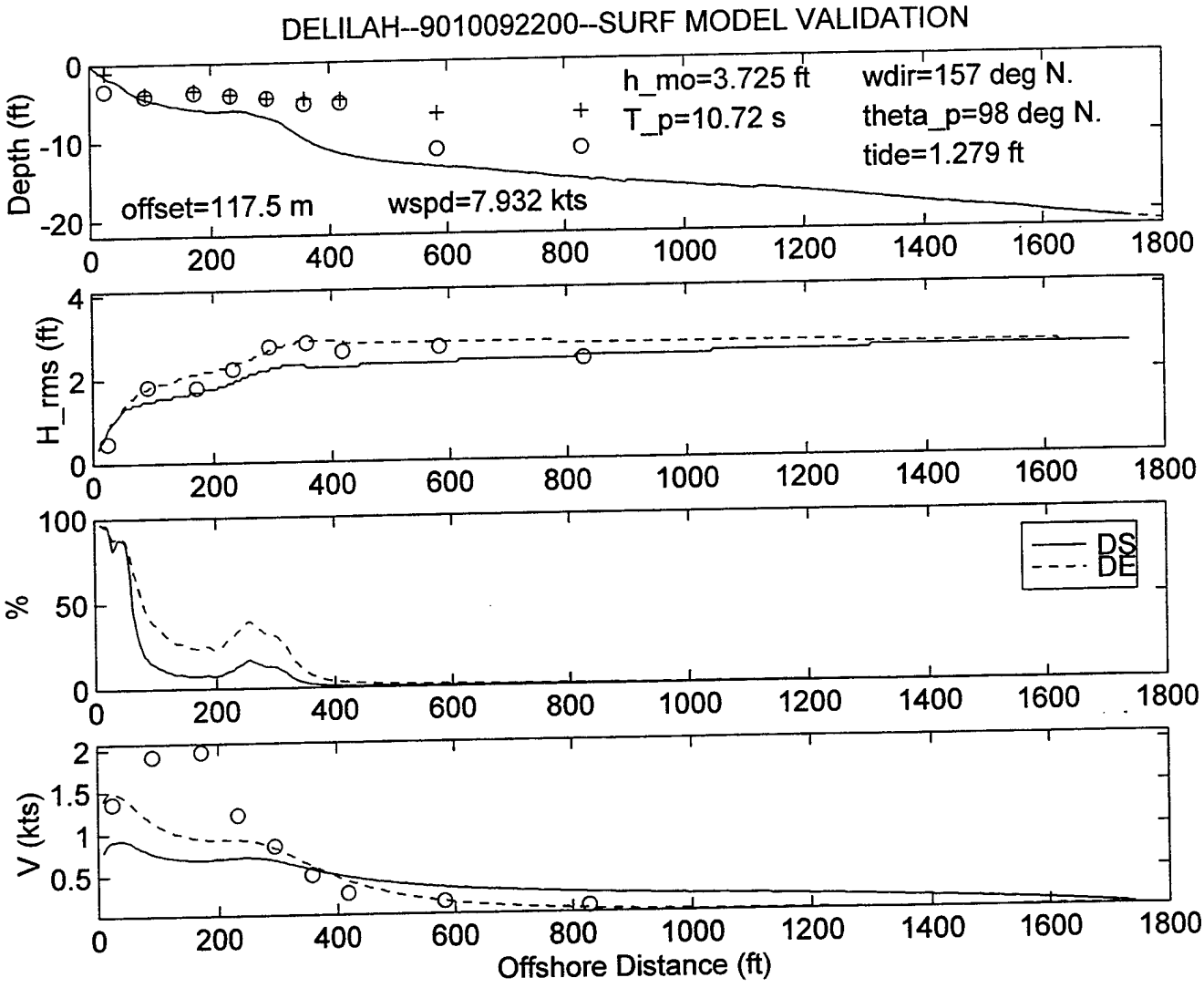
DELILAH--9010092200--SURF MODEL VALIDATION
Depth (ft)
h_mo=3.725 ft
T_p=10.72 s
wdir=157 deg N.
theta_p=98 deg N.
tide=1.279 ft
offset=117.5 m
wspd=7.932 kts
H_rms (ft)
%
DS
DE
V (kts)
Offshore Distance (ft)

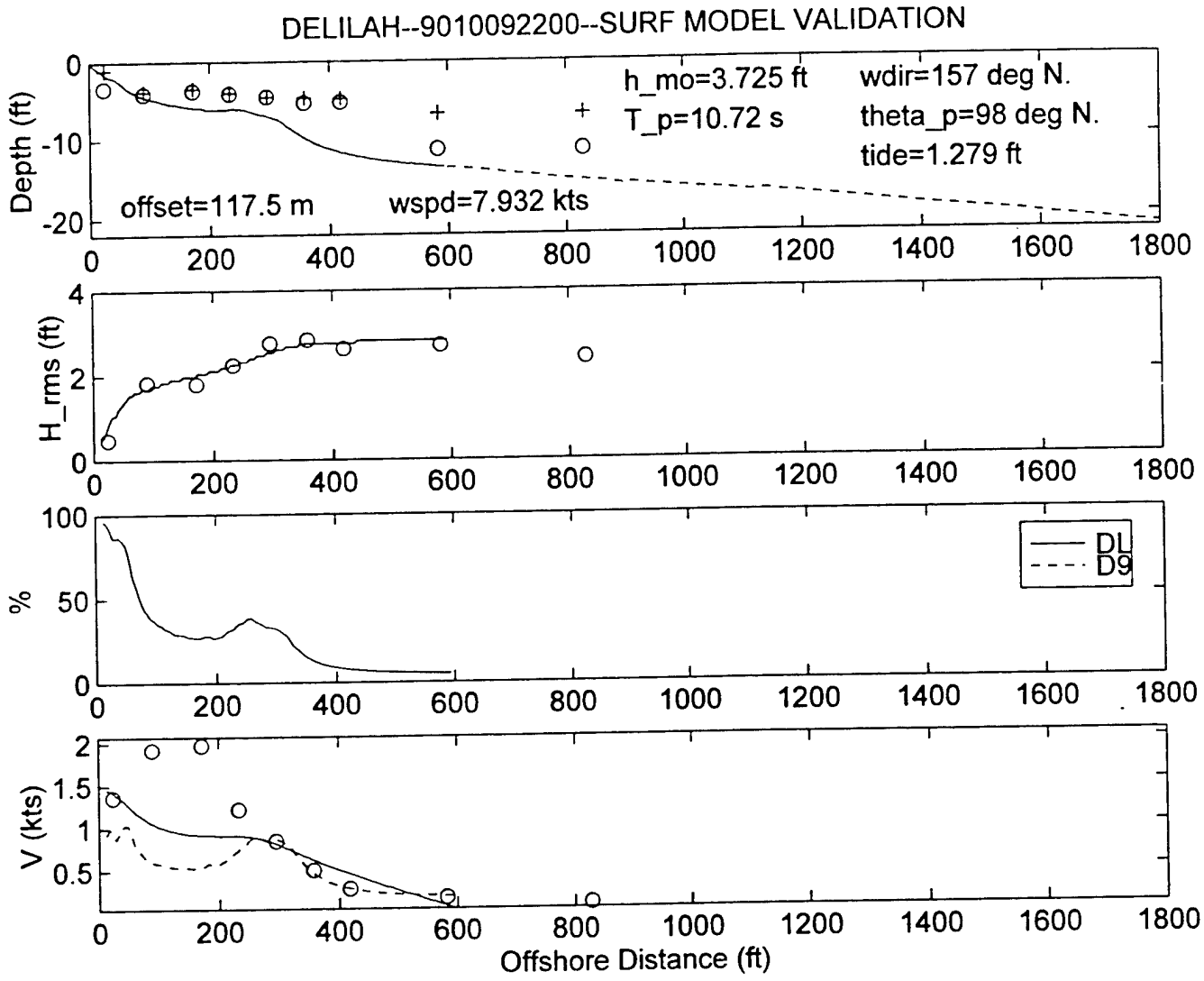
DELILAH--9010092200--SURF MODEL VALIDATION
Depth (ft)
h_mo=3.725 ft
T_p=10.72 s
wdir=157 deg N.
theta_p=98 deg N.
tide=1.279 ft
offset=117.5 m
wspd=7.932 kts
H_rms (ft)
%
DL
D9
V (kts)
Offshore Distance (ft)

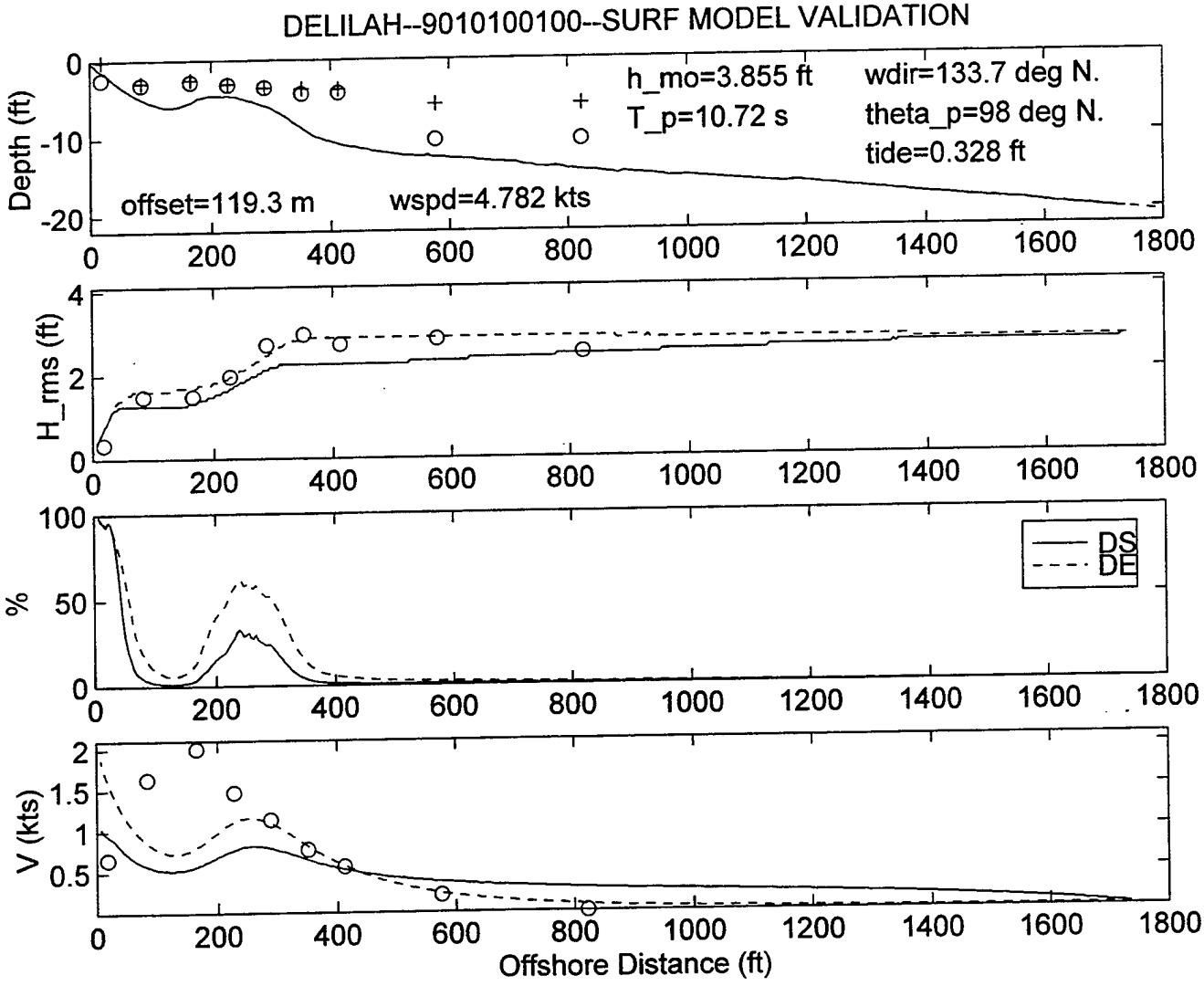
DELILAH--9010100100--SURF MODEL VALIDATION
Depth (ft)
h_mo=3.855 ft
T_p=10.72 s
wdir=133.7 deg N.
theta_p=98 deg N.
tide=0.328 ft
offset=119.3 m
wspd=4.782 kts
H_rms (ft)
%
DS
DE
V (kts)
Offshore Distance (ft)

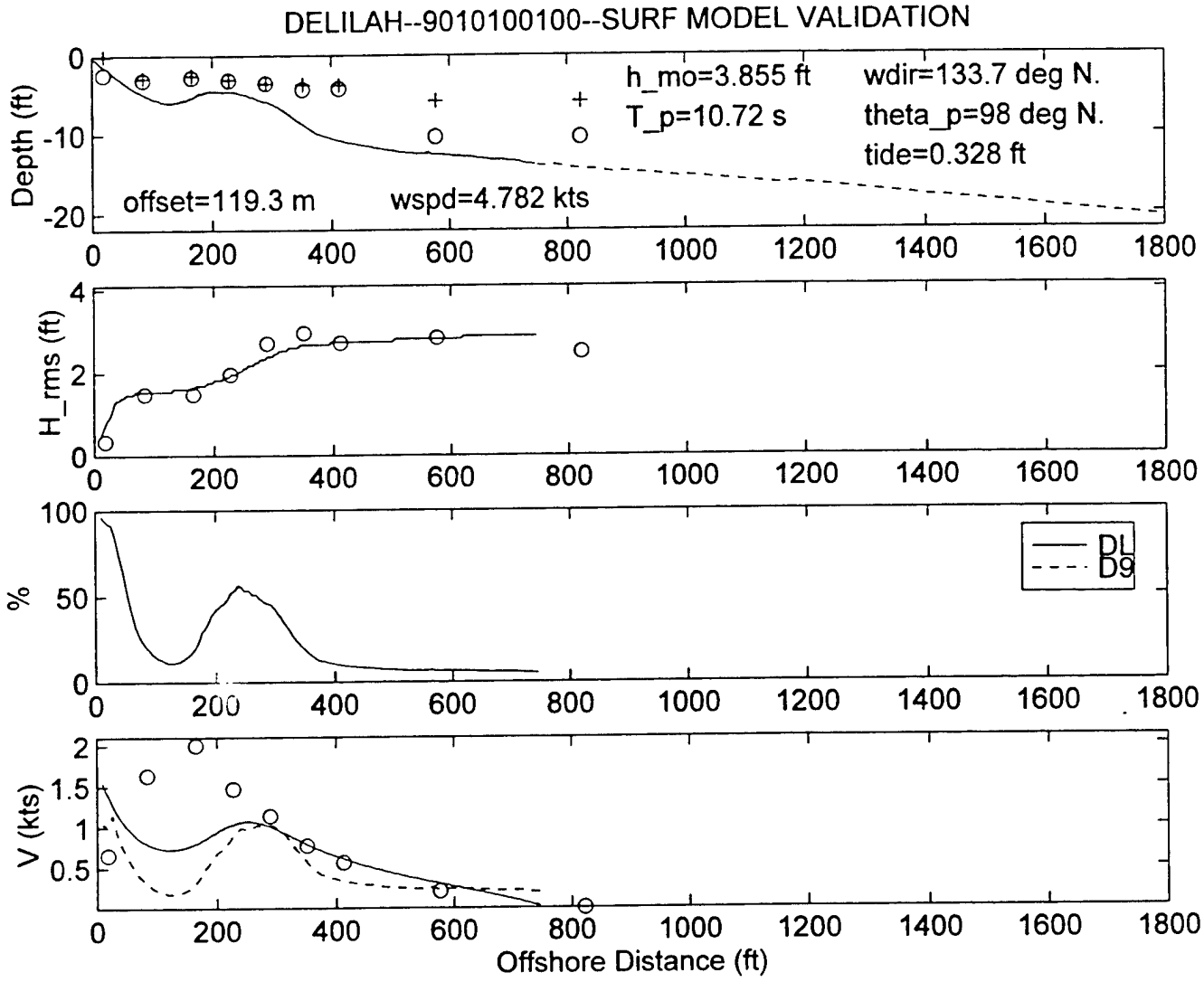
DELILAH--9010100100--SURF MODEL VALIDATION
Depth (ft)
h_mo=3.855 ft
T_p=10.72 s
wdir=133.7 deg N.
theta_p=98 deg N.
tide=0.328 ft
offset=119.3 m
wspd=4.782 kts
H_rms (ft)
%
DL
D9
V (kts)
Offshore Distance (ft)

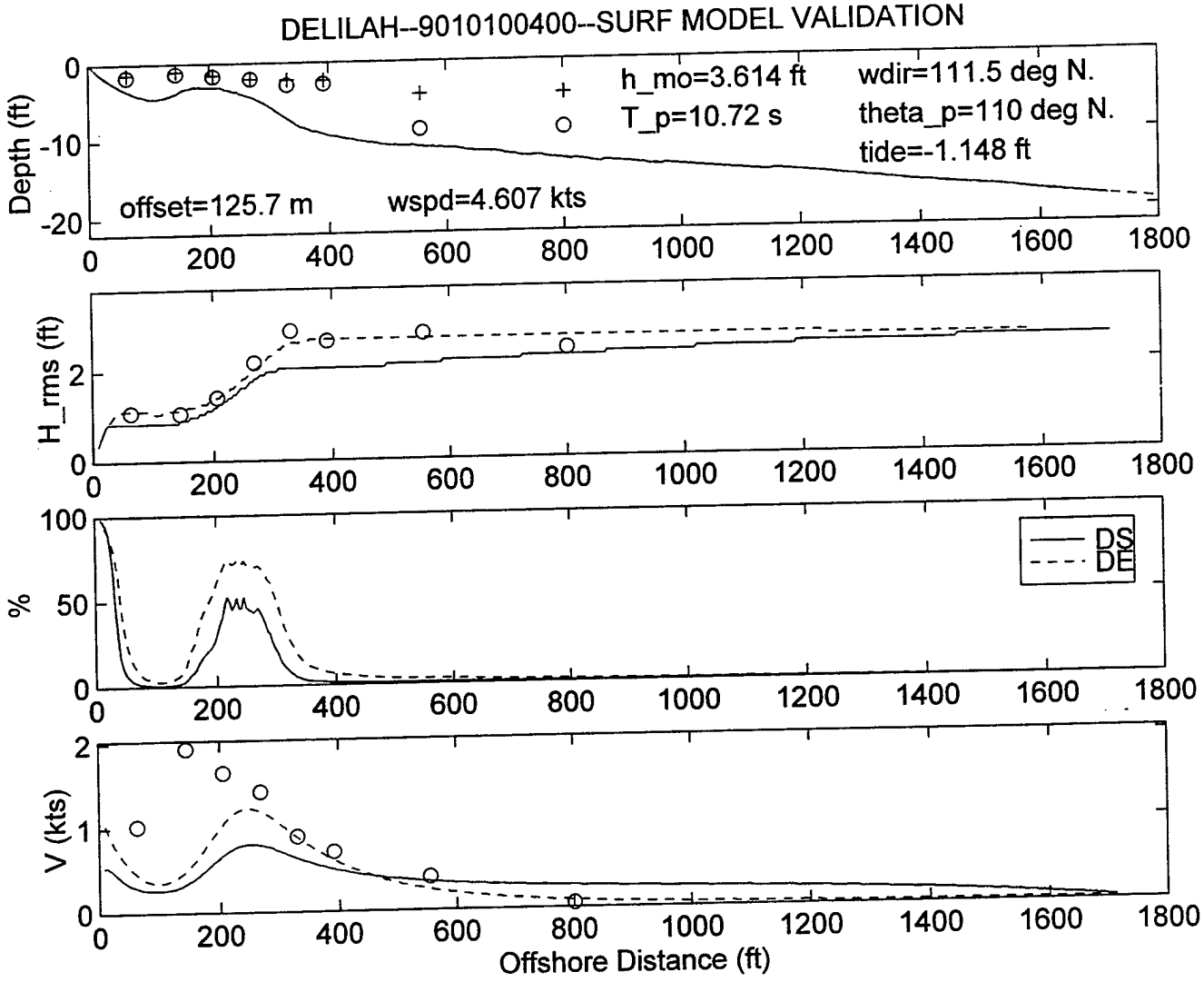
DELILAH--9010100400--SURF MODEL VALIDATION
Depth (ft)
h_mo=3.614 ft
T_p=10.72 s
wdir=111.5 deg N.
theta_p=110 deg N.
tide=-1.148 ft
offset=125.7 m
wspd=4.607 kts
H_rms (ft)
%
DS
DE
V (kts)
Offshore Distance (ft)

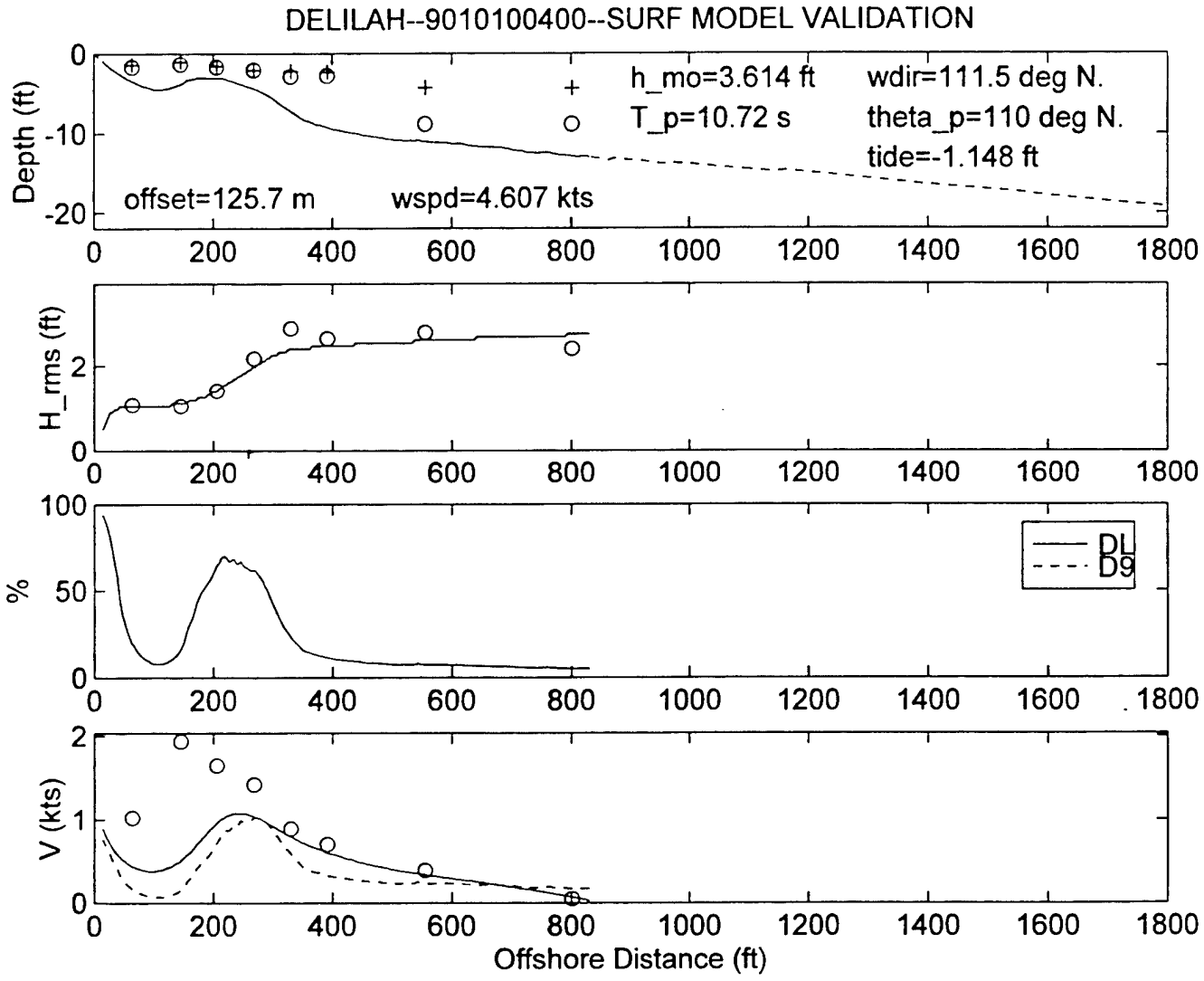
DELILAH--9010100400--SURF MODEL VALIDATION
Depth (ft)
h_mo=3.614 ft
T_p=10.72 s
wdir=111.5 deg N.
theta_p=110 deg N.
tide=-1.148 ft
offset=125.7 m
wspd=4.607 kts
H_rms (ft)
%
DL
D9
V (kts)
Offshore Distance (ft)

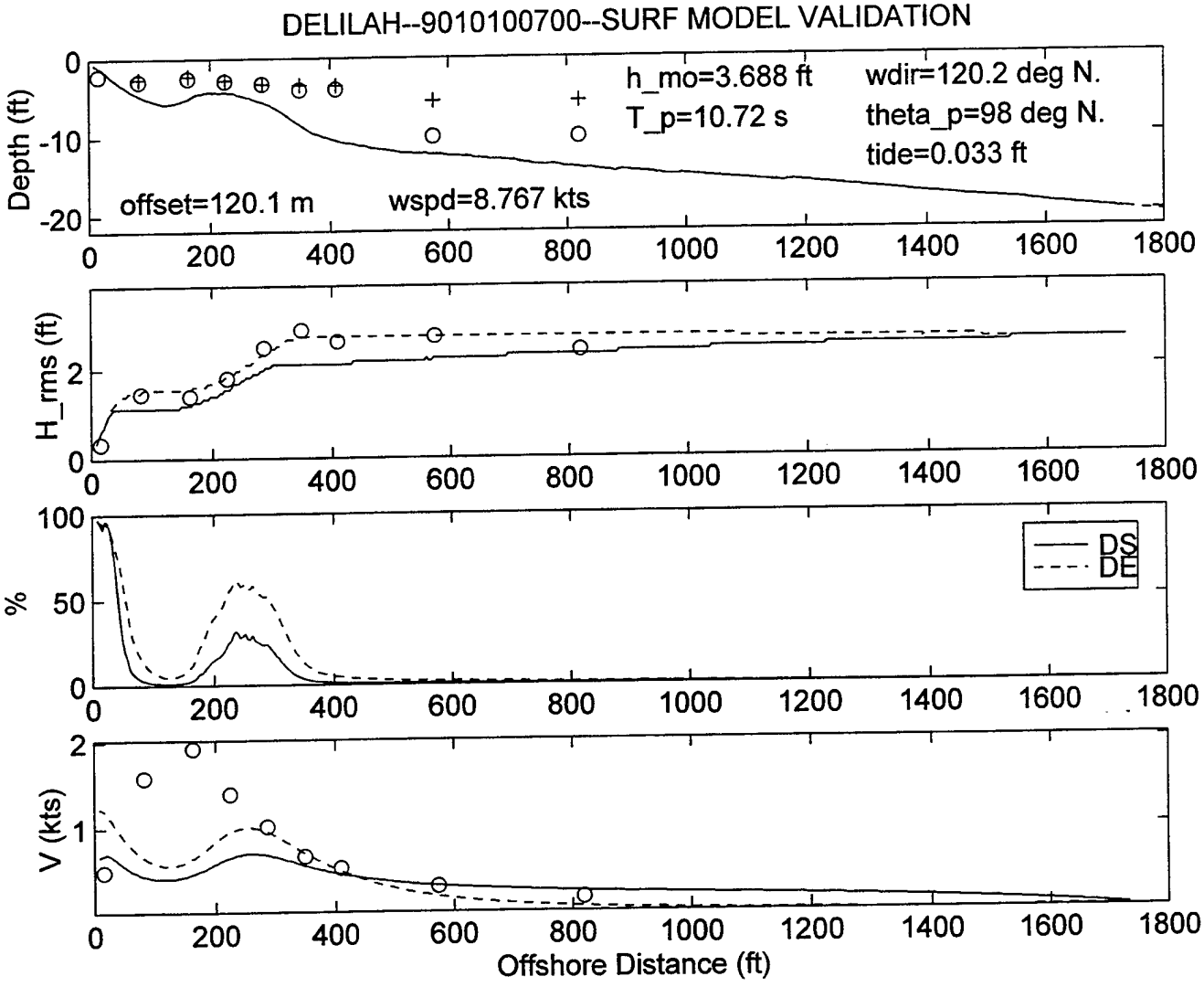
DELILAH--9010100700--SURF MODEL VALIDATION
Depth (ft)
h_mo=3.688 ft
T_p=10.72 s
wdir=120.2 deg N.
theta_p=98 deg N.
tide=0.033 ft
offset=120.1 m
wspd=8.767 kts
H_rms (ft)
%
DS
DE
V (kts)
Offshore Distance (ft)

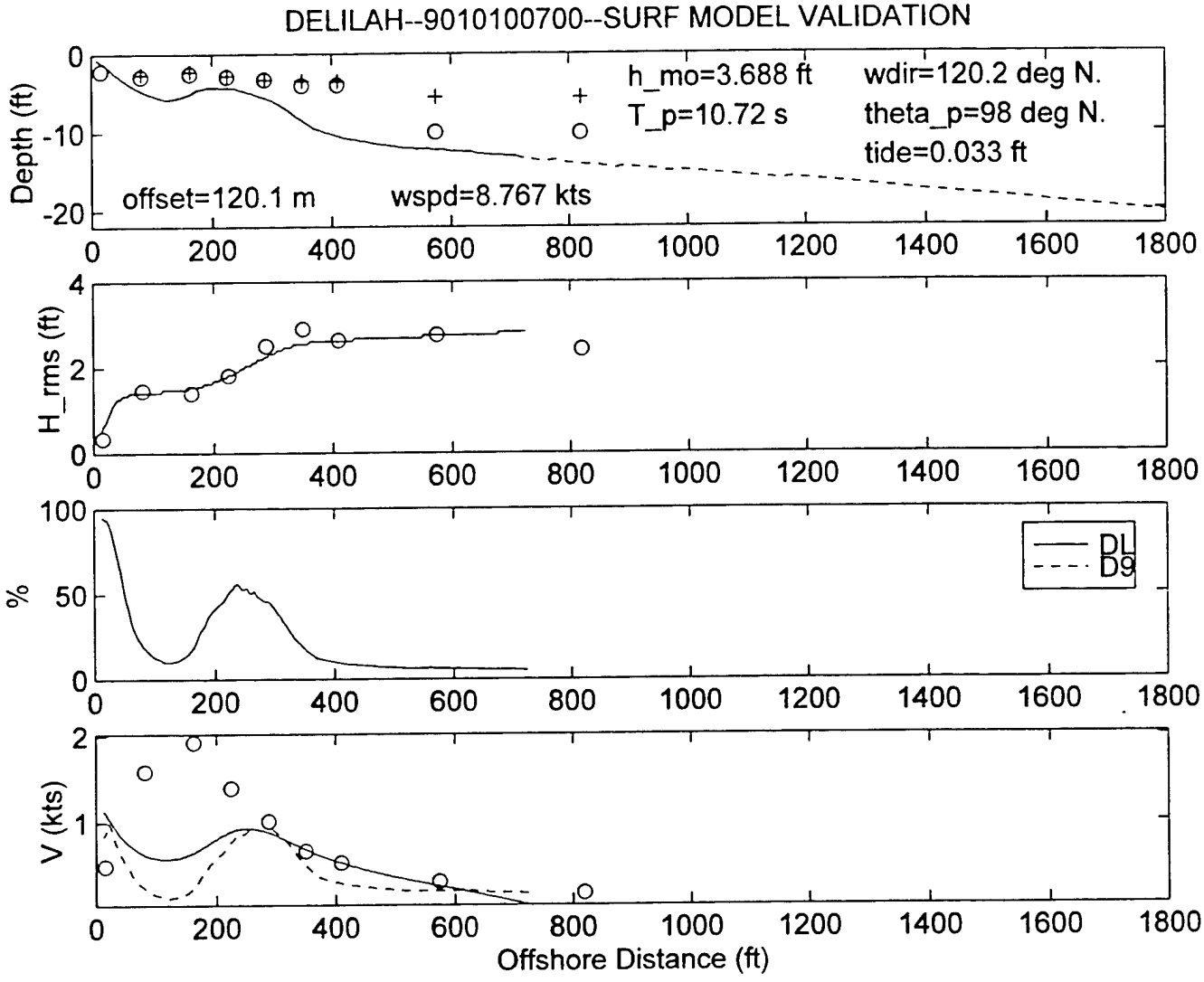
DELILAH--9010100700--SURF MODEL VALIDATION
Depth (ft)
h_mo=3.688 ft
T_p=10.72 s
wdir=120.2 deg N.
theta_p=98 deg N.
tide=0.033 ft
offset=120.1 m
wspd=8.767 kts
H_rms (ft)
%
DL
D9
V (kts)
Offshore Distance (ft)

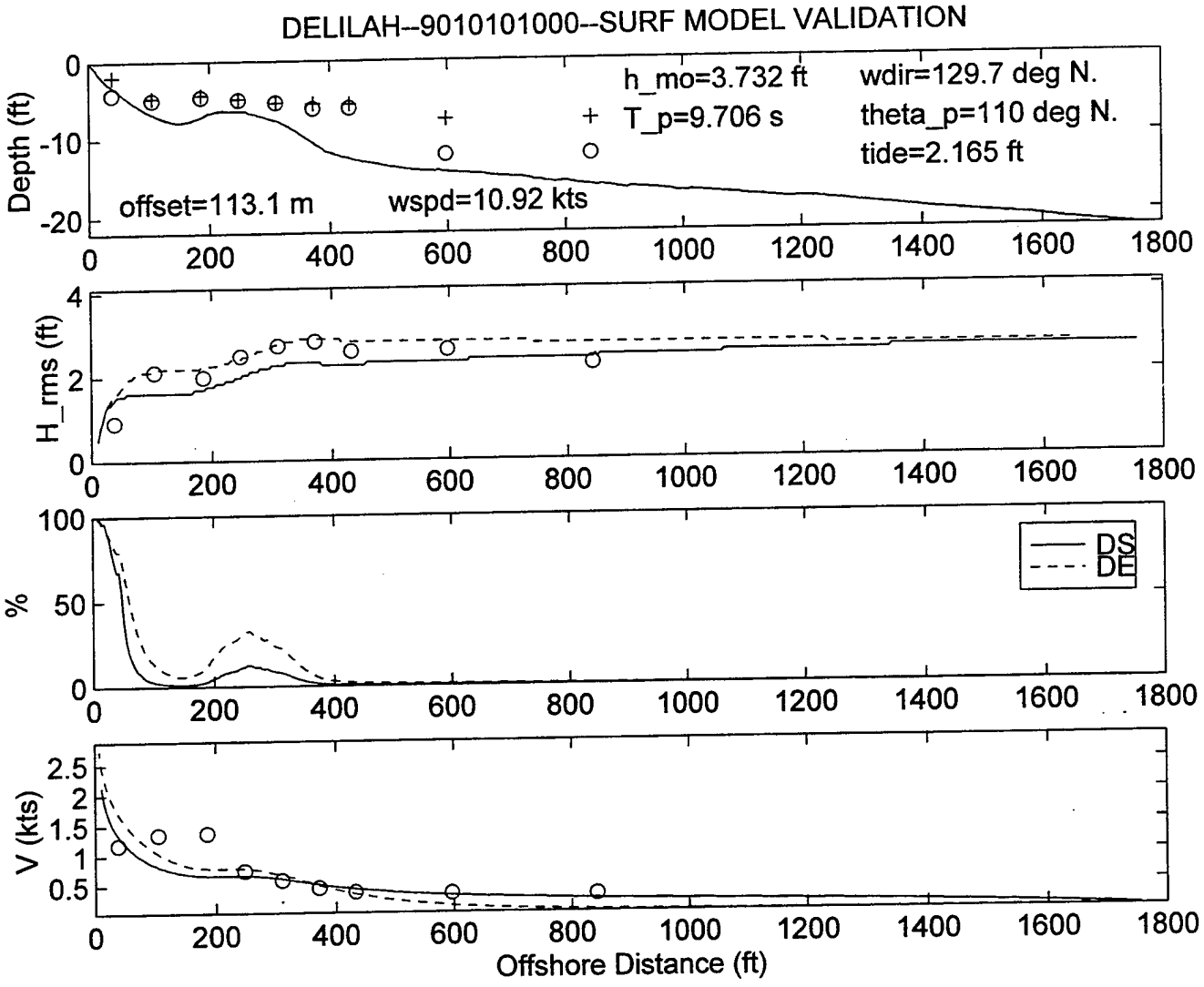
DELILAH--9010101000--SURF MODEL VALIDATION
h_mo=3.732 ft
T_p=9.706 s
wdir=129.7 deg N.
theta_p=110 deg N.
tide=2.165 ft
offset=113.1 m
wspd=10.92 kts
Depth (ft)
H_rms (ft)
%
DS
DE
V (kts)
Offshore Distance (ft)

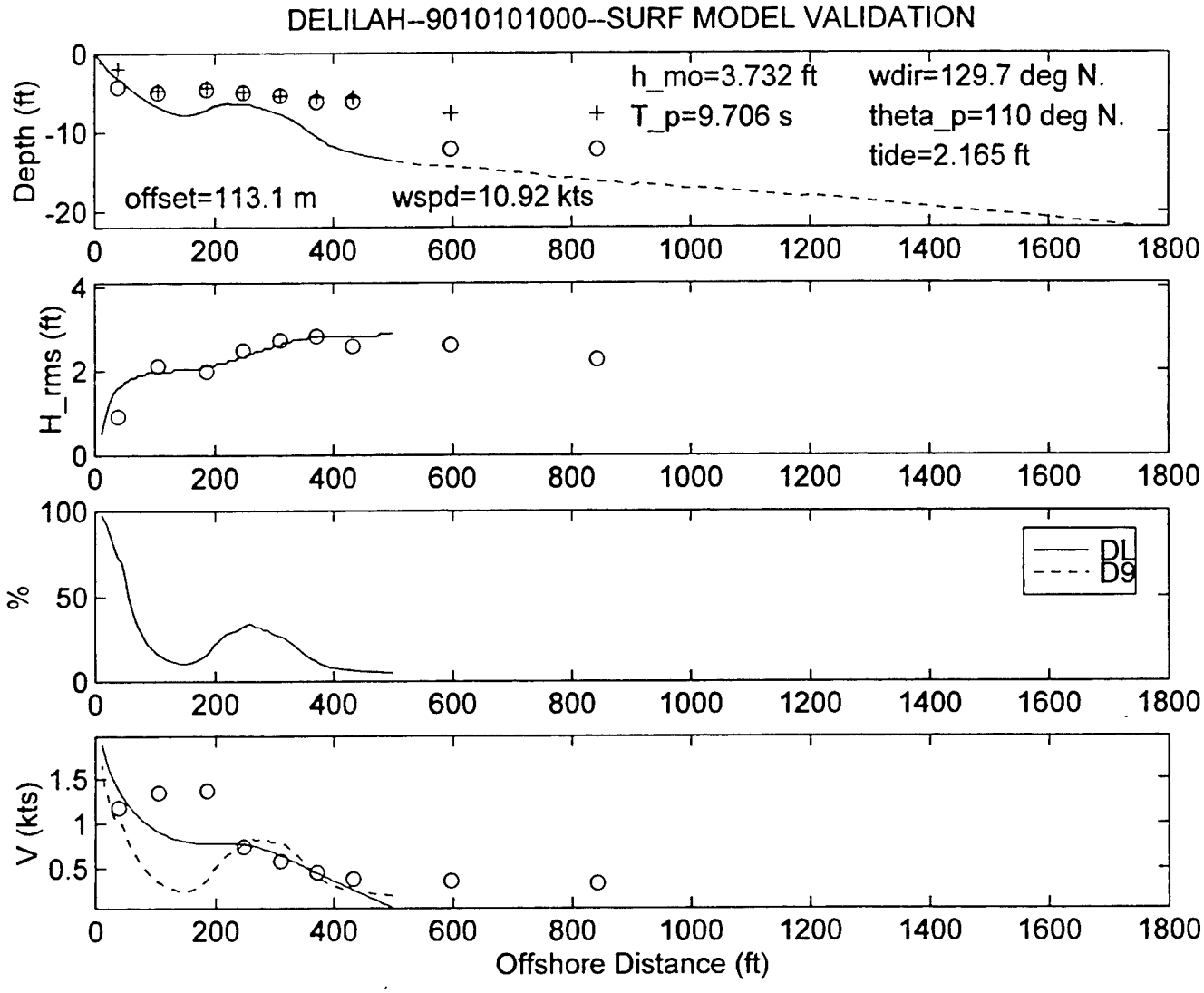
DELILAH--9010101000--SURF MODEL VALIDATION
Depth (ft)
h_mo=3.732 ft
T_p=9.706 s
wdir=129.7 deg N.
theta_p=110 deg N.
tide=2.165 ft
offset=113.1 m
wspd=10.92 kts
H_rms (ft)
%
DL
D9
V (kts)
Offshore Distance (ft)

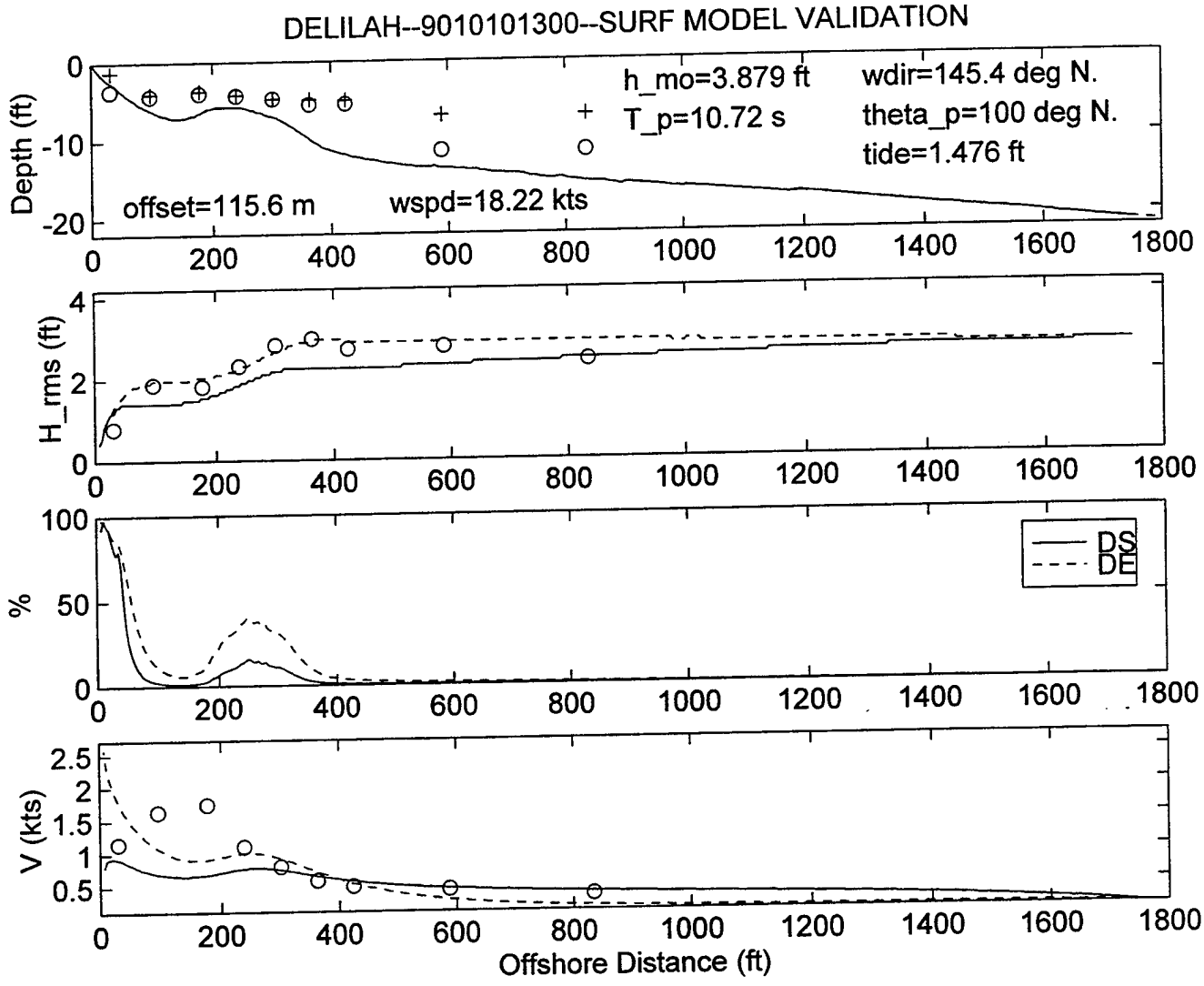
DELILAH--9010101300--SURF MODEL VALIDATION
Depth (ft)
h_mo=3.879 ft
T_p=10.72 s
wdir=145.4 deg N.
theta_p=100 deg N.
tide=1.476 ft
offset=115.6 m
wspd=18.22 kts
H_rms (ft)
%
DS
DE
V (kts)
Offshore Distance (ft)

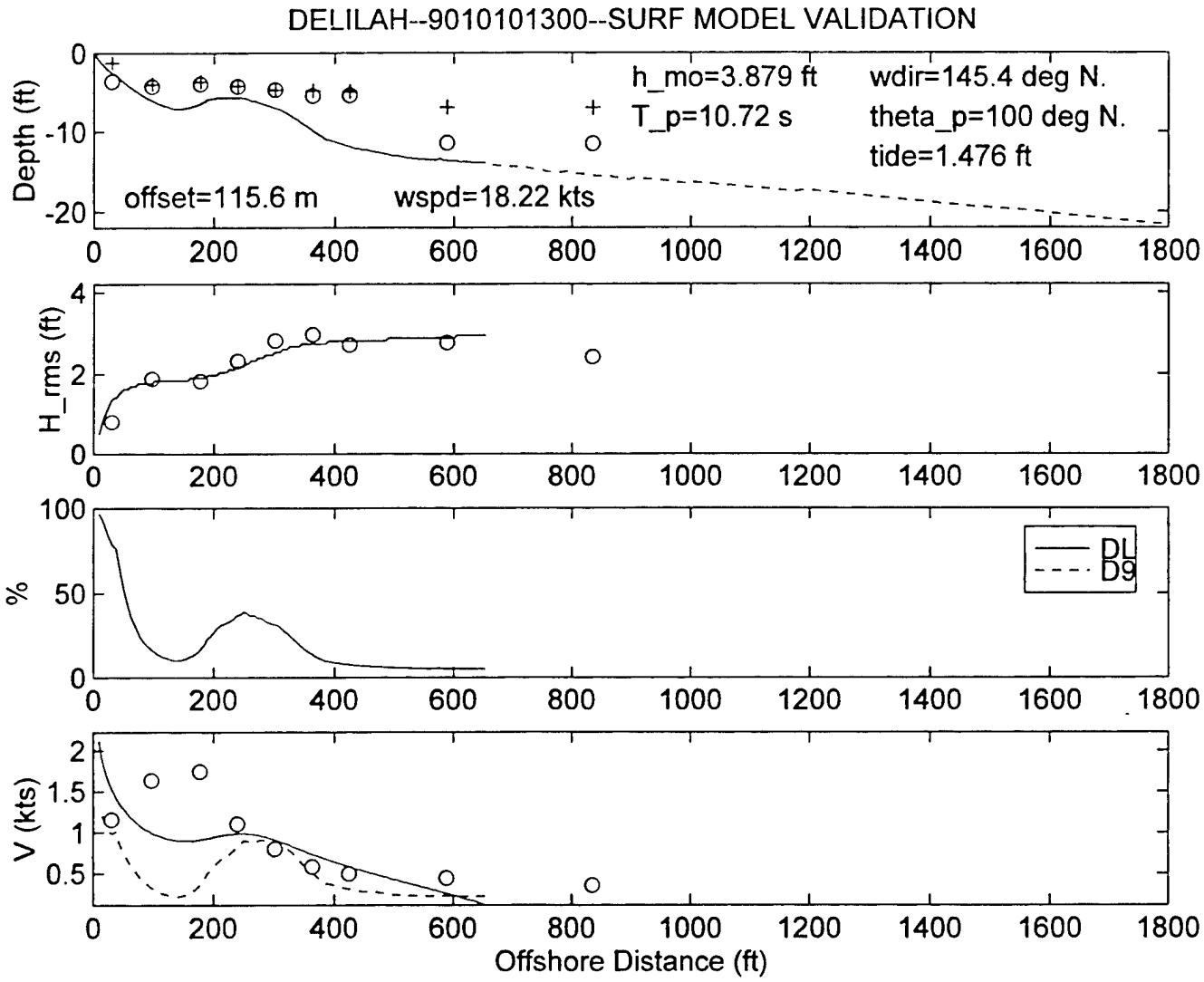
DELILAH--9010101300--SURF MODEL VALIDATION
Depth (ft)
h_mo=3.879 ft
T_p=10.72 s
wdir=145.4 deg N.
theta_p=100 deg N.
tide=1.476 ft
offset=115.6 m
wspd=18.22 kts
H_rms (ft)
%
DL
D9
V (kts)
Offshore Distance (ft)

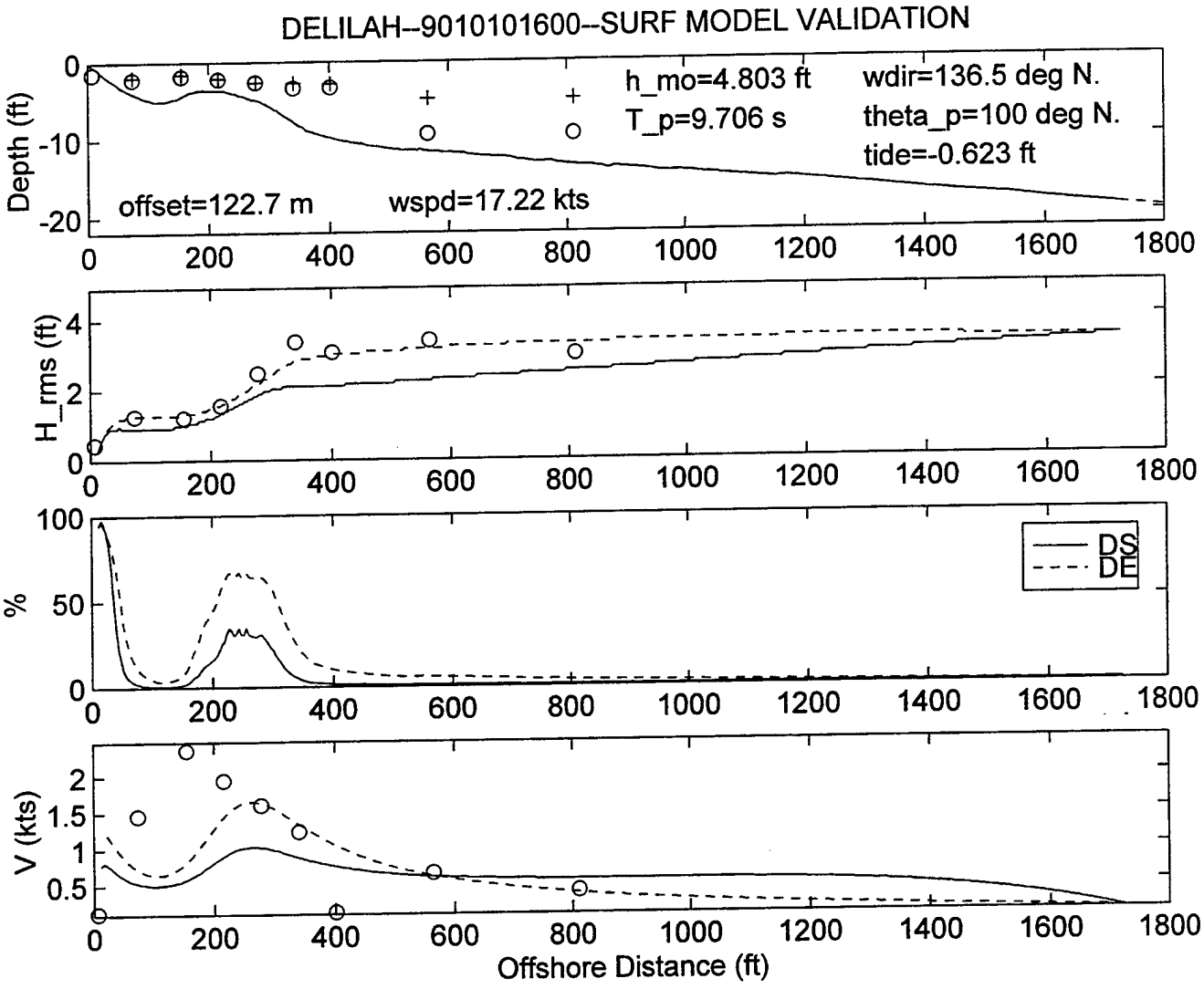
DELILAH--9010101600--SURF MODEL VALIDATION
Depth (ft)
h_mo=4.803 ft
T_p=9.706 s
wdir=136.5 deg N.
theta_p=100 deg N.
tide=-0.623 ft
offset=122.7 m
wspd=17.22 kts
H_rms (ft)
%
DS
DE
V (kts)
Offshore Distance (ft)

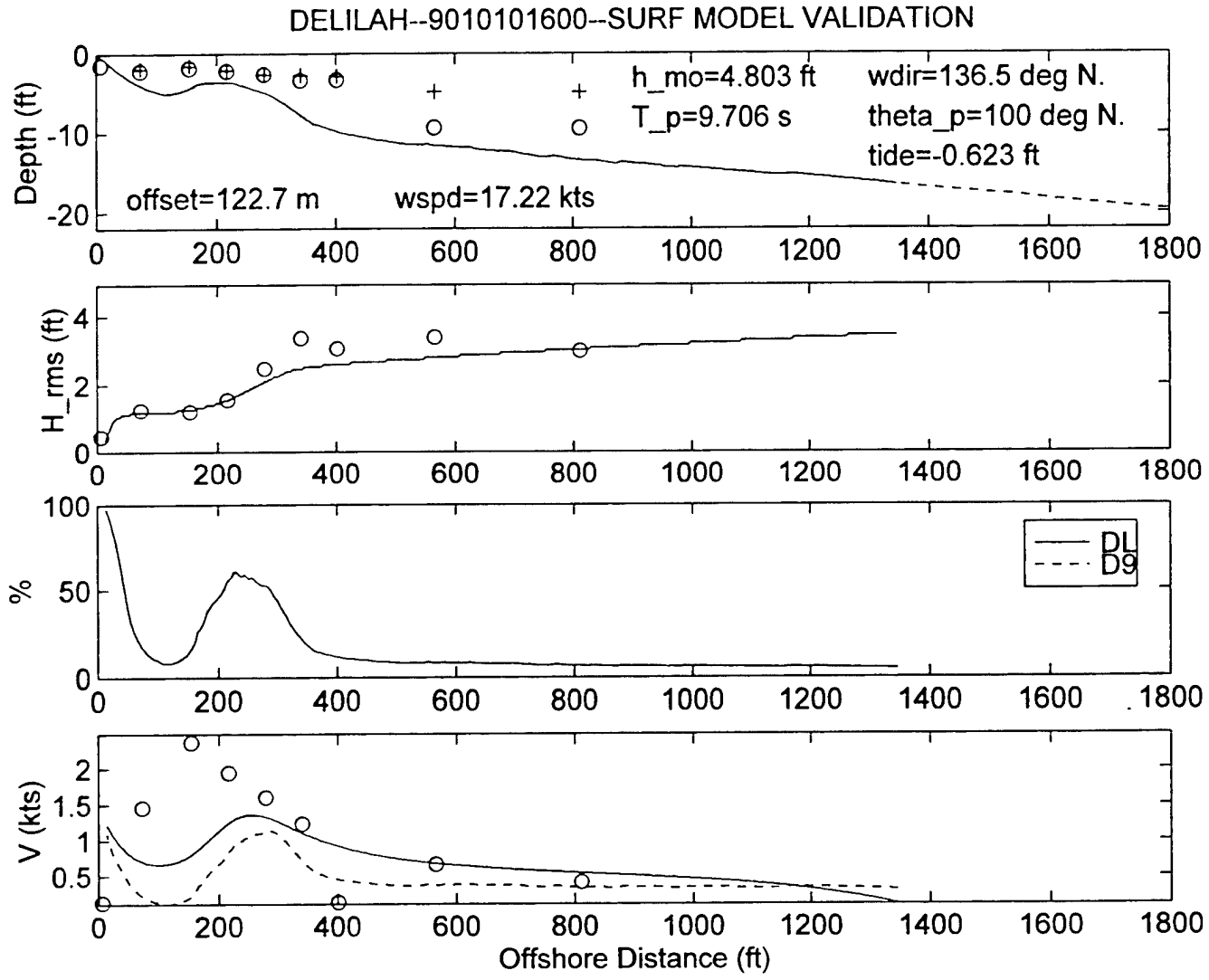
DELILAH--9010101600--SURF MODEL VALIDATION
Depth (ft)
h_mo=4.803 ft
T_p=9.706 s
wdir=136.5 deg N.
theta_p=100 deg N.
tide=-0.623 ft
offset=122.7 m
wspd=17.22 kts
H_rms (ft)
%
DL
D9
V (kts)
Offshore Distance (ft)

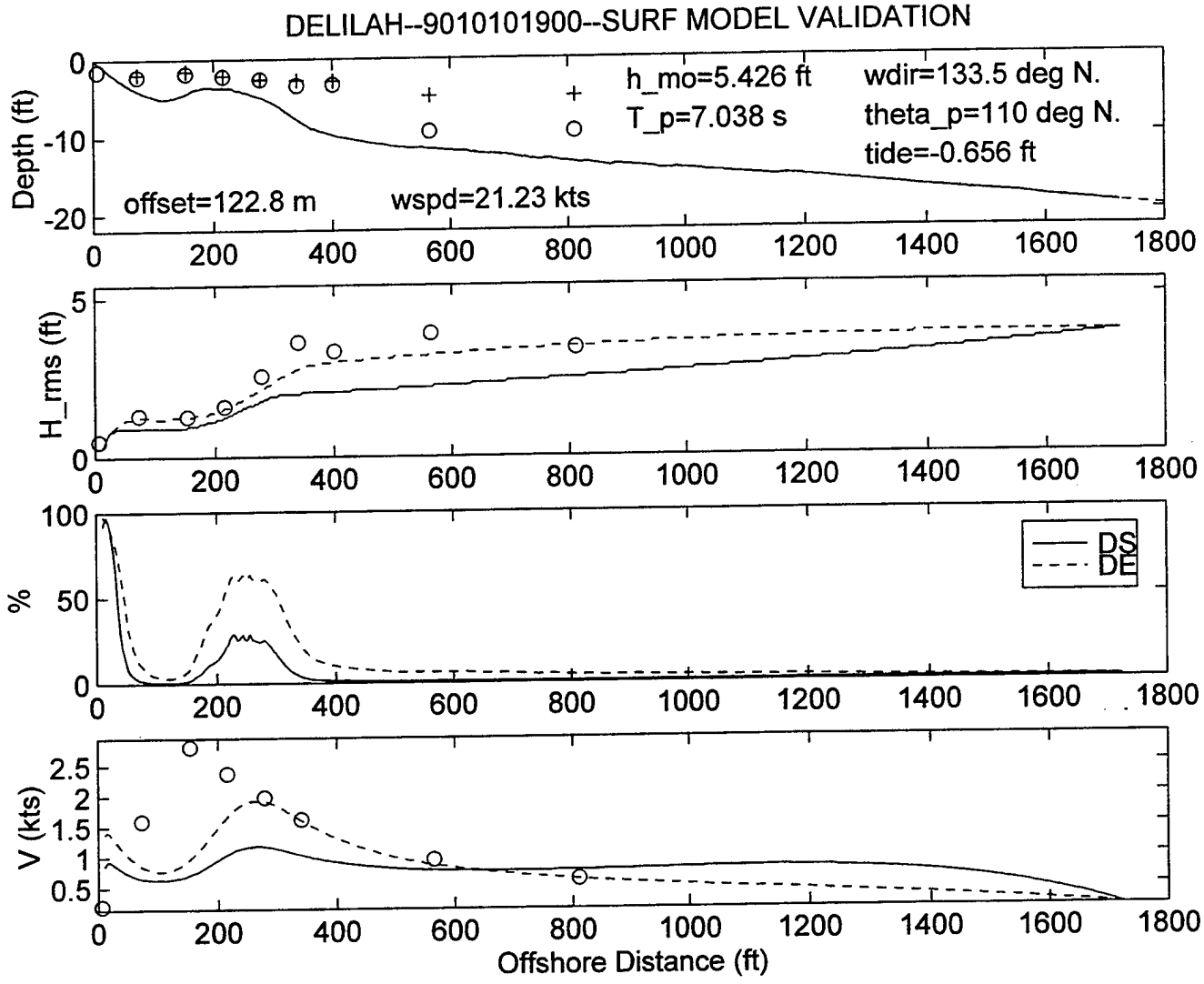
DELILAH--9010101900--SURF MODEL VALIDATION
Depth (ft)
h_mo=5.426 ft
T_p=7.038 s
wdir=133.5 deg N.
theta_p=110 deg N.
tide=-0.656 ft
offset=122.8 m
wspd=21.23 kts
H_rms (ft)
%
DS
DE
V (kts)
Offshore Distance (ft)

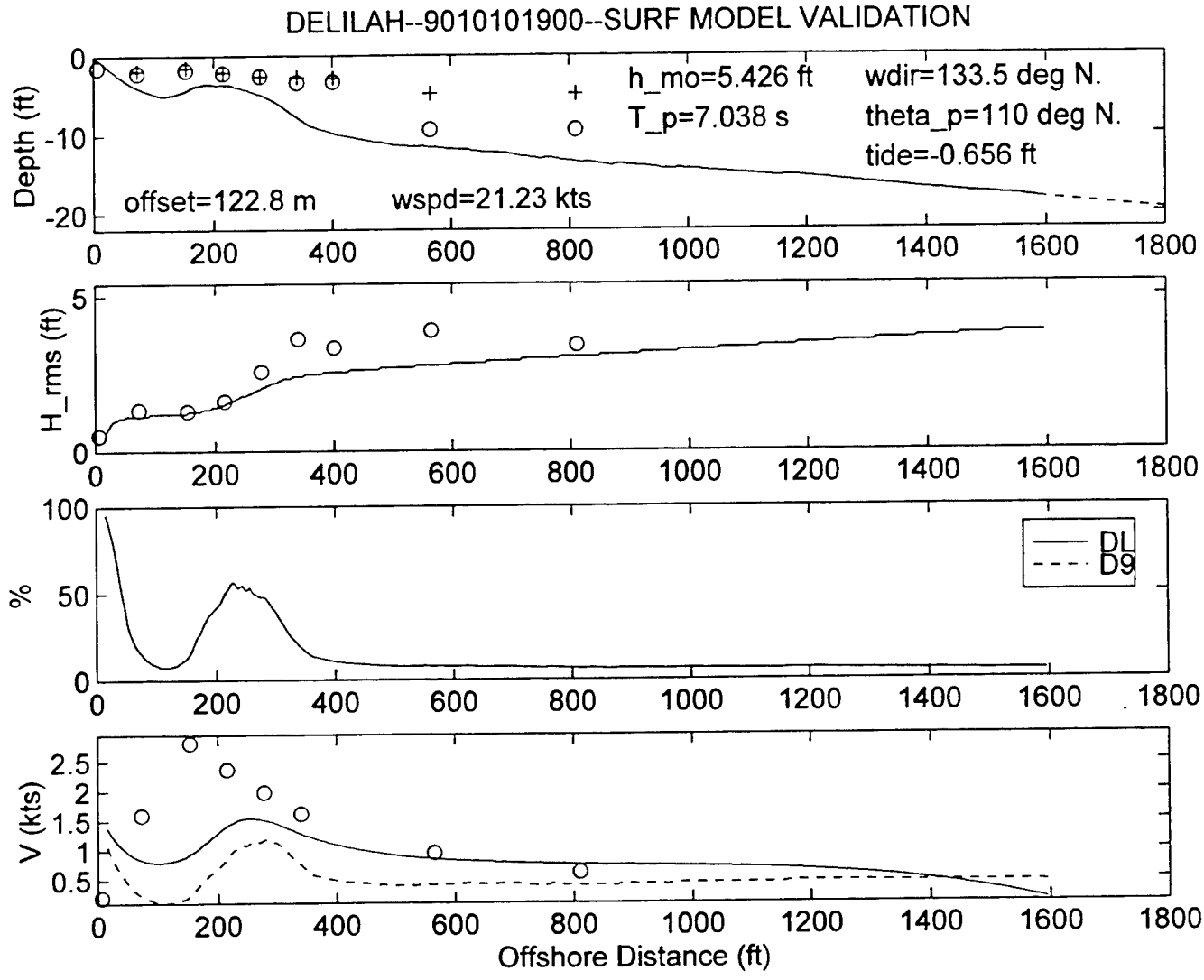
DELILAH--9010101900--SURF MODEL VALIDATION
Depth (ft)
h_mo=5.426 ft
T_p=7.038 s
wdir=133.5 deg N.
theta_p=110 deg N.
tide=-0.656 ft
offset=122.8 m
wspd=21.23 kts
H_rms (ft)
%
DL
D9
V (kts)
Offshore Distance (ft)

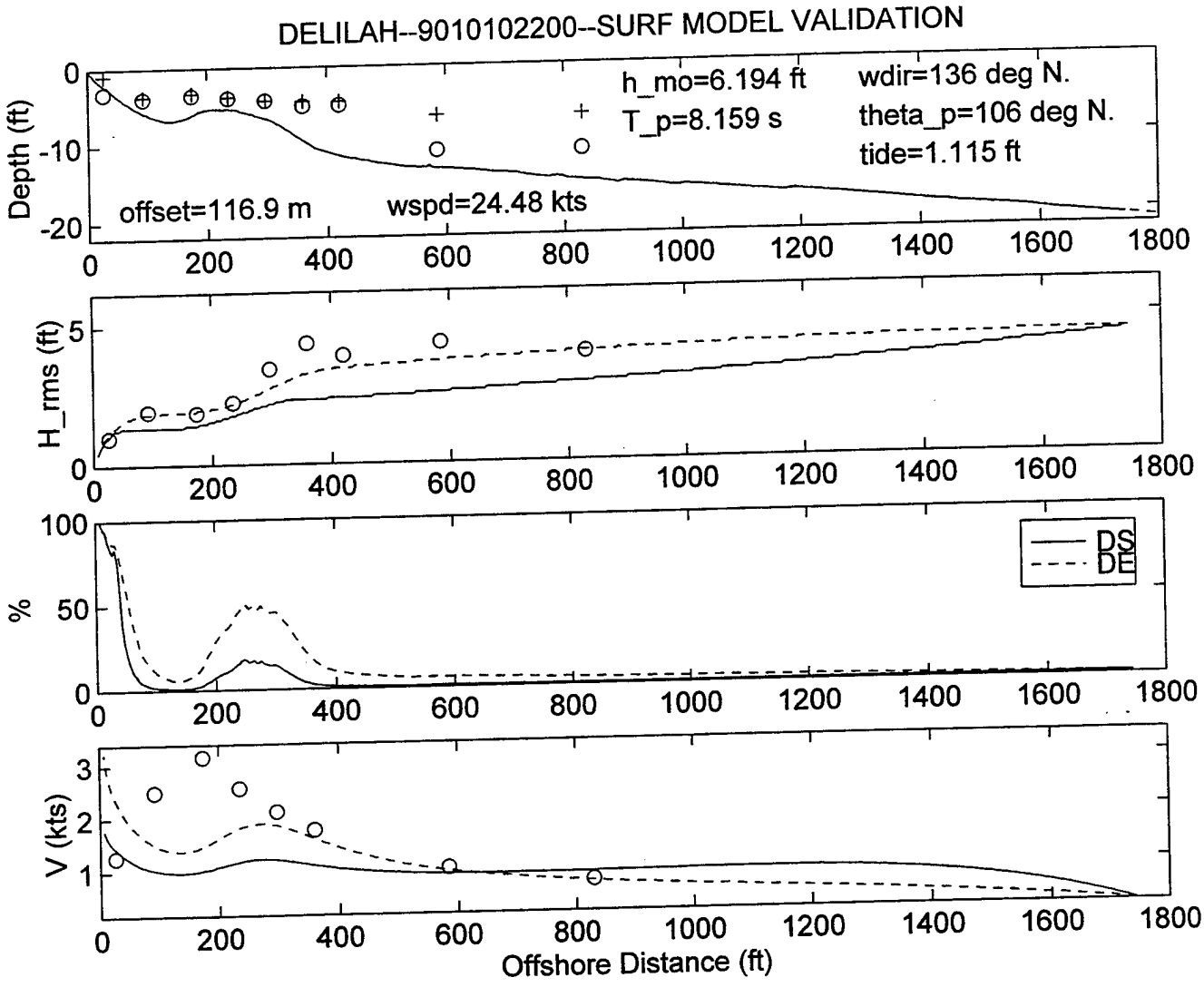
DELILAH--9010102200--SURF MODEL VALIDATION
Depth (ft)
h_mo=6.194 ft
T_p=8.159 s
wdir=136 deg N.
theta_p=106 deg N.
tide=1.115 ft
offset=116.9 m
wspd=24.48 kts
H_rms (ft)
%
DS
DE
V (kts)
Offshore Distance (ft)

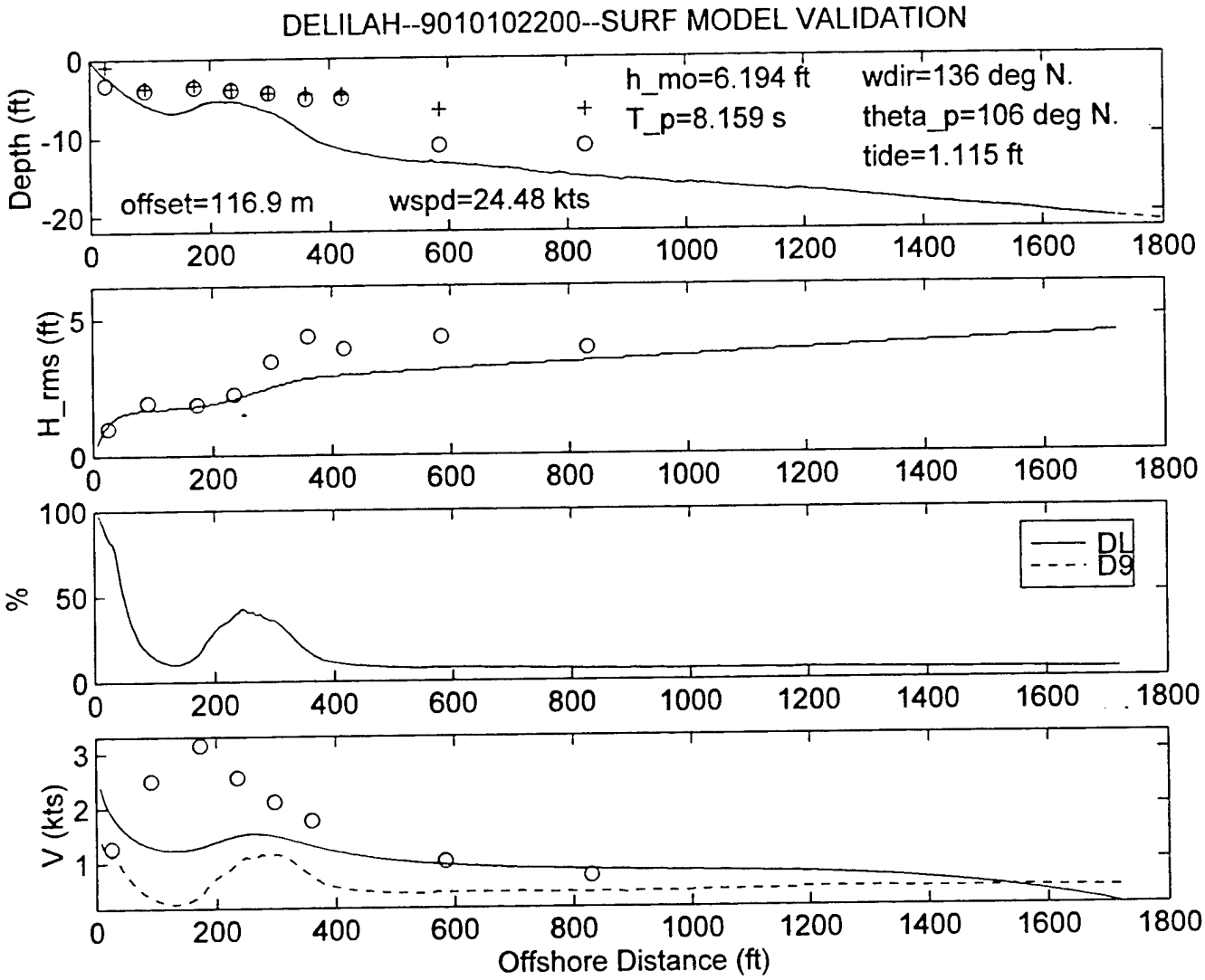
DELILAH--9010102200--SURF MODEL VALIDATION
Depth (ft)
h_mo=6.194 ft
T_p=8.159 s
wdir=136 deg N.
theta_p=106 deg N.
tide=1.115 ft
offset=116.9 m
wspd=24.48 kts
H_rms (ft)
%
DL
D9
V (kts)
Offshore Distance (ft)

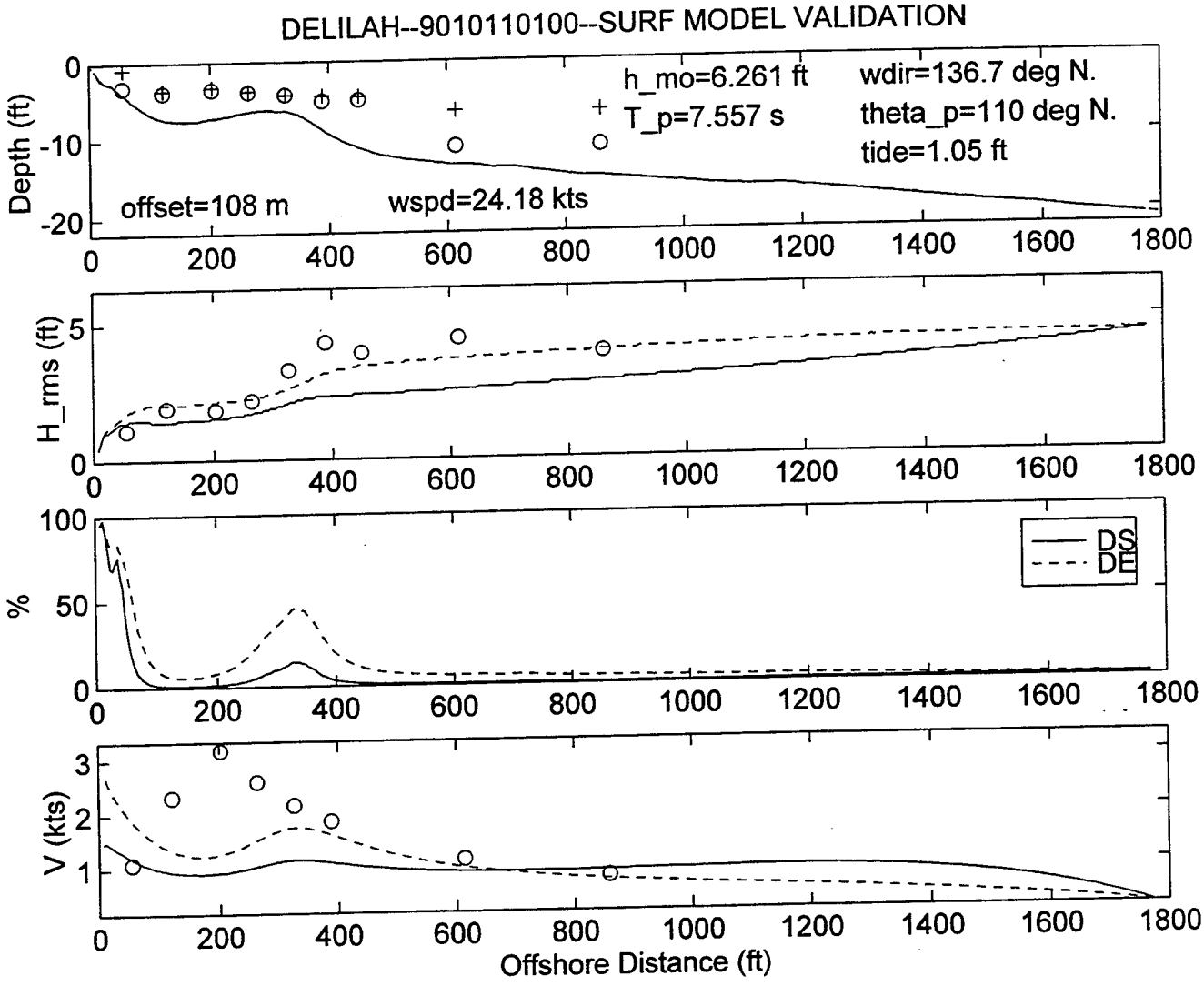
DELILAH--9010110100--SURF MODEL VALIDATION
Depth (ft)
0
-10
-20
h_mo=6.261 ft
T_p=7.557 s
wdir=136.7 deg N.
theta_p=110 deg N.
tide=1.05 ft
offset=108 m
wspd=24.18 kts
0 200 400 600 800 1000 1200 1400 1600 1800
H_rms (ft)
5
0
%
100
50
DS
DE
V (kts)
3
2
1
Offshore Distance (ft)

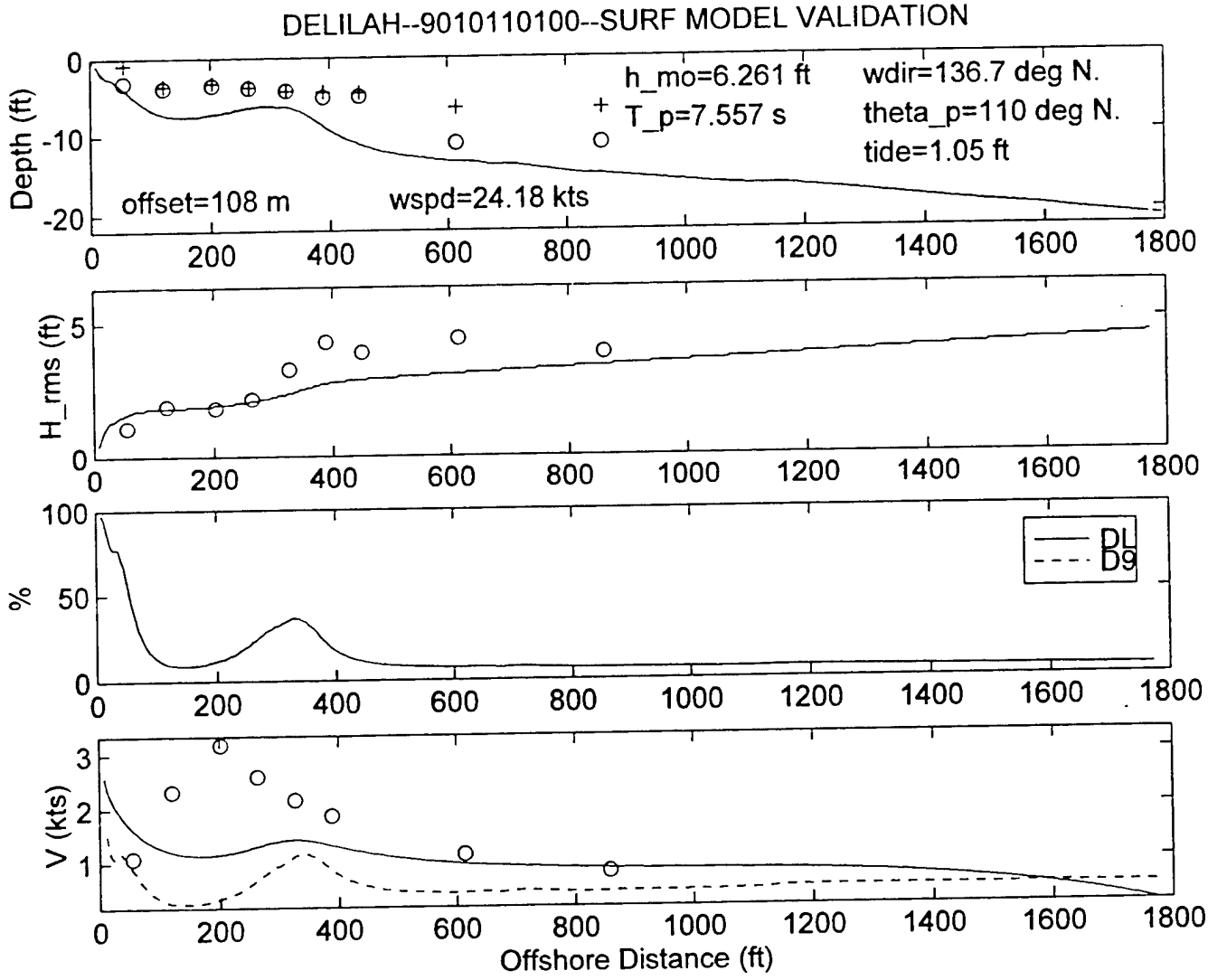
DELILAH--9010110100--SURF MODEL VALIDATION
Depth (ft)
h_mo=6.261 ft
T_p=7.557 s
wdir=136.7 deg N.
theta_p=110 deg N.
tide=1.05 ft
offset=108 m
wspd=24.18 kts
H_rms (ft)
%
DL
D9
V (kts)
Offshore Distance (ft)

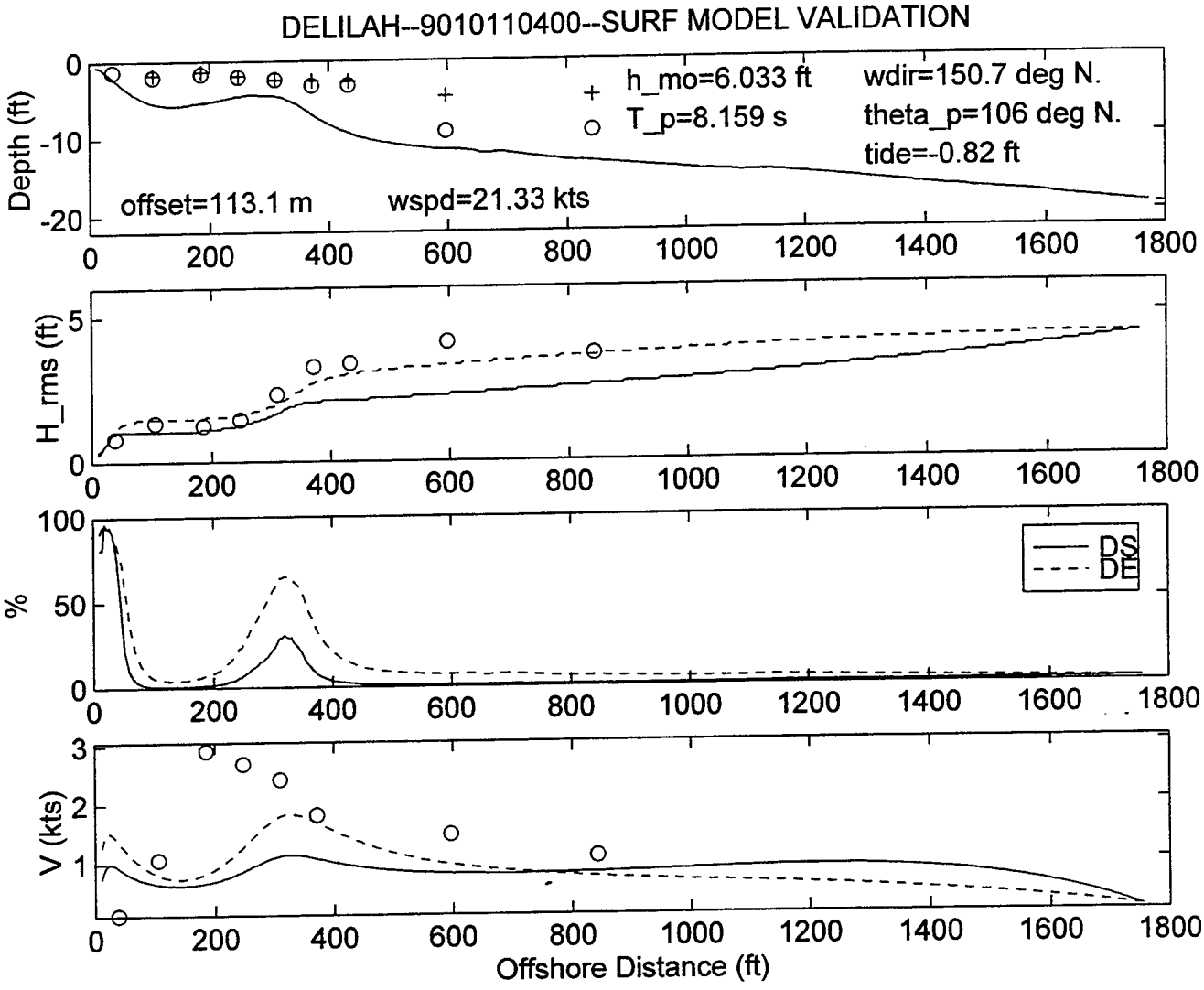
DELILAH--9010110400--SURF MODEL VALIDATION
Depth (ft)
h_mo=6.033 ft
T_p=8.159 s
wdir=150.7 deg N.
theta_p=106 deg N.
tide=-0.82 ft
offset=113.1 m
wspd=21.33 kts
H_rms (ft)
%
DS
DE
V (kts)
Offshore Distance (ft)

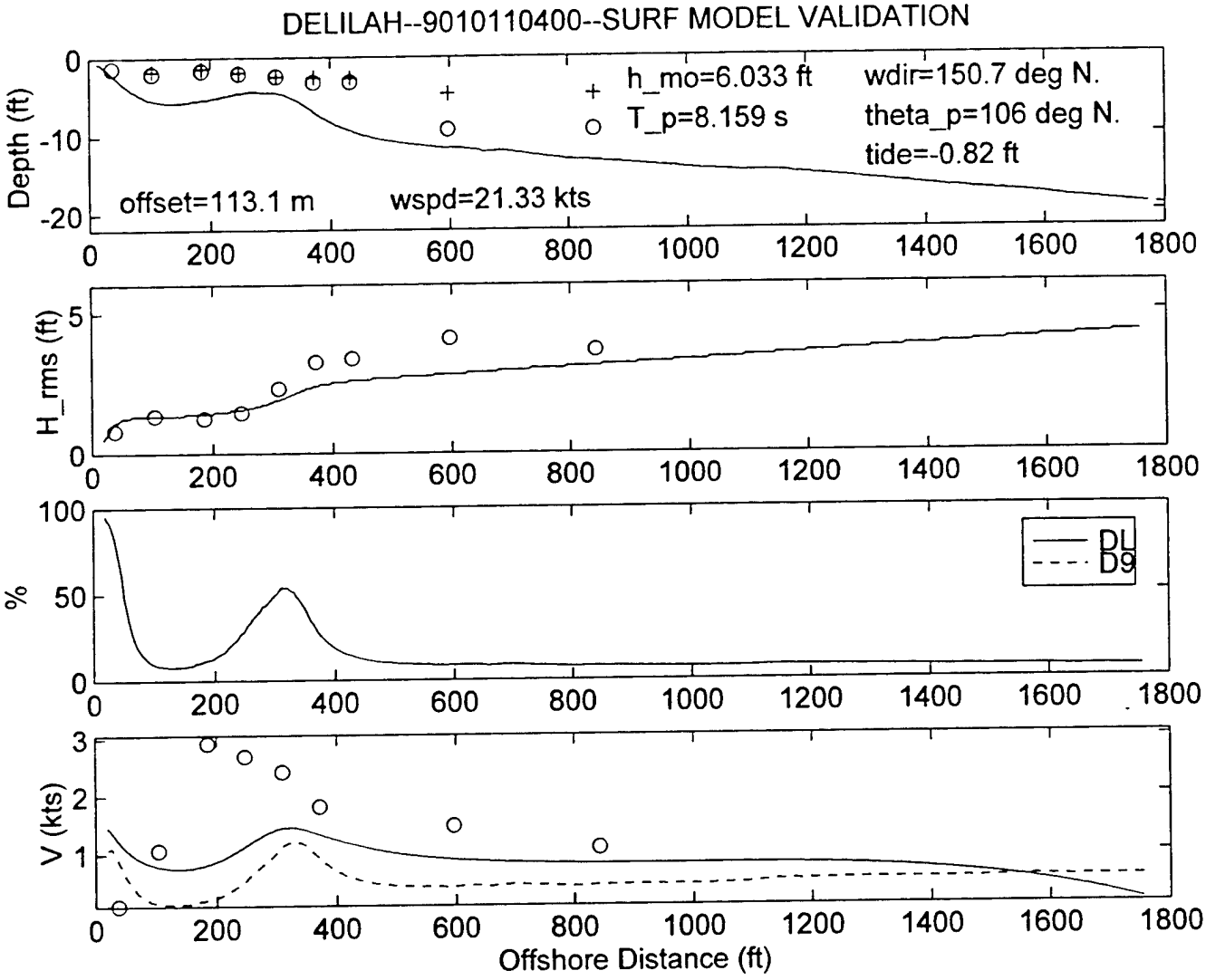
DELILAH--9010110400--SURF MODEL VALIDATION
Depth (ft)
h_mo=6.033 ft
T_p=8.159 s
wdir=150.7 deg N.
theta_p=106 deg N.
tide=-0.82 ft
offset=113.1 m
wspd=21.33 kts
H_rms (ft)
%
DL
D9
V (kts)
Offshore Distance (ft)

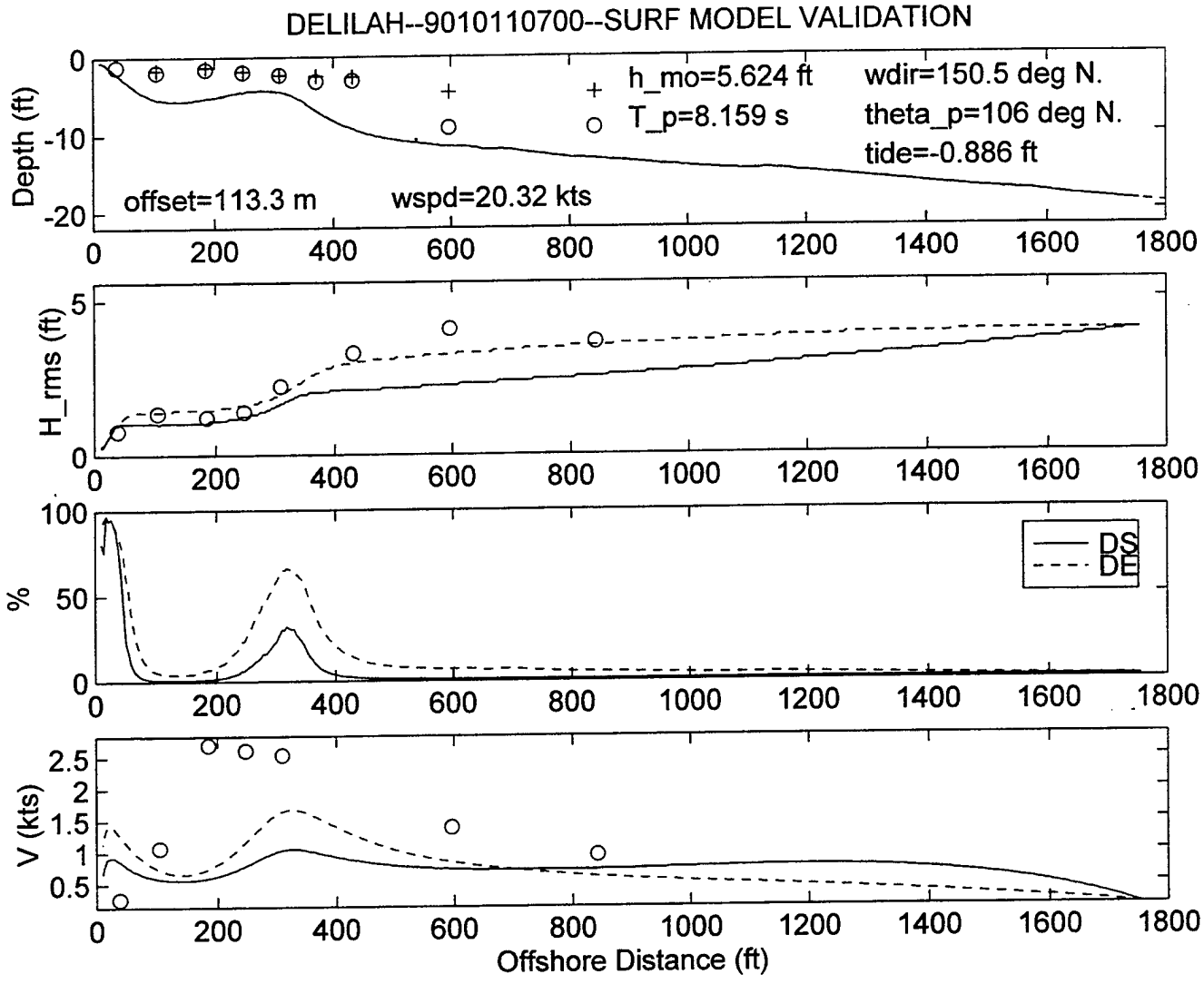
DELILAH--9010110700--SURF MODEL VALIDATION
Depth (ft)
h_mo=5.624 ft
T_p=8.159 s
wdir=150.5 deg N.
theta_p=106 deg N.
tide=-0.886 ft
offset=113.3 m
wspd=20.32 kts
H_rms (ft)
%
DS
DE
V (kts)
Offshore Distance (ft)

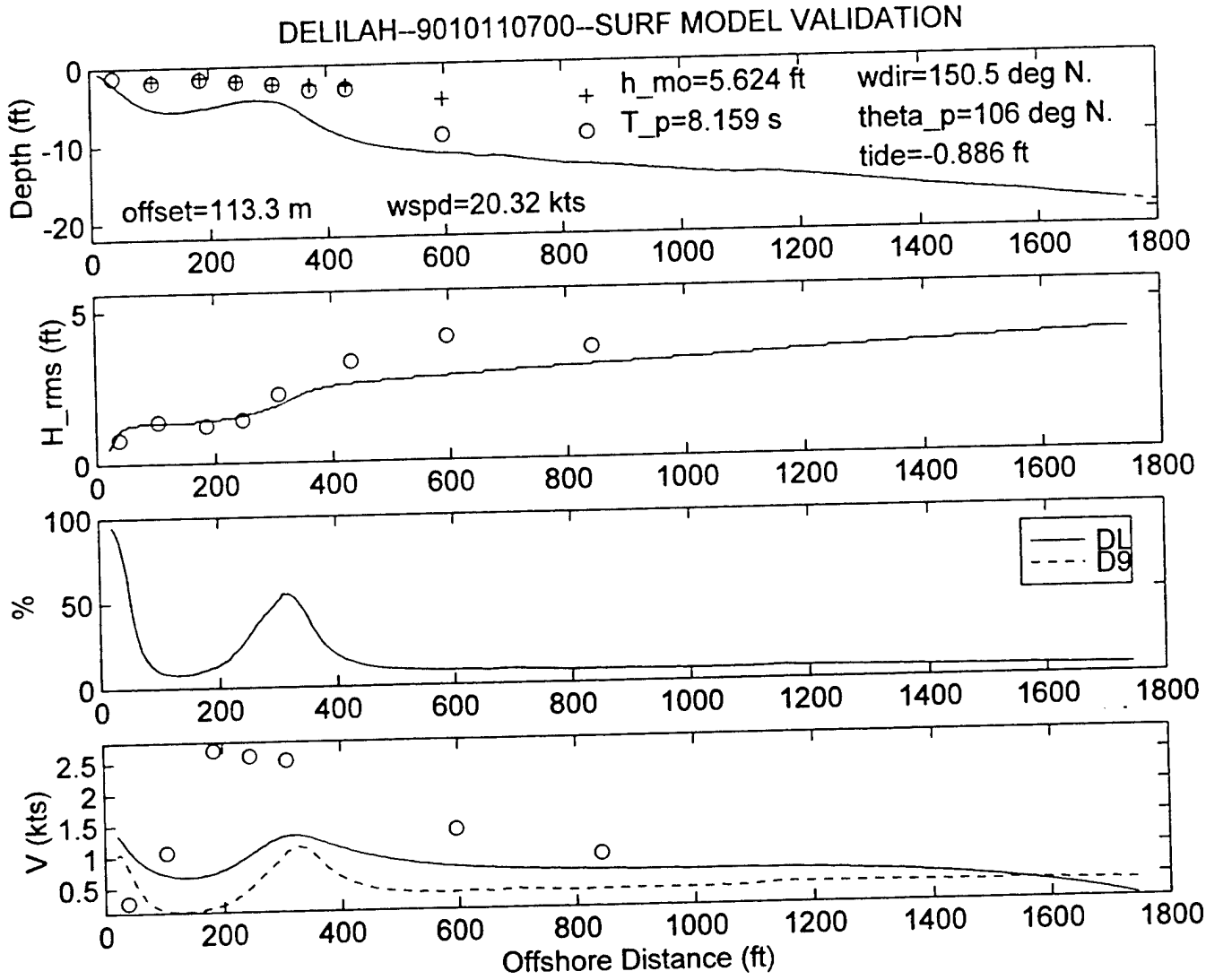
DELILAH--9010110700--SURF MODEL VALIDATION
Depth (ft)
h_mo=5.624 ft
T_p=8.159 s
wdir=150.5 deg N.
theta_p=106 deg N.
tide=-0.886 ft
offset=113.3 m
wspd=20.32 kts
H_rms (ft)
%
DL
D9
V (kts)
Offshore Distance (ft)

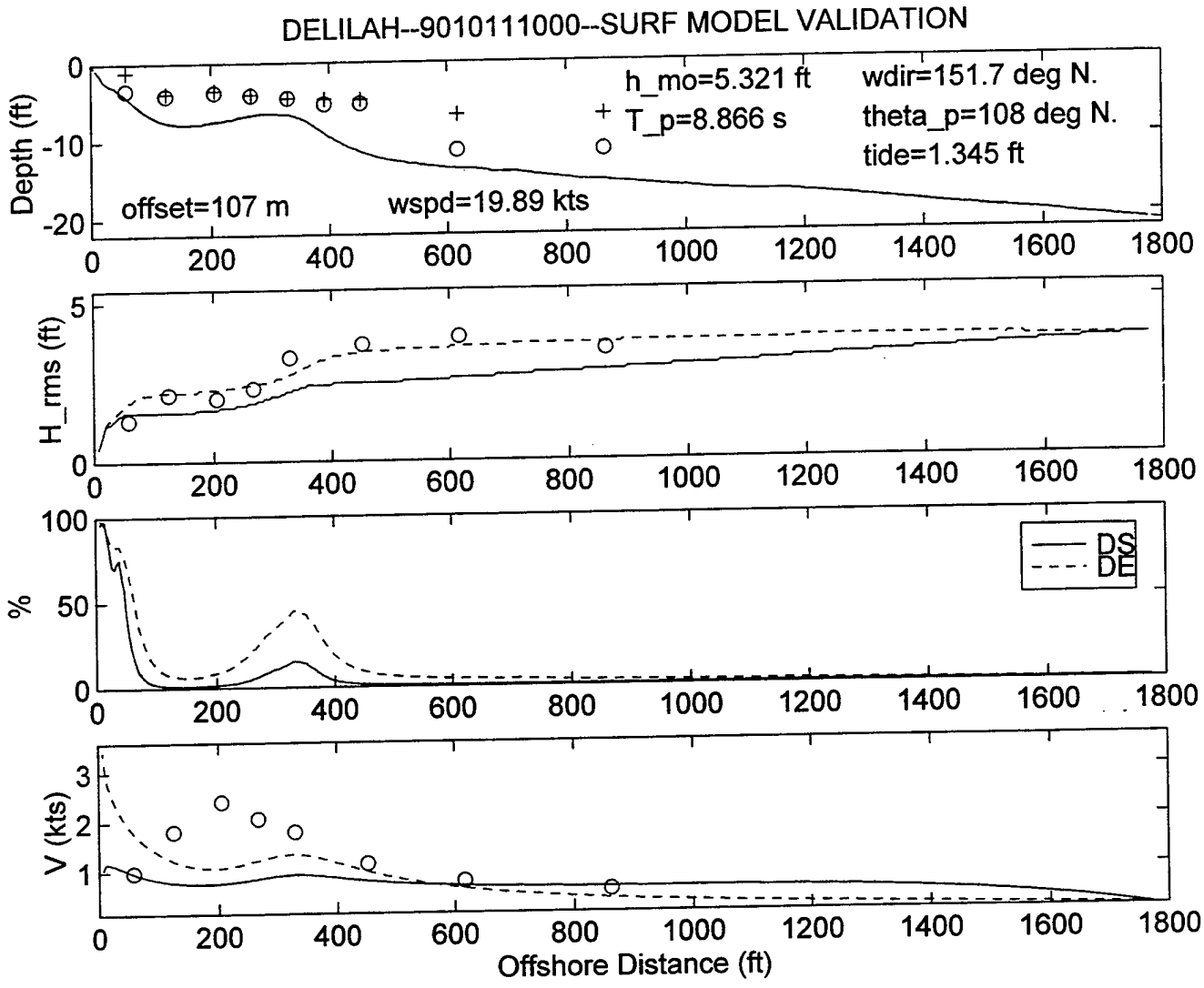
DELILAH--9010111000--SURF MODEL VALIDATION
Depth (ft)
h_mo=5.321 ft
T_p=8.866 s
wdir=151.7 deg N.
theta_p=108 deg N.
tide=1.345 ft
offset=107 m
wspd=19.89 kts
H_rms (ft)
%
DS
DE
V (kts)
Offshore Distance (ft)

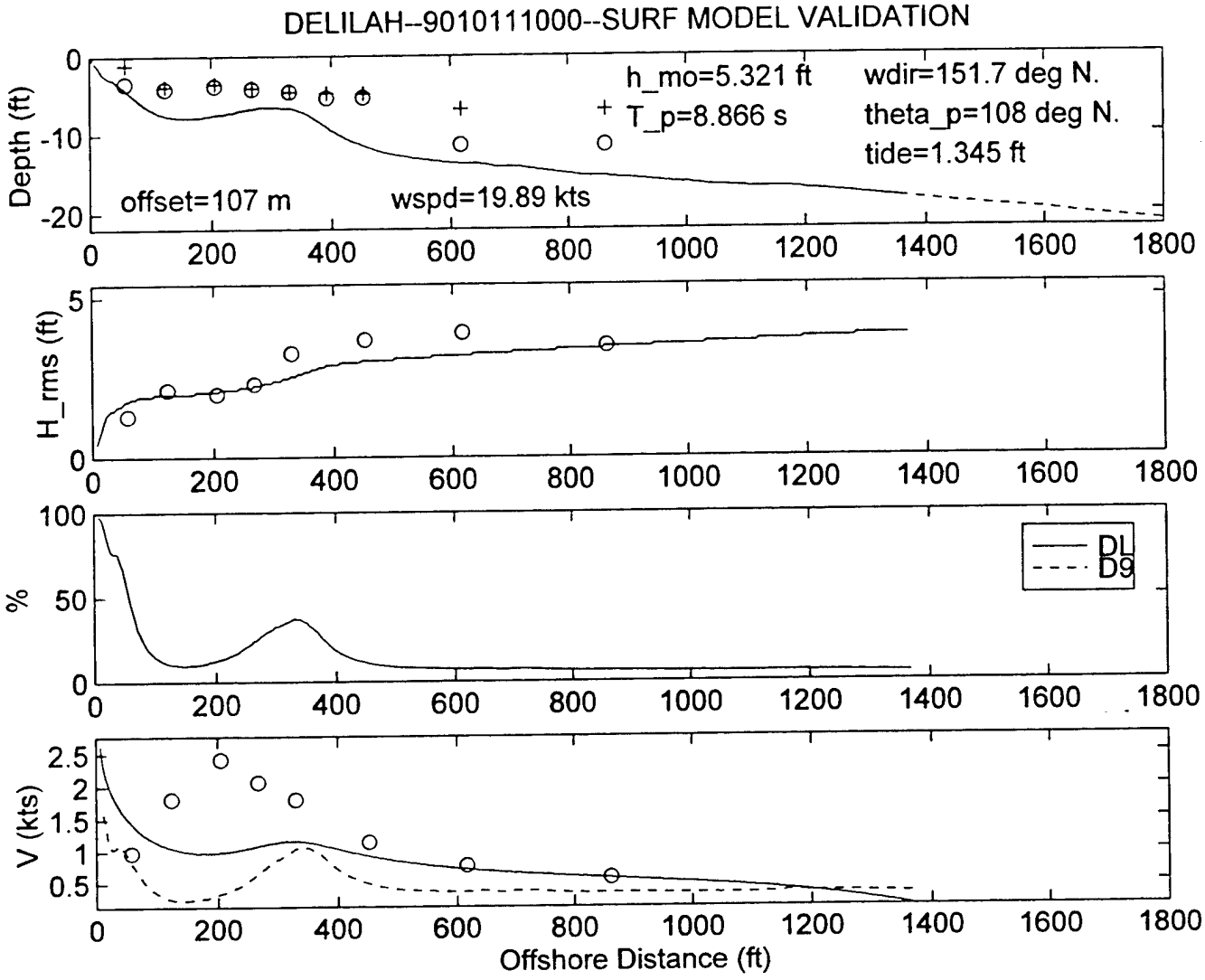
DELILAH--9010111000--SURF MODEL VALIDATION
Depth (ft)
h_mo=5.321 ft
T_p=8.866 s
wdir=151.7 deg N.
theta_p=108 deg N.
tide=1.345 ft
offset=107 m
wspd=19.89 kts
H_rms (ft)
%
DL
D9
V (kts)
Offshore Distance (ft)

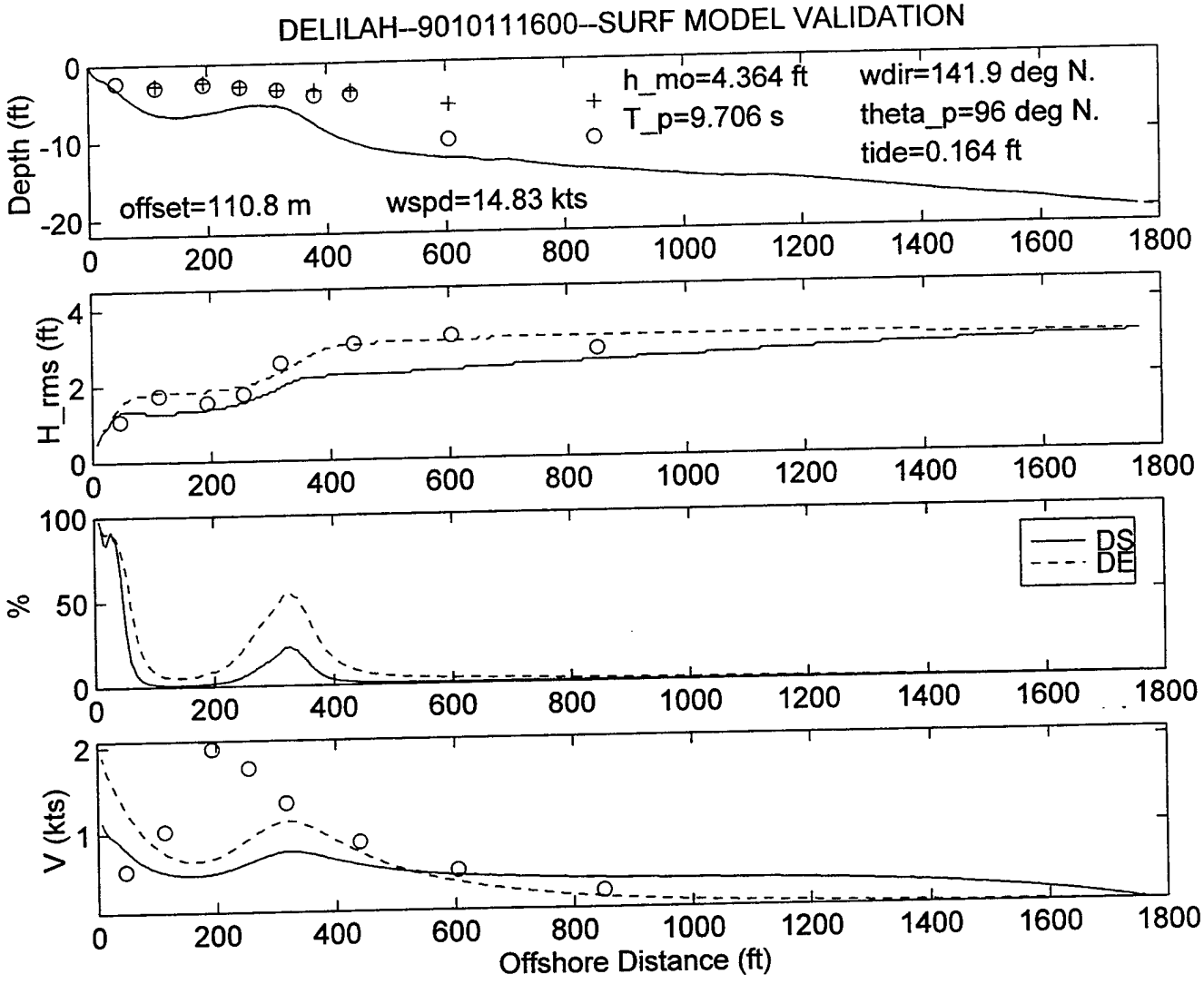
DELILAH--9010111600--SURF MODEL VALIDATION
Depth (ft)
h_mo=4.364 ft
T_p=9.706 s
wdir=141.9 deg N.
theta_p=96 deg N.
tide=0.164 ft
offset=110.8 m
wspd=14.83 kts
H_rms (ft)
%
DS
DE
V (kts)
Offshore Distance (ft)

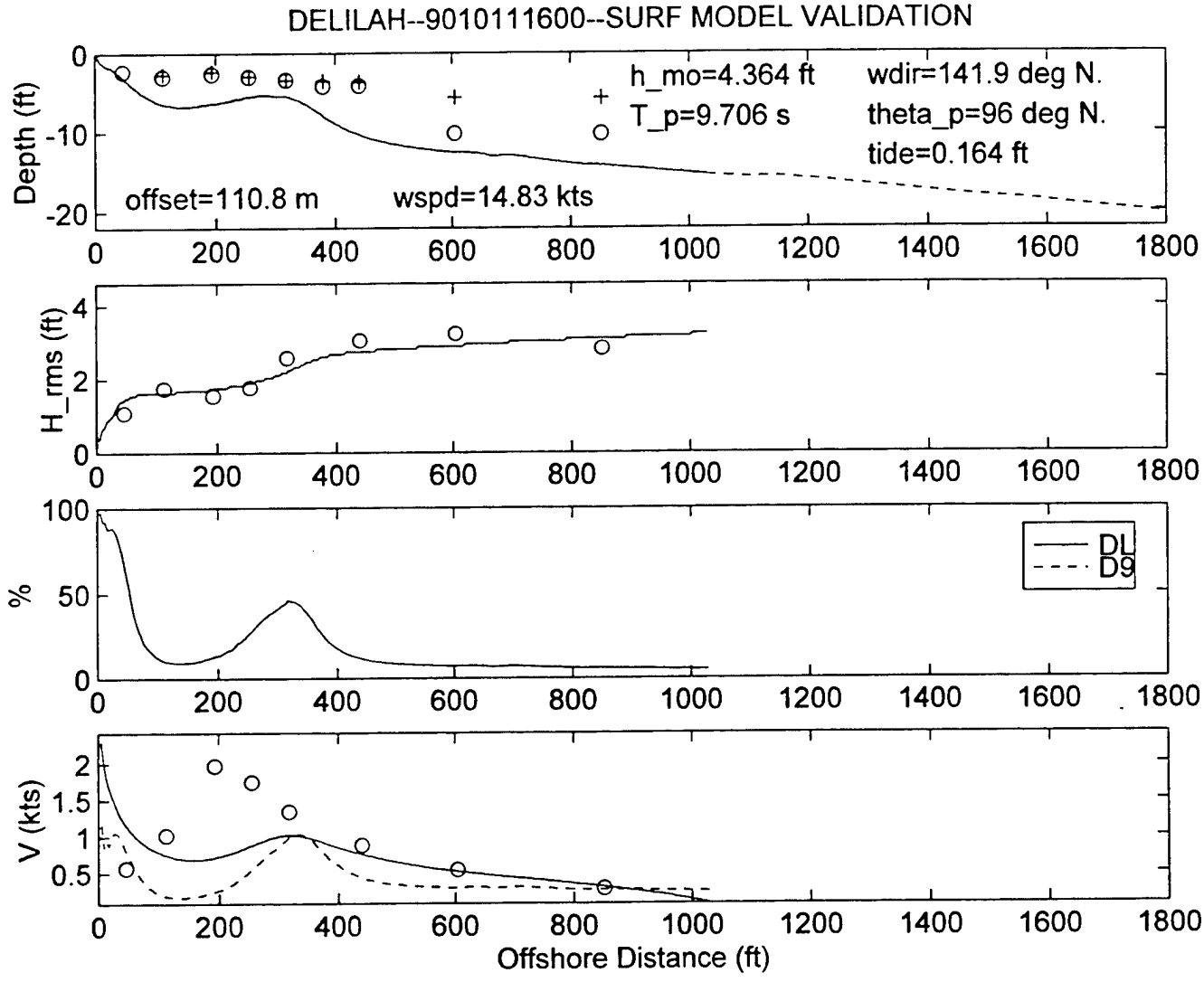
DELILAH--9010111600--SURF MODEL VALIDATION
Depth (ft)
h_mo=4.364 ft
T_p=9.706 s
wdir=141.9 deg N.
theta_p=96 deg N.
tide=0.164 ft
offset=110.8 m
wspd=14.83 kts
H_rms (ft)
%
DL
D9
V (kts)
Offshore Distance (ft)

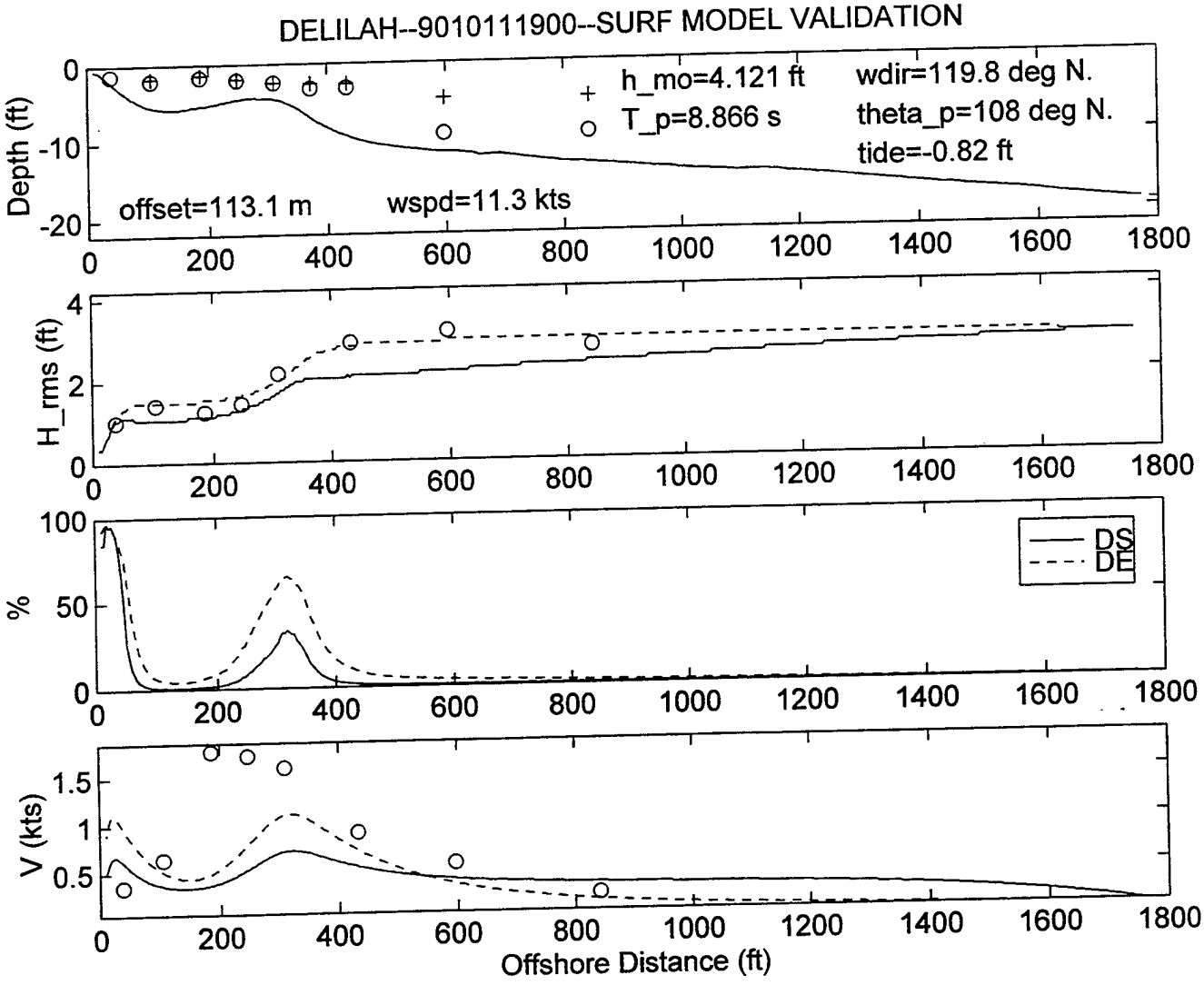
DELILAH--9010111900--SURF MODEL VALIDATION
Depth (ft)
h_mo=4.121 ft
T_p=8.866 s
wdir=119.8 deg N.
theta_p=108 deg N.
tide=-0.82 ft
offset=113.1 m
wspd=11.3 kts
H_rms (ft)
%
DS
DE
V (kts)
Offshore Distance (ft)

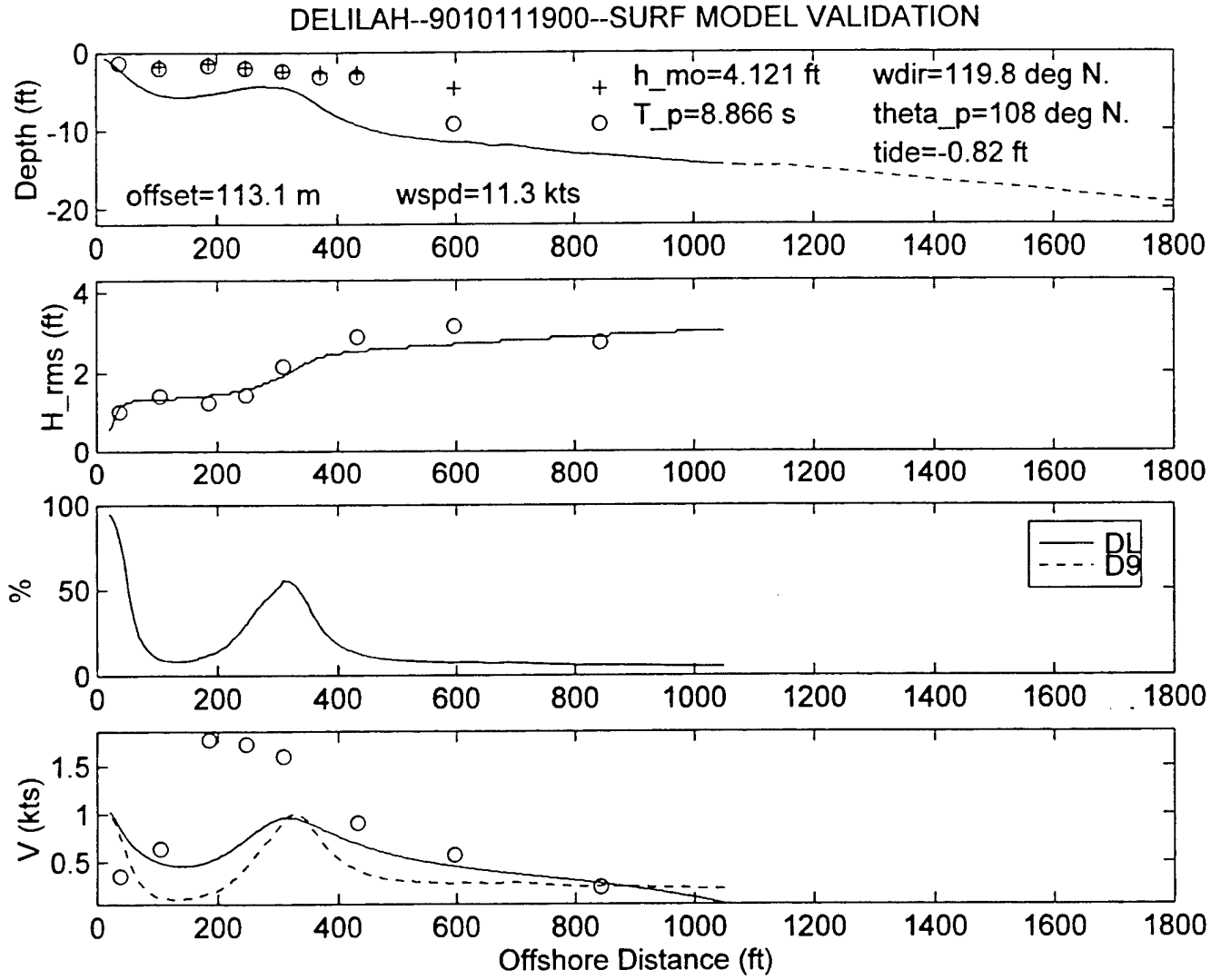
DELILAH--9010111900--SURF MODEL VALIDATION
Depth (ft)
h_mo=4.121 ft
T_p=8.866 s
wdir=119.8 deg N.
theta_p=108 deg N.
tide=-0.82 ft
offset=113.1 m
wspd=11.3 kts
H_rms (ft)
%
DL
D9
V (kts)
Offshore Distance (ft)

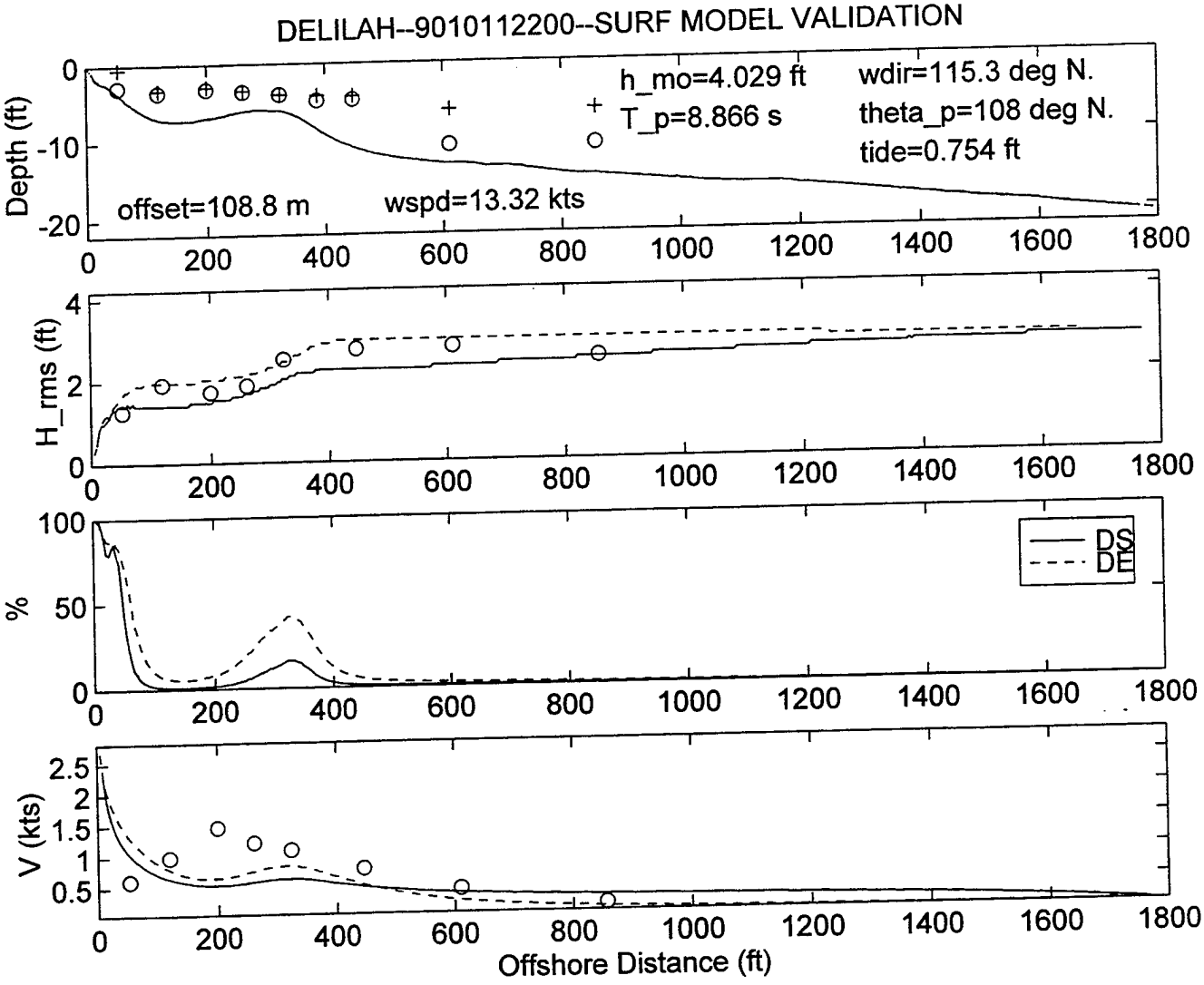
DELILAH--9010112200--SURF MODEL VALIDATION
Depth (ft)
h_mo=4.029 ft
T_p=8.866 s
wdir=115.3 deg N.
theta_p=108 deg N.
tide=0.754 ft
offset=108.8 m
wspd=13.32 kts
H_rms (ft)
%
DS
DE
V (kts)
Offshore Distance (ft)

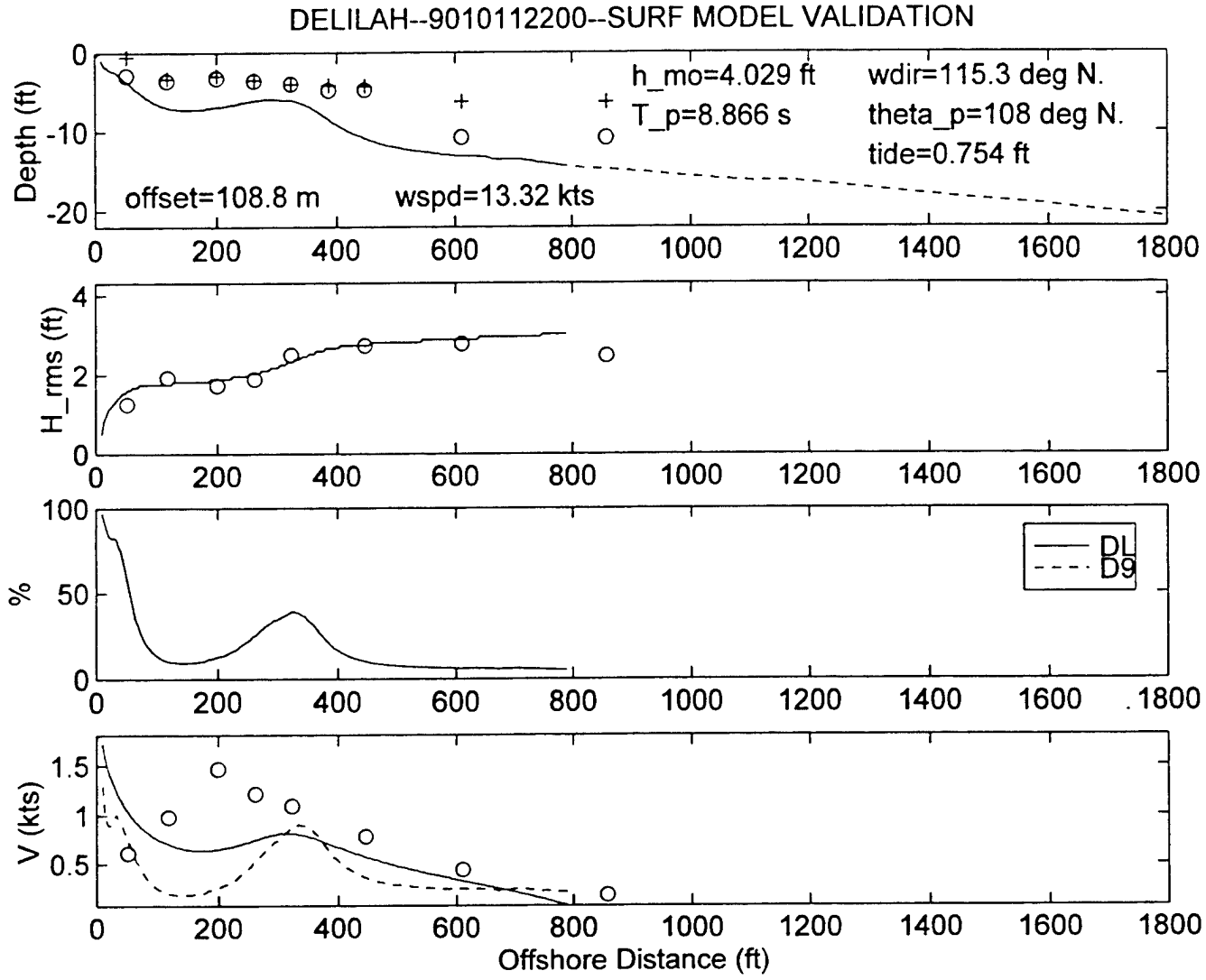
DELILAH--9010112200--SURF MODEL VALIDATION
Depth (ft)
h_mo=4.029 ft
T_p=8.866 s
wdir=115.3 deg N.
theta_p=108 deg N.
tide=0.754 ft
offset=108.8 m
wspd=13.32 kts
H_rms (ft)
%
DL
D9
V (kts)
Offshore Distance (ft)

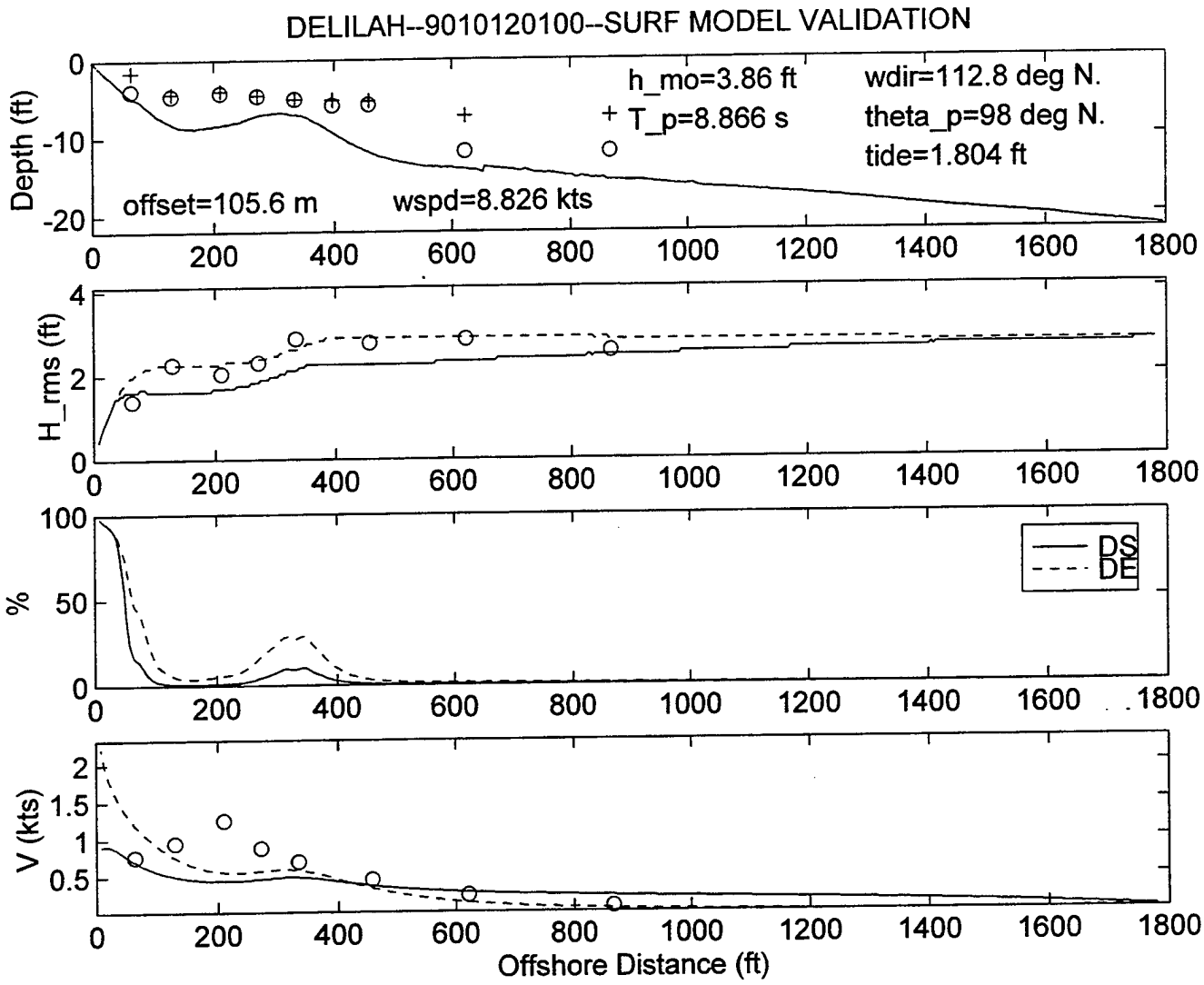
DELILAH--9010120100--SURF MODEL VALIDATION
Depth (ft)
h_mo=3.86 ft
T_p=8.866 s
wdir=112.8 deg N.
theta_p=98 deg N.
tide=1.804 ft
offset=105.6 m
wspd=8.826 kts
H_rms (ft)
%
DS
DE
V (kts)
Offshore Distance (ft)

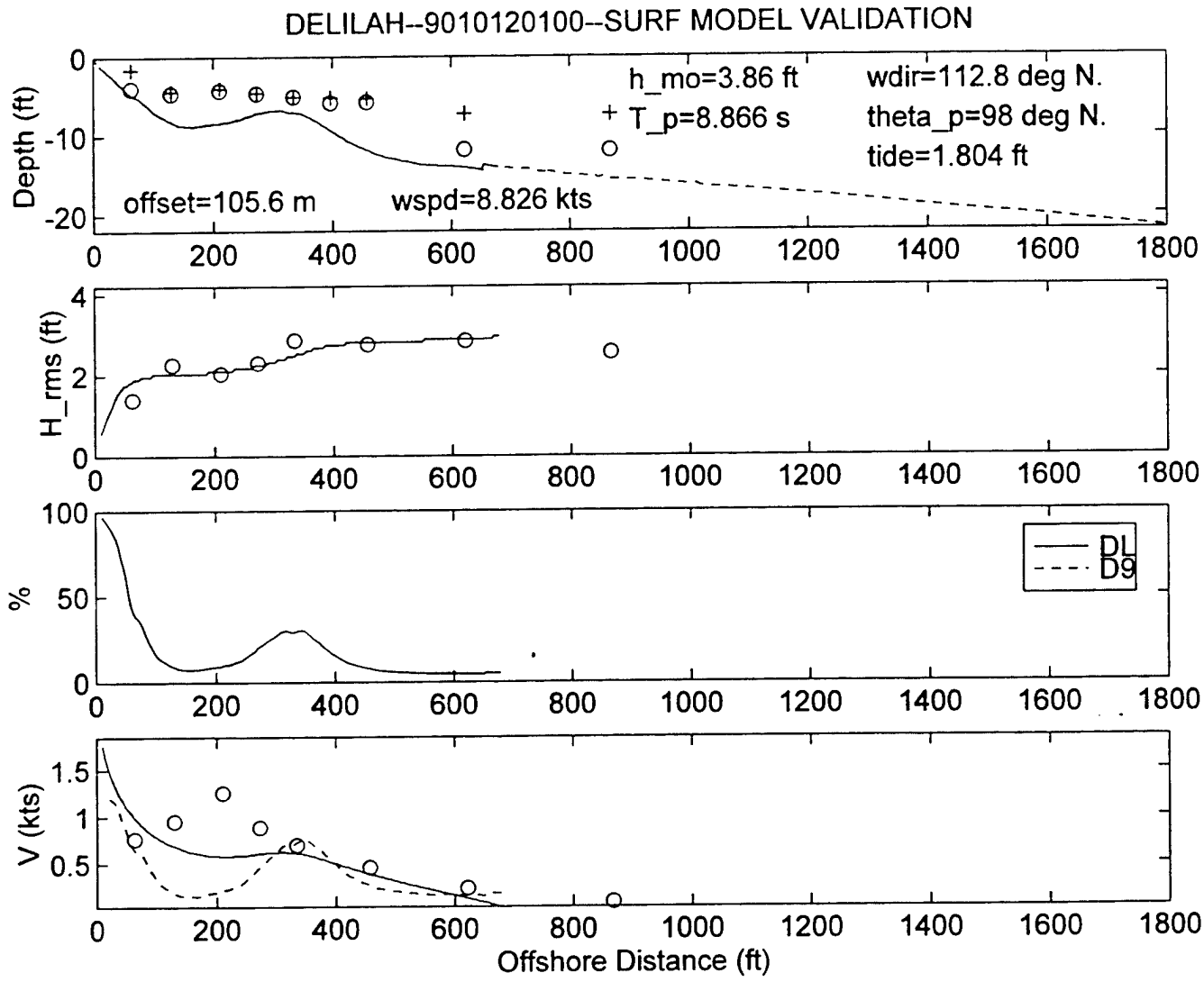
DELILAH--9010120100--SURF MODEL VALIDATION
Depth (ft)
h_mo=3.86 ft
T_p=8.866 s
wdir=112.8 deg N.
theta_p=98 deg N.
tide=1.804 ft
offset=105.6 m
wspd=8.826 kts
H_rms (ft)
%
DL
D9
V (kts)
Offshore Distance (ft)

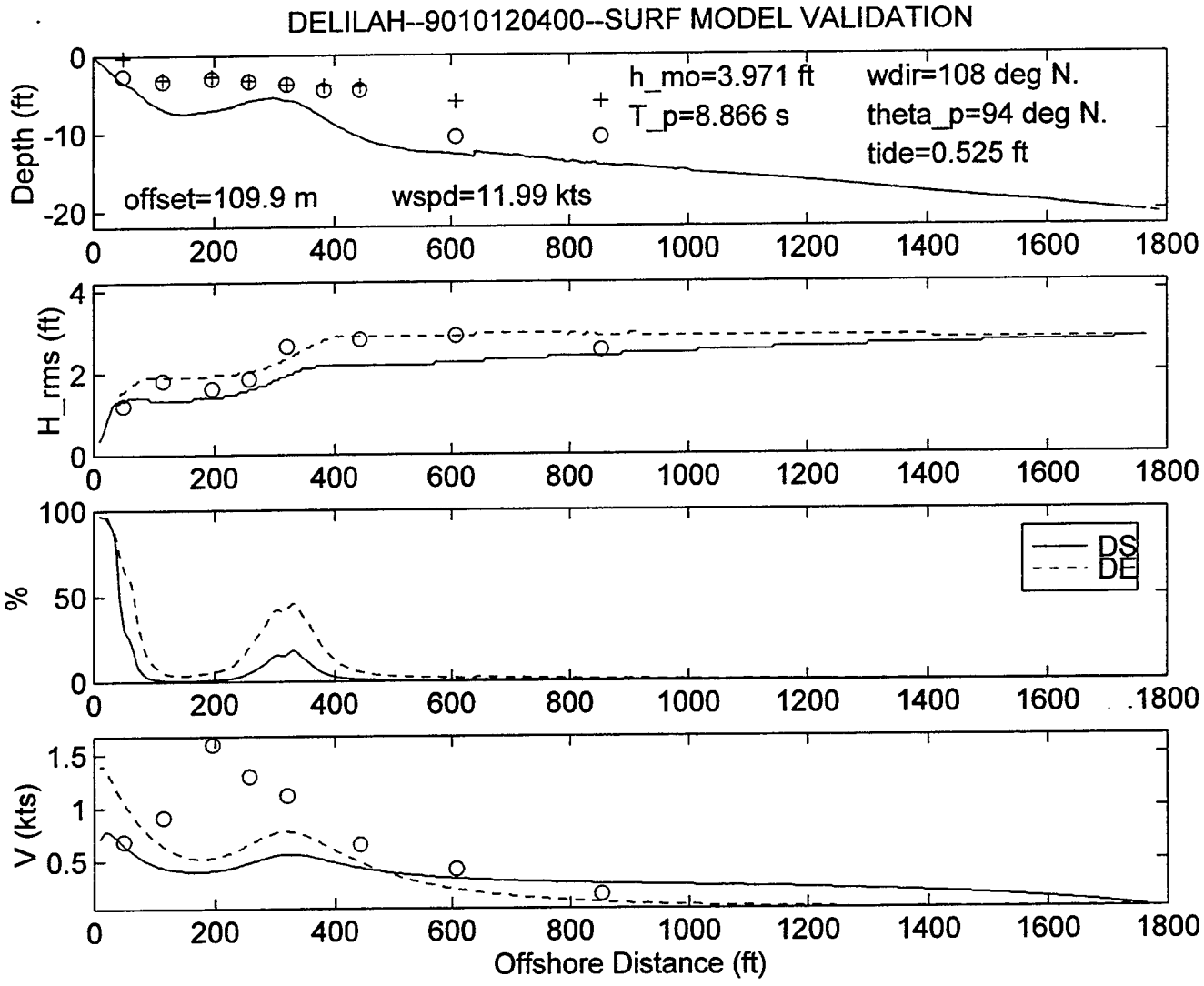
DELILAH--9010120400--SURF MODEL VALIDATION
Depth (ft)
h_mo=3.971 ft
T_p=8.866 s
wdir=108 deg N.
theta_p=94 deg N.
tide=0.525 ft
offset=109.9 m
wspd=11.99 kts
H_rms (ft)
%
DS
DE
V (kts)
Offshore Distance (ft)

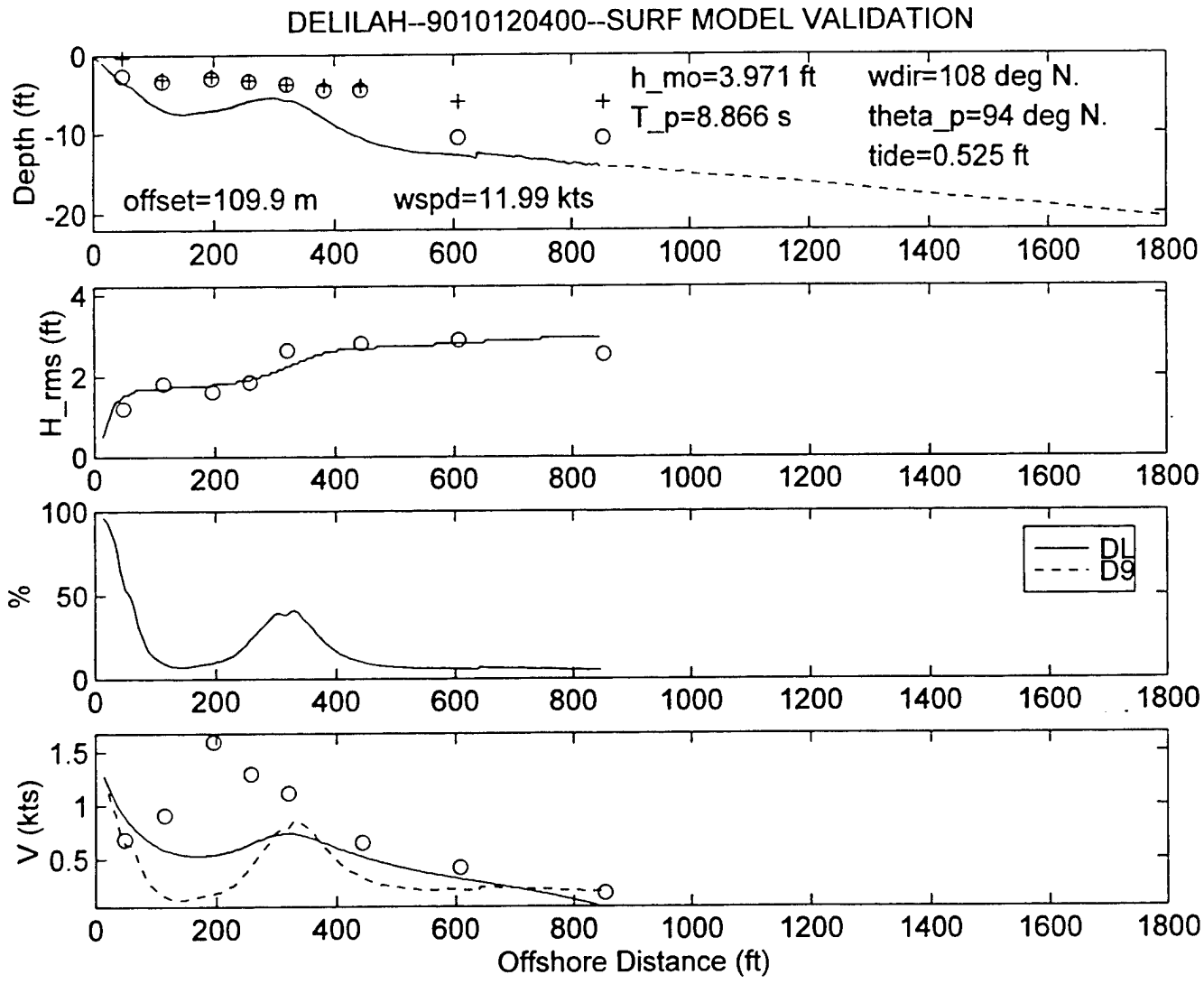
DELILAH--9010120400--SURF MODEL VALIDATION
Depth (ft)
h_mo=3.971 ft
T_p=8.866 s
wdir=108 deg N.
theta_p=94 deg N.
tide=0.525 ft
offset=109.9 m
wspd=11.99 kts
H_rms (ft)
%
DL
D9
V (kts)
Offshore Distance (ft)

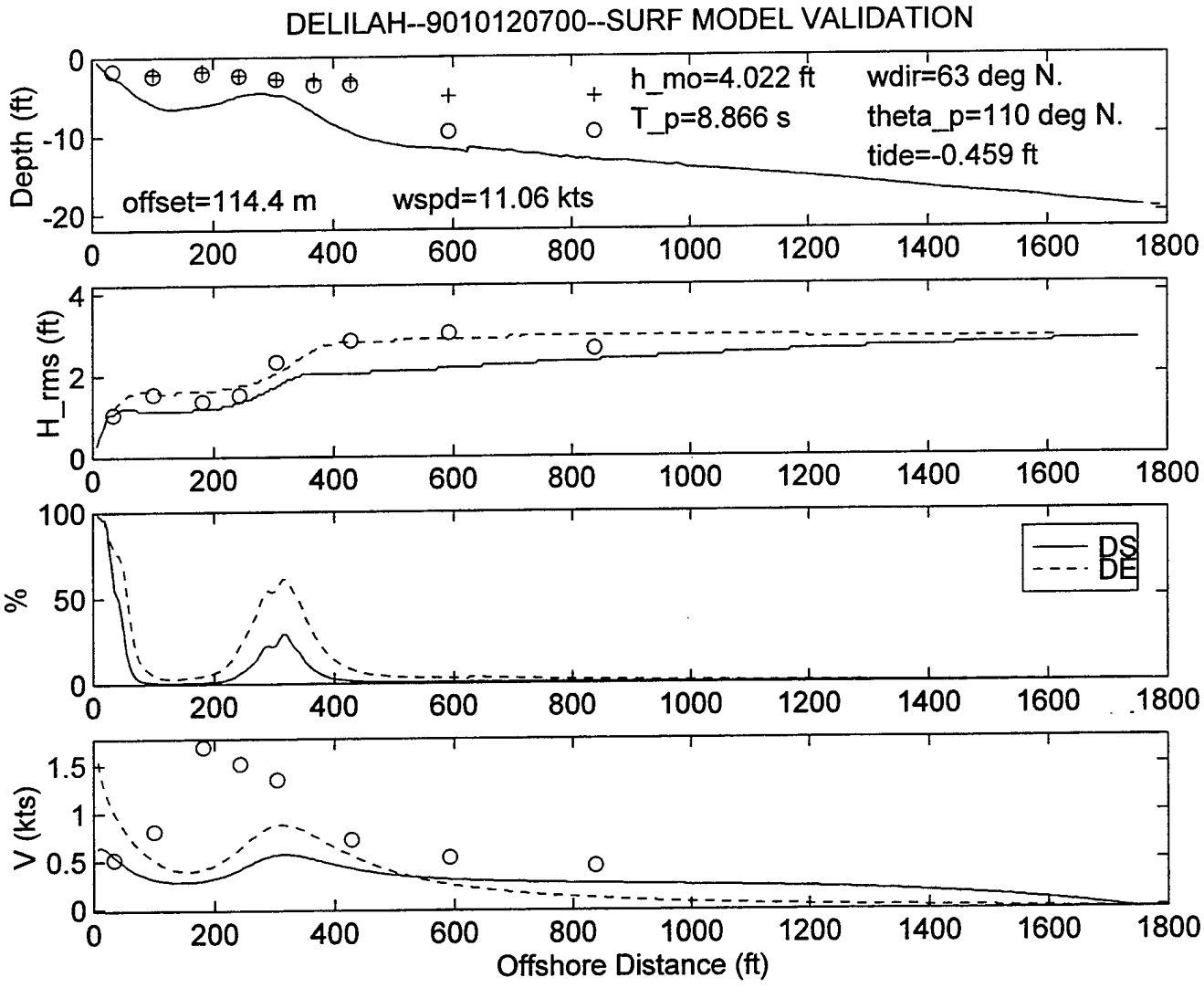
DELILAH--9010120700--SURF MODEL VALIDATION
Depth (ft)
h_mo=4.022 ft
T_p=8.866 s
wdir=63 deg N.
theta_p=110 deg N.
tide=-0.459 ft
offset=114.4 m
wspd=11.06 kts
H_rms (ft)
%
DS
DE
V (kts)
Offshore Distance (ft)

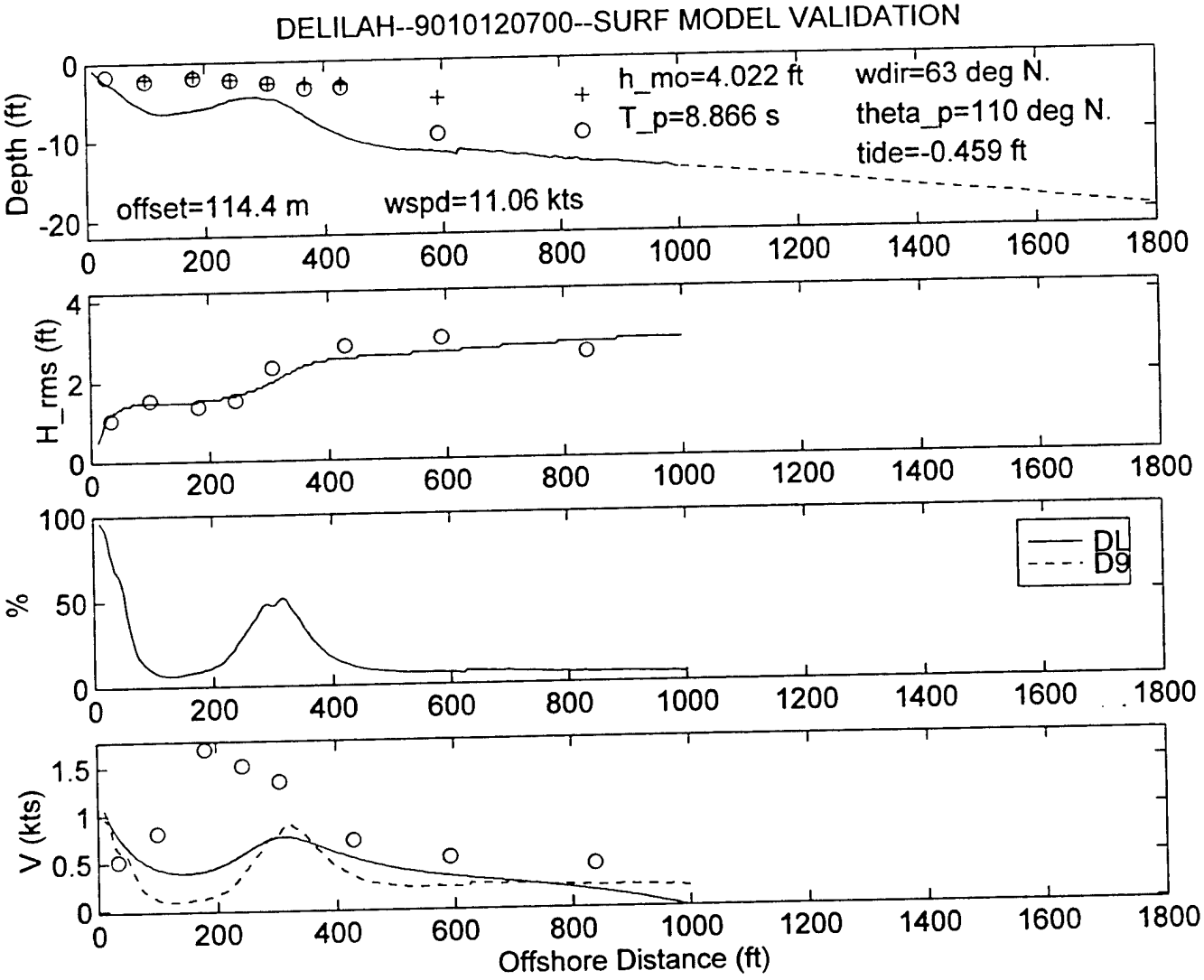
DELILAH--9010120700--SURF MODEL VALIDATION
Depth (ft)
h_mo=4.022 ft
T_p=8.866 s
wdir=63 deg N.
theta_p=110 deg N.
tide=-0.459 ft
offset=114.4 m
wspd=11.06 kts
H_rms (ft)
%
DL
D9
V (kts)
Offshore Distance (ft)

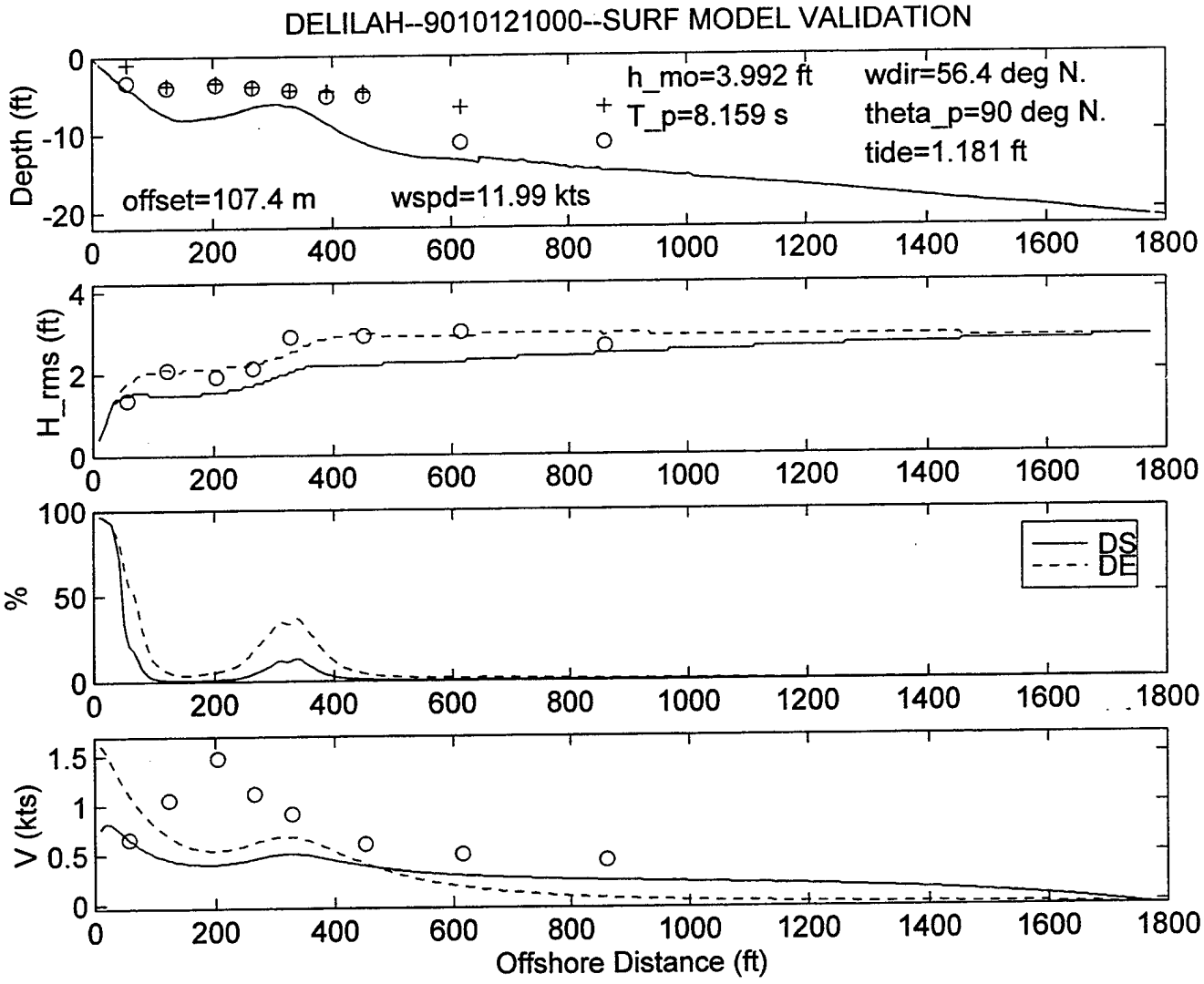
DELILAH--9010121000--SURF MODEL VALIDATION
Depth (ft)
h_mo=3.992 ft
T_p=8.159 s
wdir=56.4 deg N.
theta_p=90 deg N.
tide=1.181 ft
offset=107.4 m
wspd=11.99 kts
H_rms (ft)
%
DS
DE
V (kts)
Offshore Distance (ft)

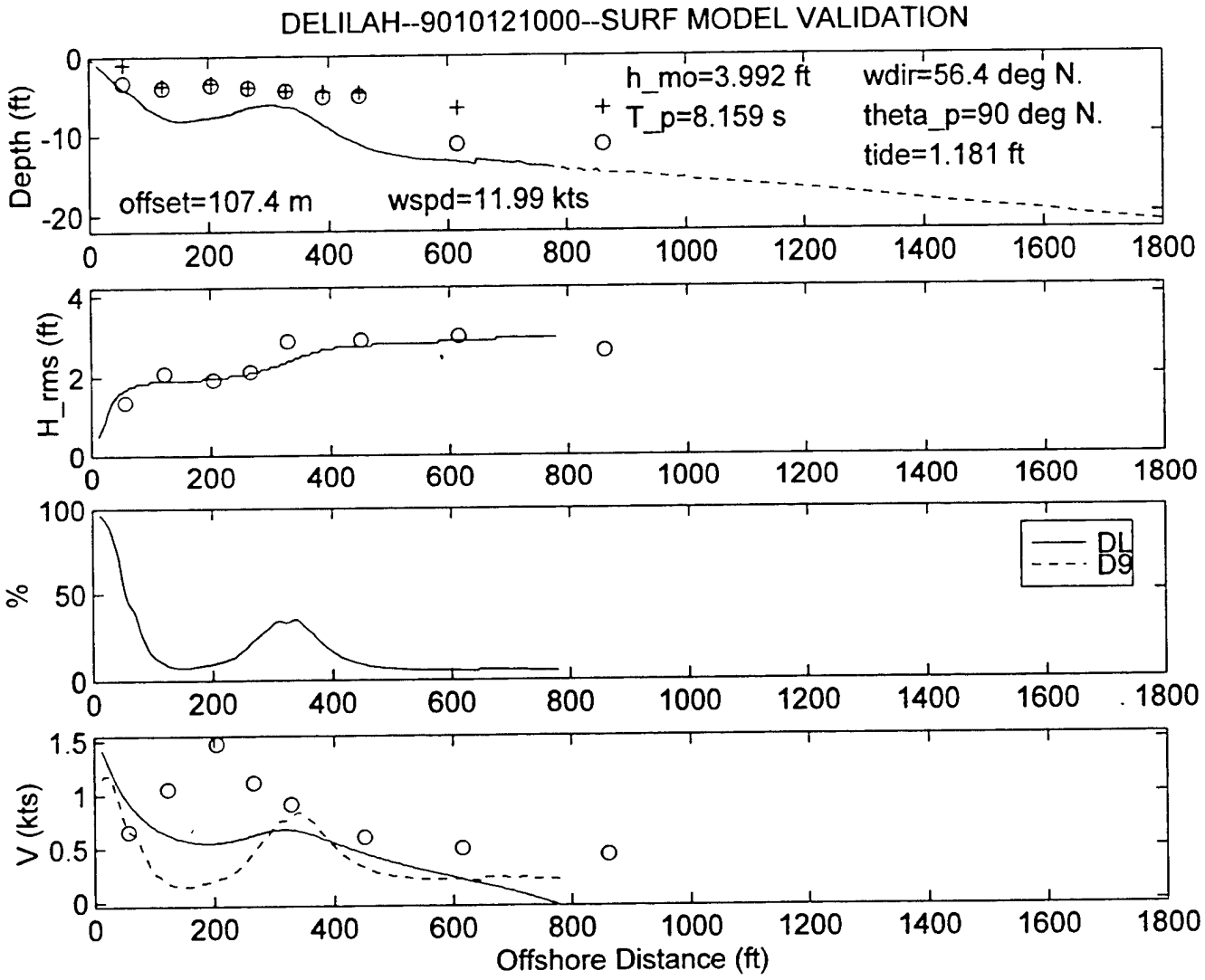
DELILAH--9010121000--SURF MODEL VALIDATION
Depth (ft)
h_mo=3.992 ft
T_p=8.159 s
wdir=56.4 deg N.
theta_p=90 deg N.
tide=1.181 ft
offset=107.4 m
wspd=11.99 kts
H_rms (ft)
%
DL
D9
V (kts)
Offshore Distance (ft)

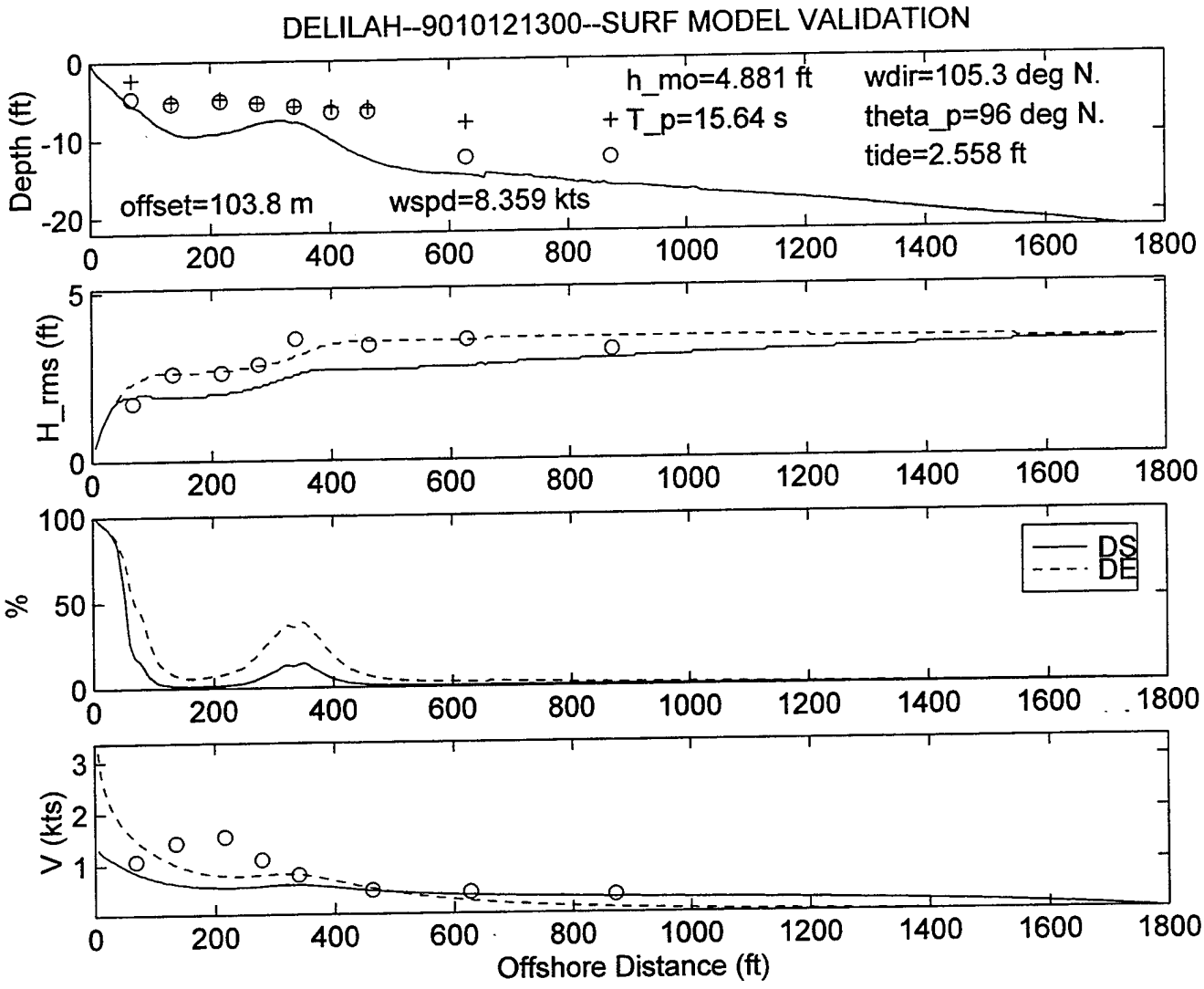
DELILAH--9010121300--SURF MODEL VALIDATION
Depth (ft)
h_mo=4.881 ft
+ T_p=15.64 s
wdir=105.3 deg N.
theta_p=96 deg N.
tide=2.558 ft
offset=103.8 m
wspd=8.359 kts
H_rms (ft)
%
DS
DE
V (kts)
Offshore Distance (ft)

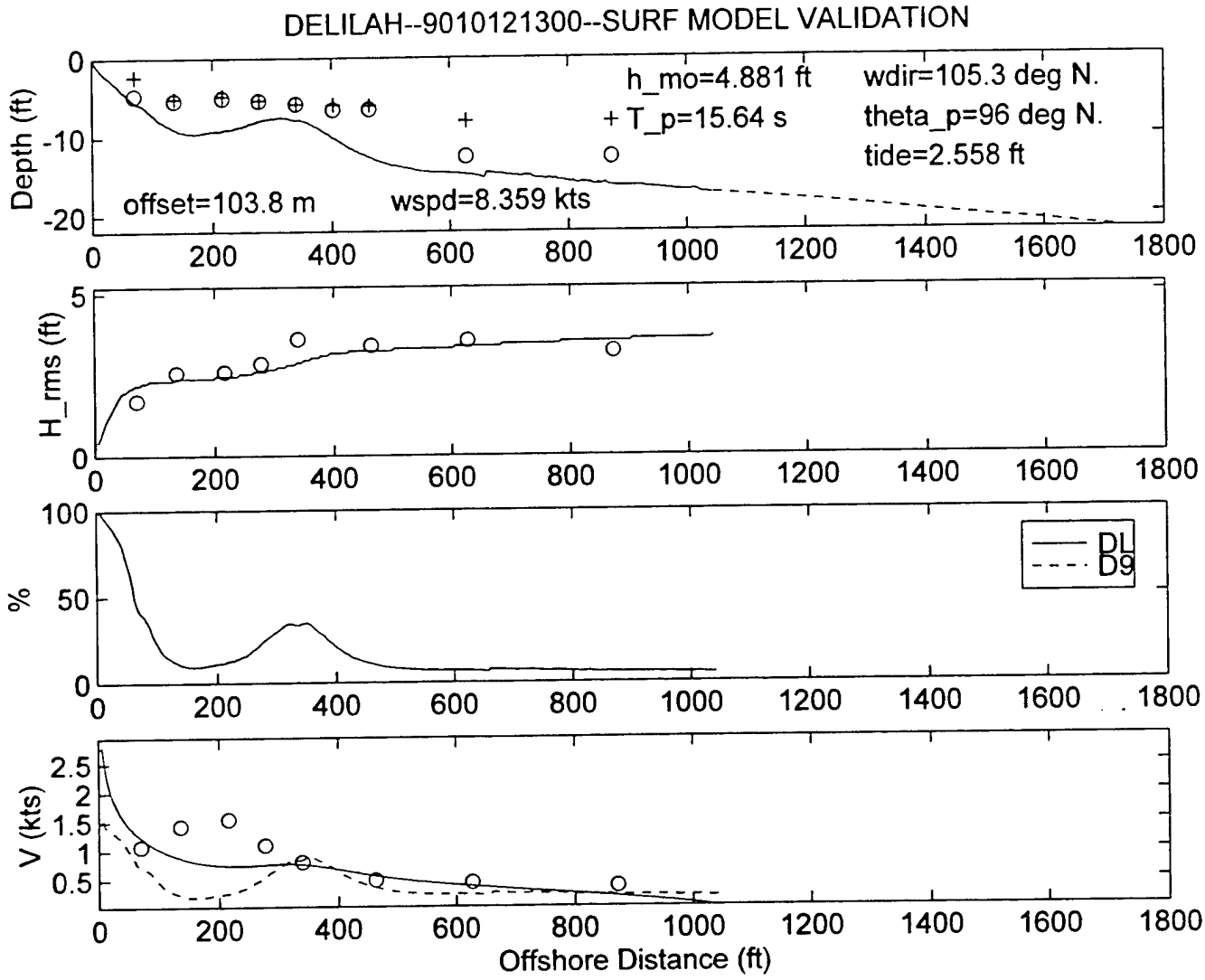
DELILAH--9010121300--SURF MODEL VALIDATION
Depth (ft)
h_mo=4.881 ft
+ T_p=15.64 s
wdir=105.3 deg N.
theta_p=96 deg N.
tide=2.558 ft
offset=103.8 m
wspd=8.359 kts
H_rms (ft)
%
DL
D9
V (kts)
Offshore Distance (ft)

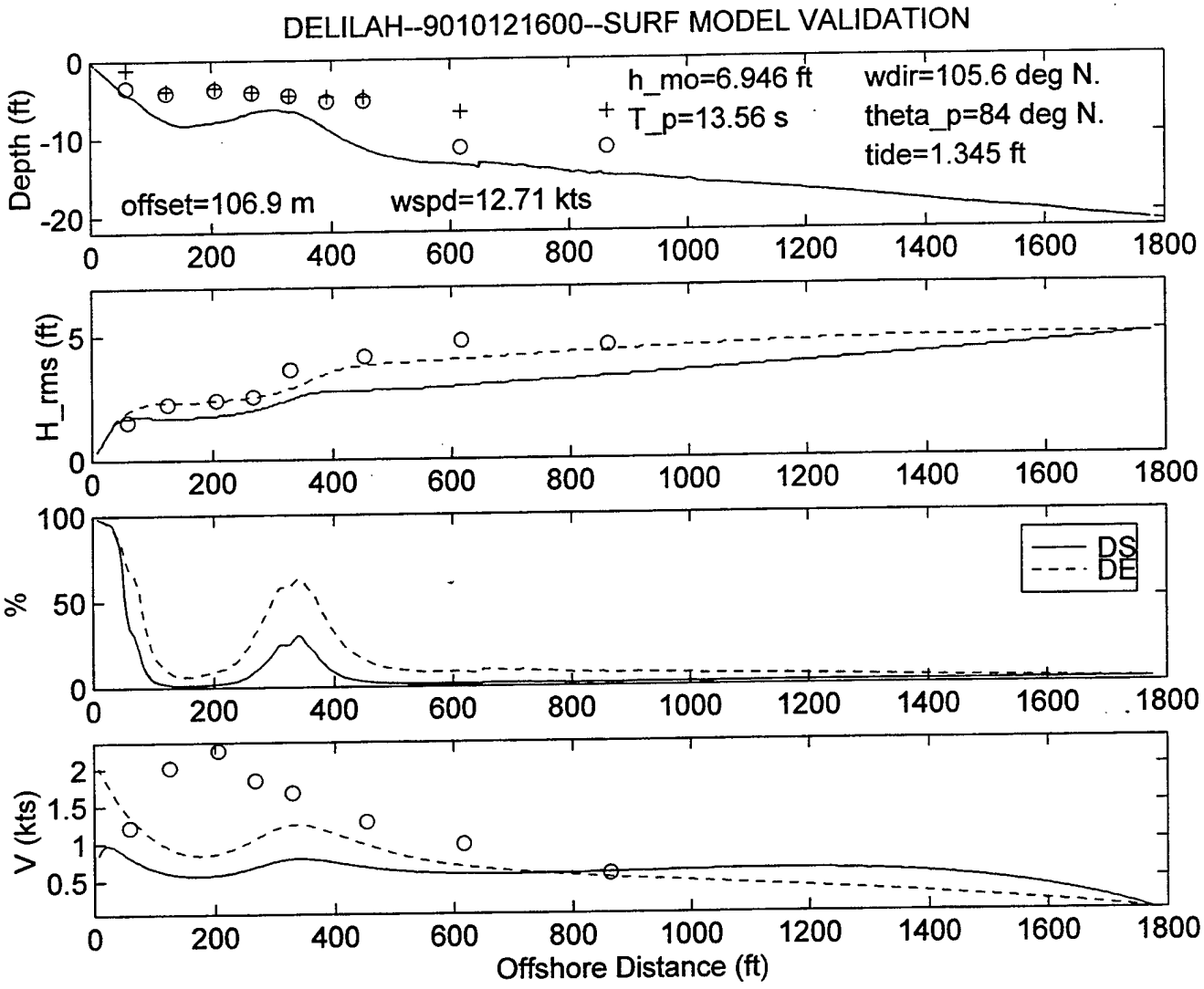
DELILAH--9010121600--SURF MODEL VALIDATION
Depth (ft)
h_mo=6.946 ft
T_p=13.56 s
wdir=105.6 deg N.
theta_p=84 deg N.
tide=1.345 ft
offset=106.9 m
wspd=12.71 kts
H_rms (ft)
%
DS
DE
V (kts)
Offshore Distance (ft)

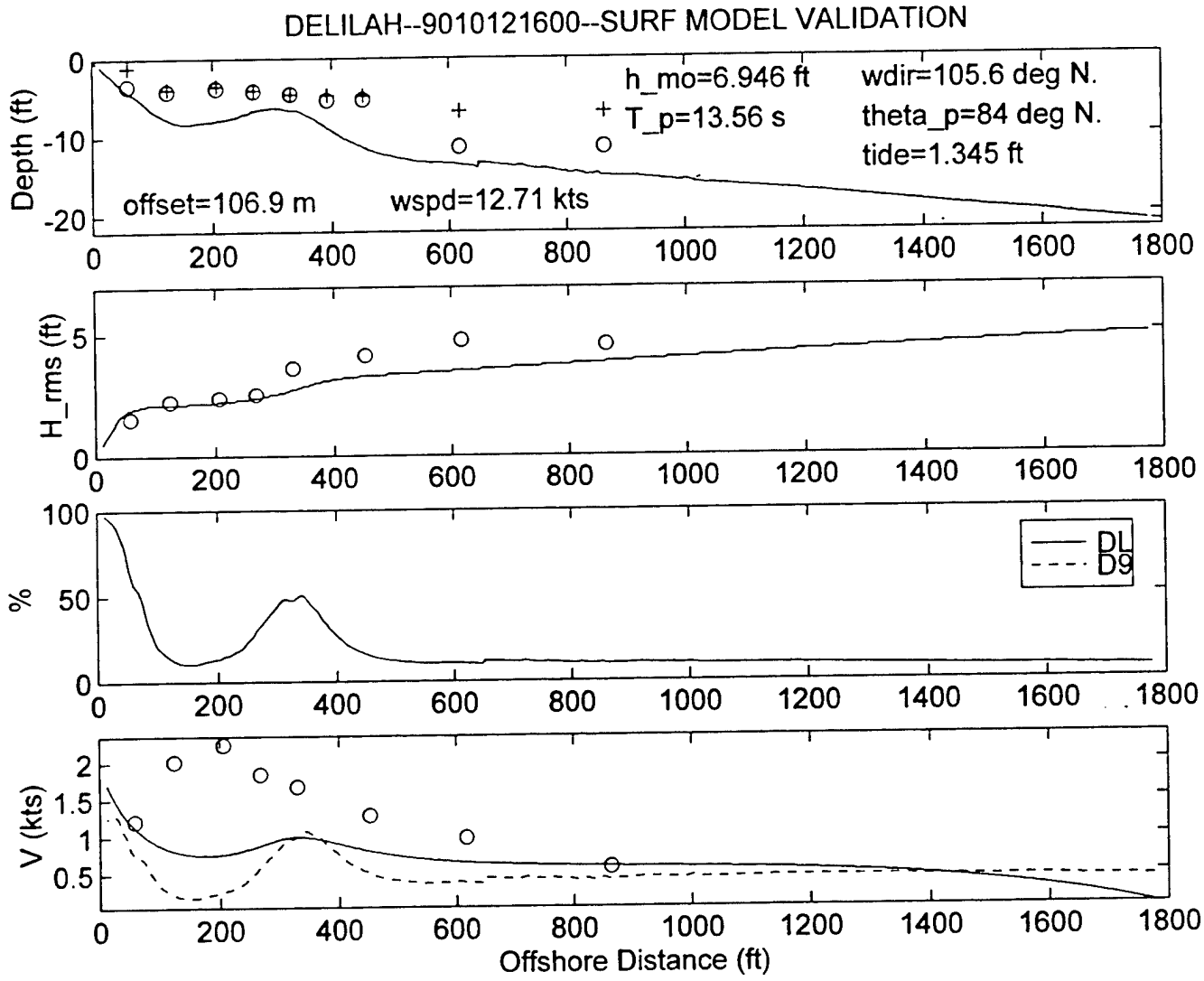
DELILAH--9010121600--SURF MODEL VALIDATION
Depth (ft)
h_mo=6.946 ft
T_p=13.56 s
wdir=105.6 deg N.
theta_p=84 deg N.
tide=1.345 ft
offset=106.9 m
wspd=12.71 kts
H_rms (ft)
%
DL
D9
V (kts)
Offshore Distance (ft)

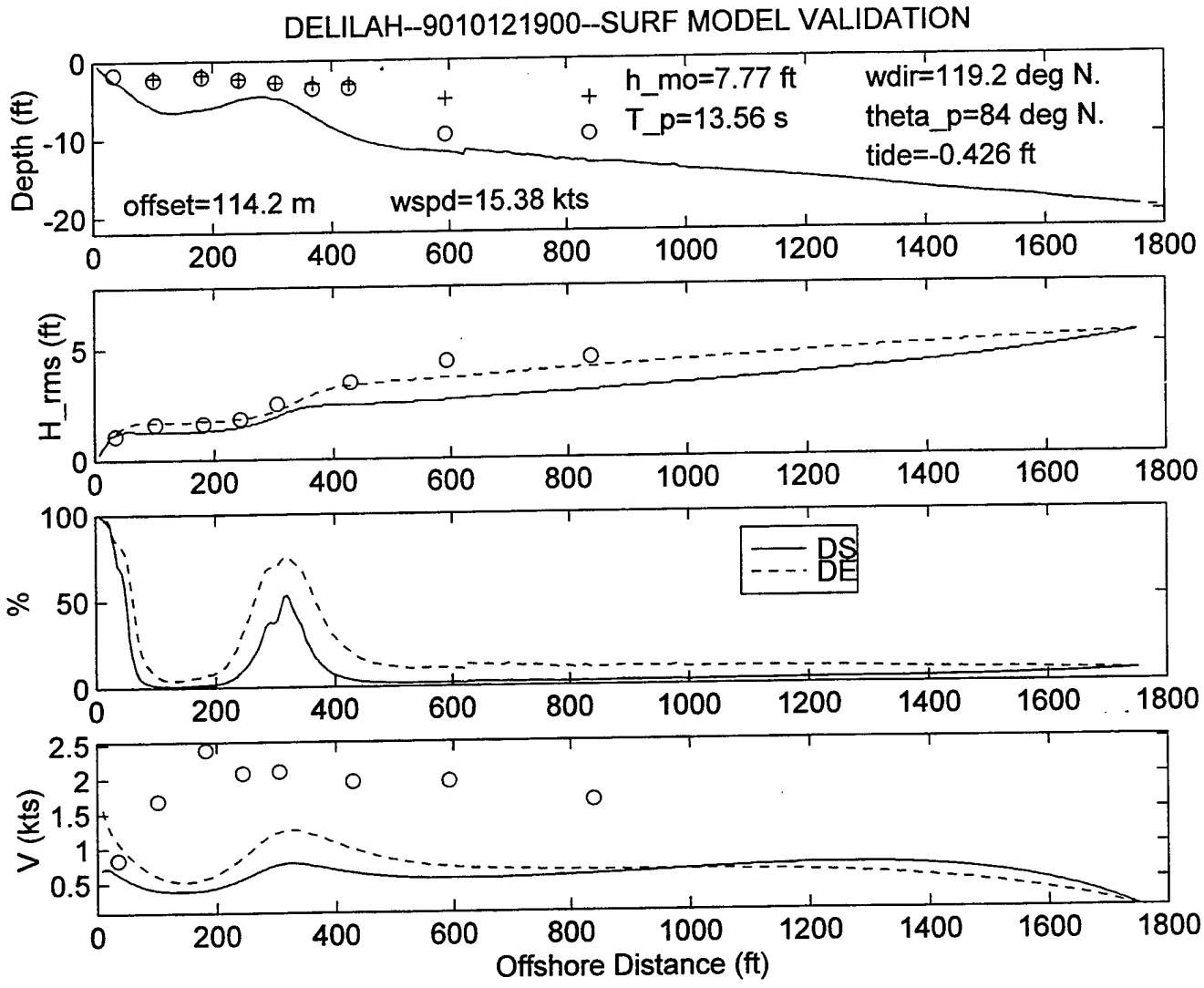
DELILAH--9010121900--SURF MODEL VALIDATION
Depth (ft)
h_mo=7.77 ft
T_p=13.56 s
wdir=119.2 deg N.
theta_p=84 deg N.
tide=-0.426 ft
offset=114.2 m
wspd=15.38 kts
H_rms (ft)
%
DS
DE
V (kts)
Offshore Distance (ft)

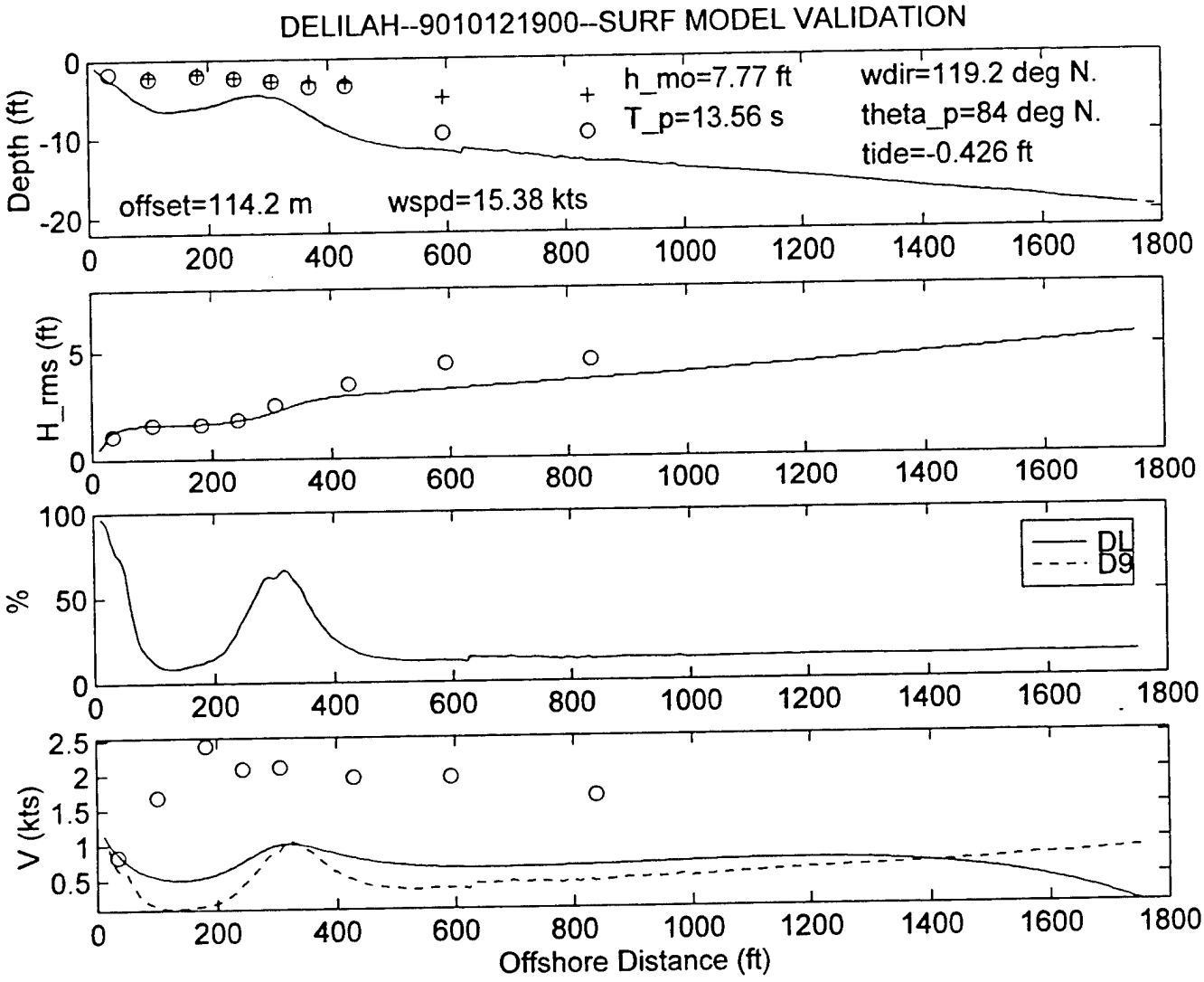
DELILAH--9010121900--SURF MODEL VALIDATION
Depth (ft)
h_mo=7.77 ft
T_p=13.56 s
wdir=119.2 deg N.
theta_p=84 deg N.
tide=-0.426 ft
offset=114.2 m
wspd=15.38 kts
H_rms (ft)
%
DL
D9
V (kts)
Offshore Distance (ft)

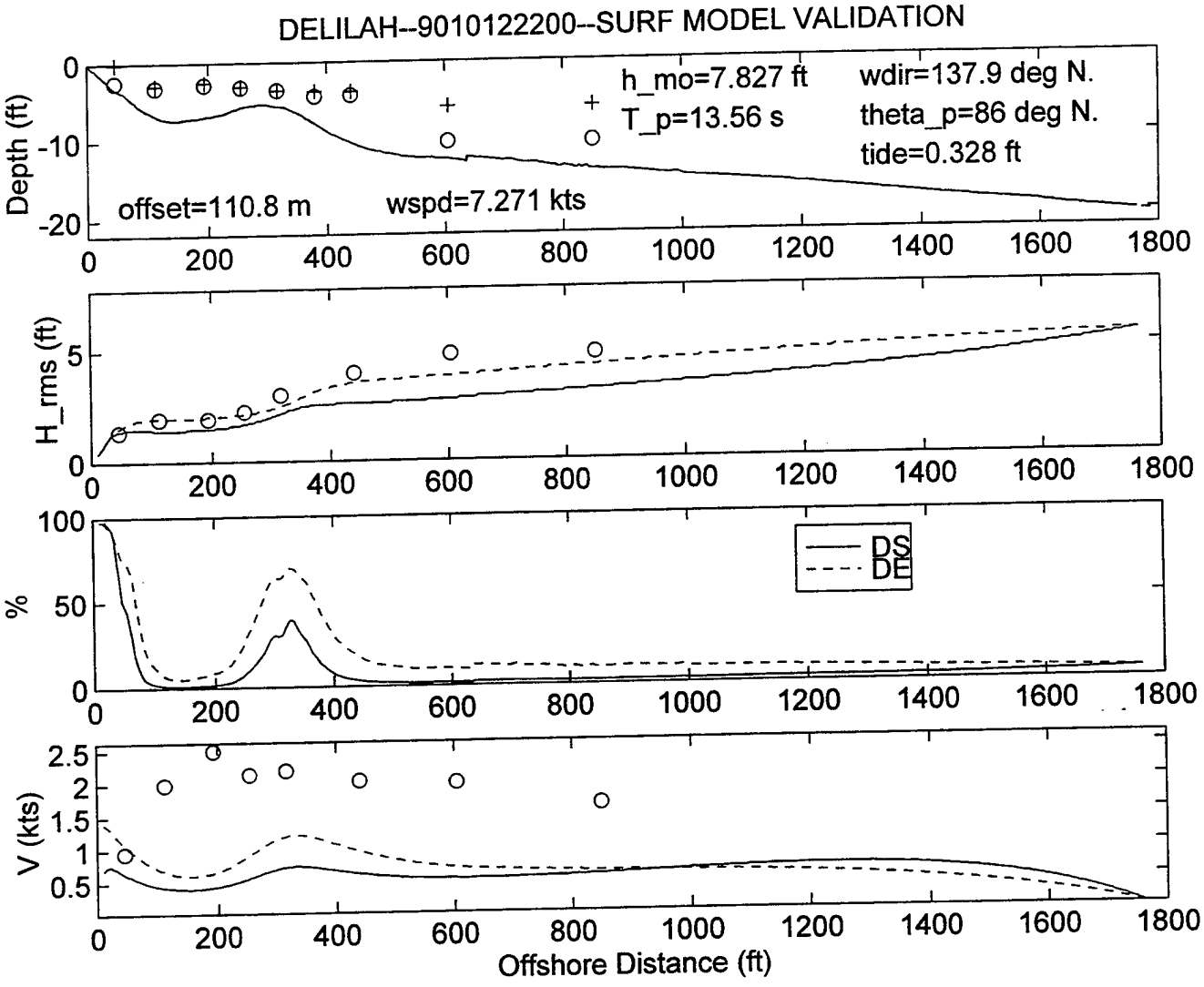
DELILAH--9010122200--SURF MODEL VALIDATION
Depth (ft)
h_mo=7.827 ft
T_p=13.56 s
wdir=137.9 deg N.
theta_p=86 deg N.
tide=0.328 ft
offset=110.8 m
wspd=7.271 kts
H_rms (ft)
%
DS
DE
V (kts)
Offshore Distance (ft)

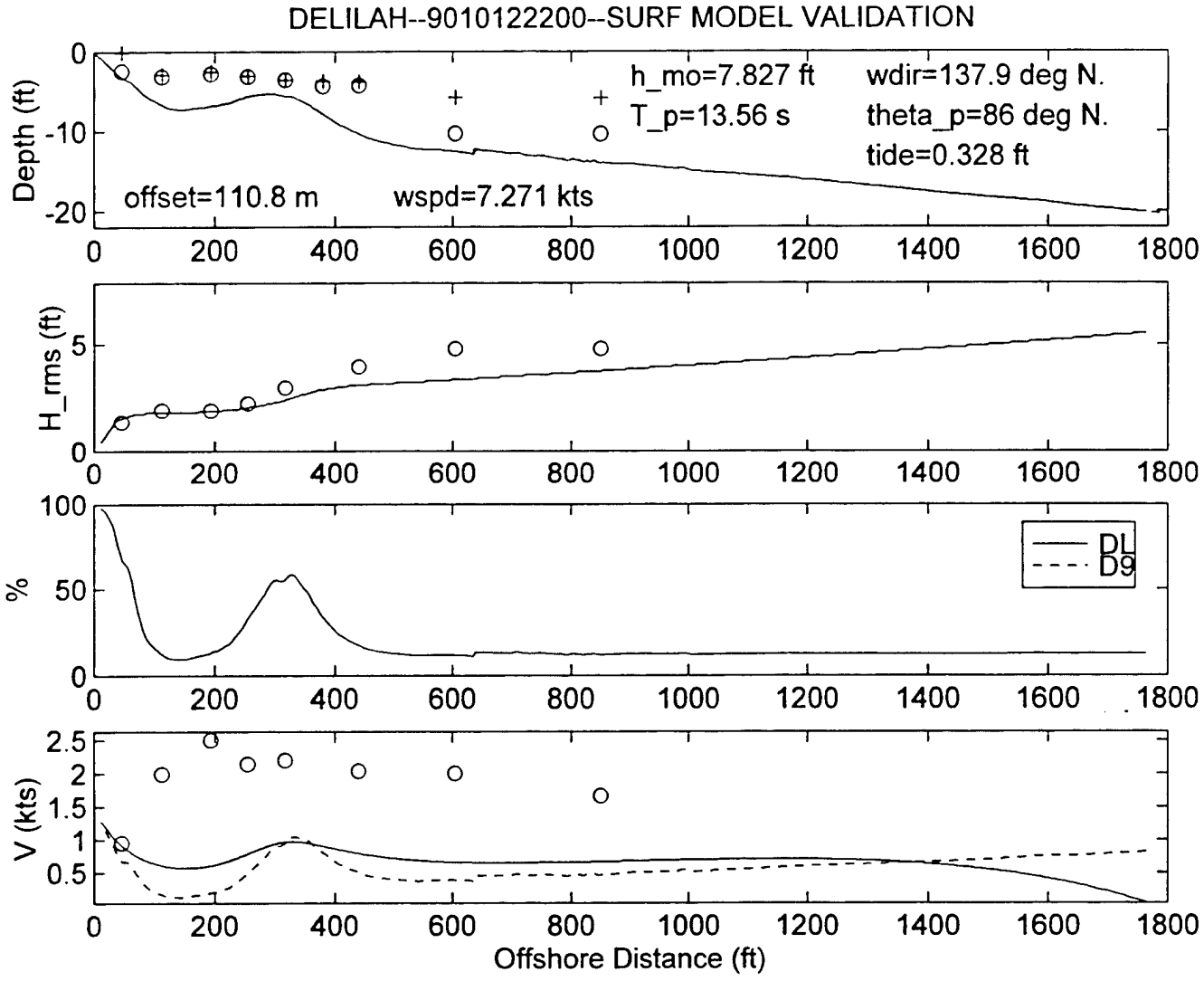
DELILAH--9010122200--SURF MODEL VALIDATION
Depth (ft)
h_mo=7.827 ft
T_p=13.56 s
wdir=137.9 deg N.
theta_p=86 deg N.
tide=0.328 ft
offset=110.8 m
wspd=7.271 kts
H_rms (ft)
%
DL
D9
V (kts)
Offshore Distance (ft)

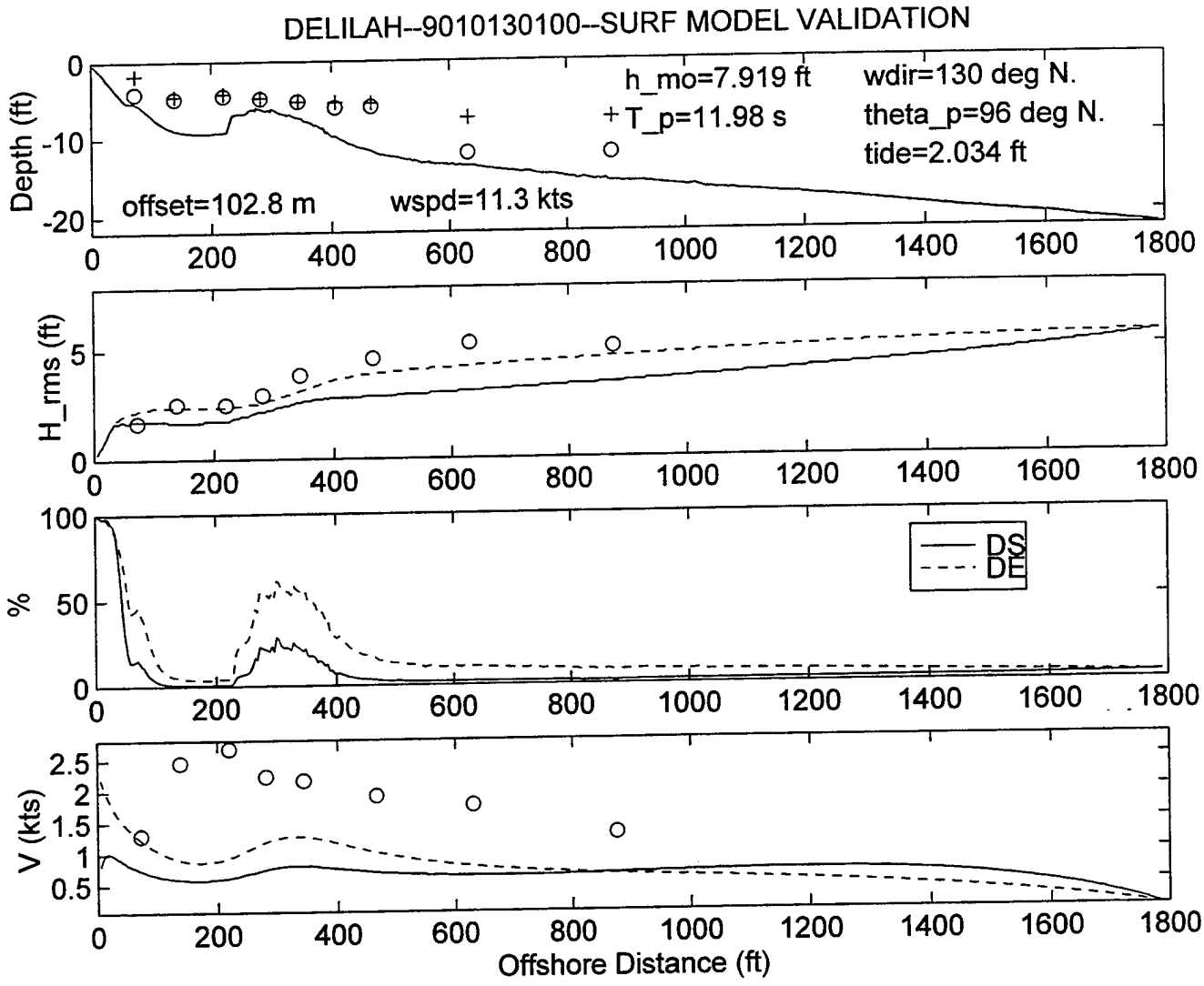
DELILAH--9010130100--SURF MODEL VALIDATION
Depth (ft)
h_mo=7.919 ft
T_p=11.98 s
wdir=130 deg N.
theta_p=96 deg N.
tide=2.034 ft
offset=102.8 m
wspd=11.3 kts
H_rms (ft)
%
DS
DE
V (kts)
Offshore Distance (ft)

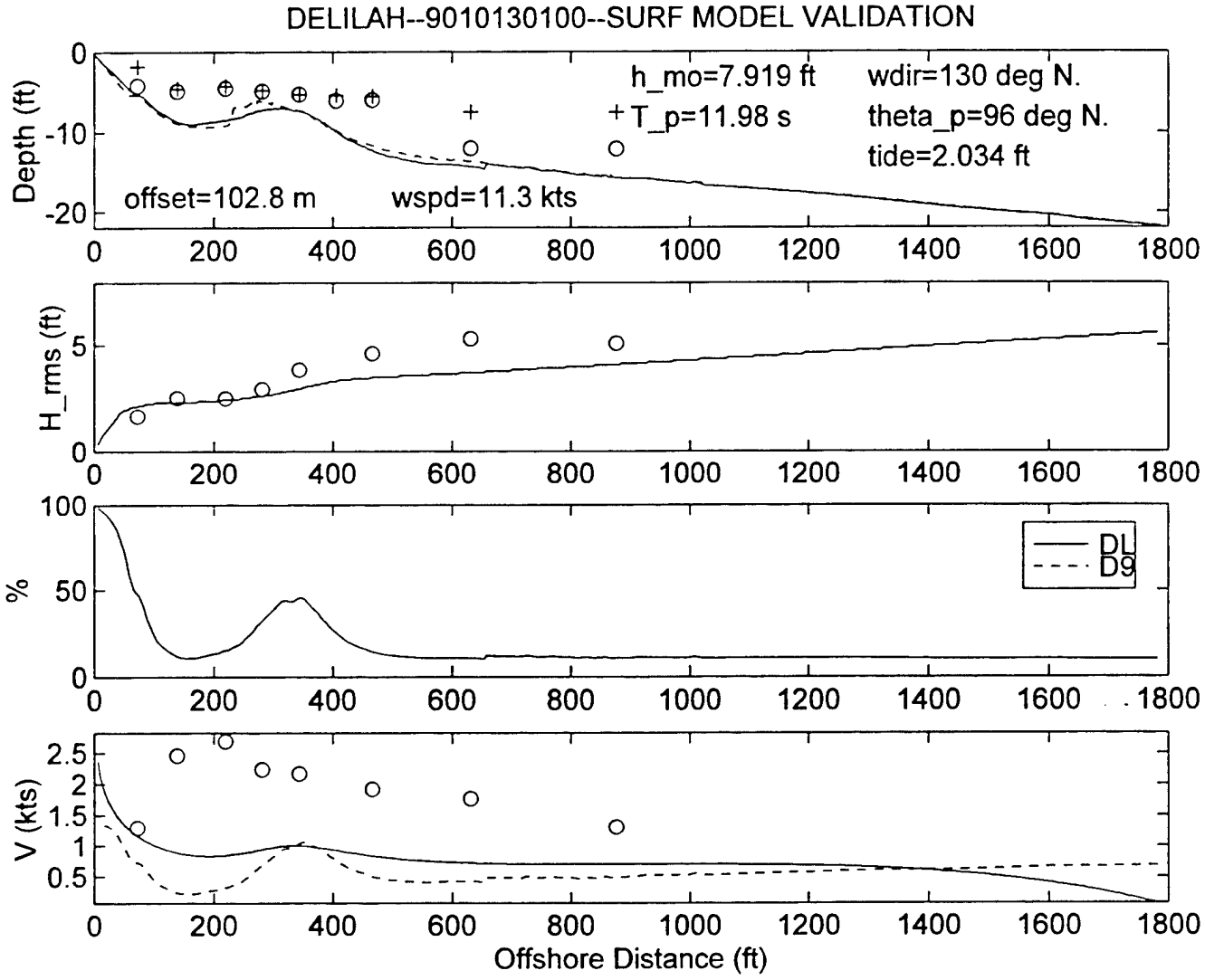
DELILAH--9010130100--SURF MODEL VALIDATION
Depth (ft)
h_mo=7.919 ft
T_p=11.98 s
wdir=130 deg N.
theta_p=96 deg N.
tide=2.034 ft
offset=102.8 m
wspd=11.3 kts
H_rms (ft)
%
DL
D9
V (kts)
Offshore Distance (ft)

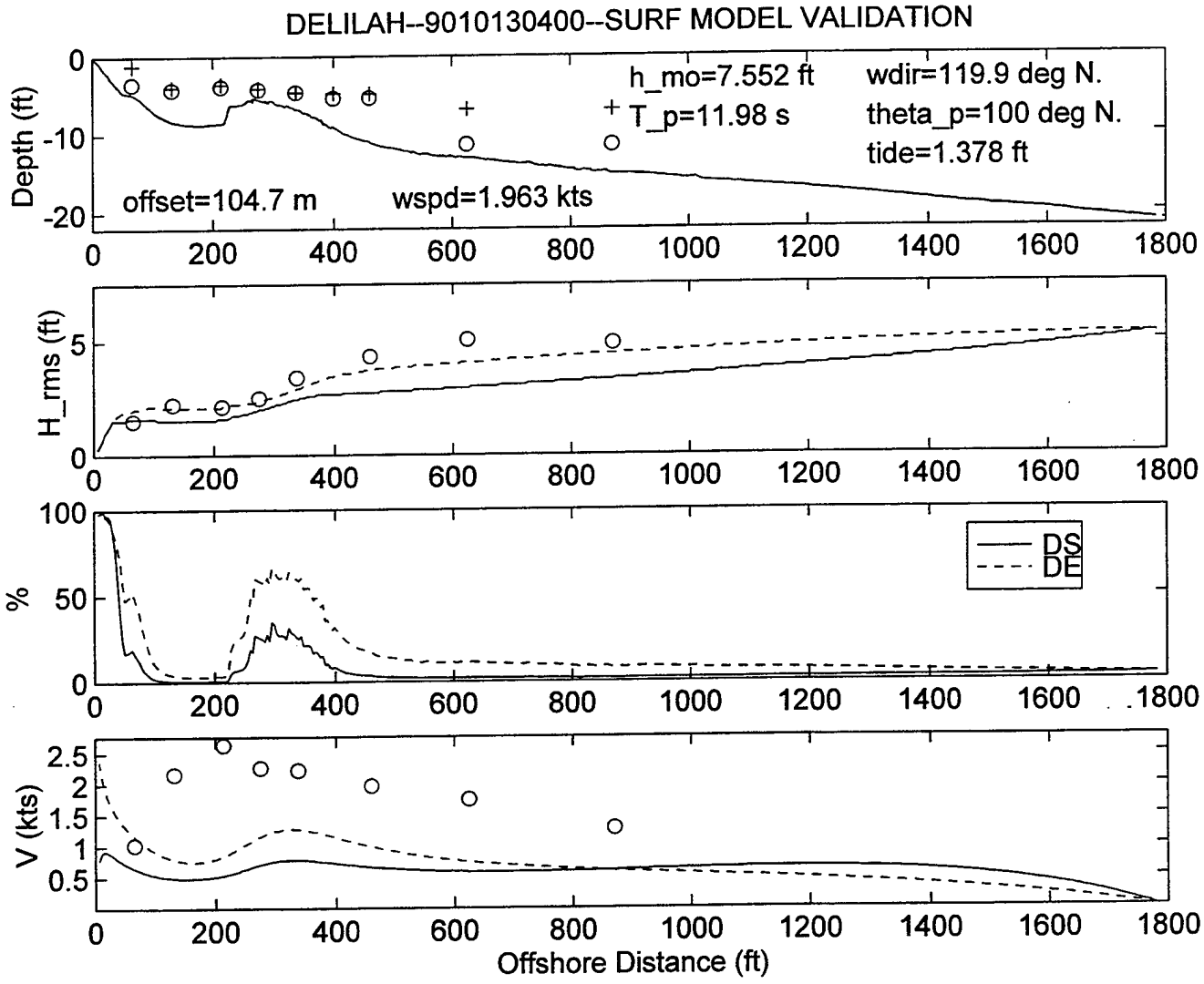
DELILAH--9010130400--SURF MODEL VALIDATION
Depth (ft)
h_mo=7.552 ft
T_p=11.98 s
wdir=119.9 deg N.
theta_p=100 deg N.
tide=1.378 ft
offset=104.7 m
wspd=1.963 kts
H_rms (ft)
%
DS
DE
V (kts)
Offshore Distance (ft)

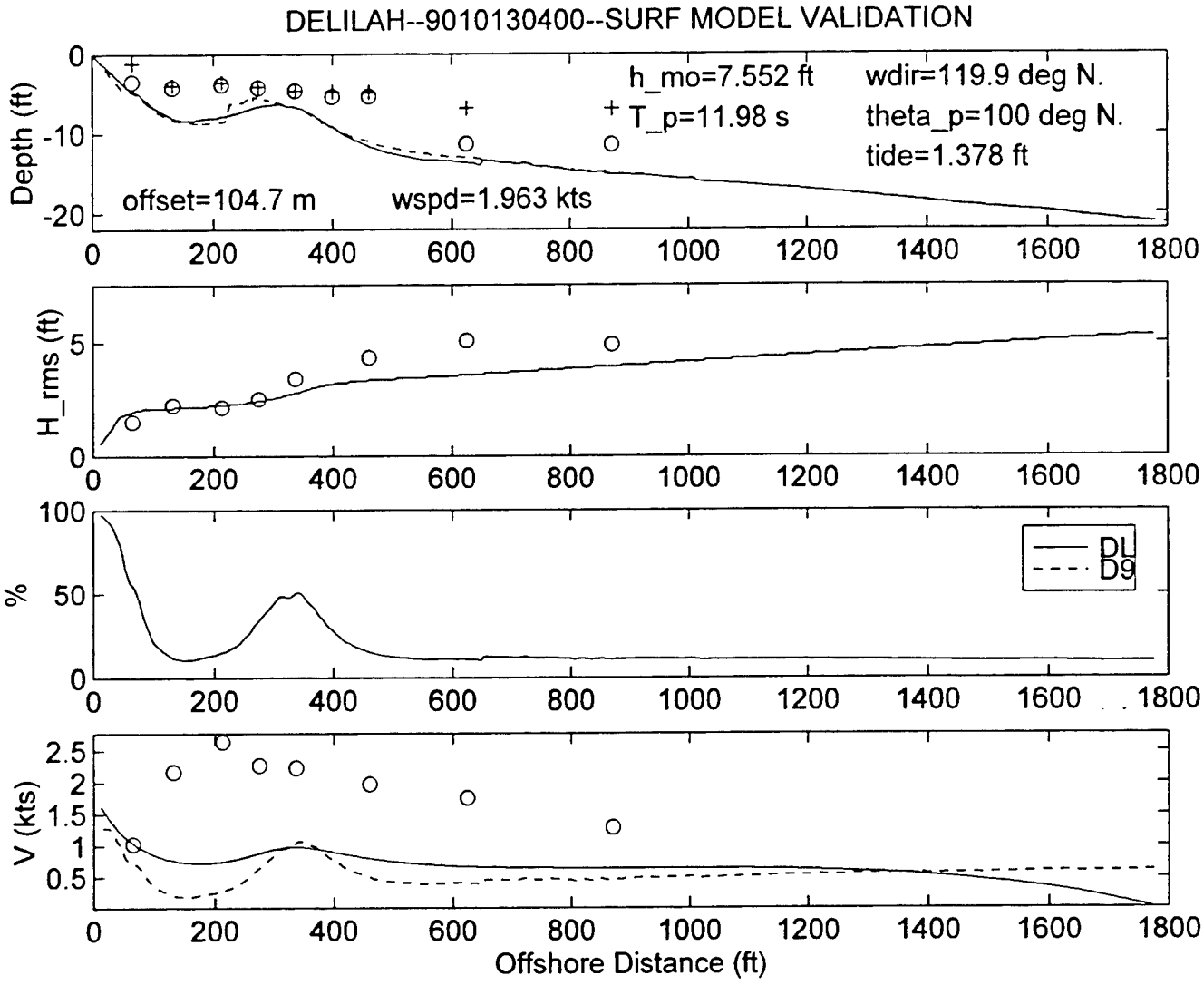
DELILAH--9010130400--SURF MODEL VALIDATION
Depth (ft)
h_mo=7.552 ft
T_p=11.98 s
wdir=119.9 deg N.
theta_p=100 deg N.
tide=1.378 ft
offset=104.7 m
wspd=1.963 kts
H_rms (ft)
%
DL
D9
V (kts)
Offshore Distance (ft)

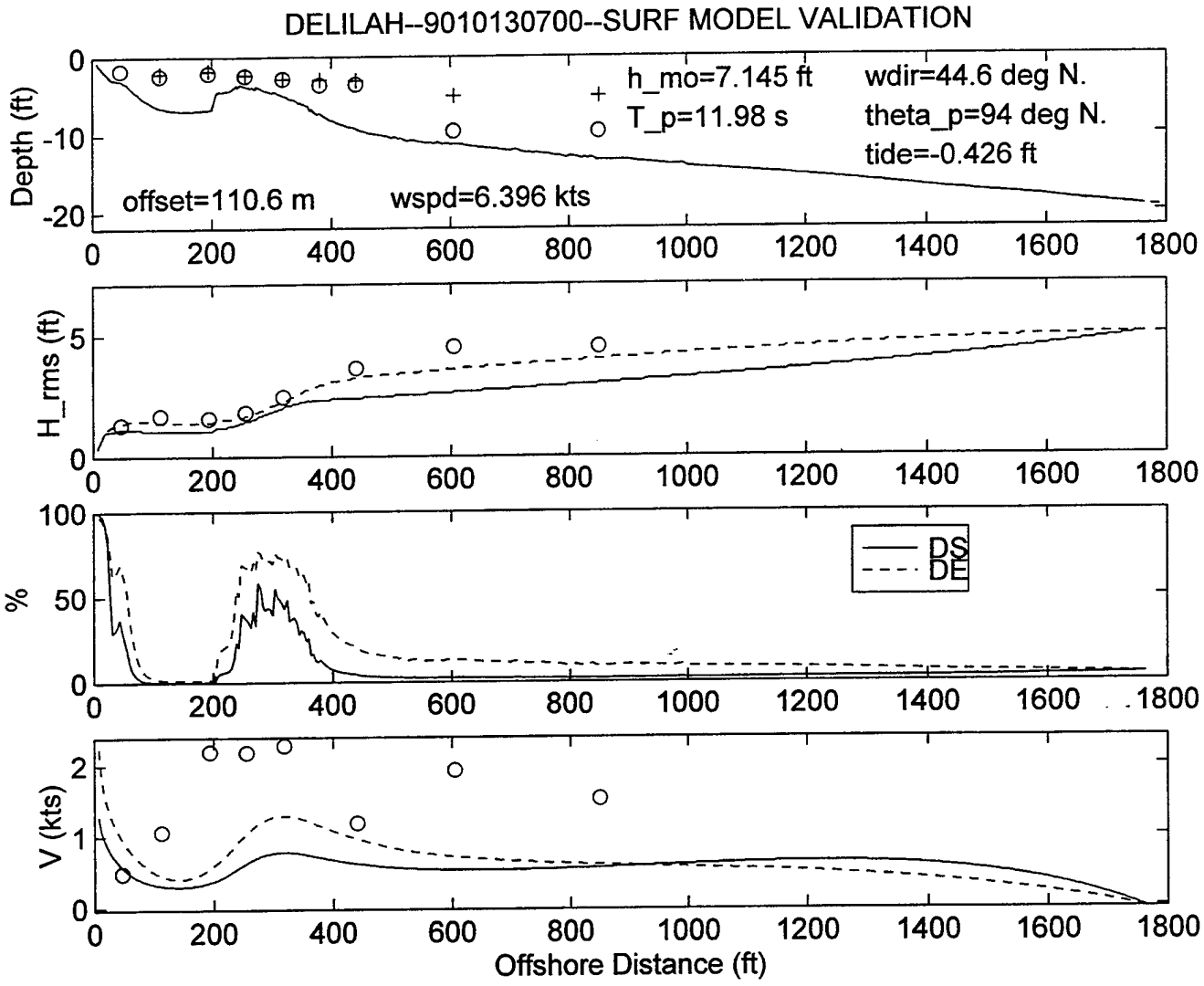
DELILAH--9010130700--SURF MODEL VALIDATION
Depth (ft)
h_mo=7.145 ft
T_p=11.98 s
wdir=44.6 deg N.
theta_p=94 deg N.
tide=-0.426 ft
offset=110.6 m
wspd=6.396 kts
H_rms (ft)
%
DS
DE
V (kts)
Offshore Distance (ft)

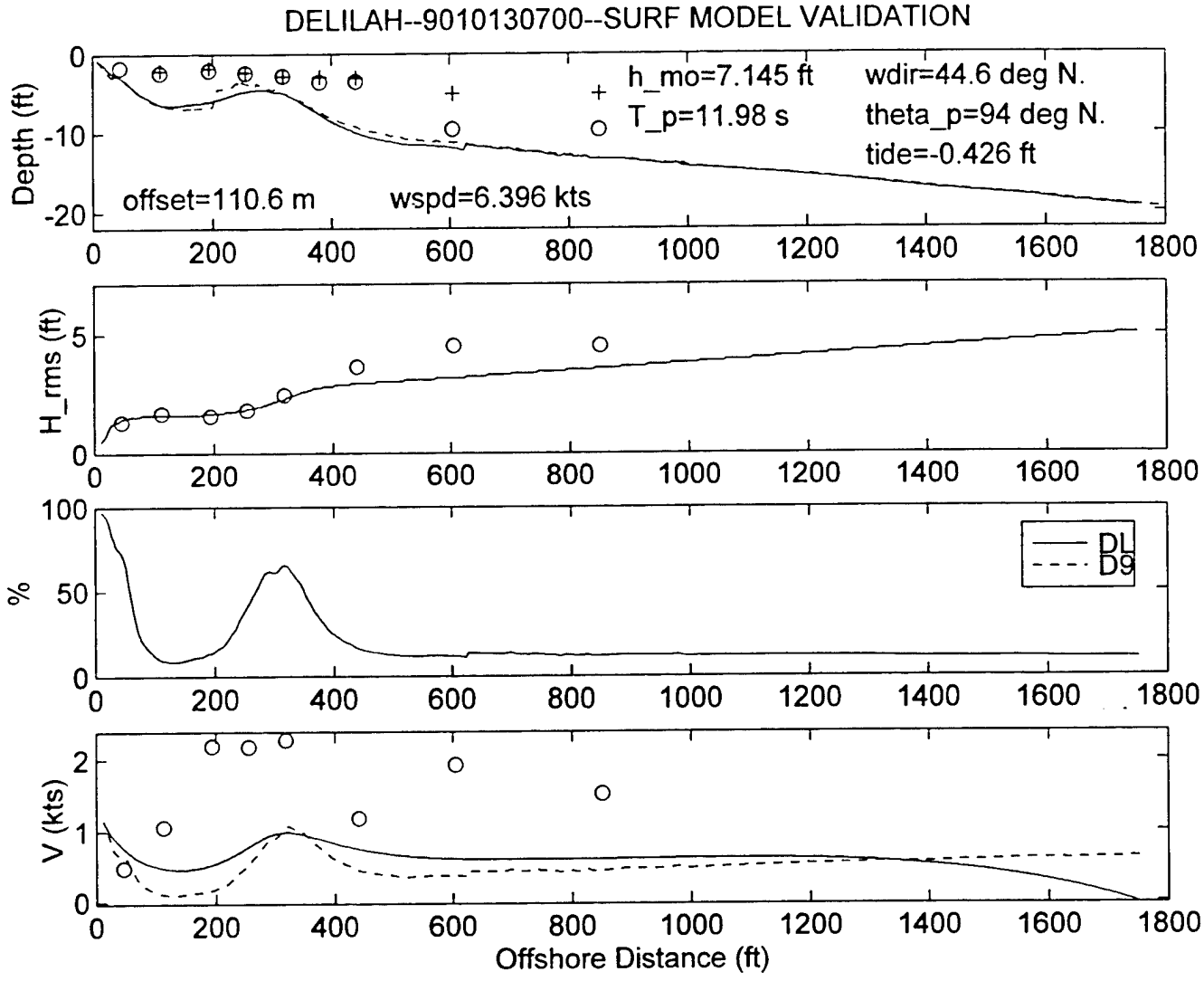
DELILAH--9010130700--SURF MODEL VALIDATION
Depth (ft)
h_mo=7.145 ft
T_p=11.98 s
wdir=44.6 deg N.
theta_p=94 deg N.
tide=-0.426 ft
offset=110.6 m
wspd=6.396 kts
H_rms (ft)
%
DL
D9
V (kts)
Offshore Distance (ft)

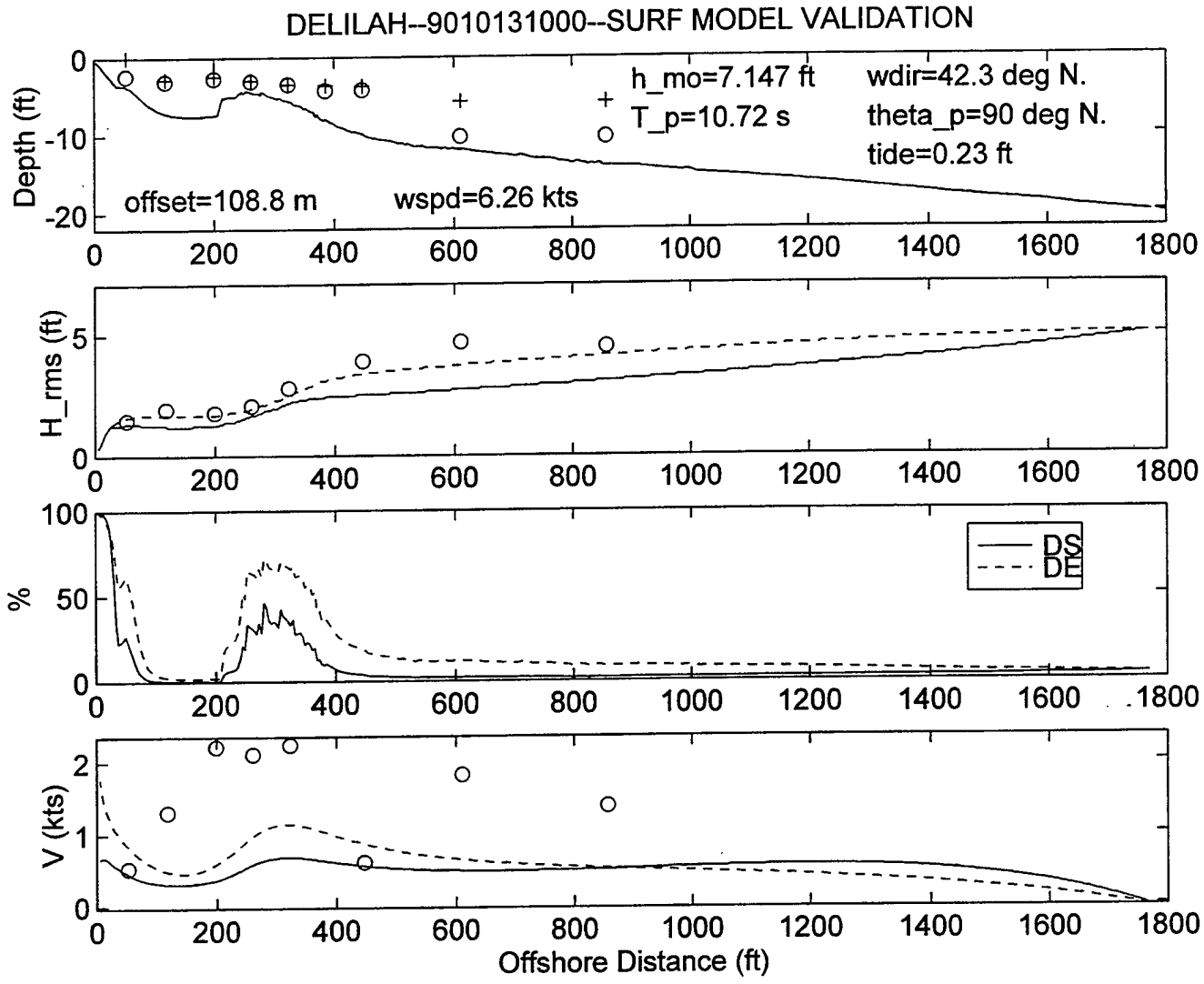
DELILAH--9010131000--SURF MODEL VALIDATION
Depth (ft)
h_mo=7.147 ft
T_p=10.72 s
wdir=42.3 deg N.
theta_p=90 deg N.
tide=0.23 ft
offset=108.8 m
wspd=6.26 kts
H_rms (ft)
%
DS
DE
V (kts)
Offshore Distance (ft)

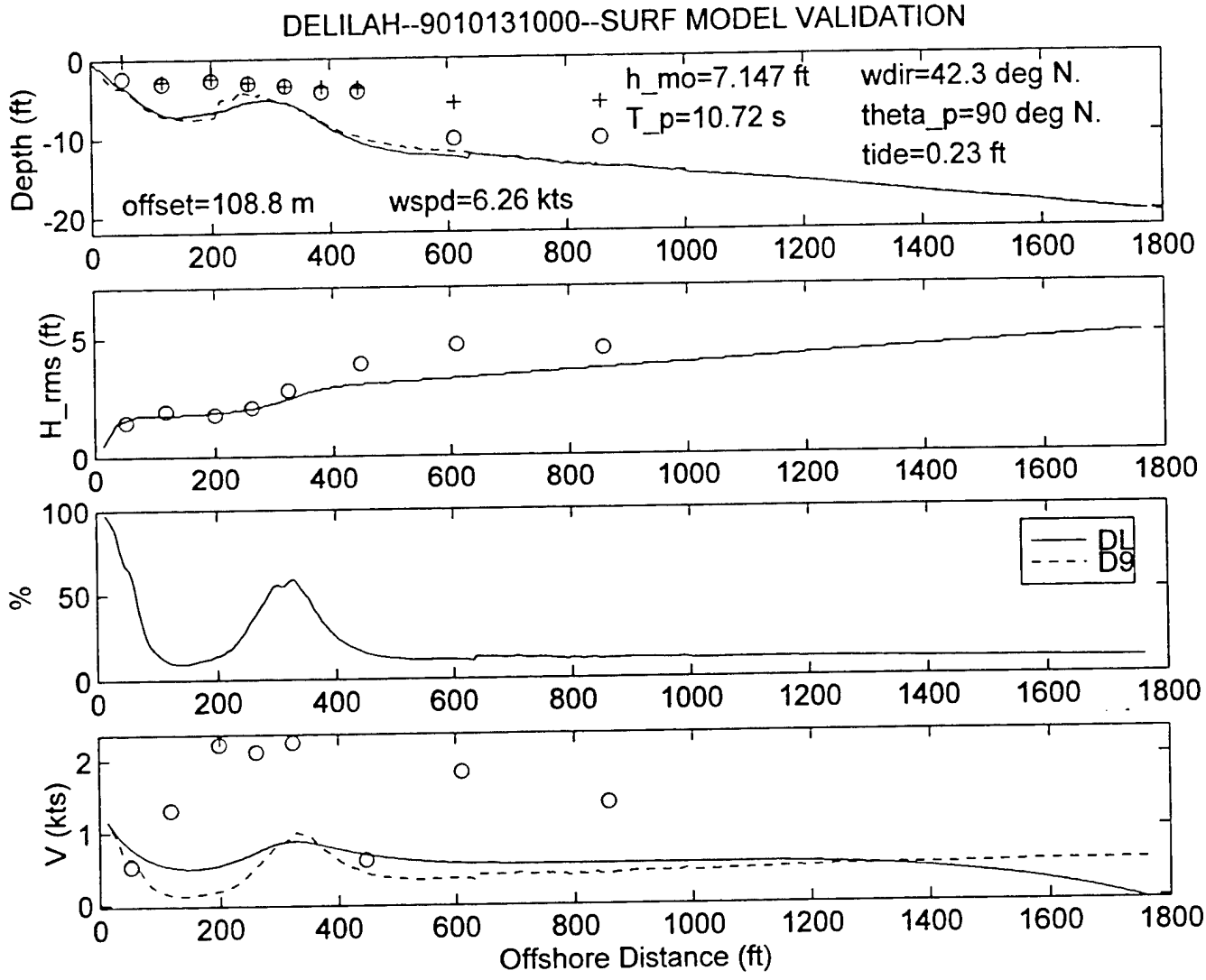
DELILAH--9010131000--SURF MODEL VALIDATION
Depth (ft)
h_mo=7.147 ft
T_p=10.72 s
wdir=42.3 deg N.
theta_p=90 deg N.
tide=0.23 ft
offset=108.8 m
wspd=6.26 kts
H_rms (ft)
%
DL
D9
V (kts)
Offshore Distance (ft)

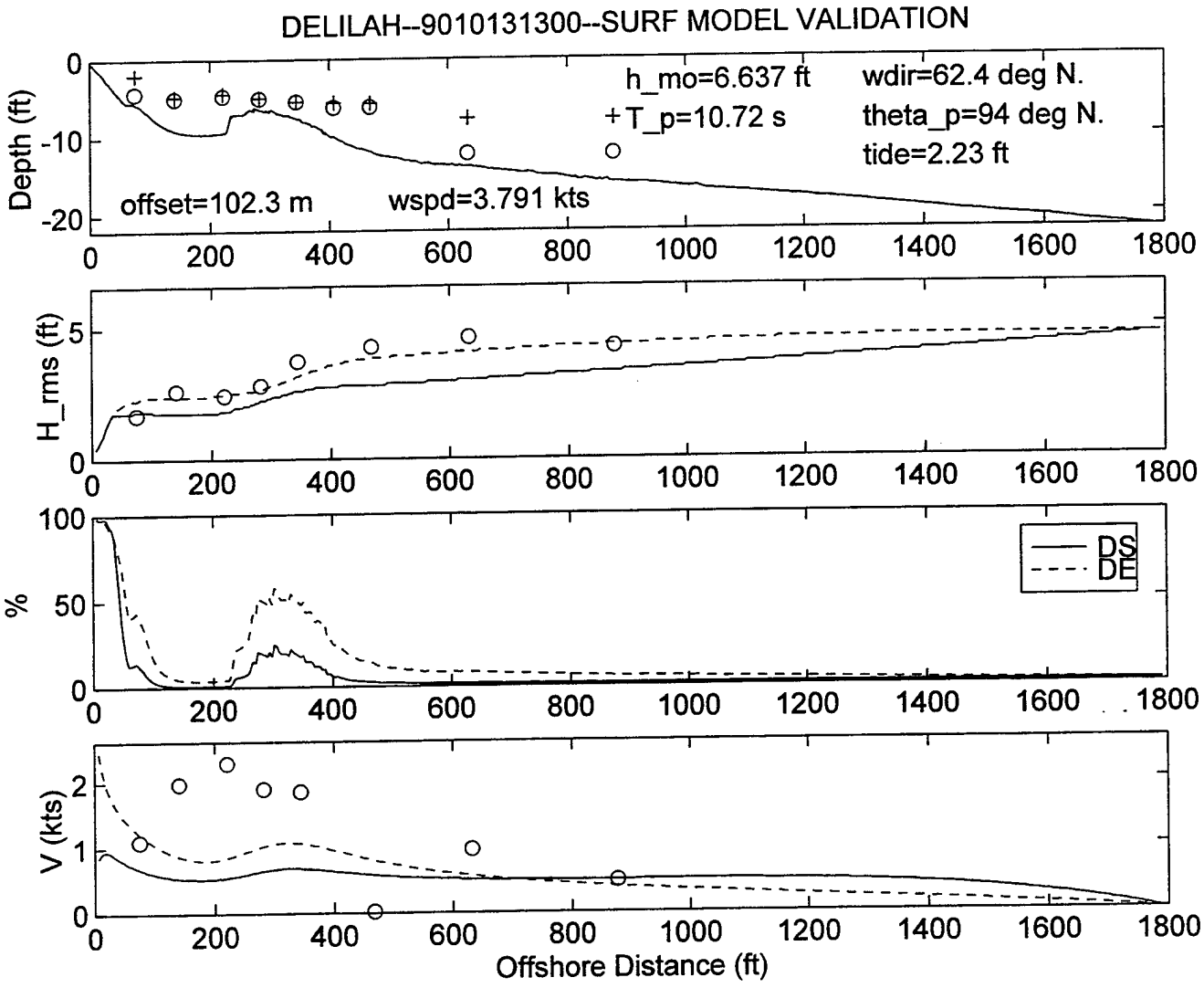
DELILAH--9010131300--SURF MODEL VALIDATION
Depth (ft)
h_mo=6.637 ft
+T_p=10.72 s
wdir=62.4 deg N.
theta_p=94 deg N.
tide=2.23 ft
offset=102.3 m
wspd=3.791 kts
H_rms (ft)
%
DS
DE
V (kts)
Offshore Distance (ft)

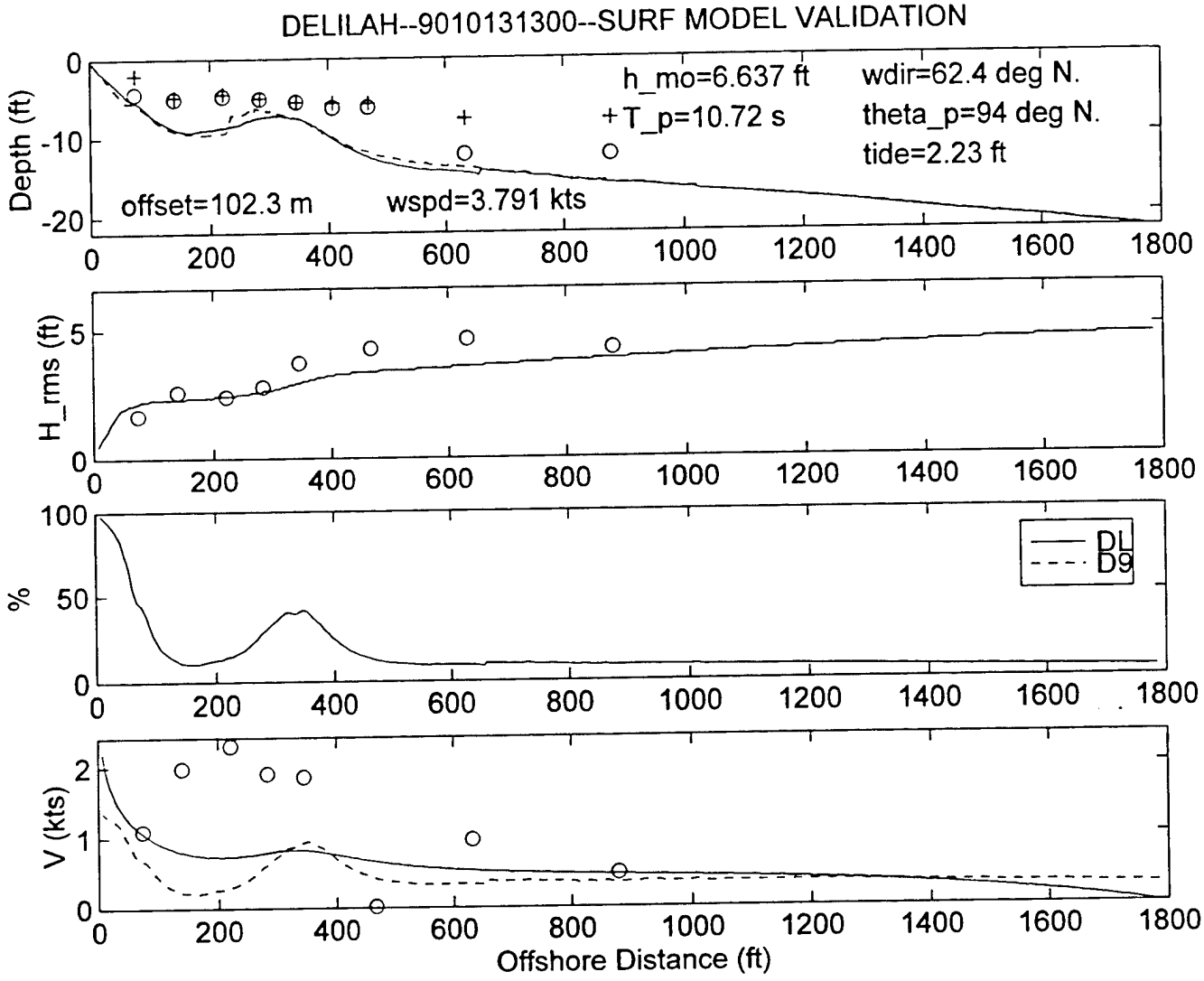
DELILAH--9010131300--SURF MODEL VALIDATION
Depth (ft)
h_mo=6.637 ft
+T_p=10.72 s
wdir=62.4 deg N.
theta_p=94 deg N.
tide=2.23 ft
offset=102.3 m
wspd=3.791 kts
H_rms (ft)
%
DL
D9
V (kts)
Offshore Distance (ft)

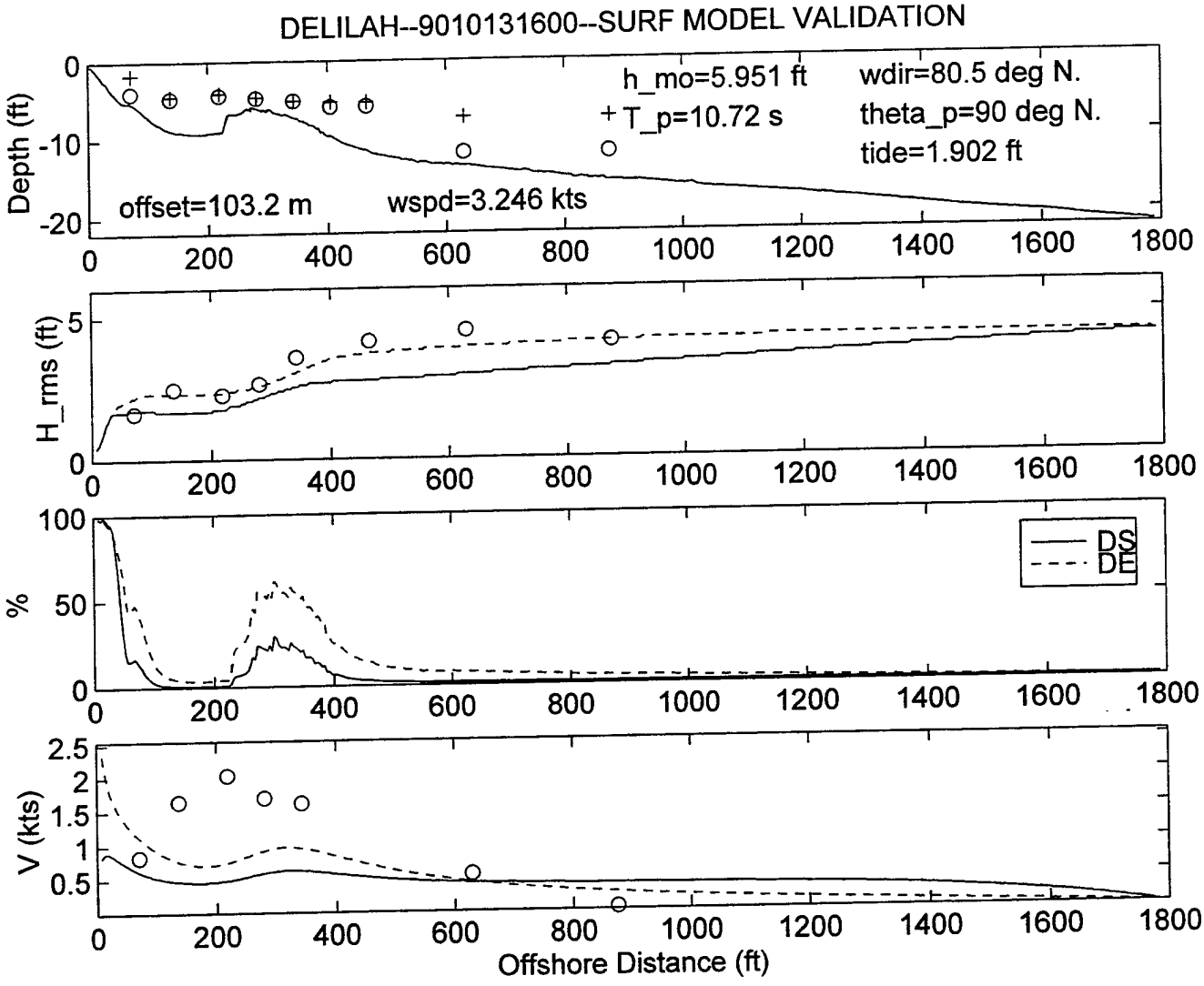
DELILAH--9010131600--SURF MODEL VALIDATION
Depth (ft)
h_mo=5.951 ft
T_p=10.72 s
wdir=80.5 deg N.
theta_p=90 deg N.
tide=1.902 ft
offset=103.2 m
wspd=3.246 kts
H_rms (ft)
%
DS
DE
V (kts)
Offshore Distance (ft)

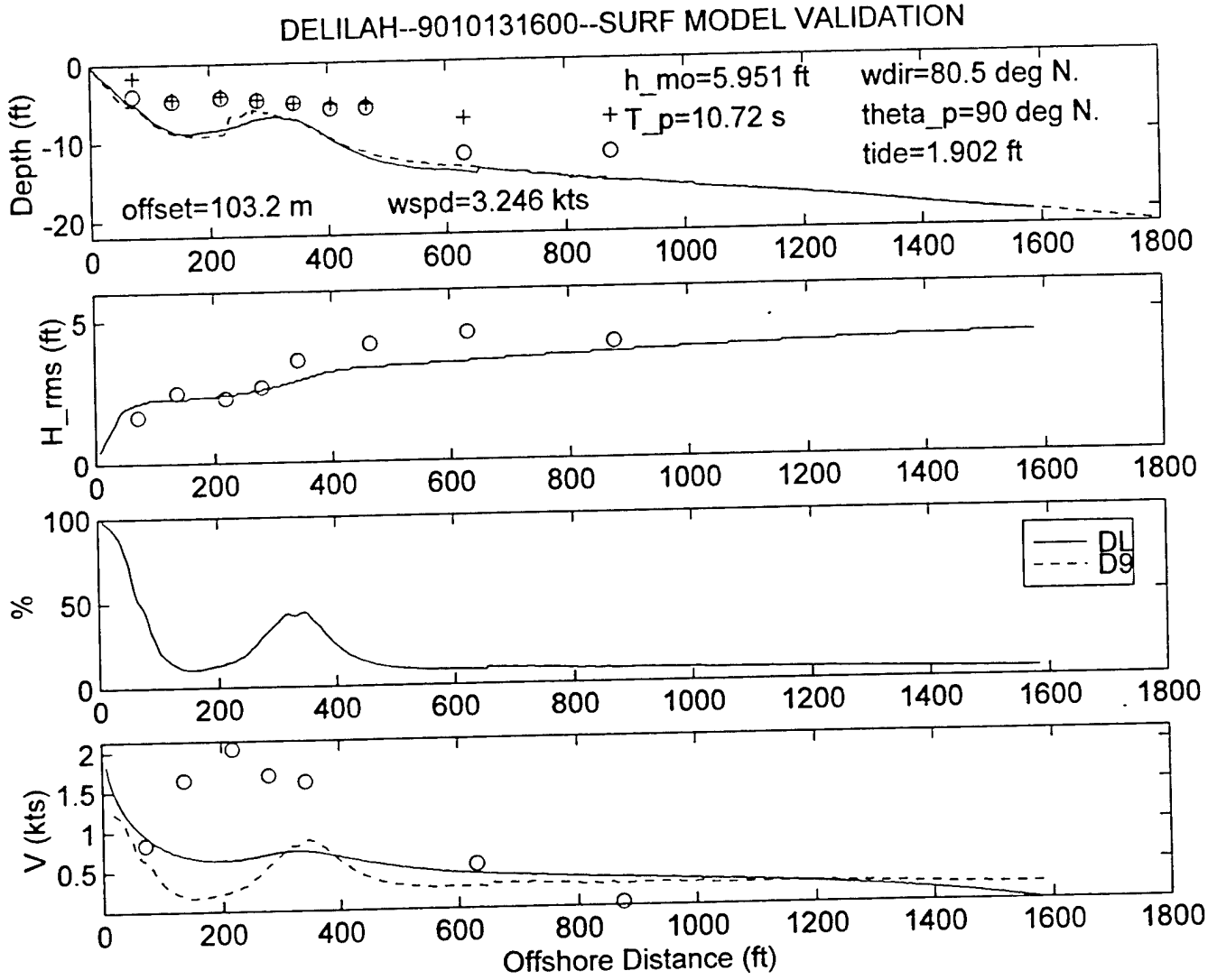
DELILAH--9010131600--SURF MODEL VALIDATION
Depth (ft)
h_mo=5.951 ft
T_p=10.72 s
wdir=80.5 deg N.
theta_p=90 deg N.
tide=1.902 ft
offset=103.2 m
wspd=3.246 kts
H_rms (ft)
%
DL
D9
V (kts)
Offshore Distance (ft)

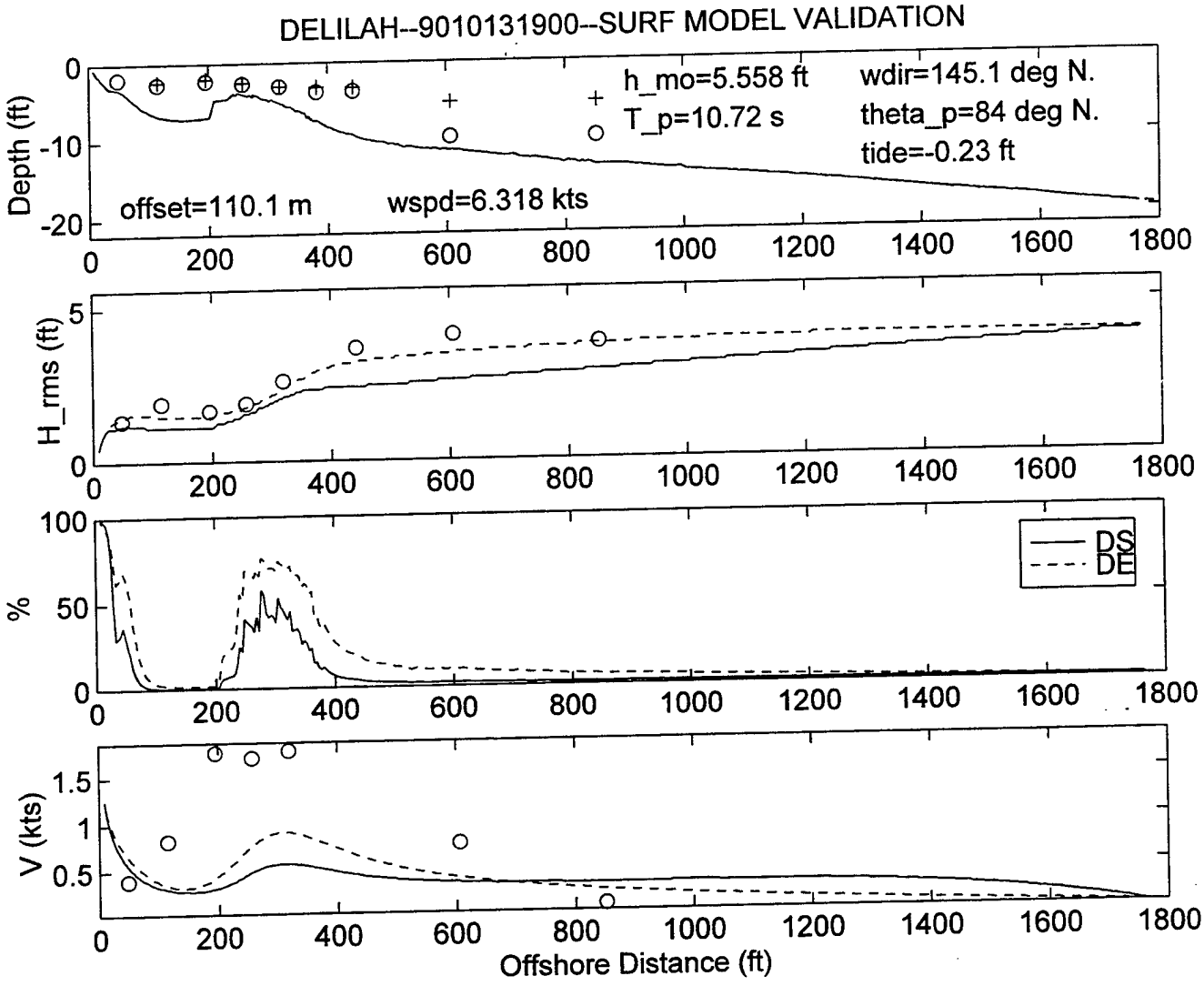
DELILAH--9010131900--SURF MODEL VALIDATION
Depth (ft)
h_mo=5.558 ft
T_p=10.72 s
wdir=145.1 deg N.
theta_p=84 deg N.
tide=-0.23 ft
offset=110.1 m
wspd=6.318 kts
H_rms (ft)
%
DS
DE
V (kts)
Offshore Distance (ft)

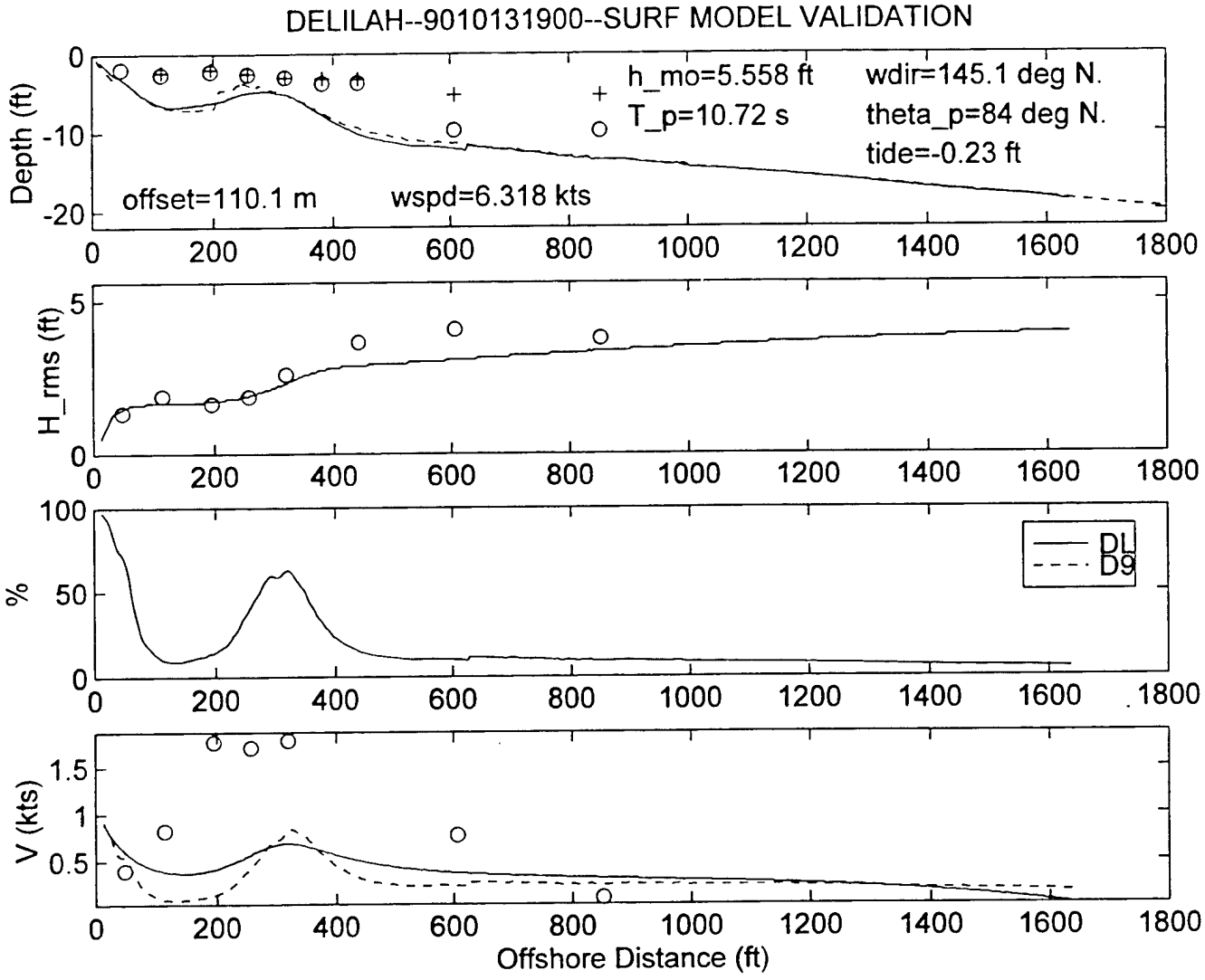
DELILAH--9010131900--SURF MODEL VALIDATION
Depth (ft)
h_mo=5.558 ft
T_p=10.72 s
wdir=145.1 deg N.
theta_p=84 deg N.
tide=-0.23 ft
offset=110.1 m
wspd=6.318 kts
H_rms (ft)
%
D1
D9
V (kts)
Offshore Distance (ft)

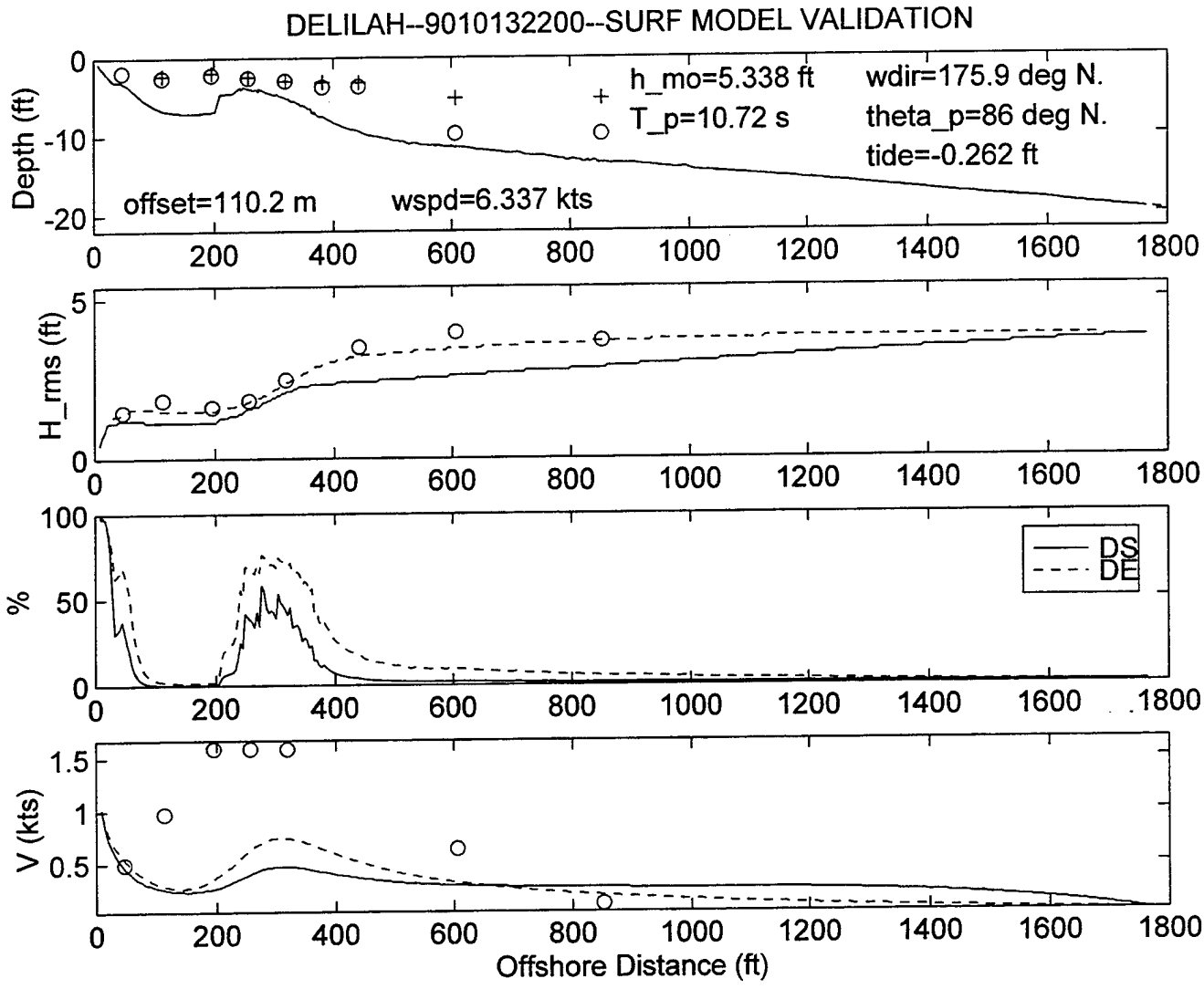
DELILAH--9010132200--SURF MODEL VALIDATION
Depth (ft)
h_mo=5.338 ft
T_p=10.72 s
wdir=175.9 deg N.
theta_p=86 deg N.
tide=-0.262 ft
offset=110.2 m
wspd=6.337 kts
H_rms (ft)
%
DS
DE
V (kts)
Offshore Distance (ft)

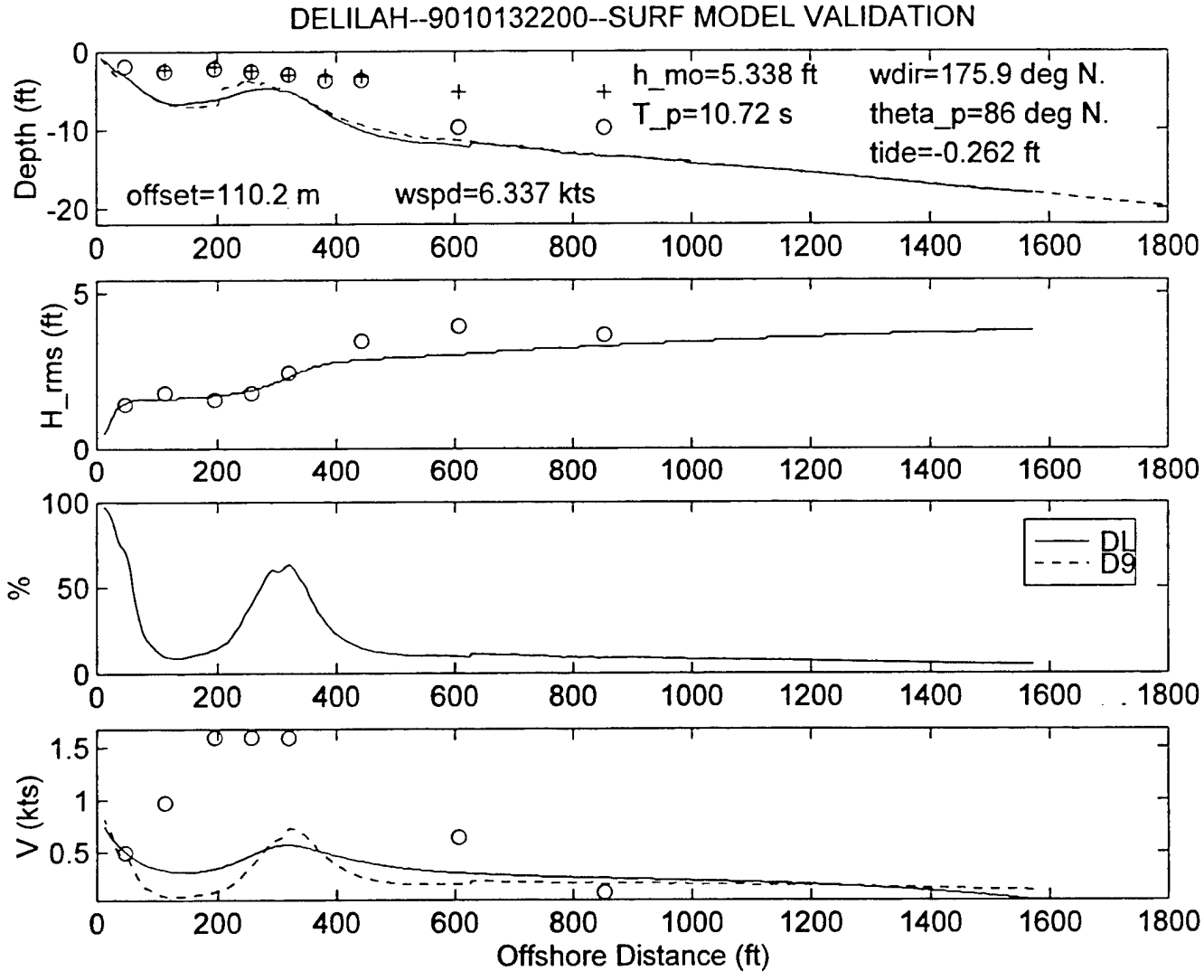
DELILAH--9010132200--SURF MODEL VALIDATION
Depth (ft)
h_mo=5.338 ft
T_p=10.72 s
wdir=175.9 deg N.
theta_p=86 deg N.
tide=-0.262 ft
offset=110.2 m
wspd=6.337 kts
H_rms (ft)
%
DL
D9
V (kts)
Offshore Distance (ft)

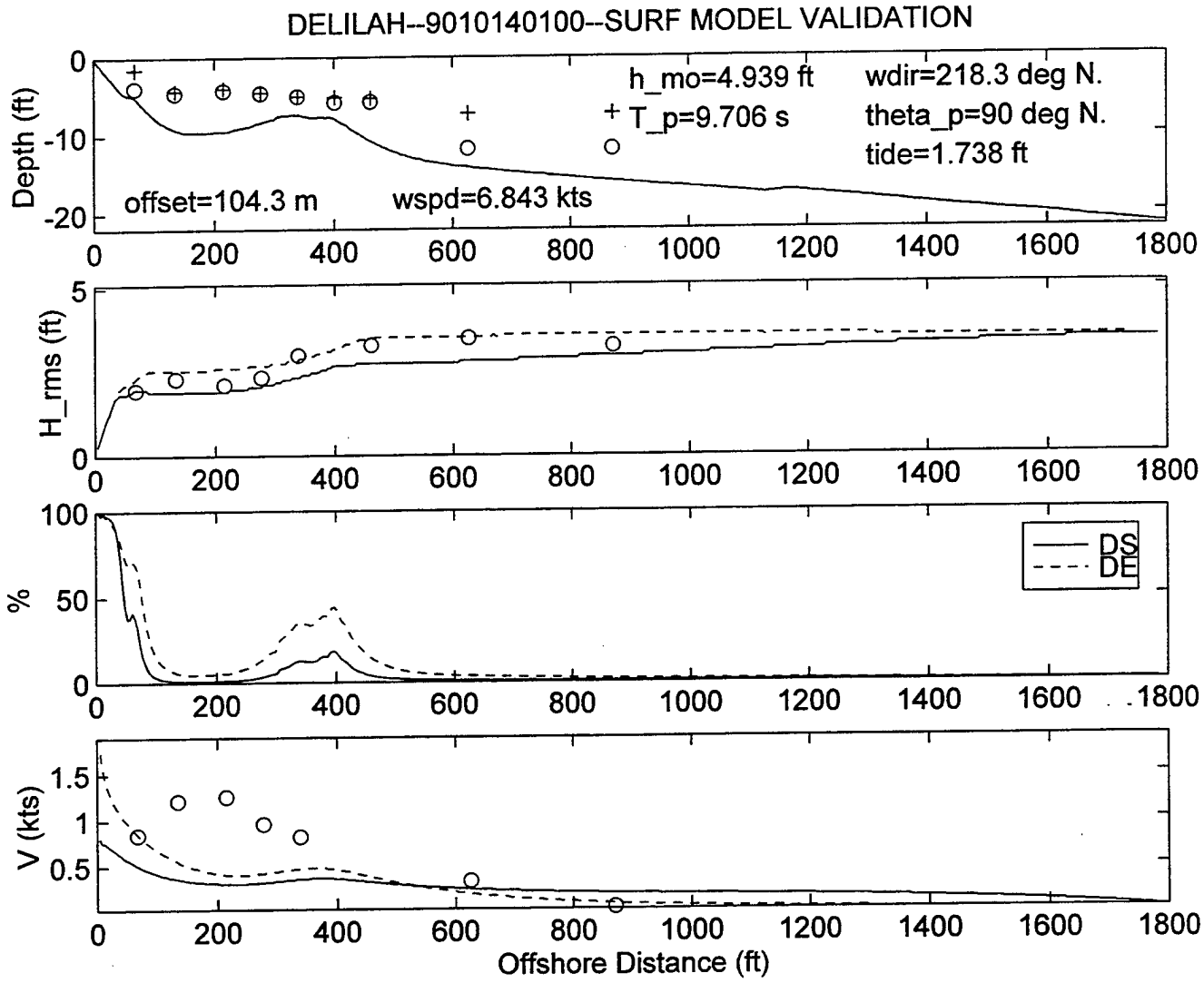
DELILAH--9010140100--SURF MODEL VALIDATION
Depth (ft)
h_mo=4.939 ft
T_p=9.706 s
wdir=218.3 deg N.
theta_p=90 deg N.
tide=1.738 ft
offset=104.3 m
wspd=6.843 kts
H_rms (ft)
%
DS
DE
V (kts)
Offshore Distance (ft)

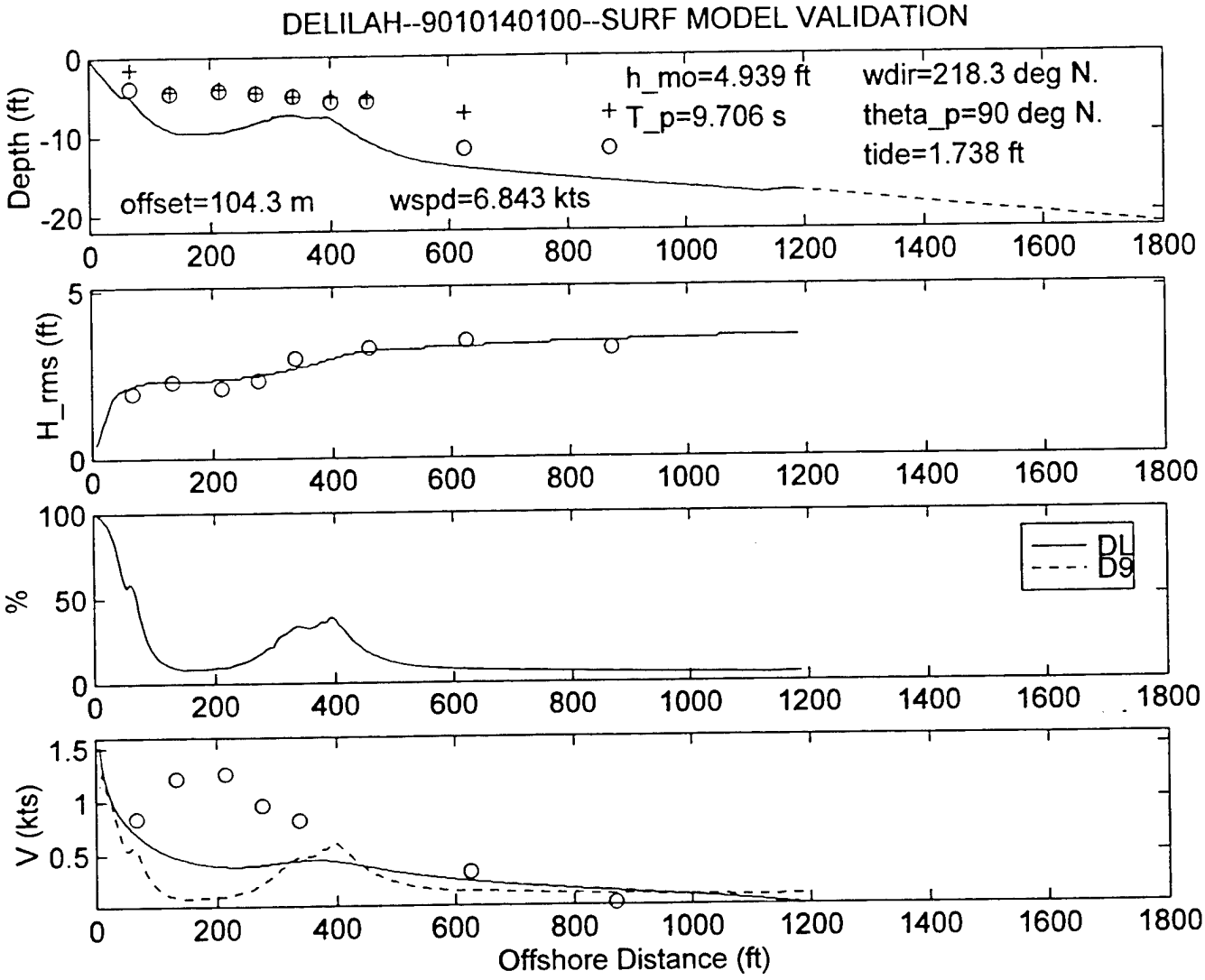
DELILAH--9010140100--SURF MODEL VALIDATION
Depth (ft)
h_mo=4.939 ft
T_p=9.706 s
wdir=218.3 deg N.
theta_p=90 deg N.
tide=1.738 ft
offset=104.3 m
wspd=6.843 kts
H_rms (ft)
%
DL
D9
V (kts)
Offshore Distance (ft)

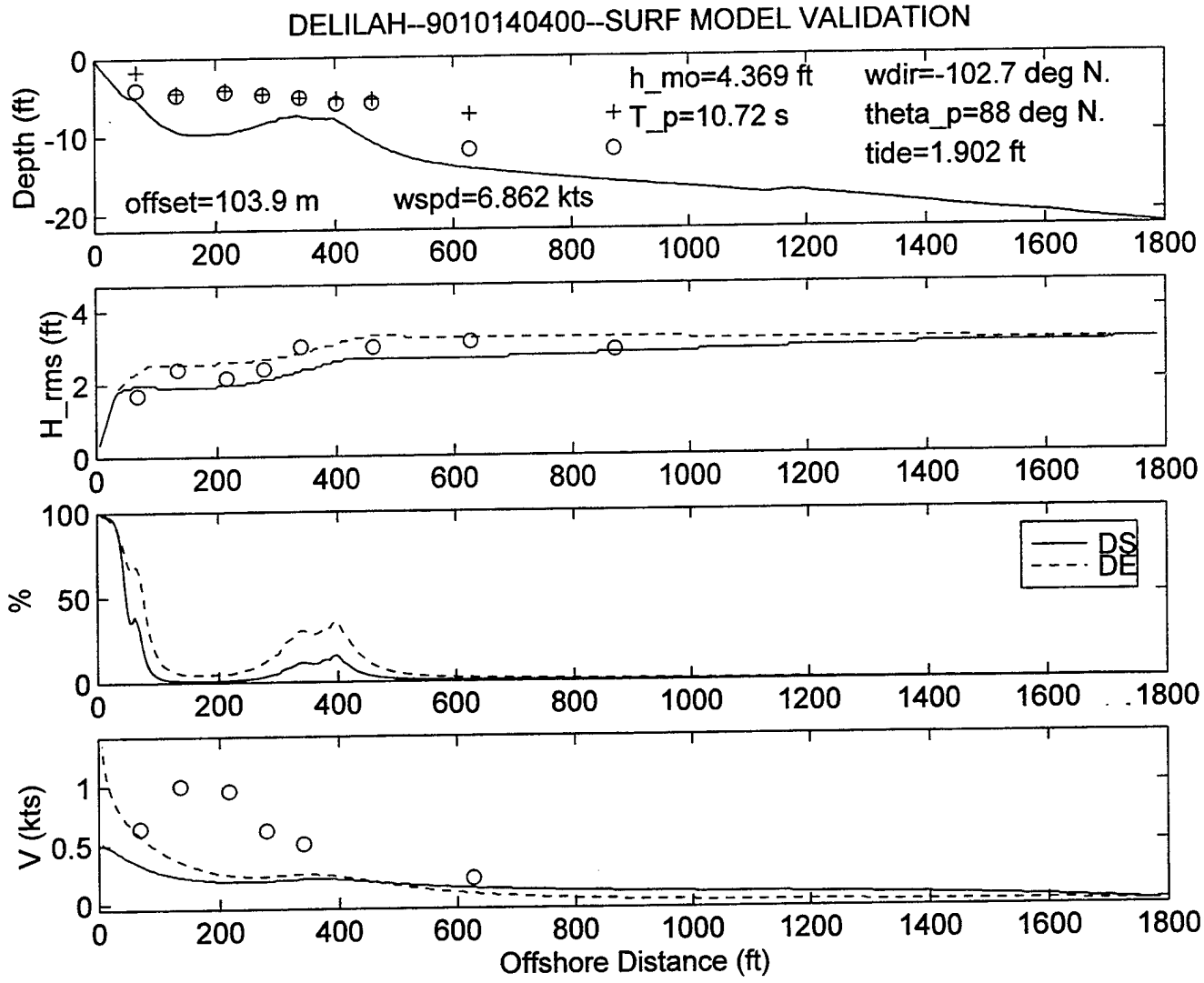
DELILAH--9010140400--SURF MODEL VALIDATION
Depth (ft)
h_mo=4.369 ft
T_p=10.72 s
wdir=-102.7 deg N.
theta_p=88 deg N.
tide=1.902 ft
offset=103.9 m
wspd=6.862 kts
H_rms (ft)
%
DS
DE
V (kts)
Offshore Distance (ft)

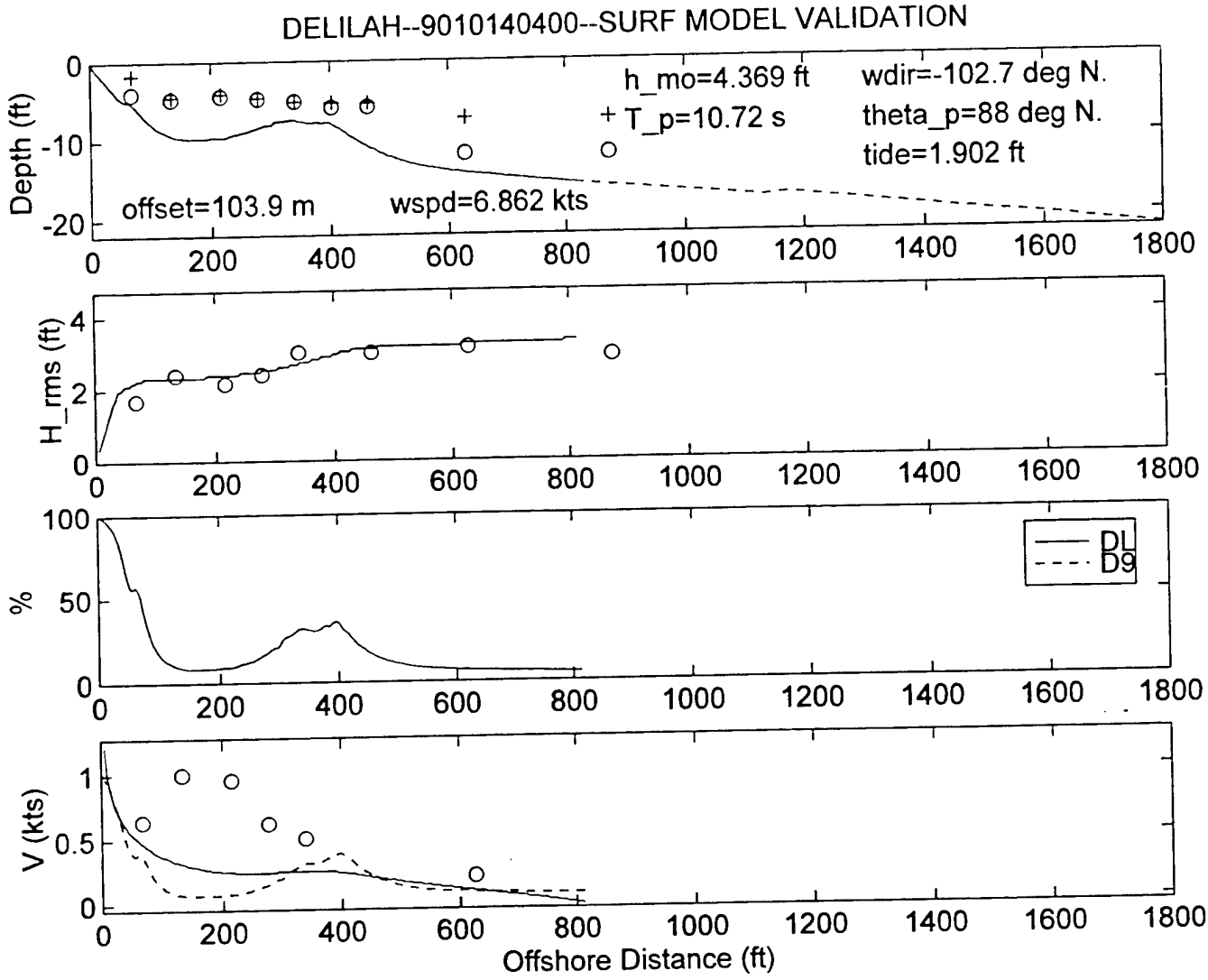
DELILAH--9010140400--SURF MODEL VALIDATION
Depth (ft)
h_mo=4.369 ft
T_p=10.72 s
wdir=-102.7 deg N.
theta_p=88 deg N.
tide=1.902 ft
offset=103.9 m
wspd=6.862 kts
H_rms (ft)
%
DL
D9
V (kts)
Offshore Distance (ft)

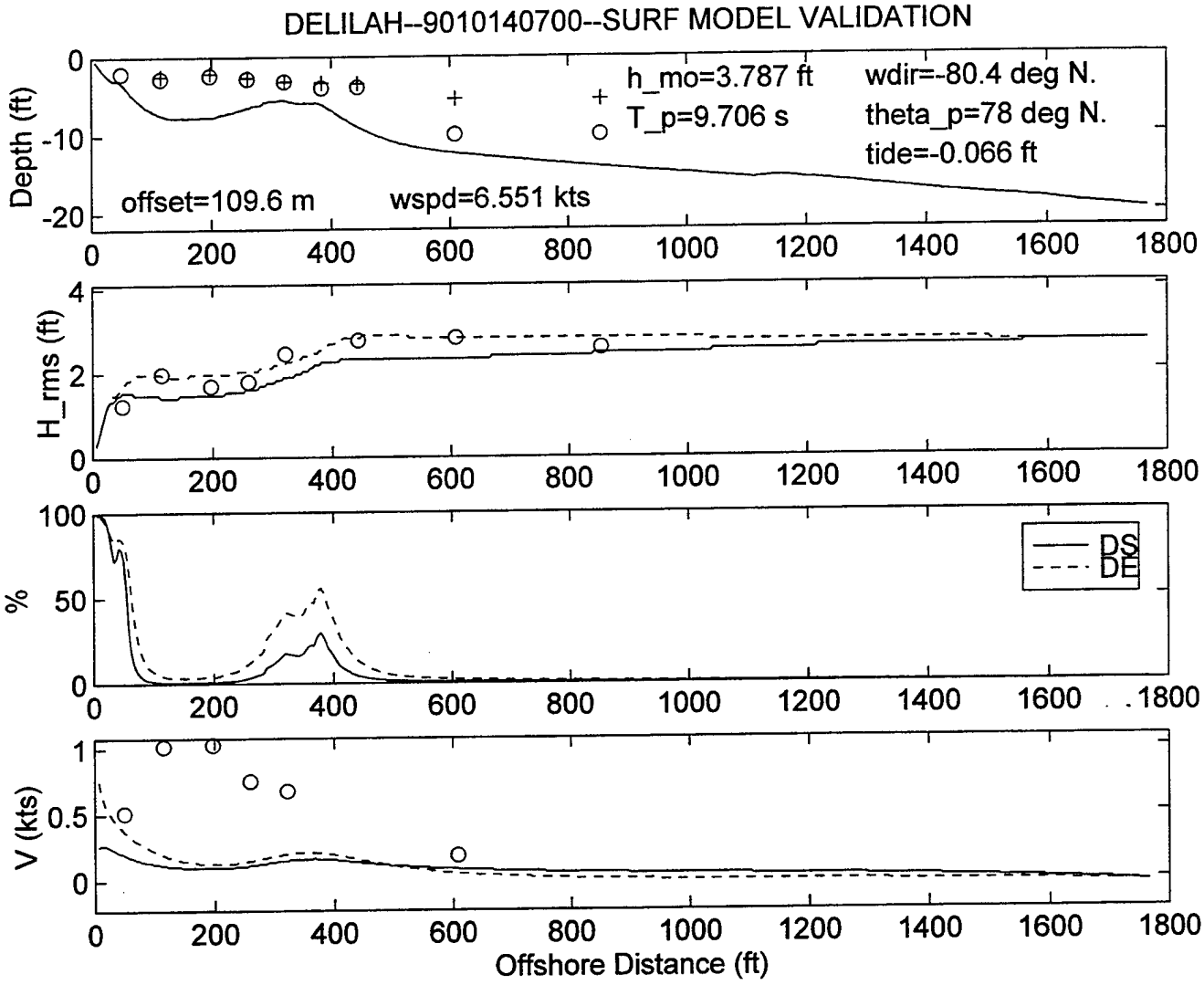
DELILAH--9010140700--SURF MODEL VALIDATION
Depth (ft)
h_mo=3.787 ft
T_p=9.706 s
wdir=-80.4 deg N.
theta_p=78 deg N.
tide=-0.066 ft
offset=109.6 m
wspd=6.551 kts
H_rms (ft)
%
DS
DE
V (kts)
Offshore Distance (ft)

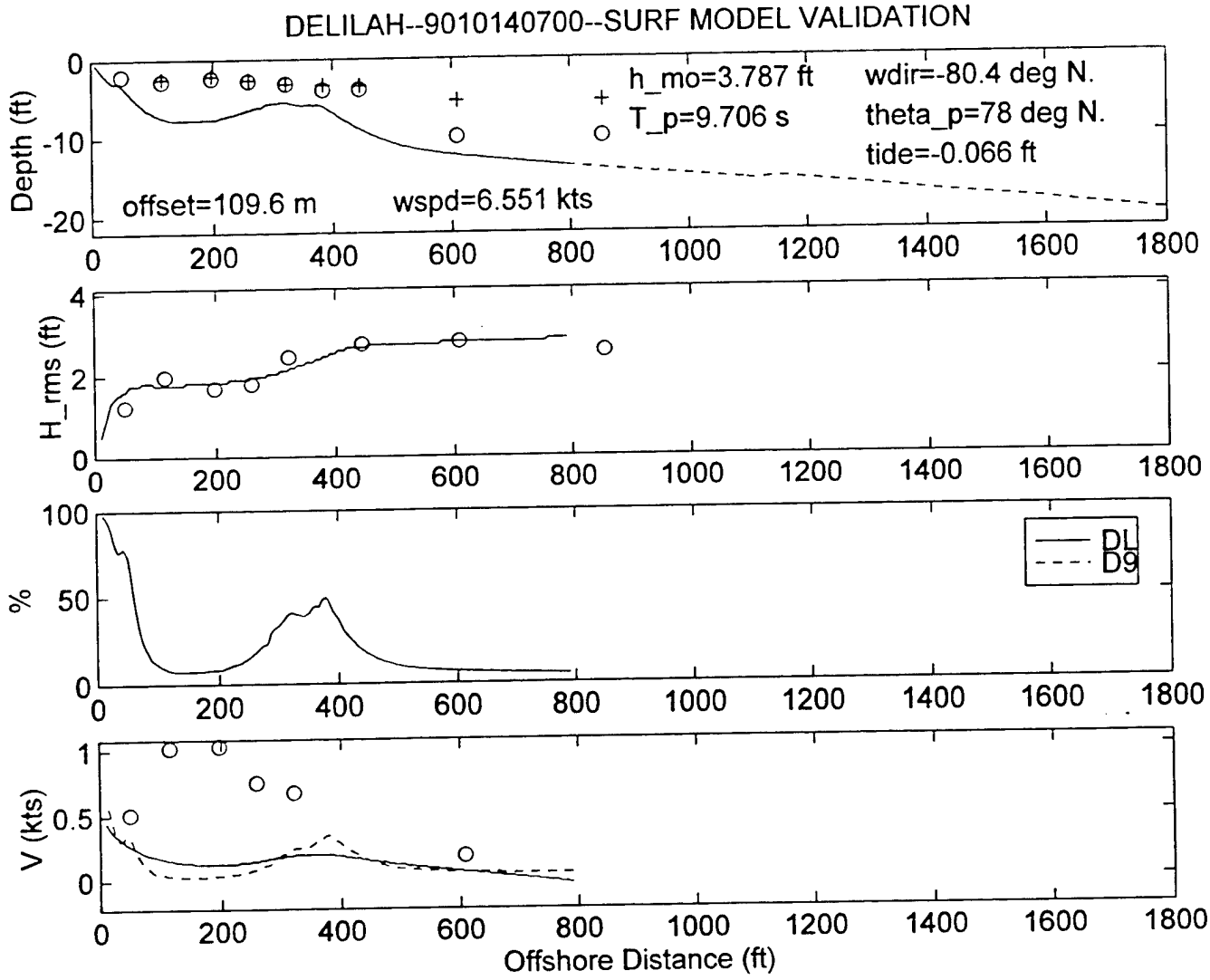
DELILAH--9010140700--SURF MODEL VALIDATION
Depth (ft)
h_mo=3.787 ft
T_p=9.706 s
wdir=-80.4 deg N.
theta_p=78 deg N.
tide=-0.066 ft
offset=109.6 m
wspd=6.551 kts
H_rms (ft)
%
DL
D9
V (kts)
Offshore Distance (ft)

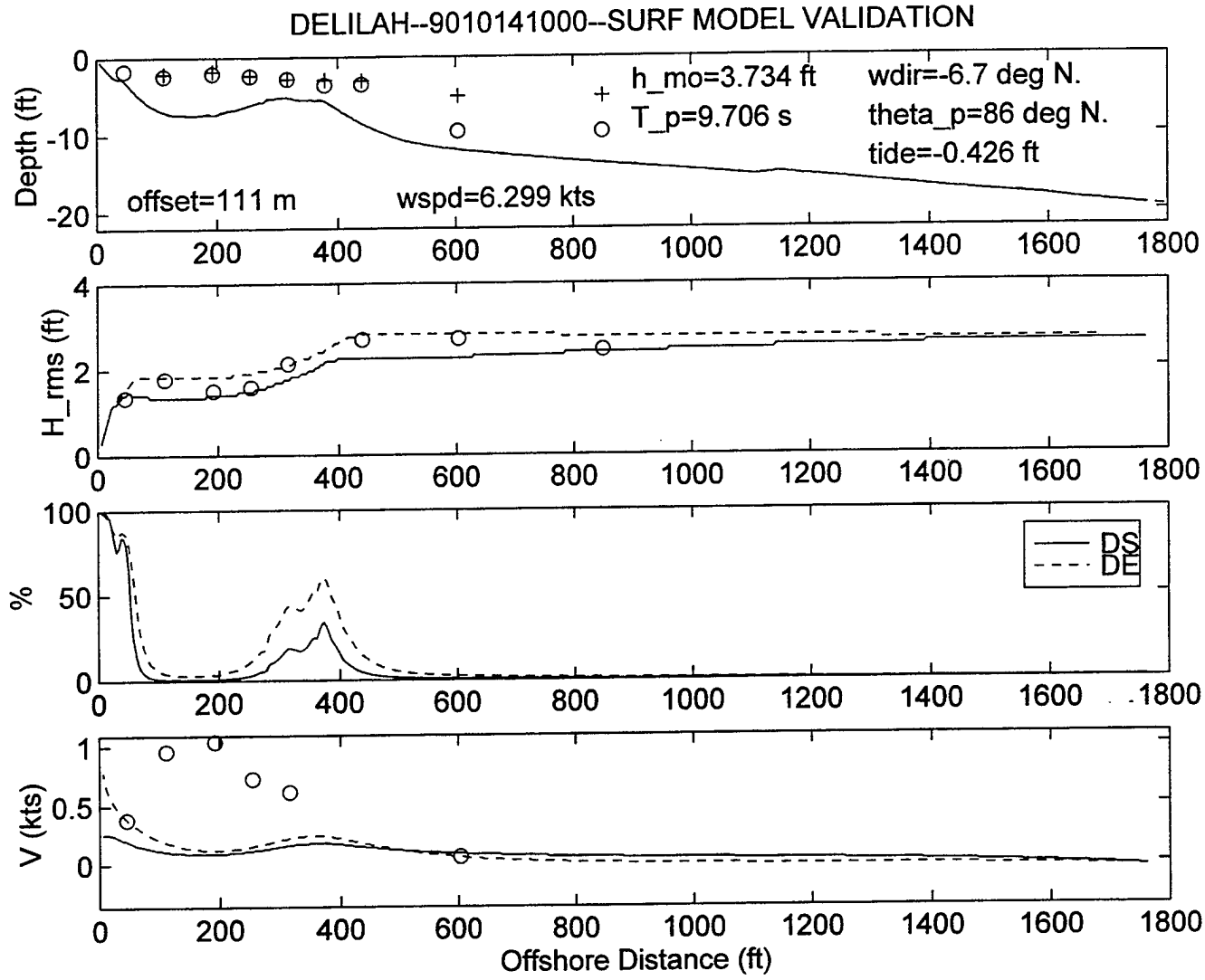
DELILAH--9010141000--SURF MODEL VALIDATION
Depth (ft)
h_mo=3.734 ft
T_p=9.706 s
wdir=-6.7 deg N.
theta_p=86 deg N.
tide=-0.426 ft
offset=111 m
wspd=6.299 kts
H_rms (ft)
%
DS
DE
V (kts)
Offshore Distance (ft)

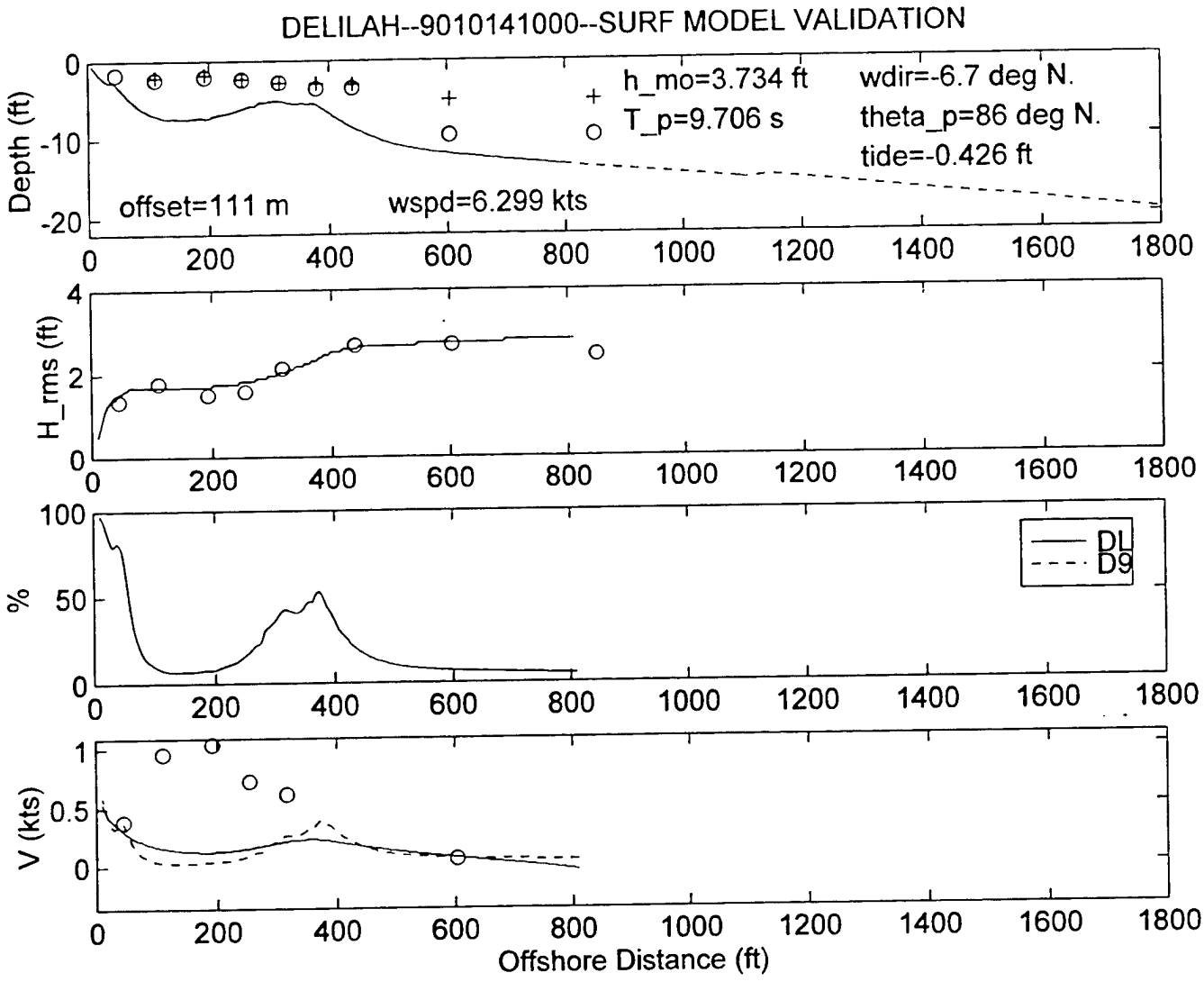
DELILAH--9010141000--SURF MODEL VALIDATION
Depth (ft)
h_mo=3.734 ft
T_p=9.706 s
wdir=-6.7 deg N.
theta_p=86 deg N.
tide=-0.426 ft
offset=111 m
wspd=6.299 kts
H_rms (ft)
%
DL
D9
V (kts)
Offshore Distance (ft)

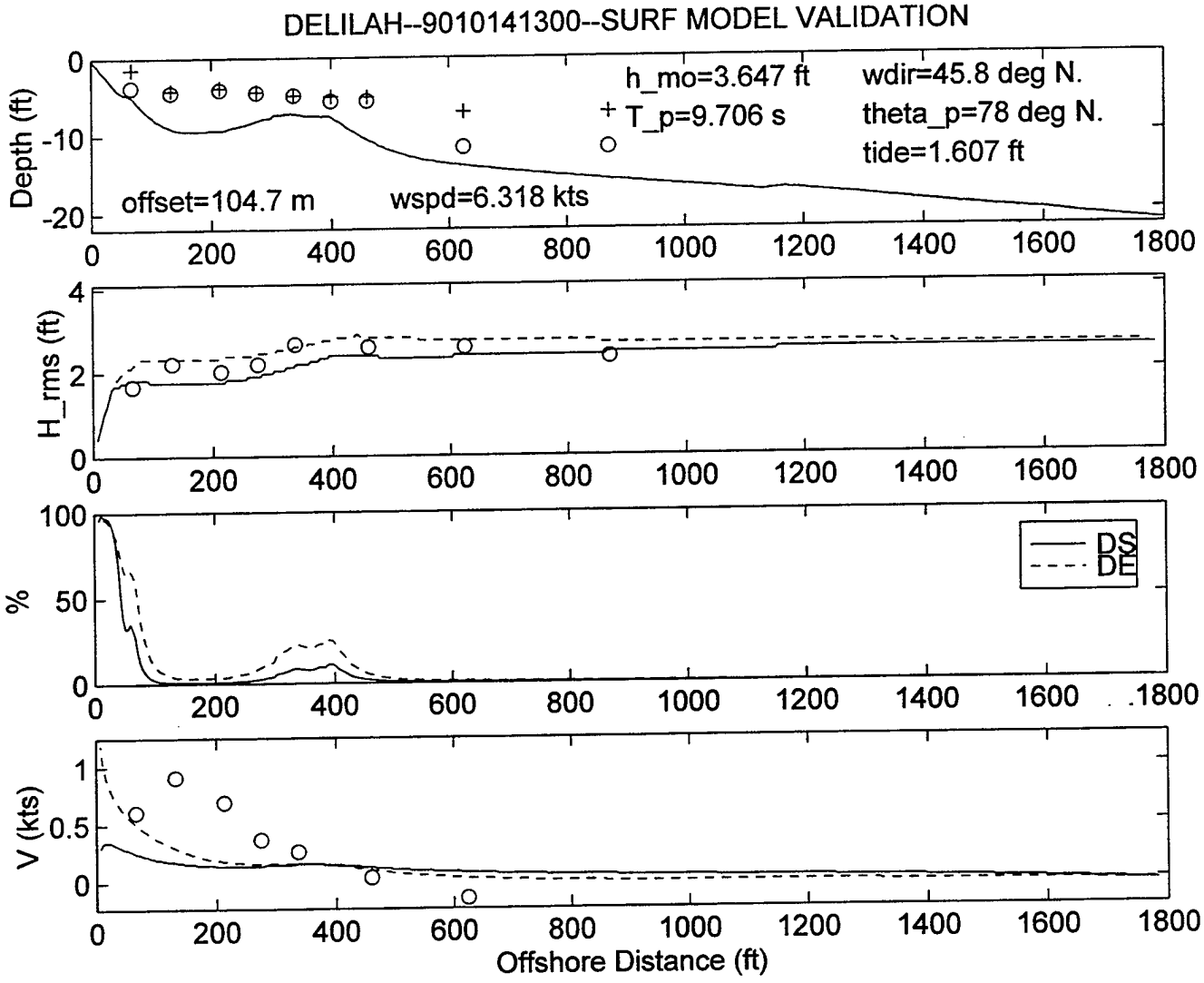
DELILAH--9010141300--SURF MODEL VALIDATION
Depth (ft)
h_mo=3.647 ft
T_p=9.706 s
wdir=45.8 deg N.
theta_p=78 deg N.
tide=1.607 ft
offset=104.7 m
wspd=6.318 kts
H_rms (ft)
%
DS
DE
V (kts)
Offshore Distance (ft)

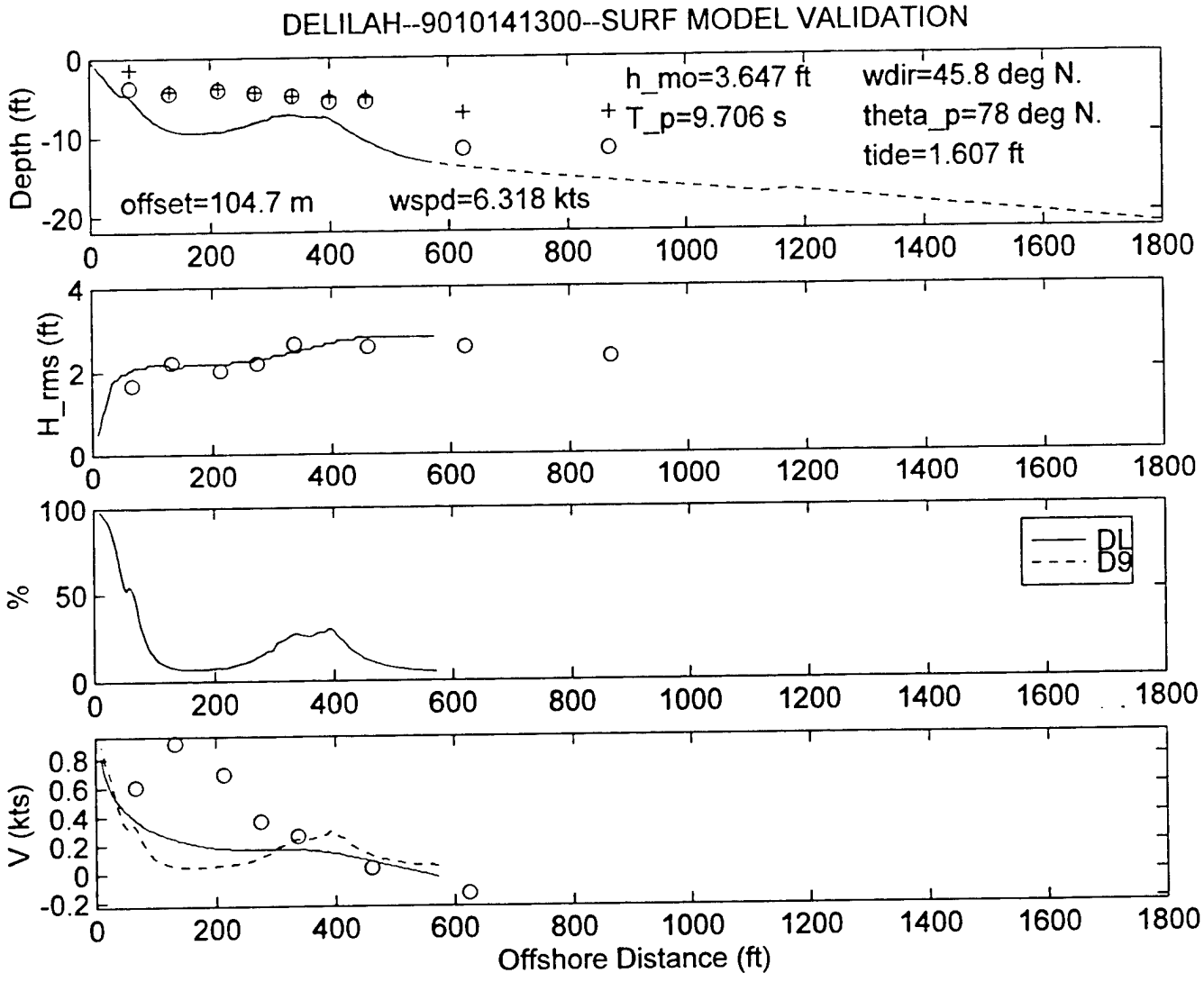
DELILAH--9010141300--SURF MODEL VALIDATION
Depth (ft)
h_mo=3.647 ft
T_p=9.706 s
wdir=45.8 deg N.
theta_p=78 deg N.
tide=1.607 ft
offset=104.7 m
wspd=6.318 kts
H_rms (ft)
%
DL
D9
V (kts)
Offshore Distance (ft)

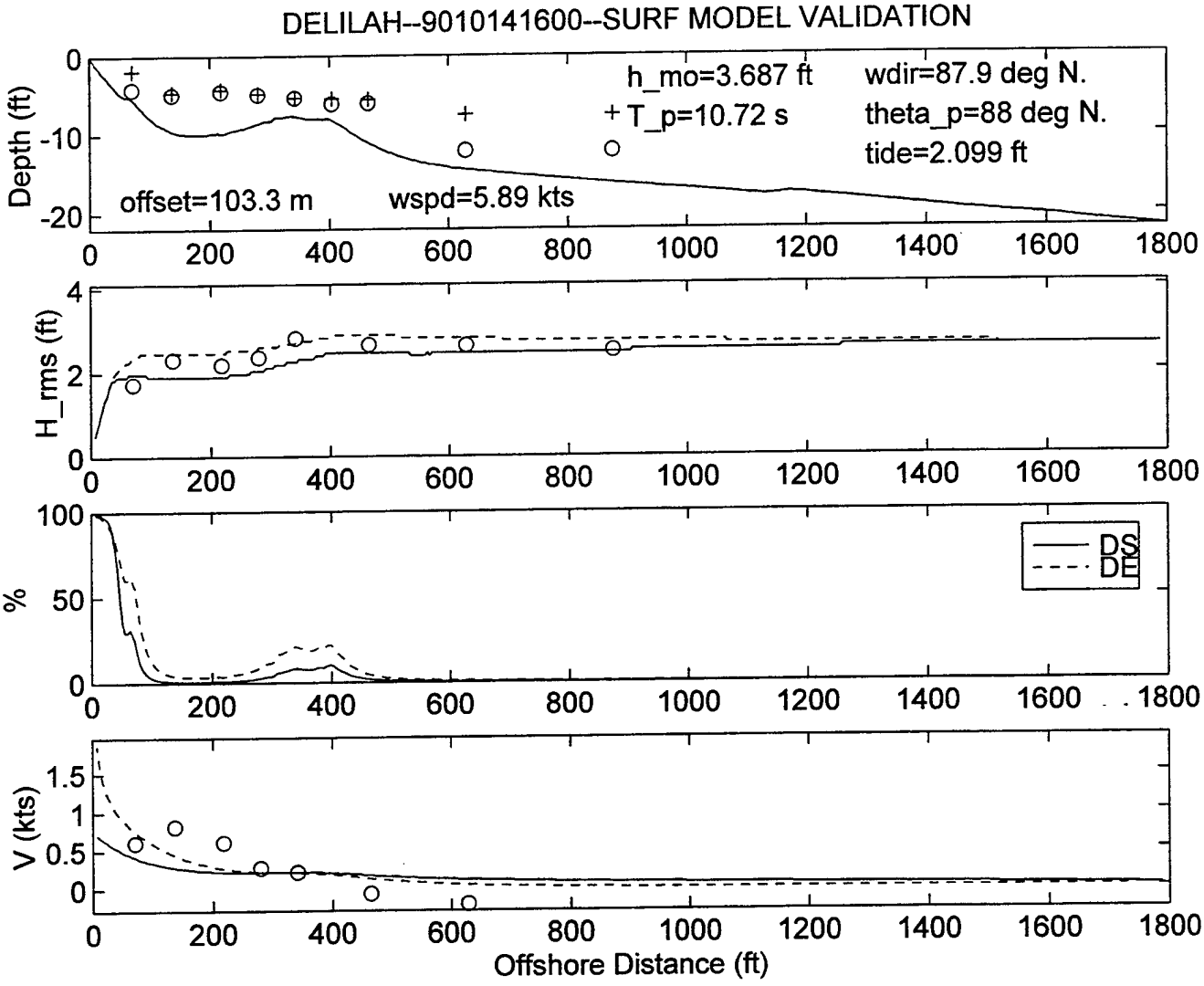
DELILAH--9010141600--SURF MODEL VALIDATION
Depth (ft)
h_mo=3.687 ft
T_p=10.72 s
wdir=87.9 deg N.
theta_p=88 deg N.
tide=2.099 ft
offset=103.3 m
wspd=5.89 kts
H_rms (ft)
%
DS
DE
V (kts)
Offshore Distance (ft)

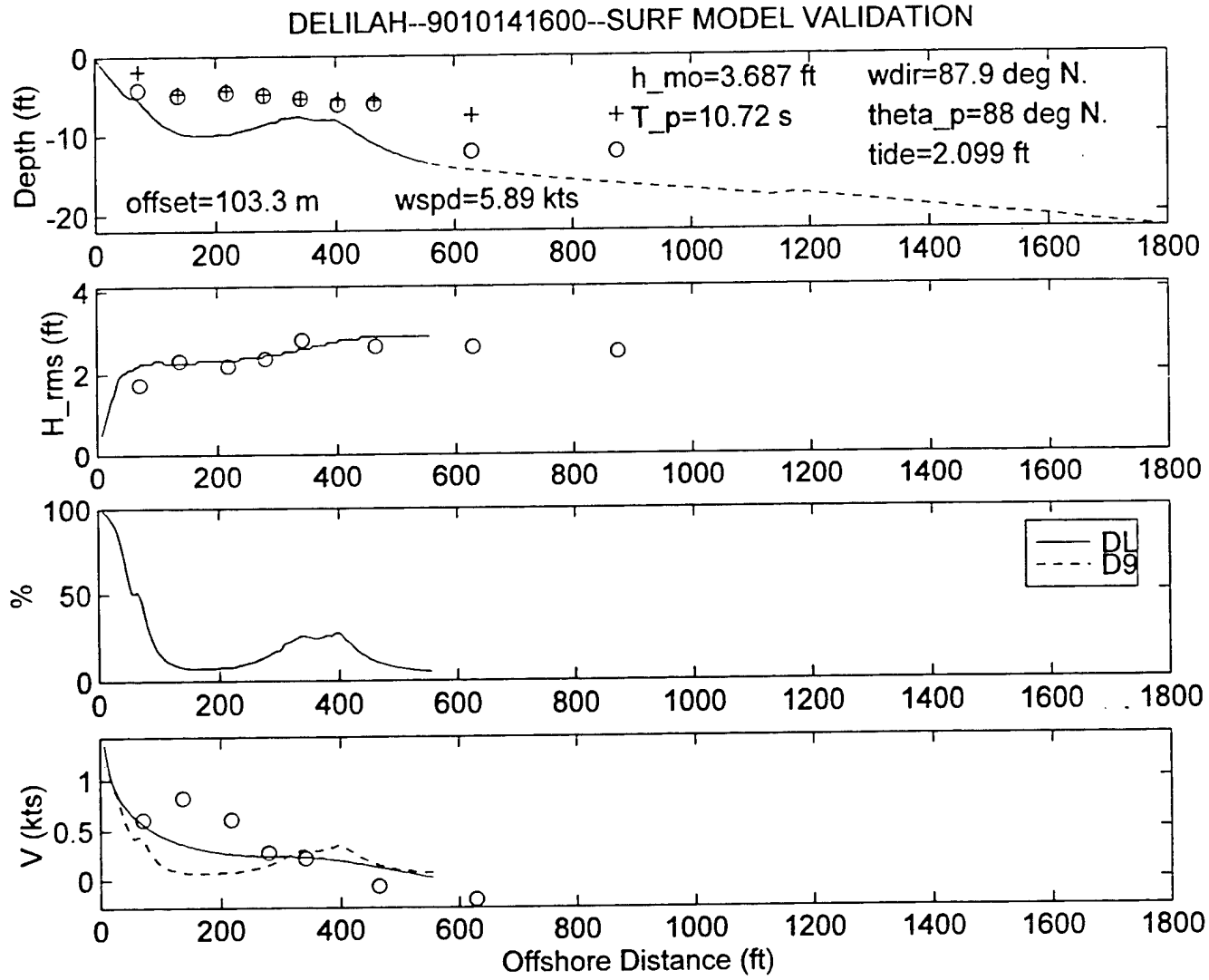
DELILAH--9010141600--SURF MODEL VALIDATION
Depth (ft)
h_mo=3.687 ft
T_p=10.72 s
wdir=87.9 deg N.
theta_p=88 deg N.
tide=2.099 ft
offset=103.3 m
wspd=5.89 kts
H_rms (ft)
%
DL
D9
V (kts)
Offshore Distance (ft)

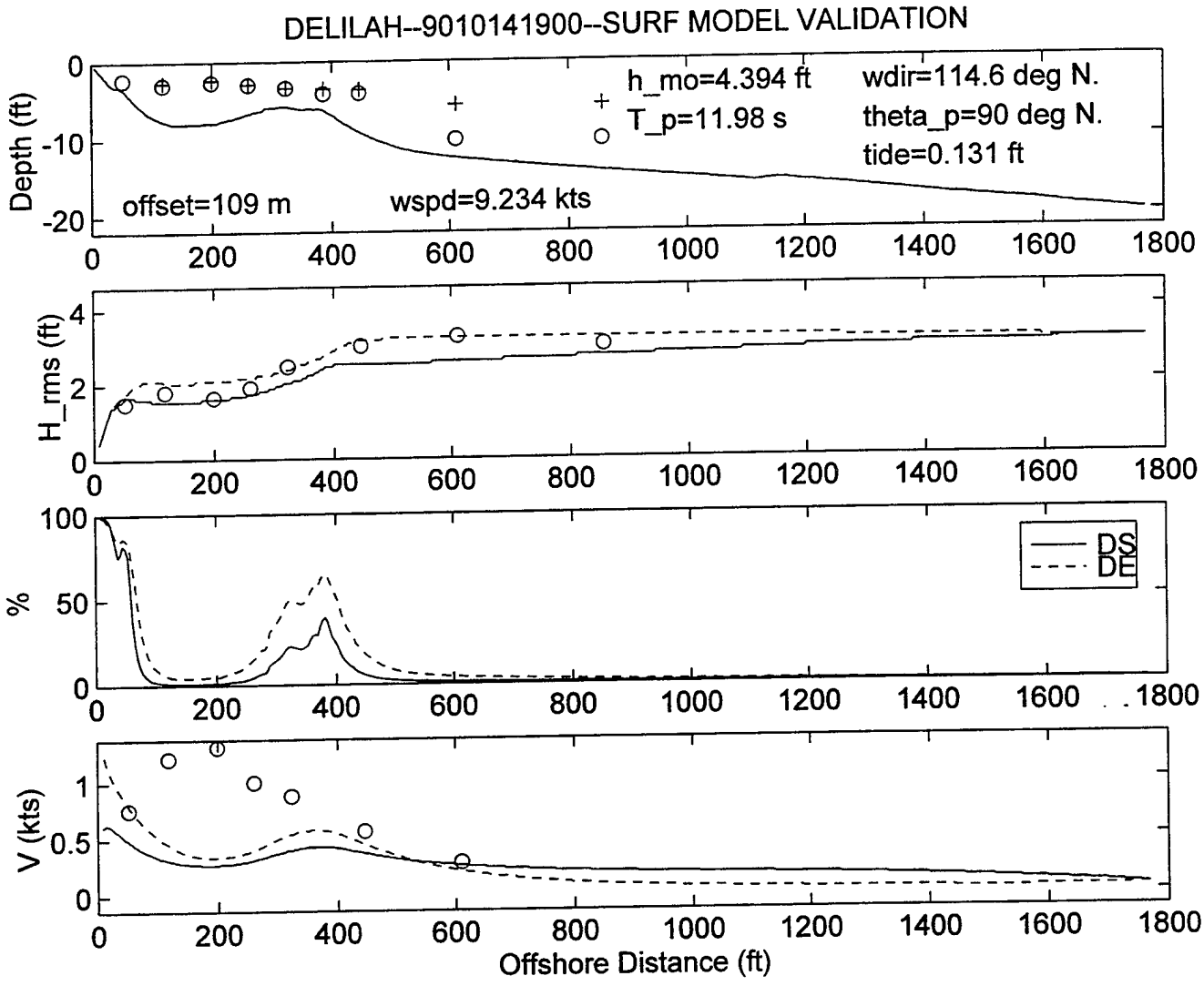
DELILAH--9010141900--SURF MODEL VALIDATION
Depth (ft)
h_mo=4.394 ft
T_p=11.98 s
wdir=114.6 deg N.
theta_p=90 deg N.
tide=0.131 ft
offset=109 m
wspd=9.234 kts
H_rms (ft)
%
DS
DE
V (kts)
Offshore Distance (ft)

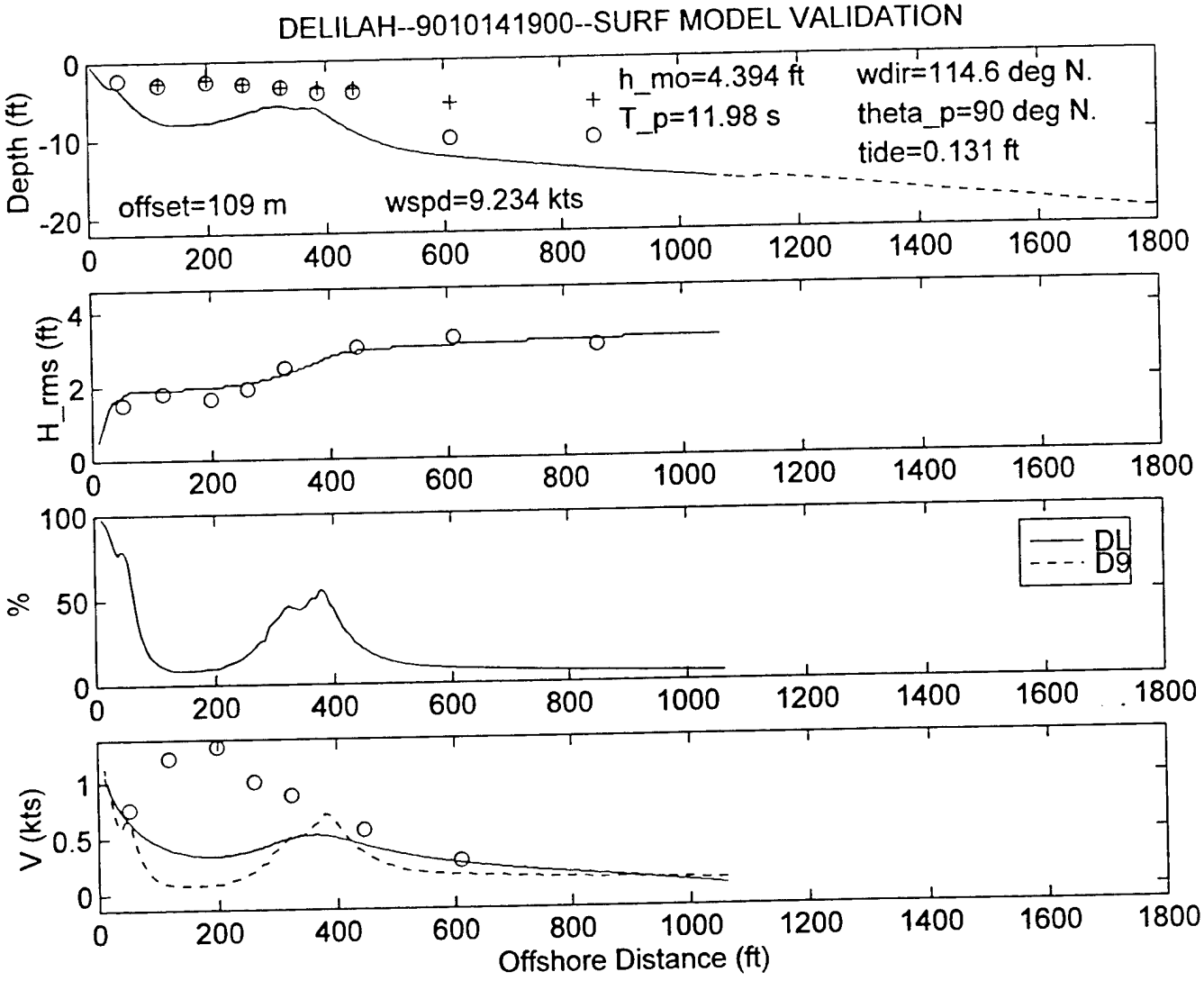
DELILAH--9010141900--SURF MODEL VALIDATION
Depth (ft)
h_mo=4.394 ft
T_p=11.98 s
wdir=114.6 deg N.
theta_p=90 deg N.
tide=0.131 ft
offset=109 m
wspd=9.234 kts
H_rms (ft)
%
DL
D9
V (kts)
Offshore Distance (ft)

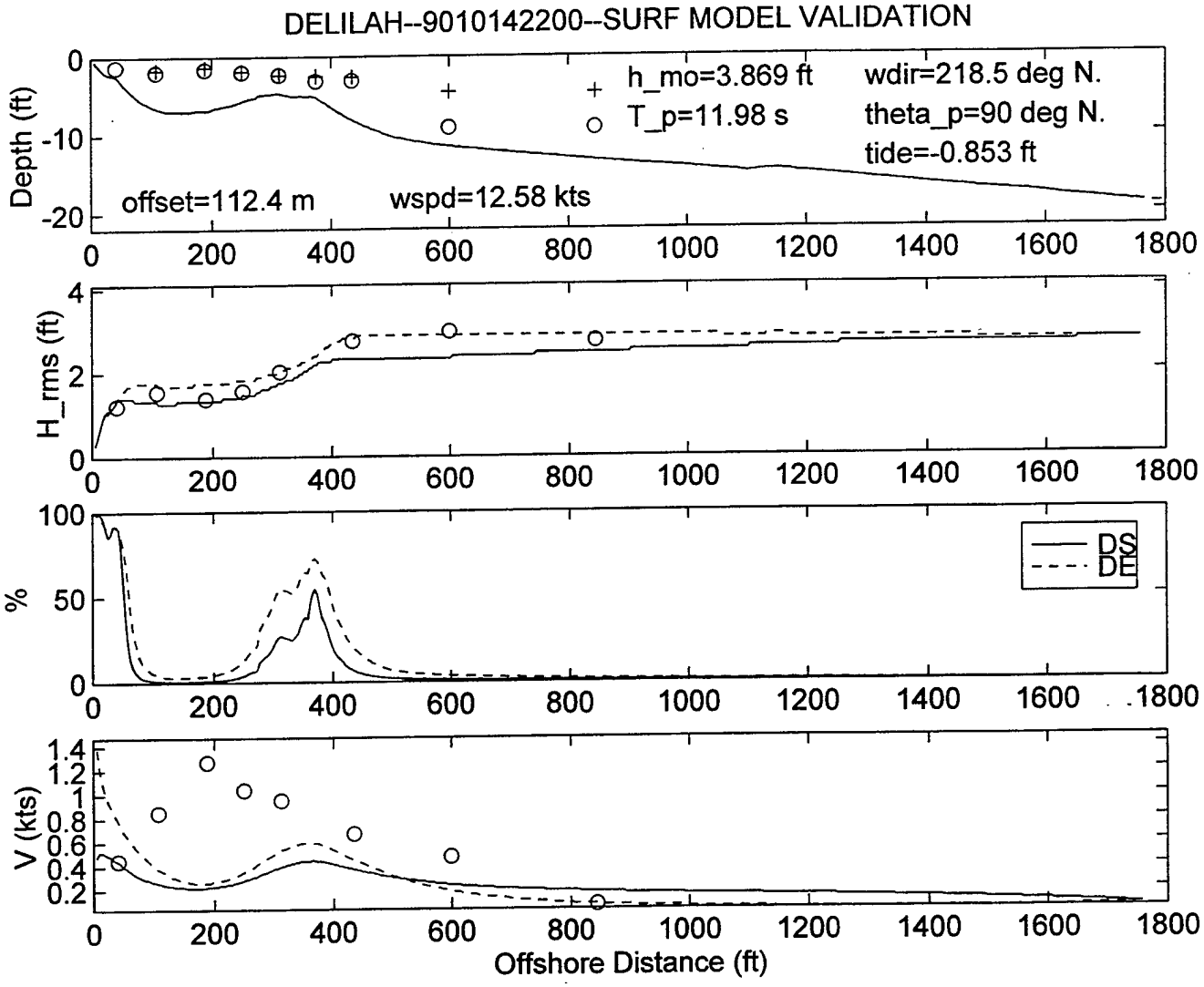
DELILAH--9010142200--SURF MODEL VALIDATION
Depth (ft)
h_mo=3.869 ft
T_p=11.98 s
wdir=218.5 deg N.
theta_p=90 deg N.
tide=-0.853 ft
offset=112.4 m
wspd=12.58 kts
H_rms (ft)
%
DS
DE
V (kts)
Offshore Distance (ft)

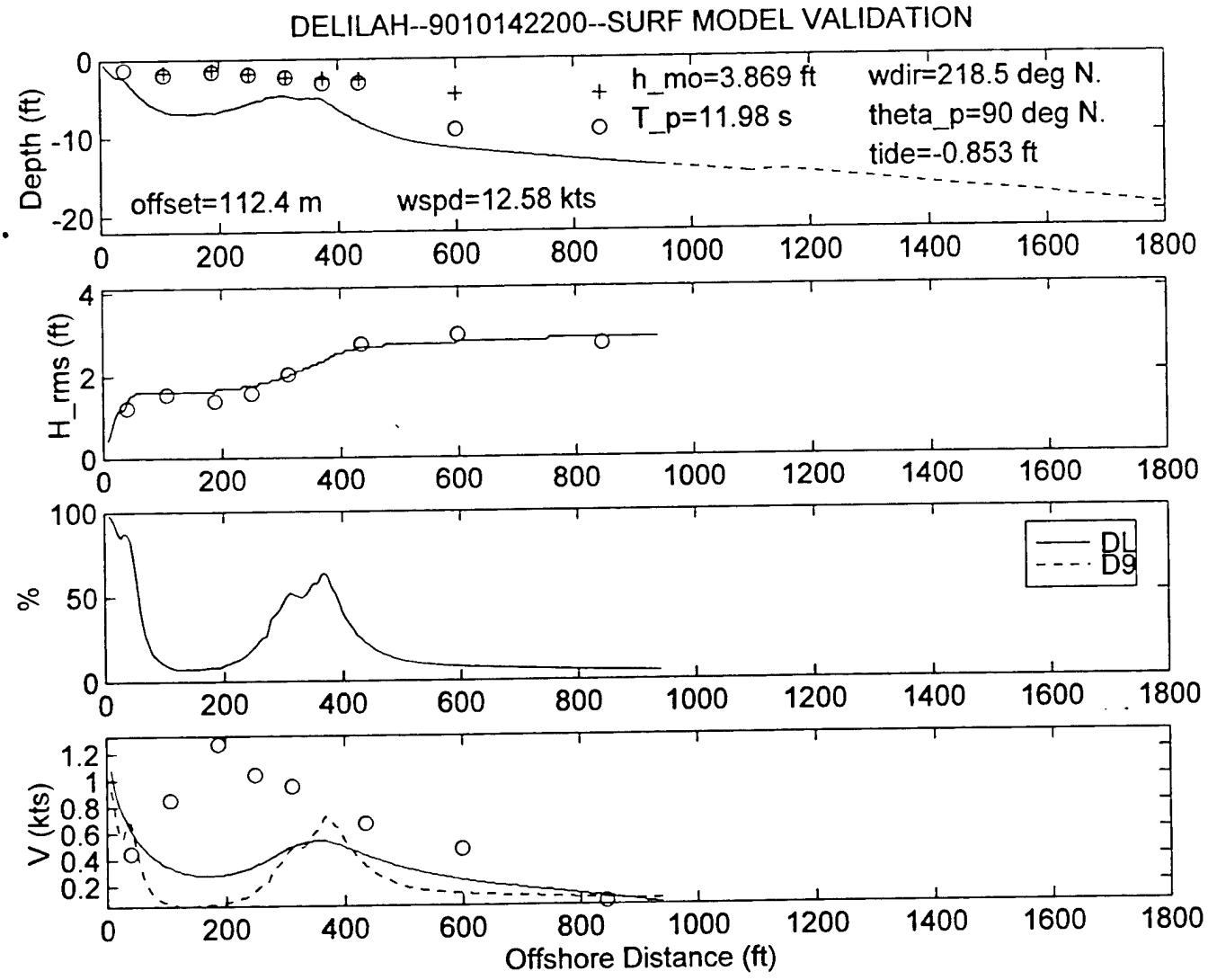
DELILAH--9010142200--SURF MODEL VALIDATION
Depth (ft)
h_mo=3.869 ft
T_p=11.98 s
wdir=218.5 deg N.
theta_p=90 deg N.
tide=-0.853 ft
offset=112.4 m
wspd=12.58 kts
H_rms (ft)
%
DL
D9
V (kts)
Offshore Distance (ft)

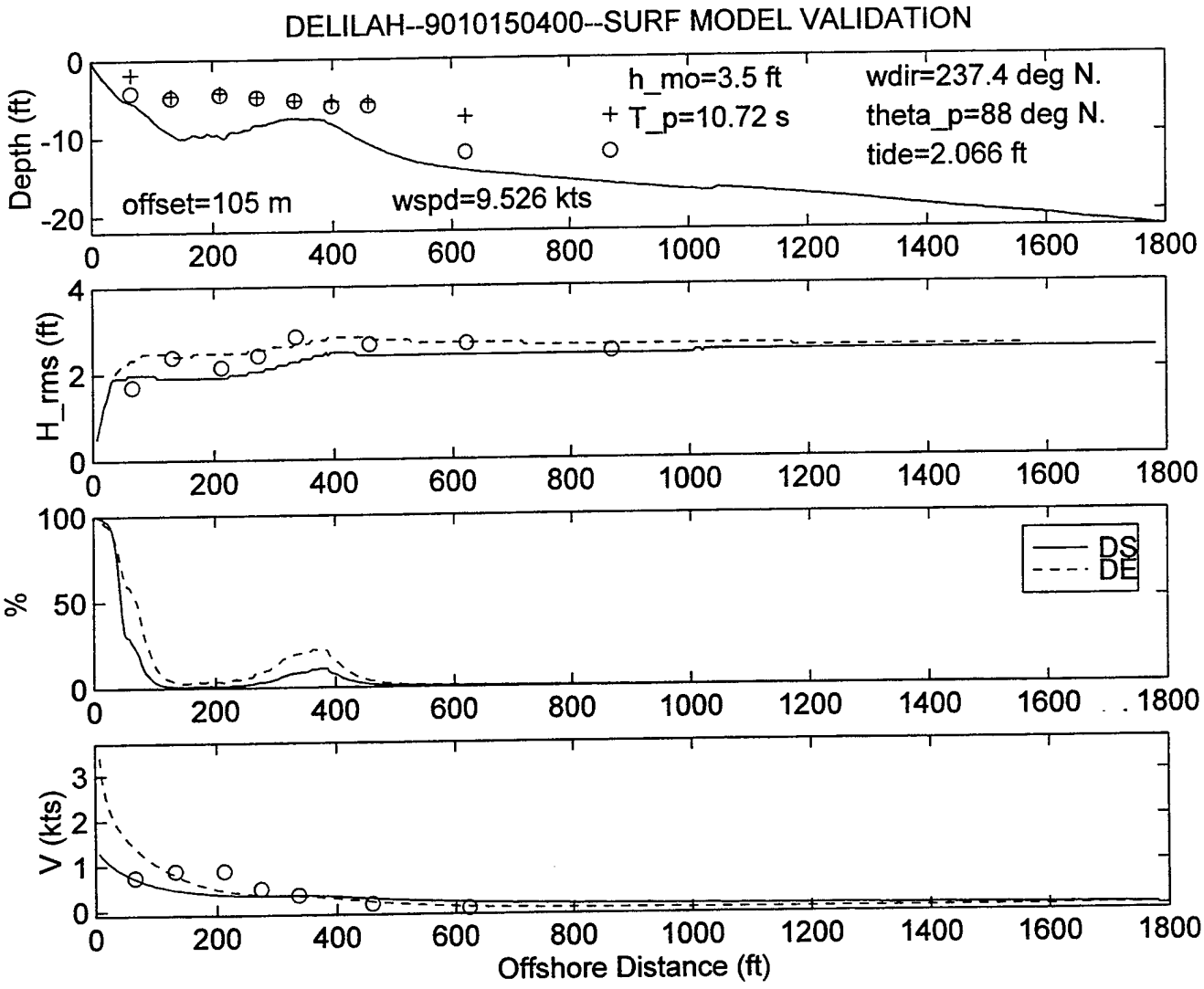
DELILAH--9010150400--SURF MODEL VALIDATION
Depth (ft)
h_mo=3.5 ft
T_p=10.72 s
wdir=237.4 deg N.
theta_p=88 deg N.
tide=2.066 ft
offset=105 m
wspd=9.526 kts
H_rms (ft)
%
DS
DM
V (kts)
Offshore Distance (ft)

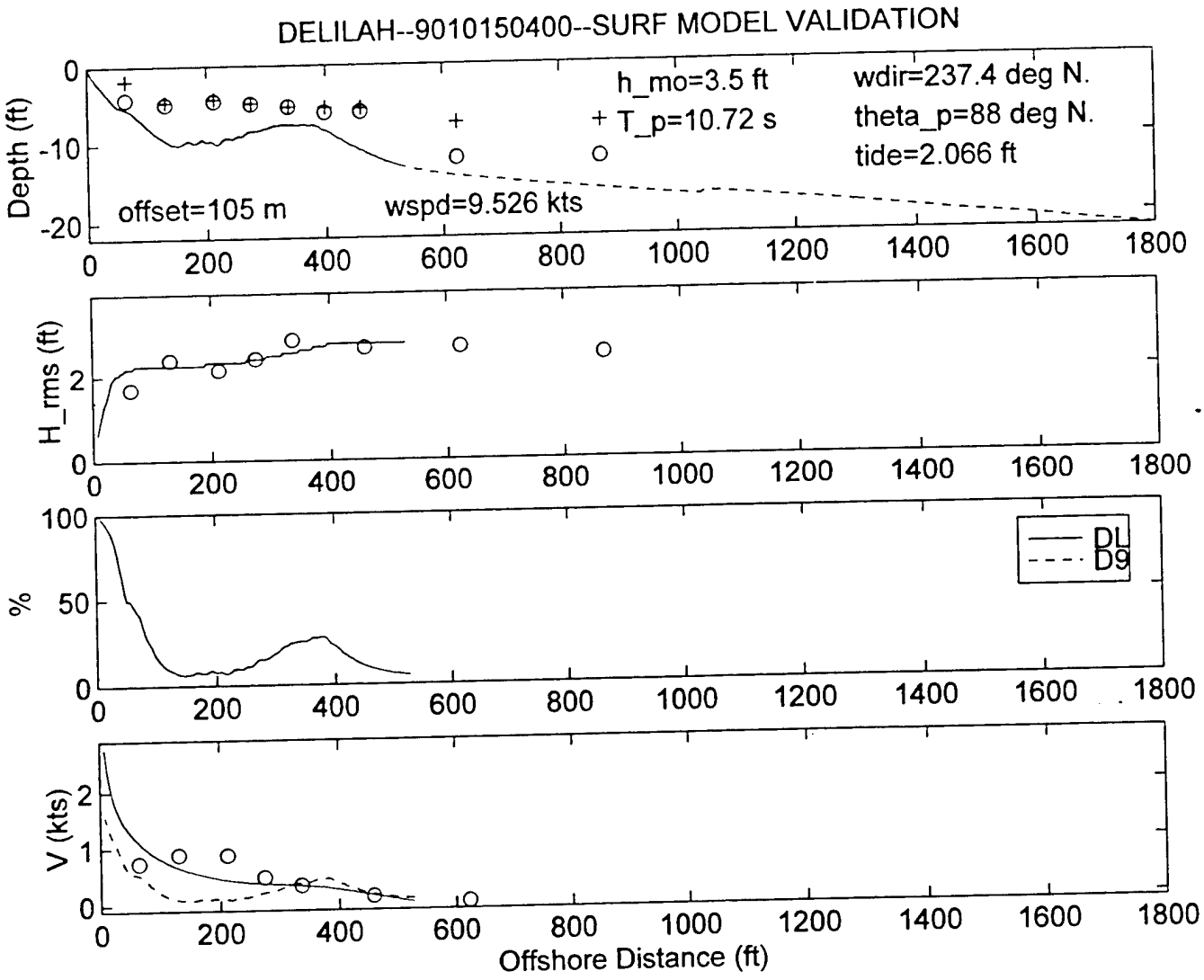
DELILAH--9010150400--SURF MODEL VALIDATION
Depth (ft)
h_mo=3.5 ft
T_p=10.72 s
wdir=237.4 deg N.
theta_p=88 deg N.
tide=2.066 ft
offset=105 m
wspd=9.526 kts
H_rms (ft)
%
DL
D9
V (kts)
Offshore Distance (ft)

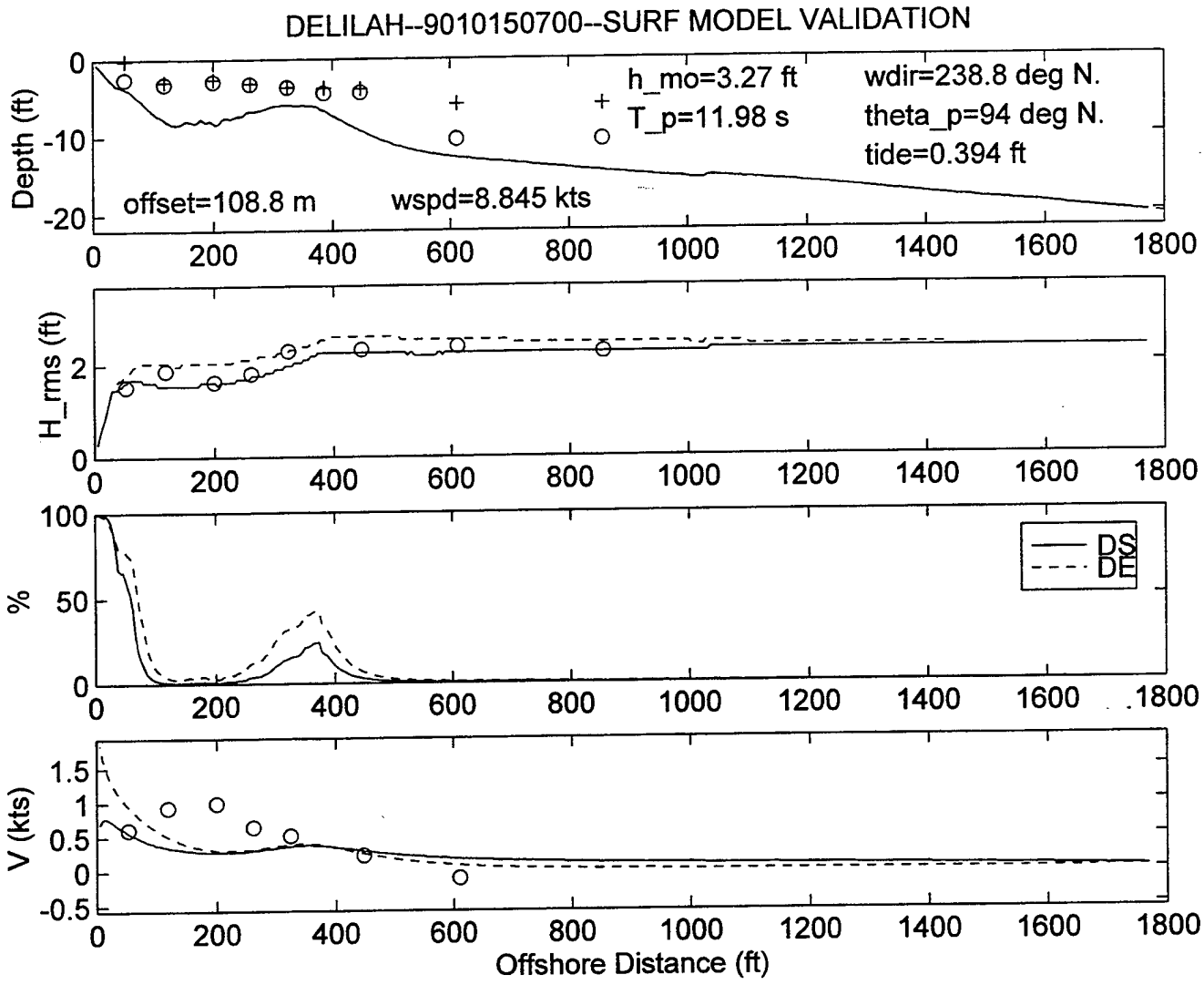
DELILAH--9010150700--SURF MODEL VALIDATION
Depth (ft)
h_mo=3.27 ft
T_p=11.98 s
wdir=238.8 deg N.
theta_p=94 deg N.
tide=0.394 ft
offset=108.8 m
wspd=8.845 kts
H_rms (ft)
%
DS
DM
V (kts)
Offshore Distance (ft)

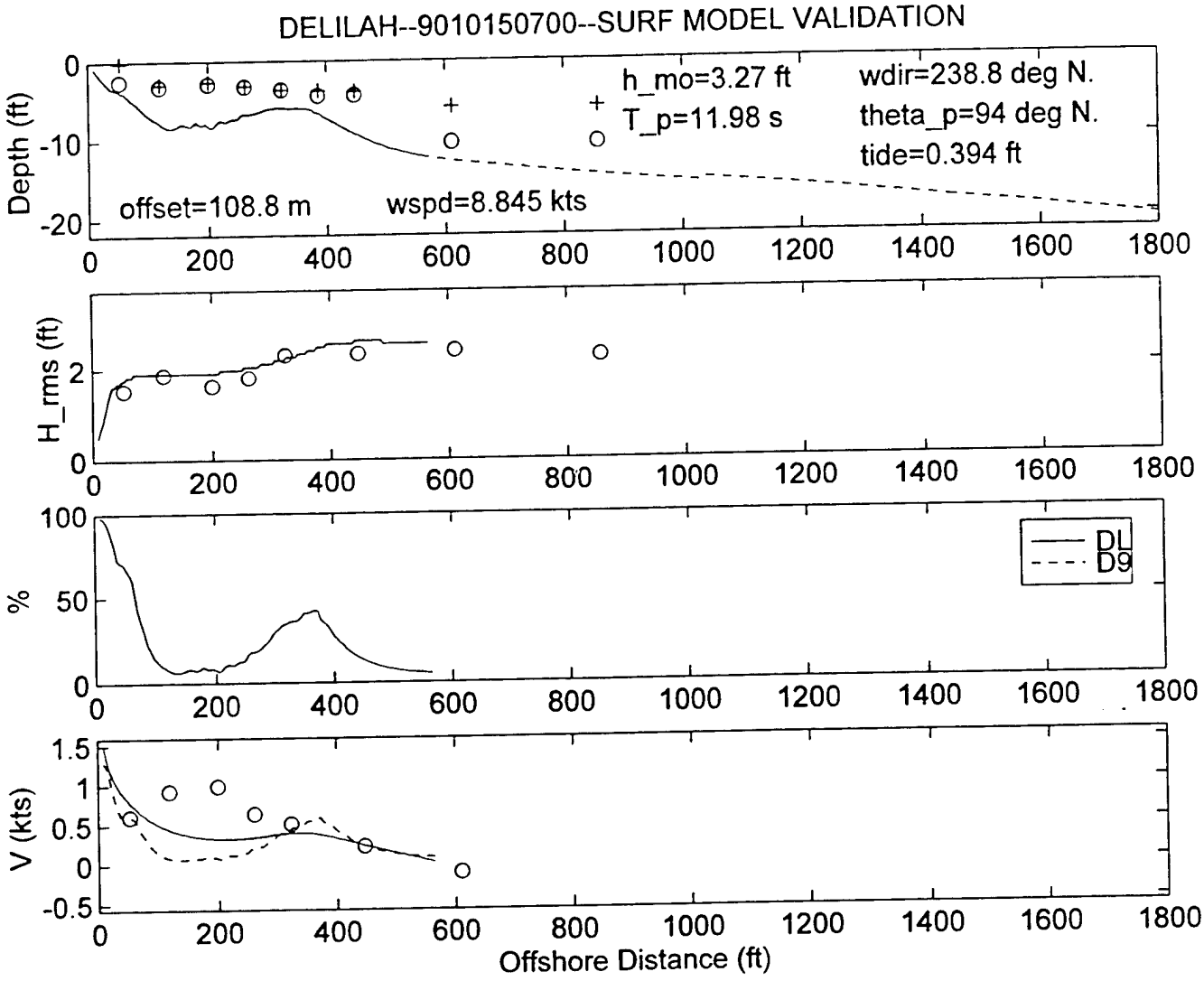
DELILAH--9010150700--SURF MODEL VALIDATION
Depth (ft)
h_mo=3.27 ft
T_p=11.98 s
wdir=238.8 deg N.
theta_p=94 deg N.
tide=0.394 ft
offset=108.8 m
wspd=8.845 kts
H_rms (ft)
%
DL
D9
V (kts)
Offshore Distance (ft)

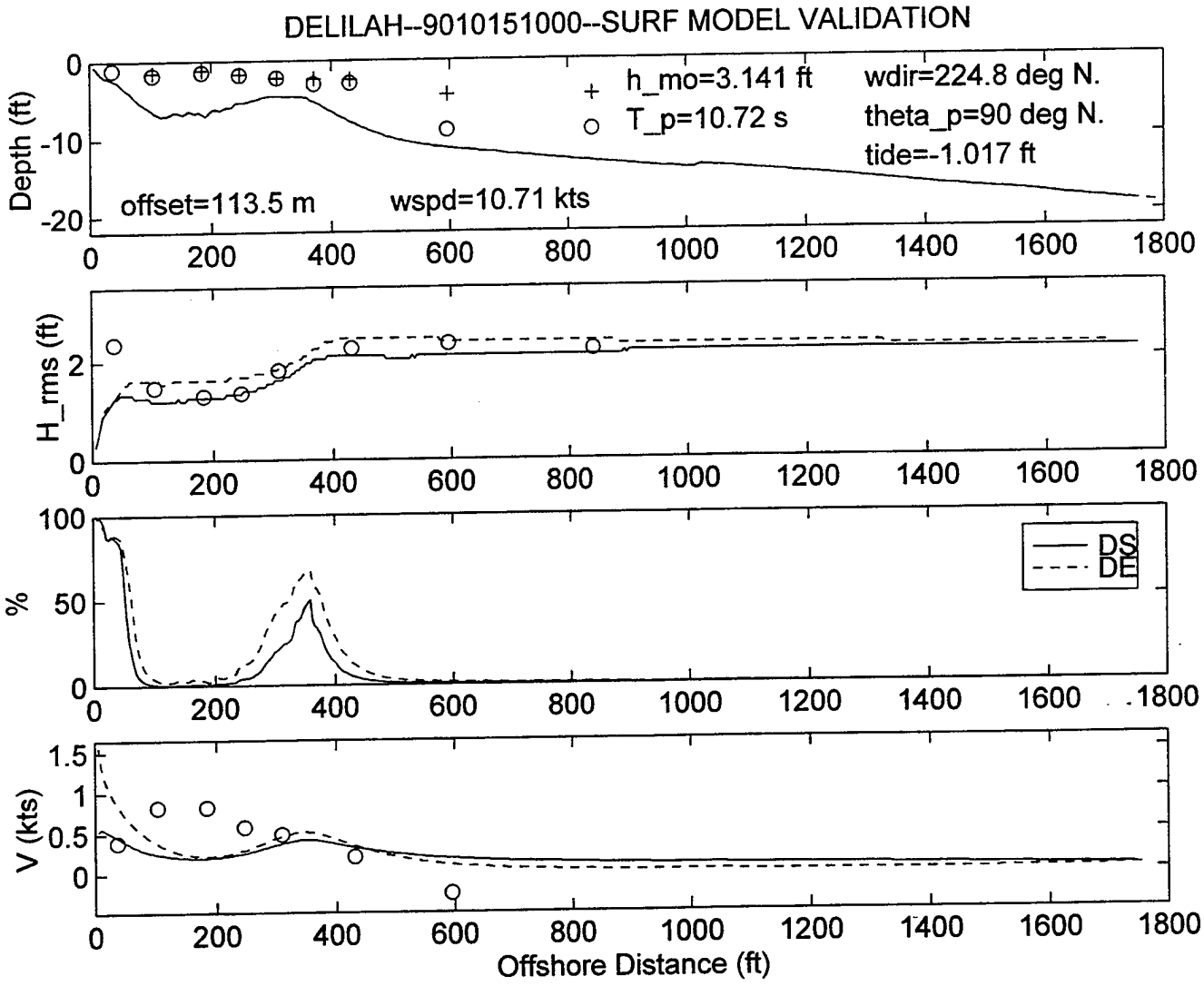
DELILAH--9010151000--SURF MODEL VALIDATION
Depth (ft)
h_mo=3.141 ft
T_p=10.72 s
wdir=224.8 deg N.
theta_p=90 deg N.
tide=-1.017 ft
offset=113.5 m
wspd=10.71 kts
H_rms (ft)
%
DS
DE
V (kts)
Offshore Distance (ft)

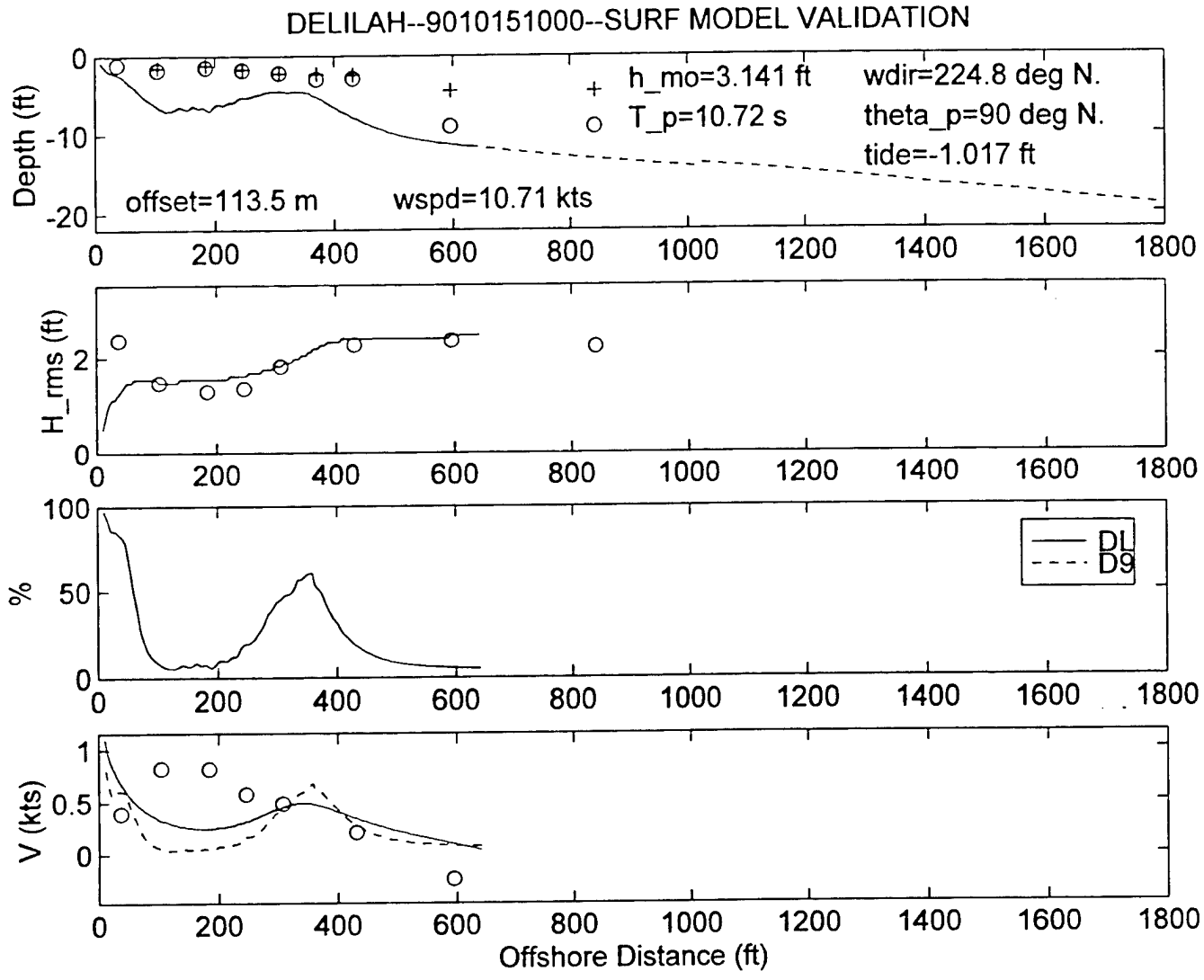
DELILAH--9010151000--SURF MODEL VALIDATION
Depth (ft)
h_mo=3.141 ft
T_p=10.72 s
wdir=224.8 deg N.
theta_p=90 deg N.
tide=-1.017 ft
offset=113.5 m
wspd=10.71 kts
H_rms (ft)
%
DL
D9
V (kts)
Offshore Distance (ft)

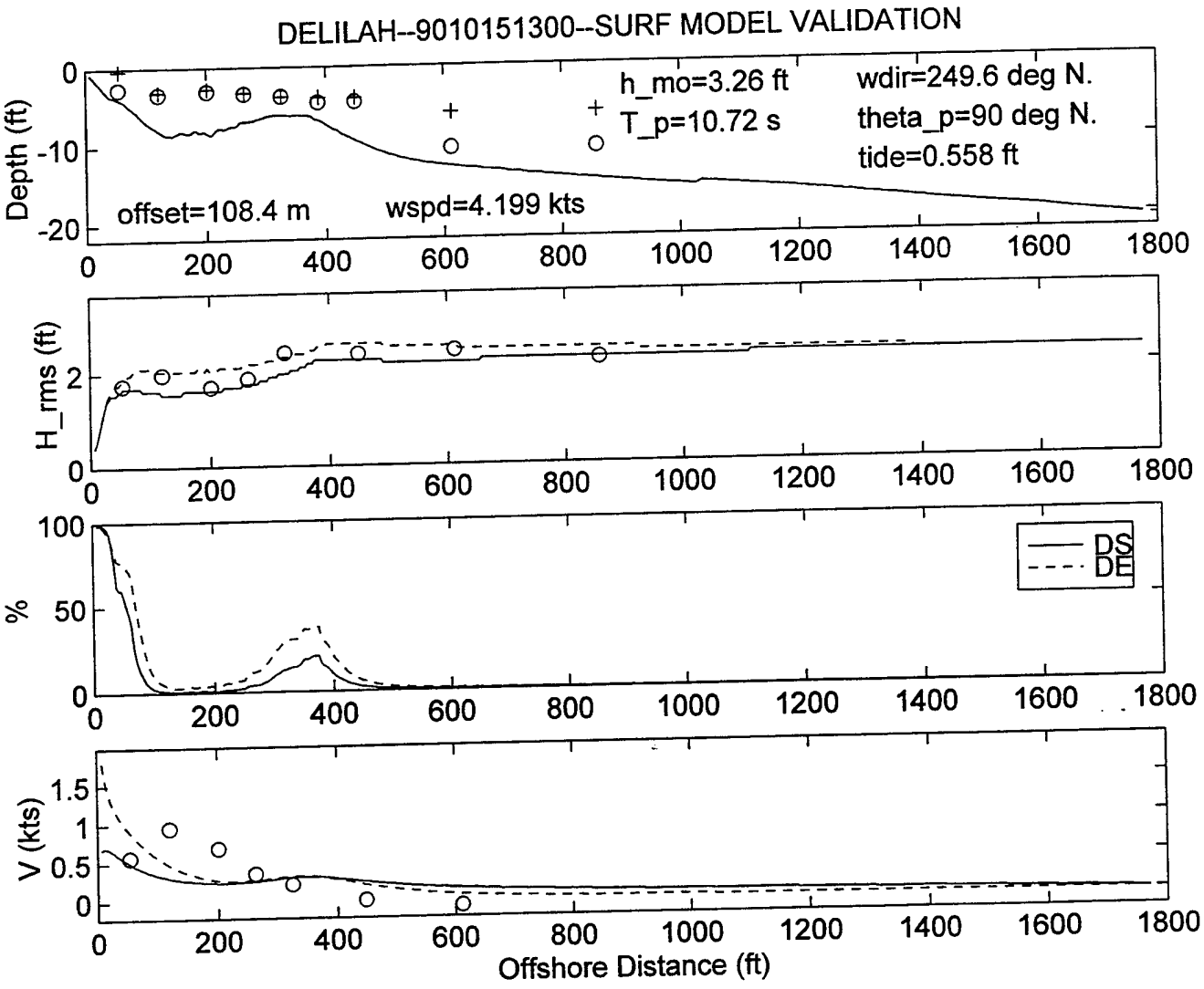
DELILAH--9010151300--SURF MODEL VALIDATION
Depth (ft)
h_mo=3.26 ft
T_p=10.72 s
wdir=249.6 deg N.
theta_p=90 deg N.
tide=0.558 ft
offset=108.4 m
wspd=4.199 kts
H_rms (ft)
%
DS
DE
V (kts)
Offshore Distance (ft)

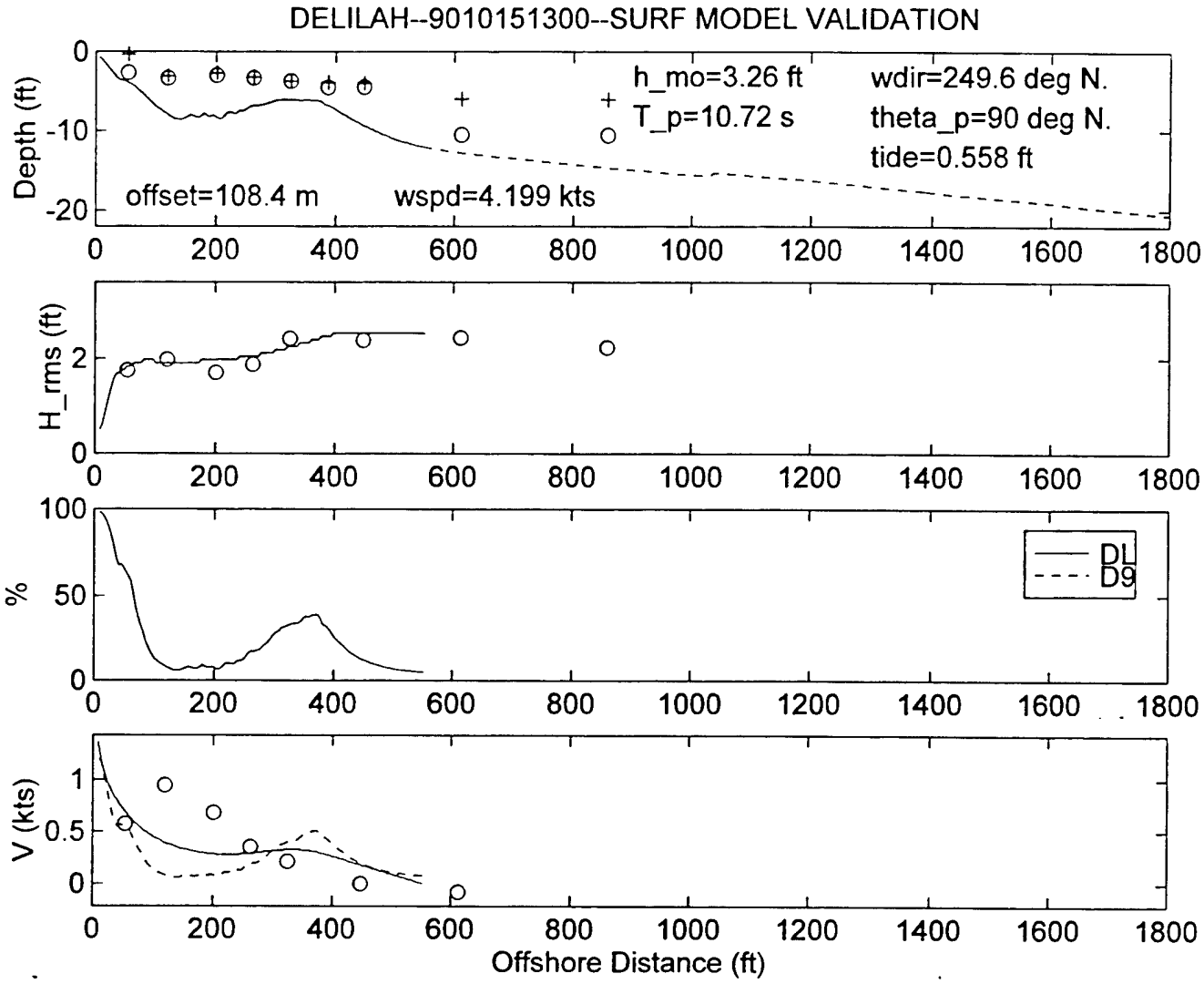
DELILAH--9010151300--SURF MODEL VALIDATION
Depth (ft)
h_mo=3.26 ft
T_p=10.72 s
wdir=249.6 deg N.
theta_p=90 deg N.
tide=0.558 ft
offset=108.4 m
wspd=4.199 kts
H_rms (ft)
%
DL
D9
V (kts)
Offshore Distance (ft)

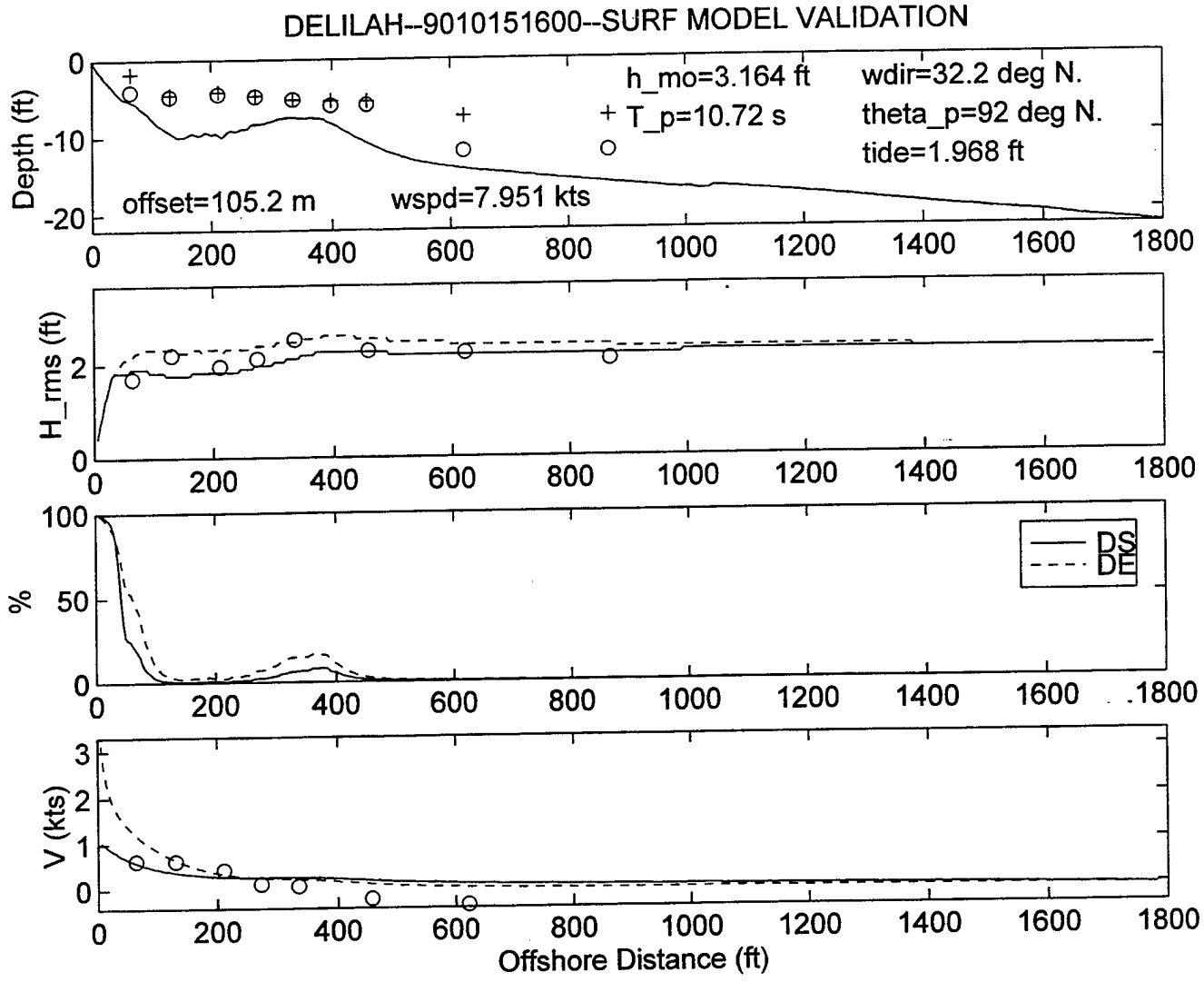
DELILAH--9010151600--SURF MODEL VALIDATION
Depth (ft)
h_mo=3.164 ft
T_p=10.72 s
wdir=32.2 deg N.
theta_p=92 deg N.
tide=1.968 ft
offset=105.2 m
wspd=7.951 kts
H_rms (ft)
%
DS
DE
V (kts)
Offshore Distance (ft)

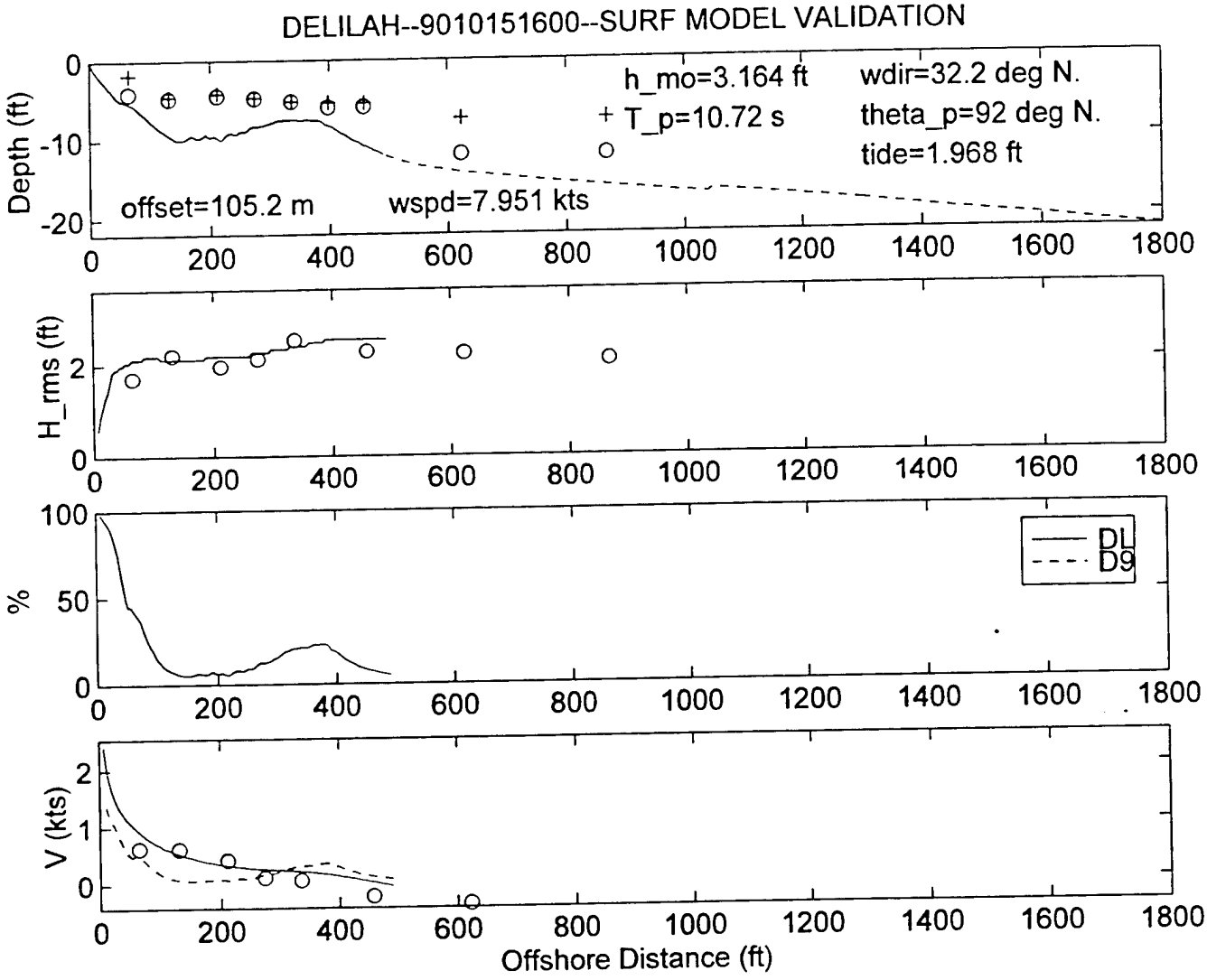
DELILAH--9010151600--SURF MODEL VALIDATION
Depth (ft)
h_mo=3.164 ft
T_p=10.72 s
wdir=32.2 deg N.
theta_p=92 deg N.
tide=1.968 ft
offset=105.2 m
wspd=7.951 kts
H_rms (ft)
%
DL
D9
V (kts)
Offshore Distance (ft)

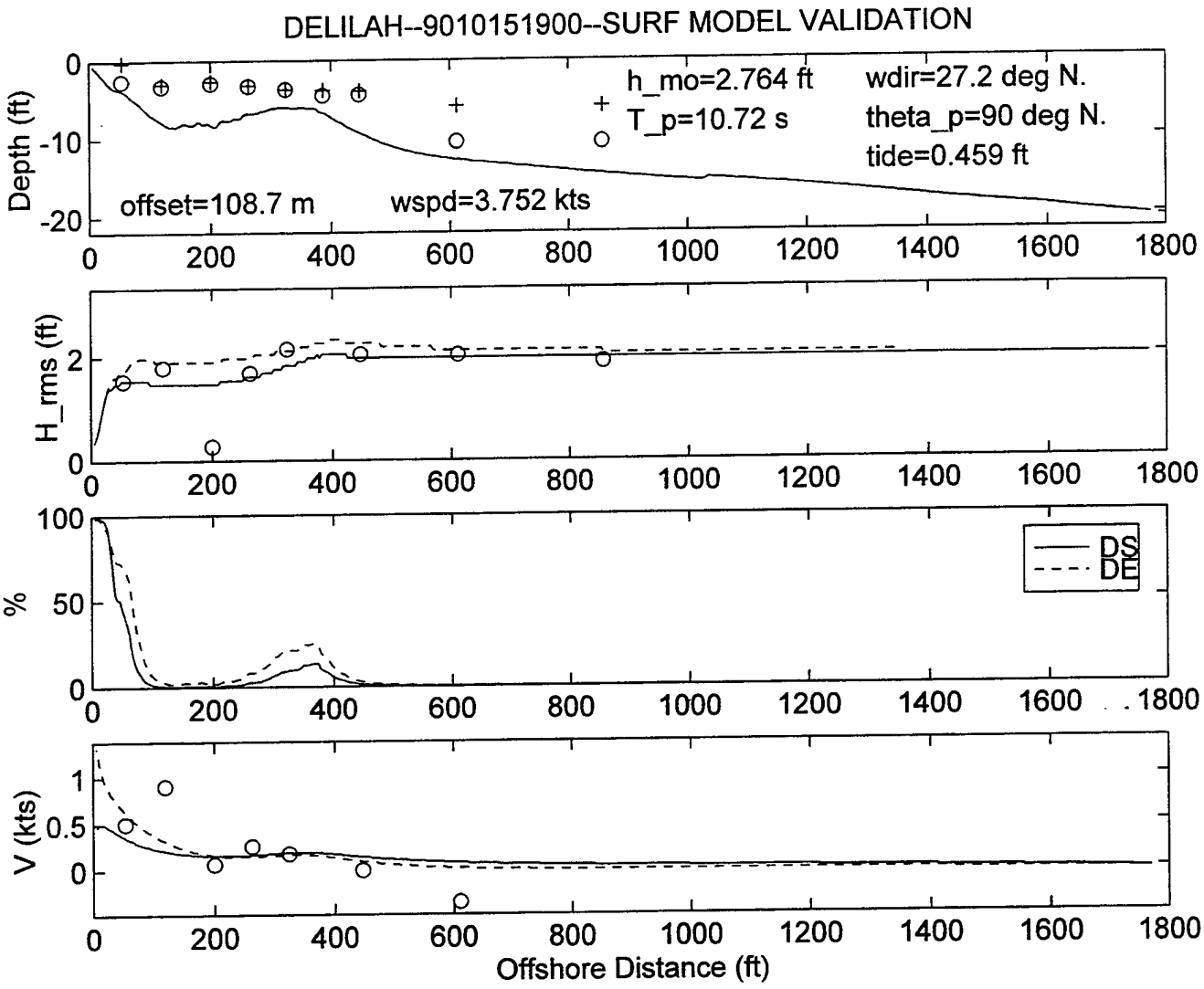
DELILAH--9010151900--SURF MODEL VALIDATION
Depth (ft)
h_mo=2.764 ft
T_p=10.72 s
wdir=27.2 deg N.
theta_p=90 deg N.
tide=0.459 ft
offset=108.7 m
wspd=3.752 kts
H_rms (ft)
%
DS
DE
V (kts)
Offshore Distance (ft)

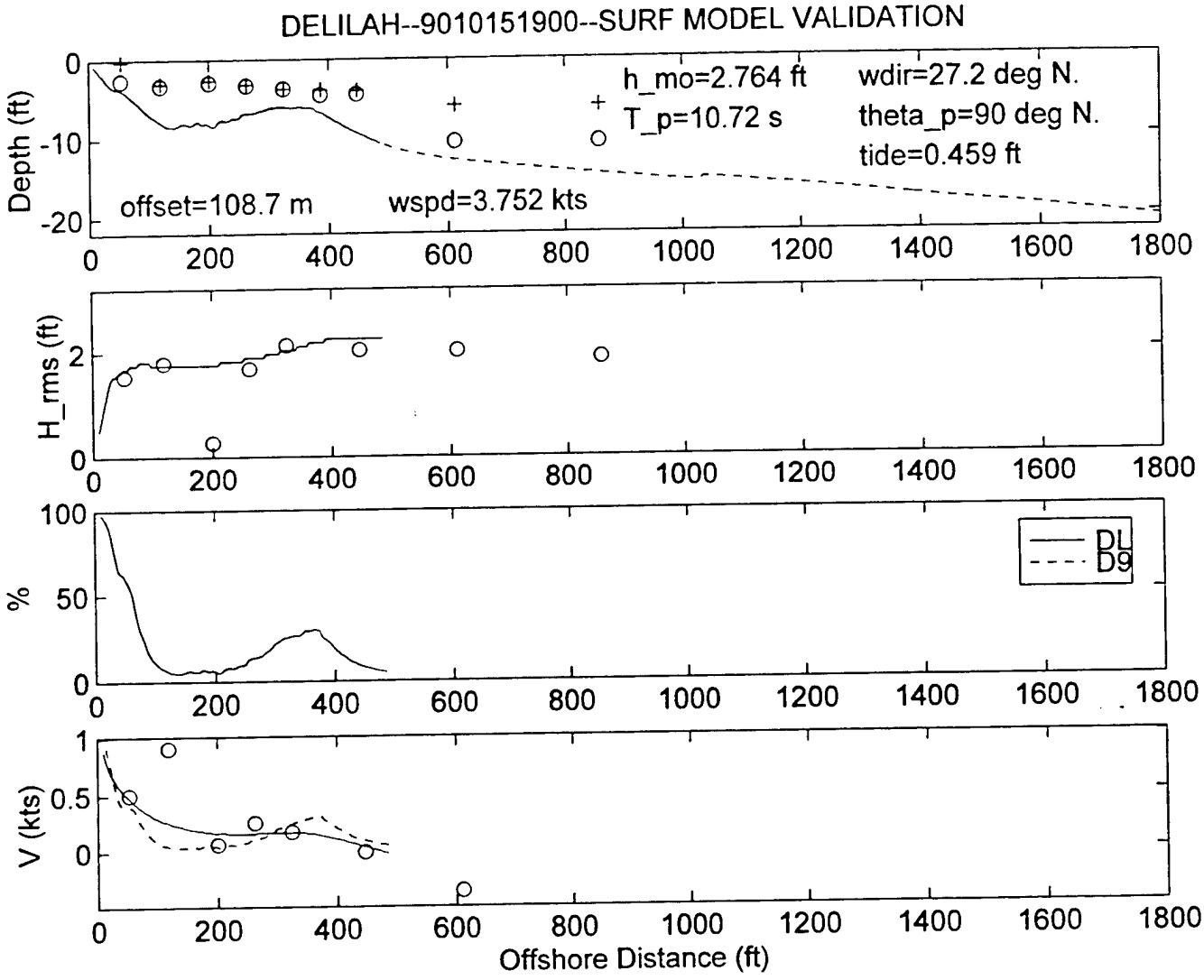
DELILAH--9010151900--SURF MODEL VALIDATION
Depth (ft)
h_mo=2.764 ft
T_p=10.72 s
wdir=27.2 deg N.
theta_p=90 deg N.
tide=0.459 ft
offset=108.7 m
wspd=3.752 kts
H_rms (ft)
%
DL
D9
V (kts)
Offshore Distance (ft)

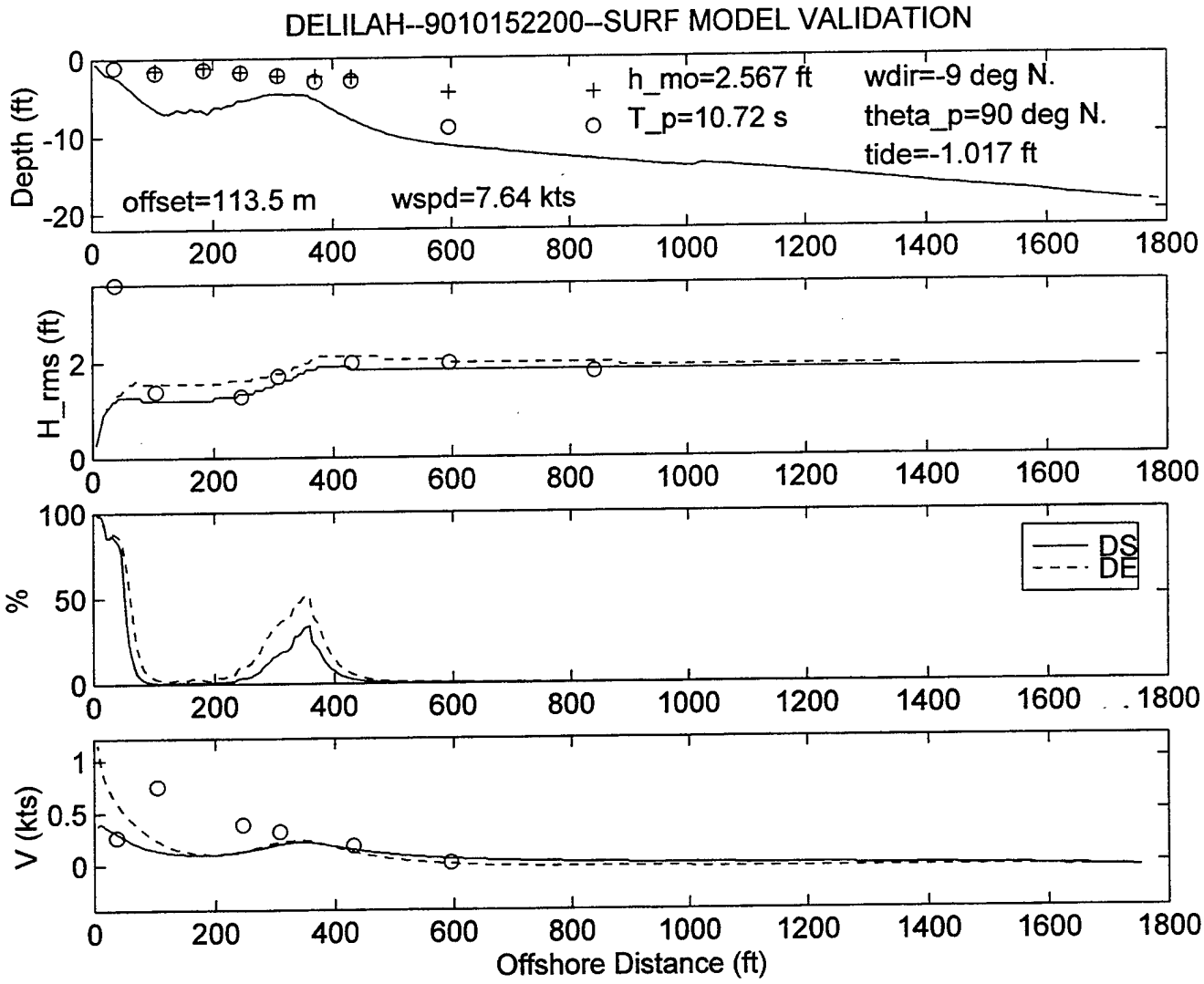
DELILAH--9010152200--SURF MODEL VALIDATION
Depth (ft)
h_mo=2.567 ft
T_p=10.72 s
wdir=-9 deg N.
theta_p=90 deg N.
tide=-1.017 ft
offset=113.5 m
wspd=7.64 kts
H_rms (ft)
%
DS
DE
V (kts)
Offshore Distance (ft)

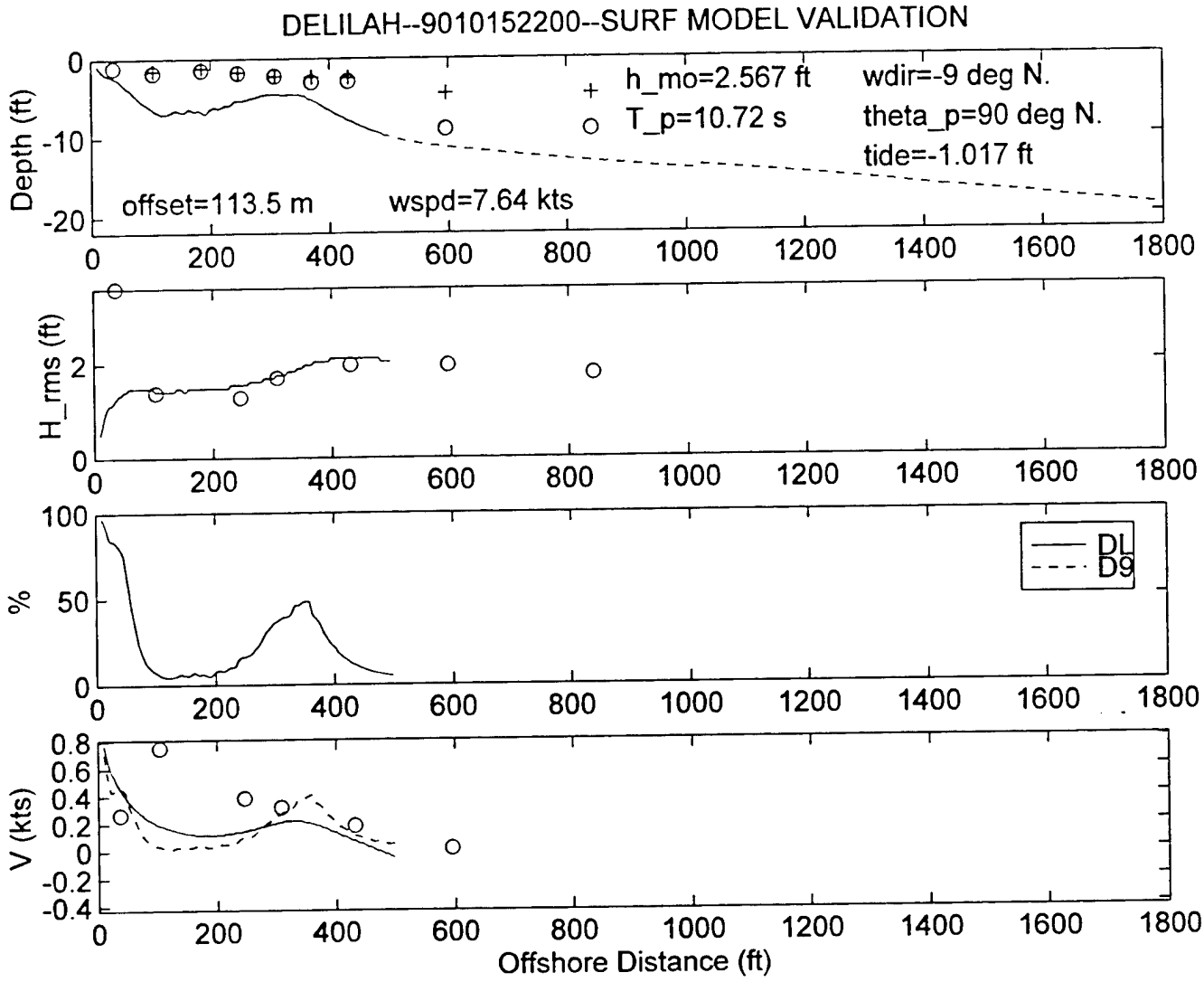
DELILAH--9010152200--SURF MODEL VALIDATION
Depth (ft)
h_mo=2.567 ft
T_p=10.72 s
wdir=-9 deg N.
theta_p=90 deg N.
tide=-1.017 ft
offset=113.5 m
wspd=7.64 kts
H_rms (ft)
%
DL
D9
V (kts)
Offshore Distance (ft)

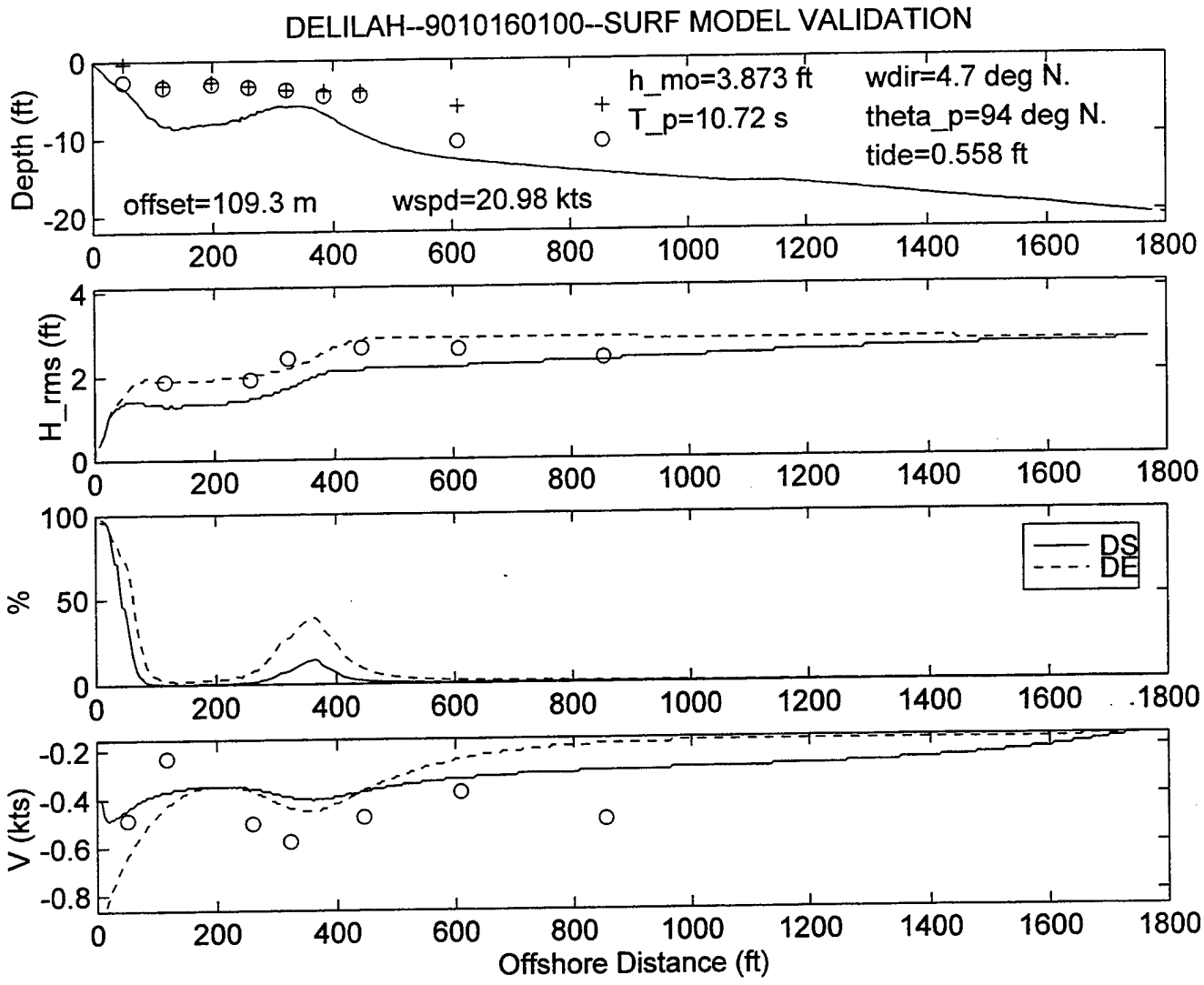
DELILAH--9010160100--SURF MODEL VALIDATION
Depth (ft)
h_mo=3.873 ft
T_p=10.72 s
wdir=4.7 deg N.
theta_p=94 deg N.
tide=0.558 ft
offset=109.3 m
wspd=20.98 kts
H_rms (ft)
%
DS
DE
V (kts)
Offshore Distance (ft)

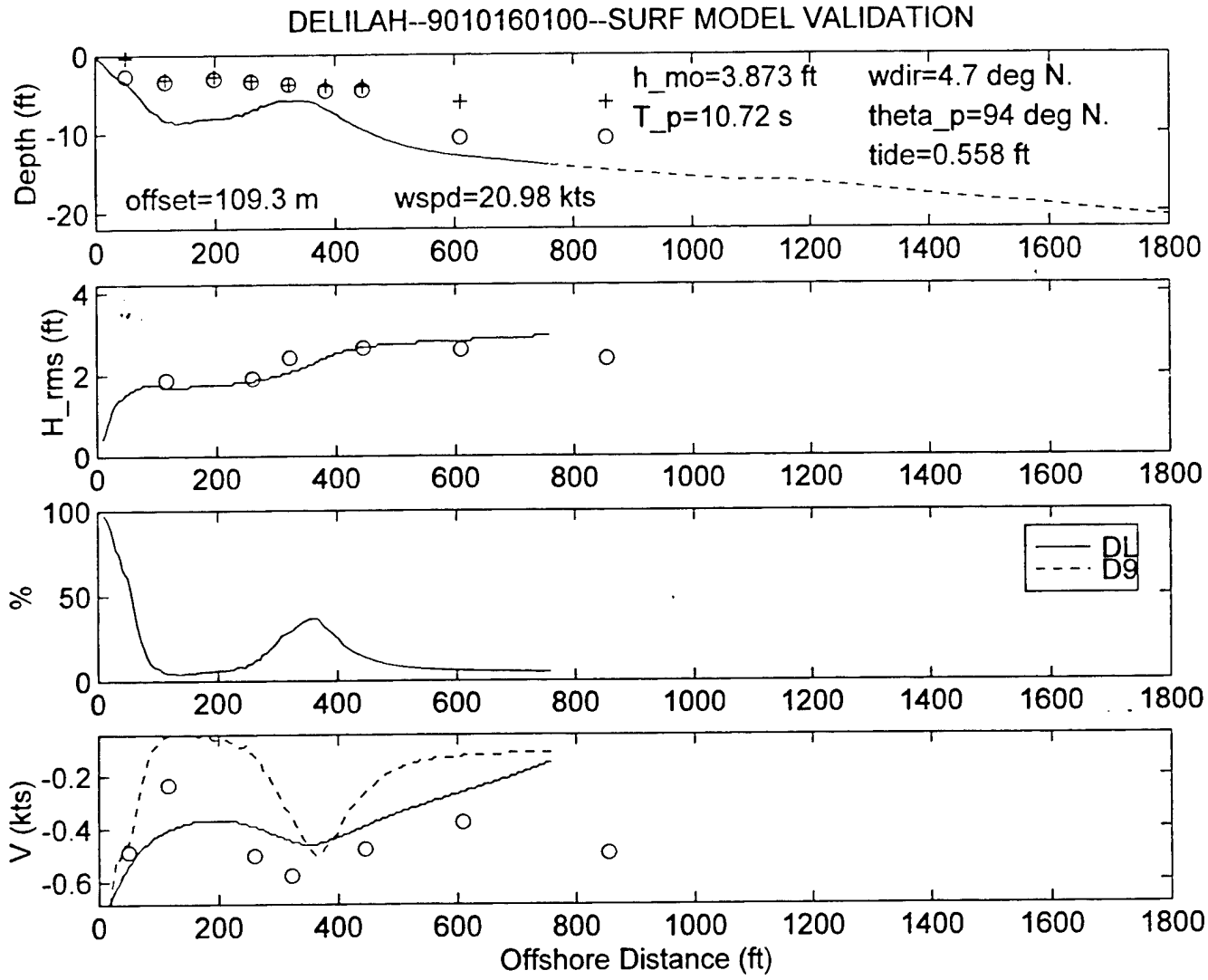
DELILAH--9010160100--SURF MODEL VALIDATION
Depth (ft)
h_mo=3.873 ft
T_p=10.72 s
wdir=4.7 deg N.
theta_p=94 deg N.
tide=0.558 ft
offset=109.3 m
wspd=20.98 kts
H_rms (ft)
%
DL
D9
V (kts)
Offshore Distance (ft)

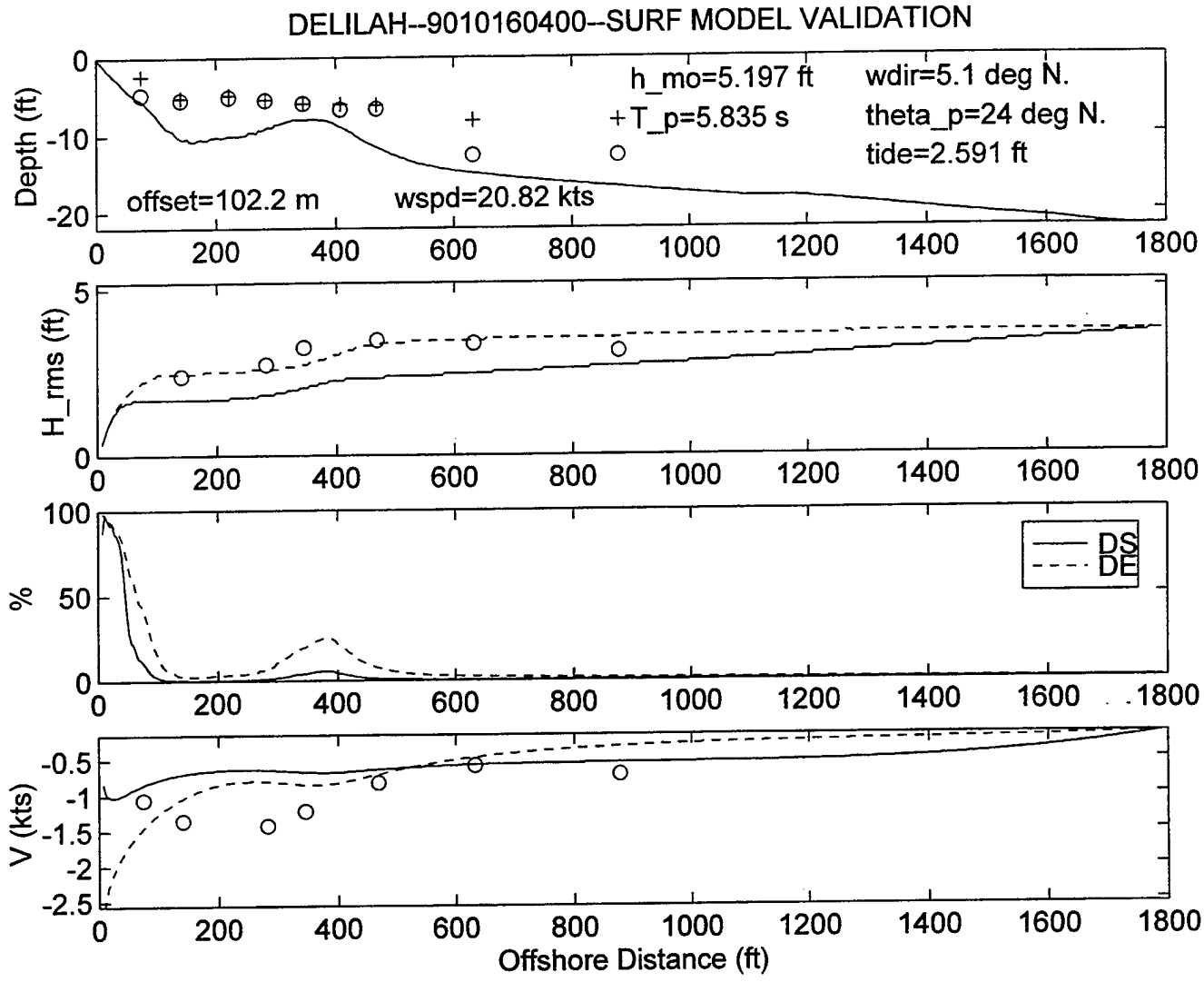
DELILAH--9010160400--SURF MODEL VALIDATION
Depth (ft)
h_mo=5.197 ft
+T_p=5.835 s
wdir=5.1 deg N.
theta_p=24 deg N.
tide=2.591 ft
offset=102.2 m
wspd=20.82 kts
H_rms (ft)
%
DS
DE
V (kts)
Offshore Distance (ft)

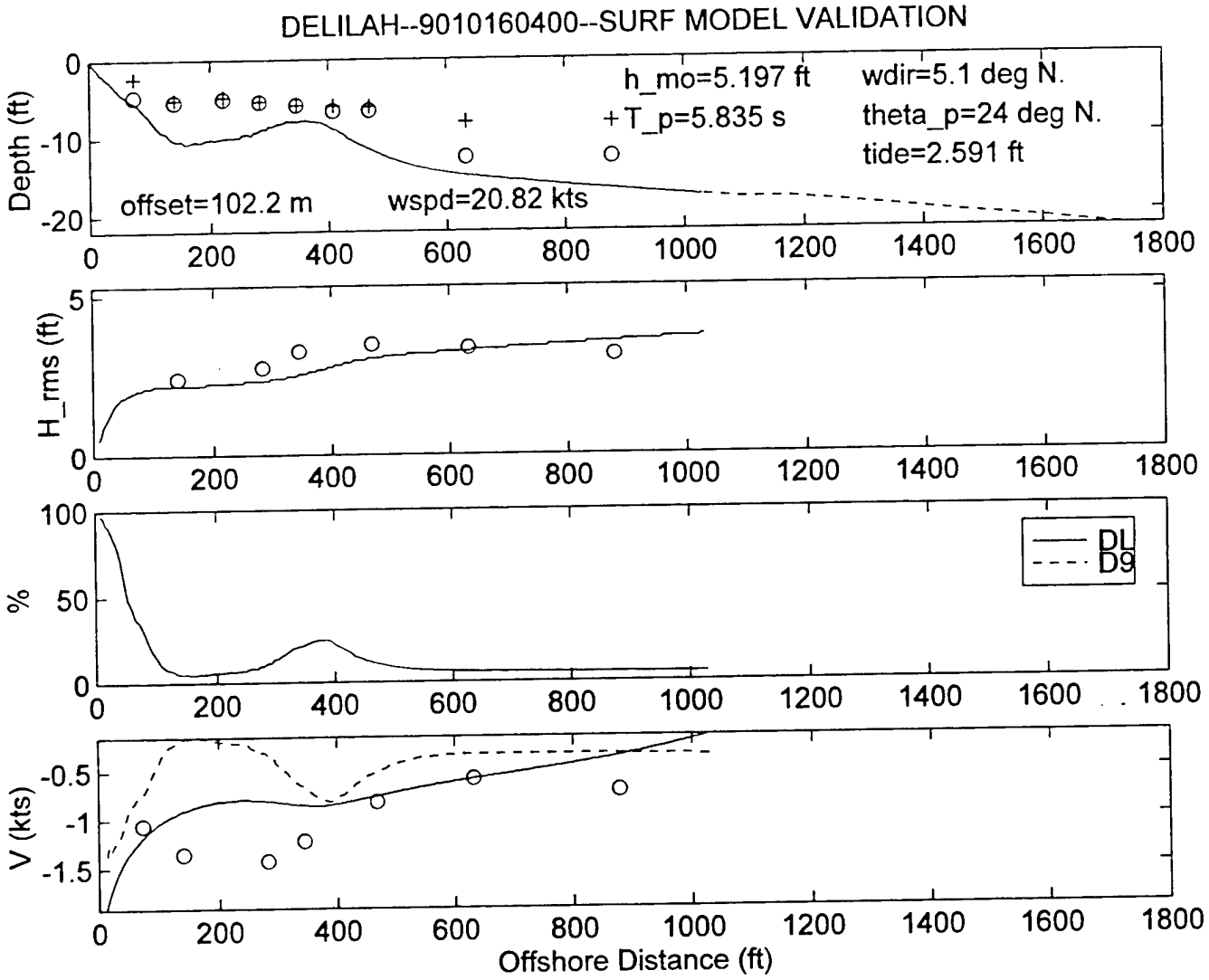
DELILAH--9010160400--SURF MODEL VALIDATION
Depth (ft)
h_mo=5.197 ft
+T_p=5.835 s
wdir=5.1 deg N.
theta_p=24 deg N.
tide=2.591 ft
offset=102.2 m
wspd=20.82 kts
H_rms (ft)
%
DL
D9
V (kts)
Offshore Distance (ft)

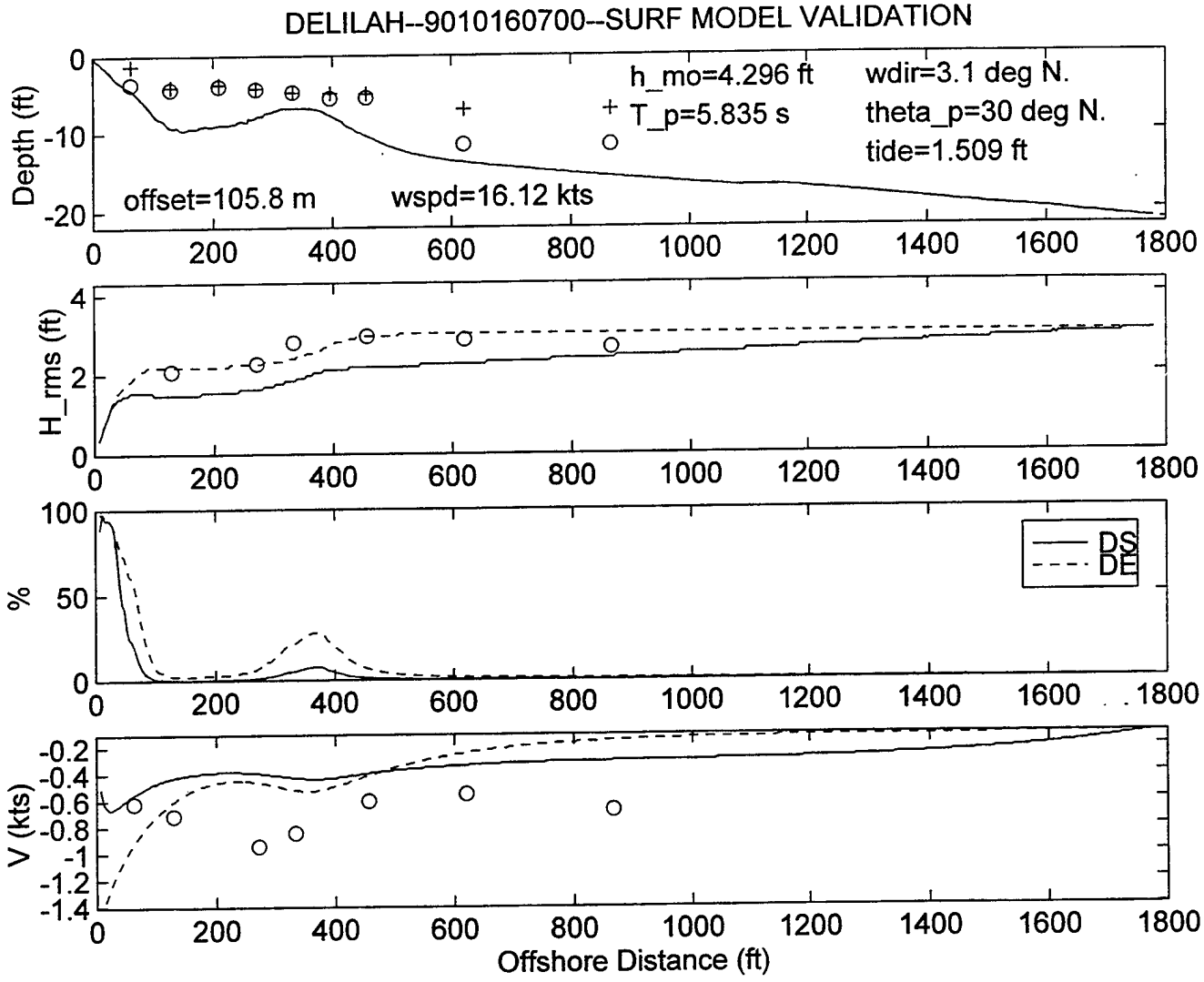
DELILAH--9010160700--SURF MODEL VALIDATION
Depth (ft)
h_mo=4.296 ft
T_p=5.835 s
wdir=3.1 deg N.
theta_p=30 deg N.
tide=1.509 ft
offset=105.8 m
wspd=16.12 kts
H_rms (ft)
%
DS
DE
V (kts)
Offshore Distance (ft)

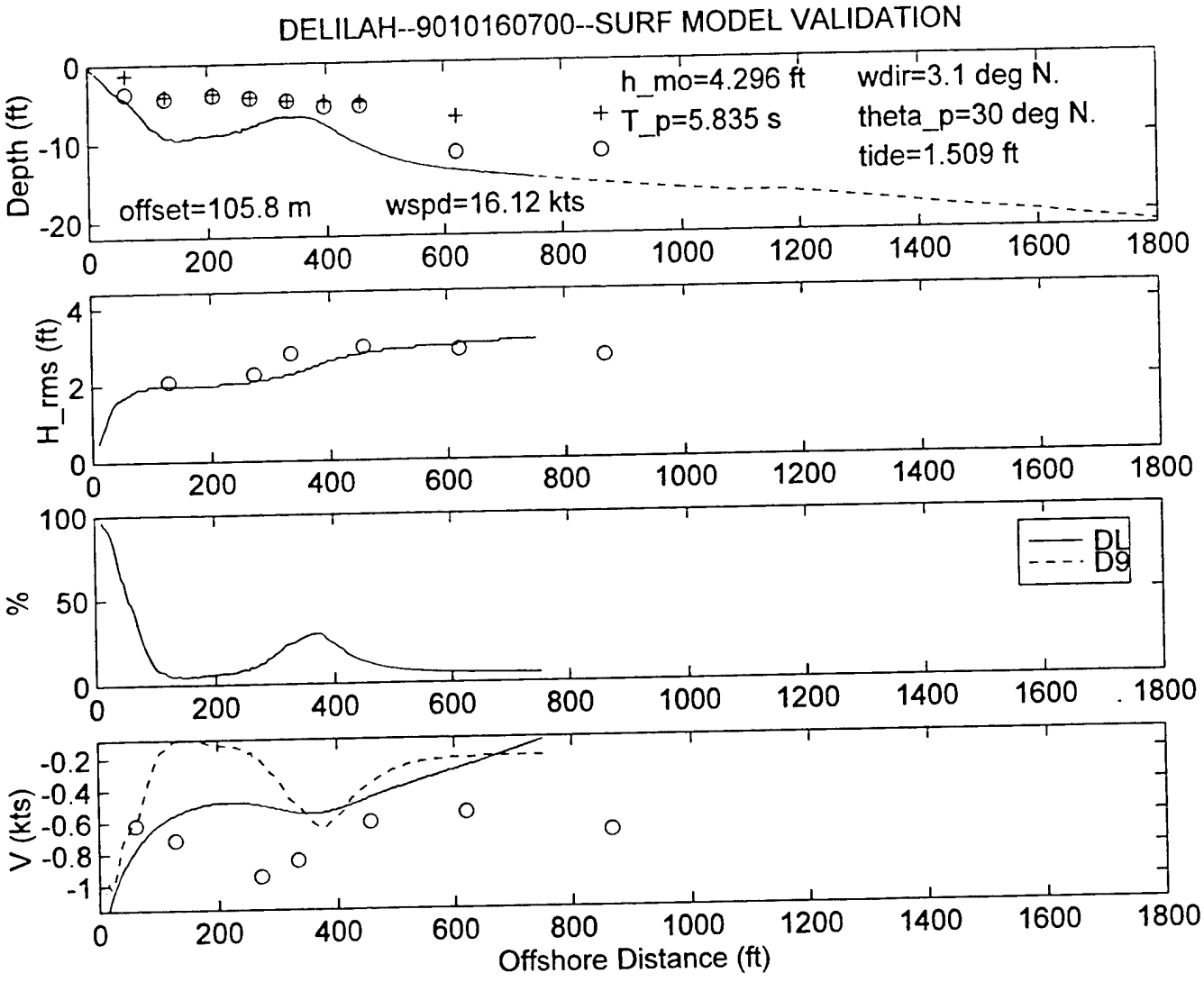
DELILAH--9010160700--SURF MODEL VALIDATION
Depth (ft)
h_mo=4.296 ft
T_p=5.835 s
wdir=3.1 deg N.
theta_p=30 deg N.
tide=1.509 ft
offset=105.8 m
wspd=16.12 kts
H_rms (ft)
%
DL
D9
V (kts)
Offshore Distance (ft)

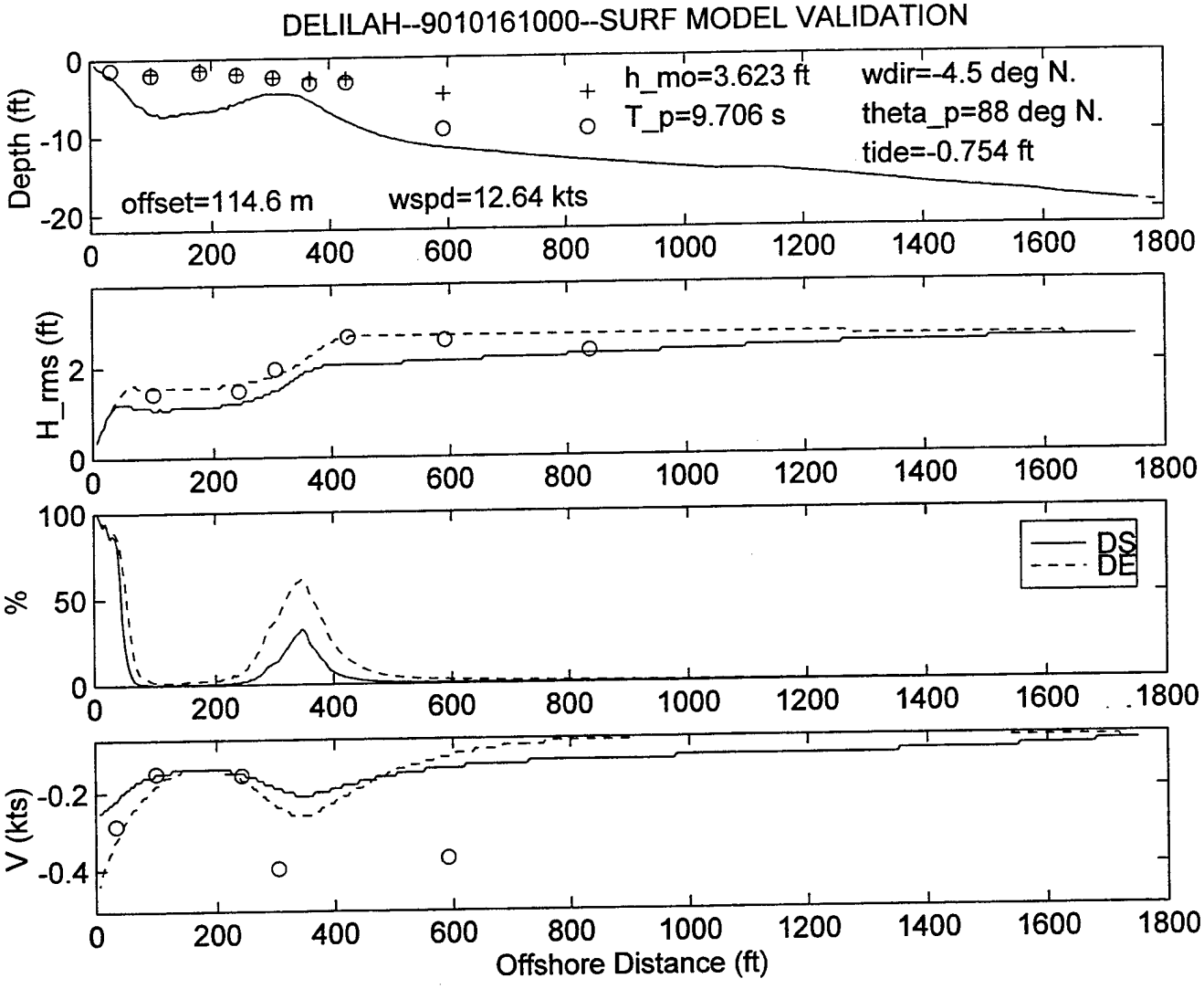
DELILAH--9010161000--SURF MODEL VALIDATION
Depth (ft)
h_mo=3.623 ft
T_p=9.706 s
wdir=-4.5 deg N.
theta_p=88 deg N.
tide=-0.754 ft
offset=114.6 m
wspd=12.64 kts
H_rms (ft)
%
DS
DE
V (kts)
Offshore Distance (ft)

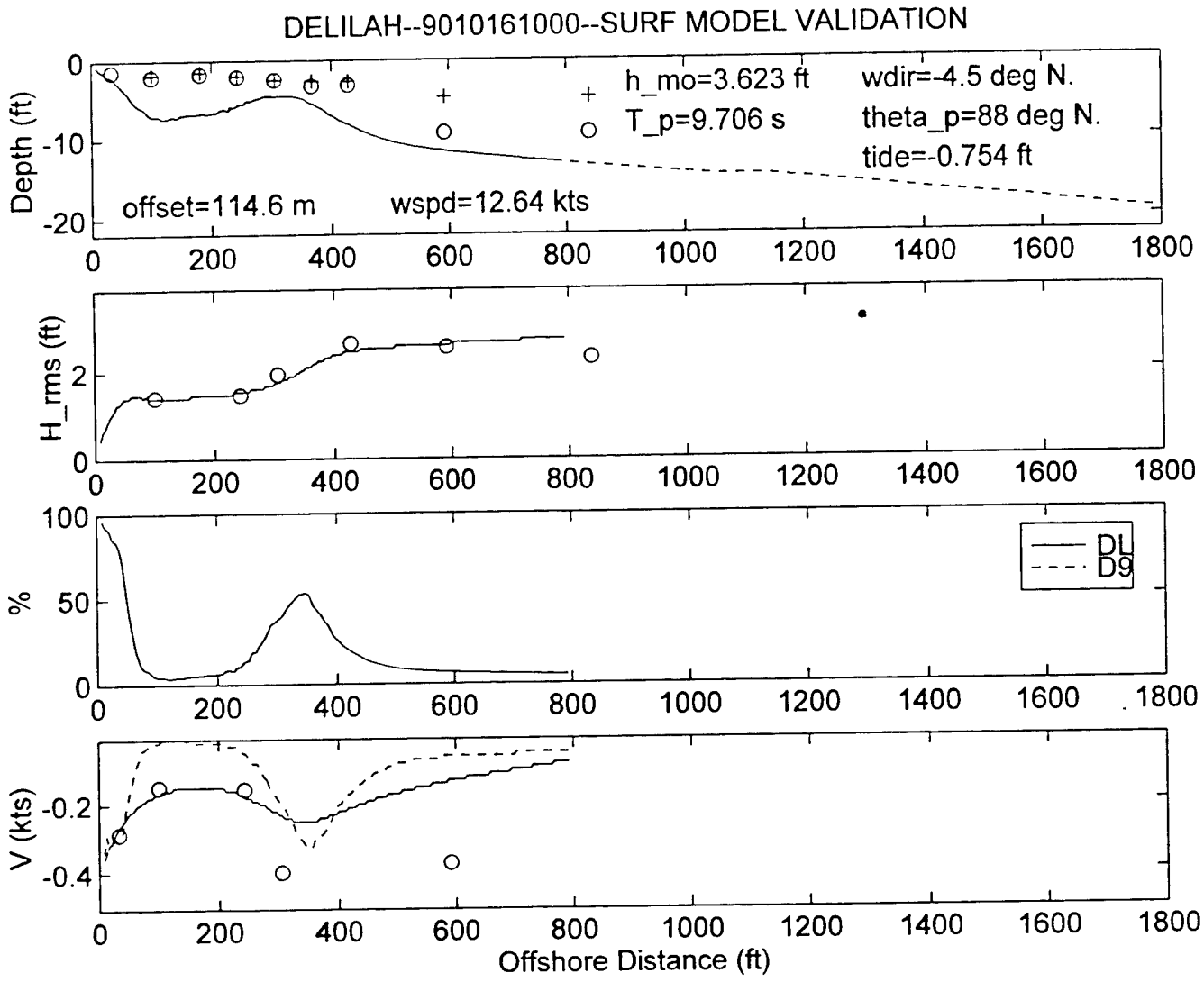
DELILAH--9010161000--SURF MODEL VALIDATION
Depth (ft)
h_mo=3.623 ft
T_p=9.706 s
wdir=-4.5 deg N.
theta_p=88 deg N.
tide=-0.754 ft
offset=114.6 m
wspd=12.64 kts
H_rms (ft)
%
DL
D9
V (kts)
Offshore Distance (ft)

Appendix C
Scatter Plots

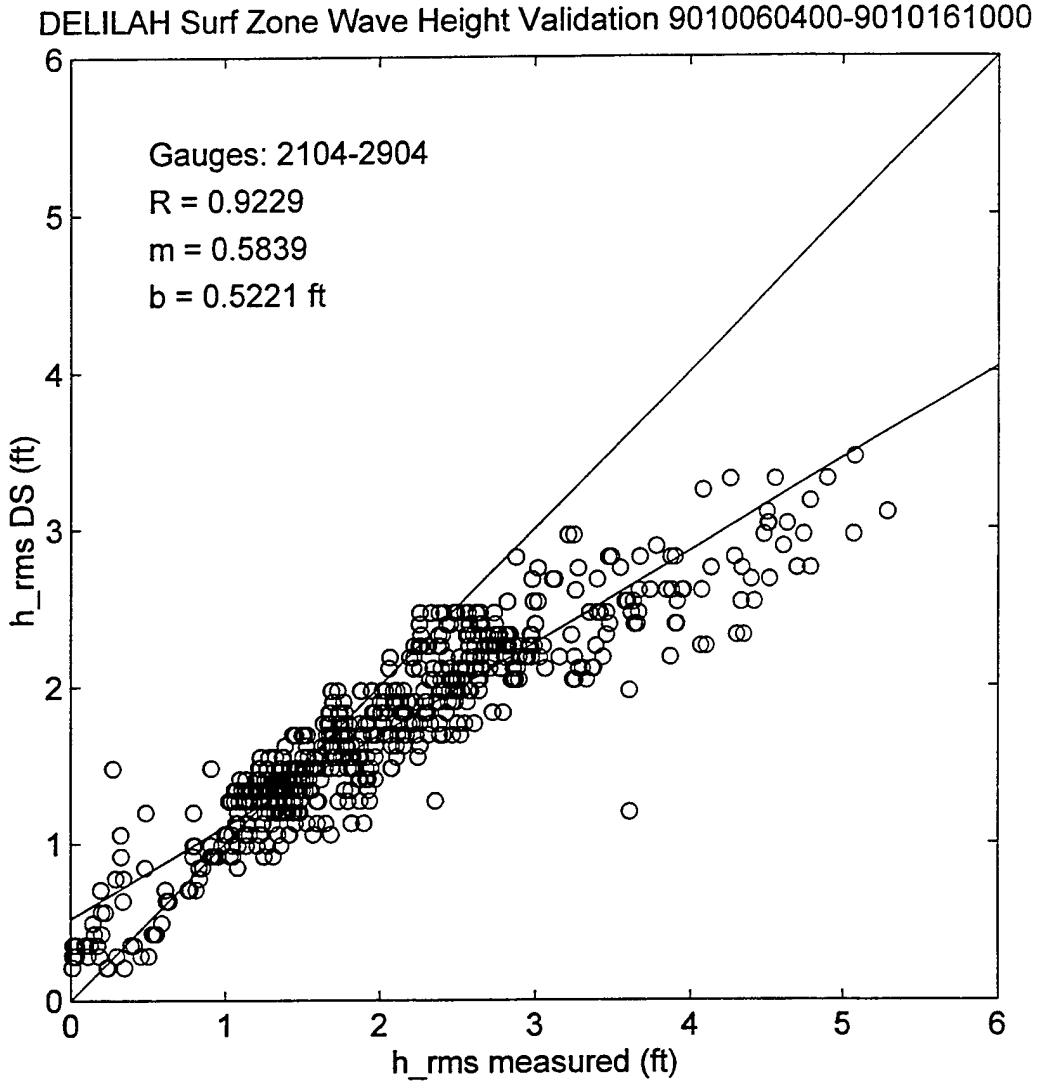
DELILAH Surf Zone Wave Height Validation 9010060400-9010161000
Gauges: 2104-2904
R = 0.9229
m = 0.5839
b = 0.5221 ft
h_rms DS (ft)
h_rms measured (ft)
0
1
2
3
4
5
6

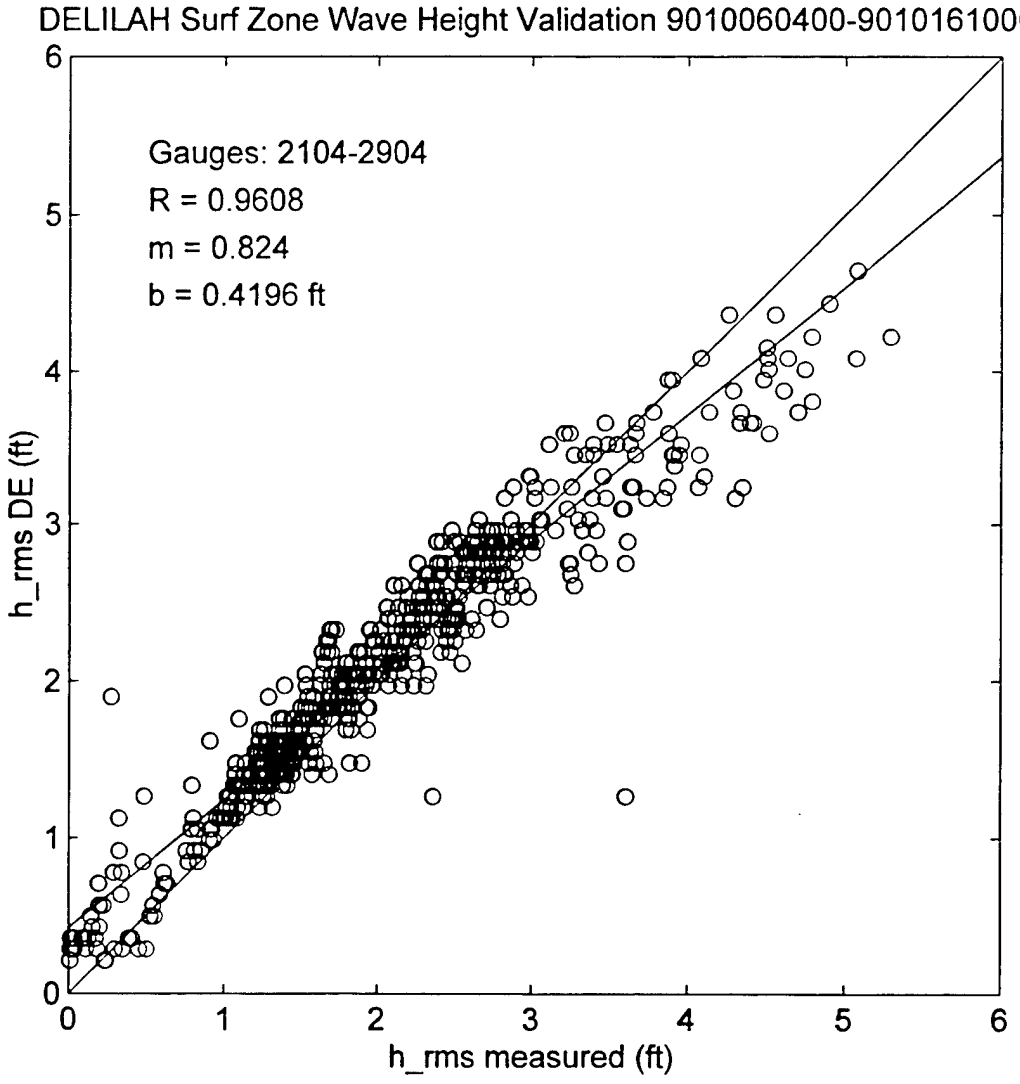
DELILAH Surf Zone Wave Height Validation 9010060400-9010161000
Gauges: 2104-2904
R = 0.9608
m = 0.824
b = 0.4196 ft
h_rms DE (ft)
h_rms measured (ft)
0
1
2
3
4
5
6

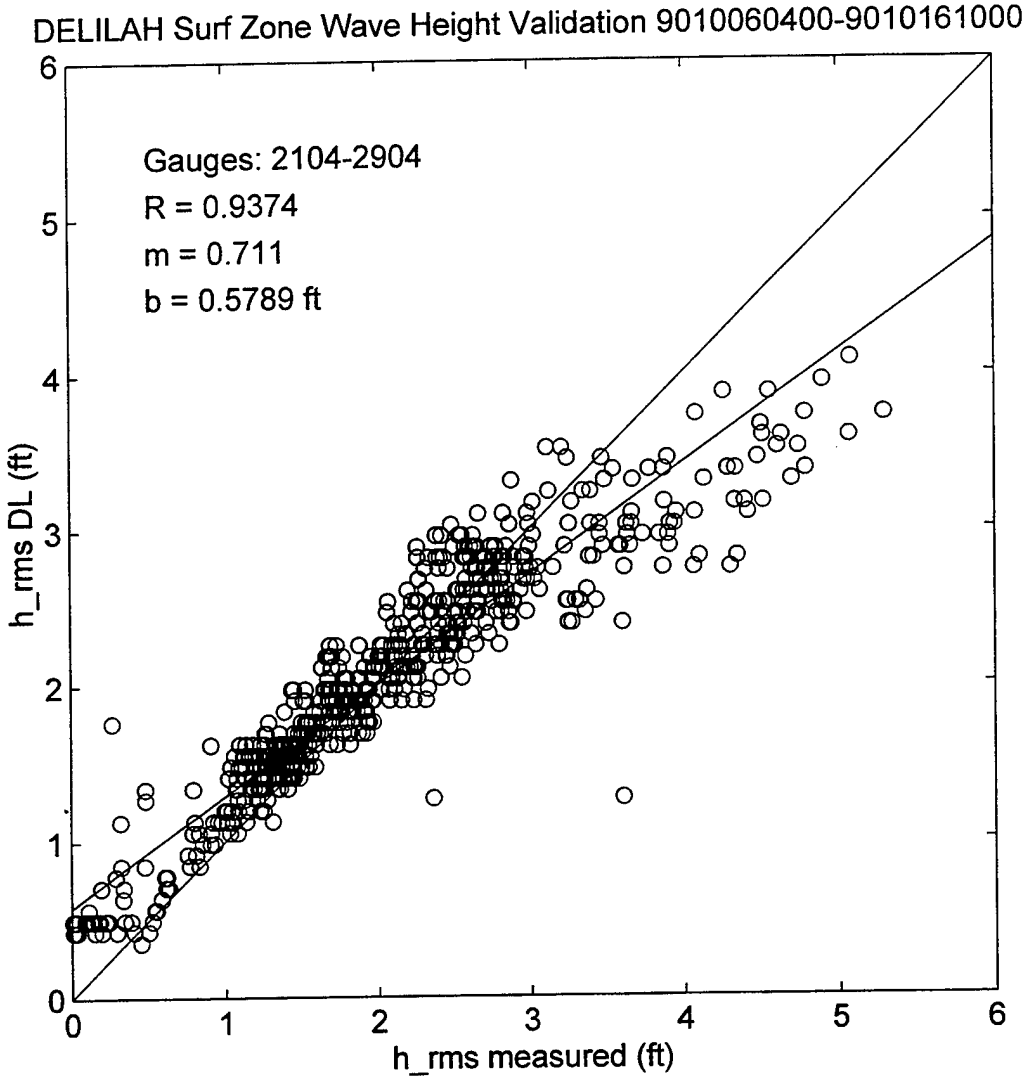
DELILAH Surf Zone Wave Height Validation 9010060400-9010161000
Gauges: 2104-2904
R = 0.9374
m = 0.711
b = 0.5789 ft
h_rms DL (ft)
h_rms measured (ft)
0
1
2
3
4
5
6

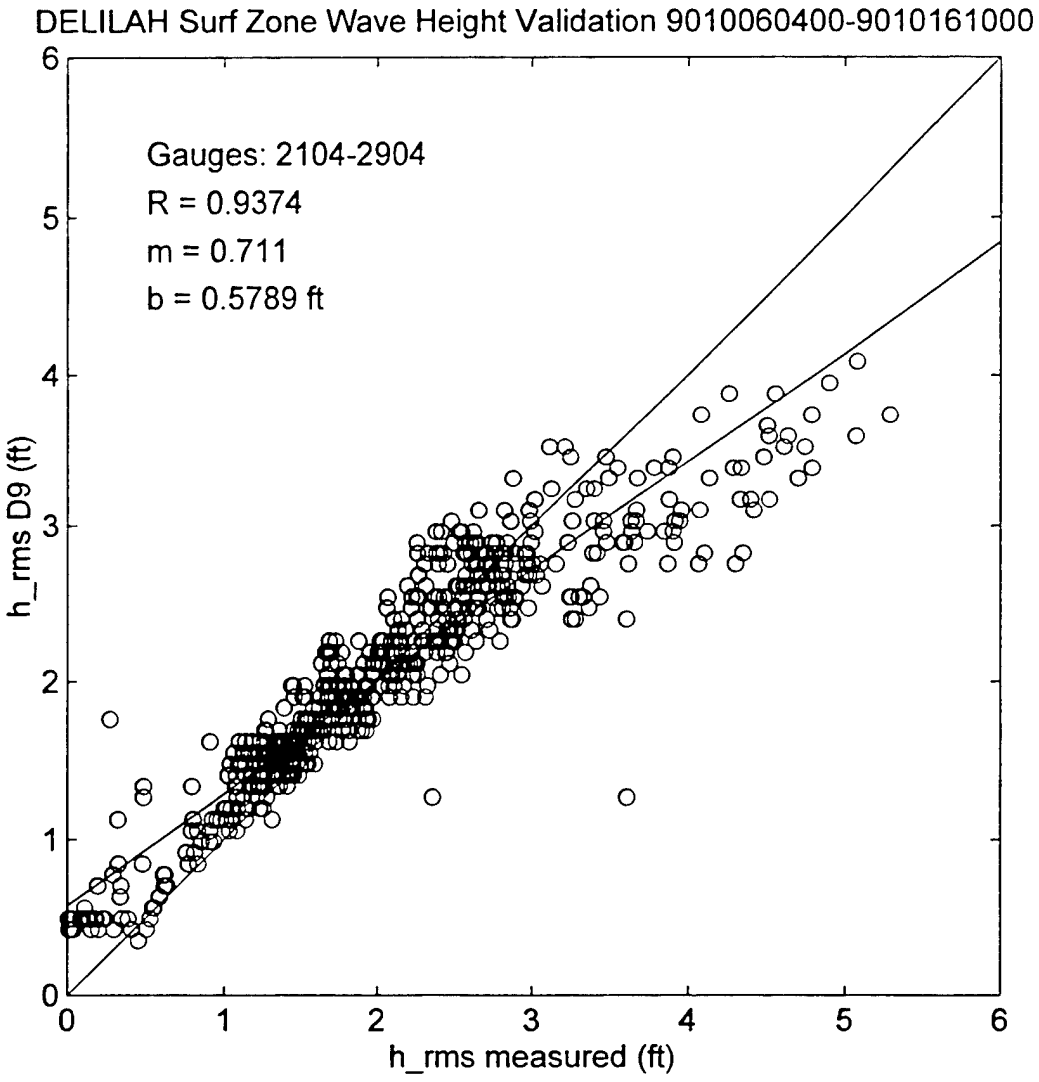
DELILAH Surf Zone Wave Height Validation 9010060400-9010161000
Gauges: 2104-2904
R = 0.9374
m = 0.711
b = 0.5789 ft
h_rms D9 (ft)
h_rms measured (ft)
0
1
2
3
4
5
6

DELILAH Surf Zone Wave Height Validation 9010060400-9010161000

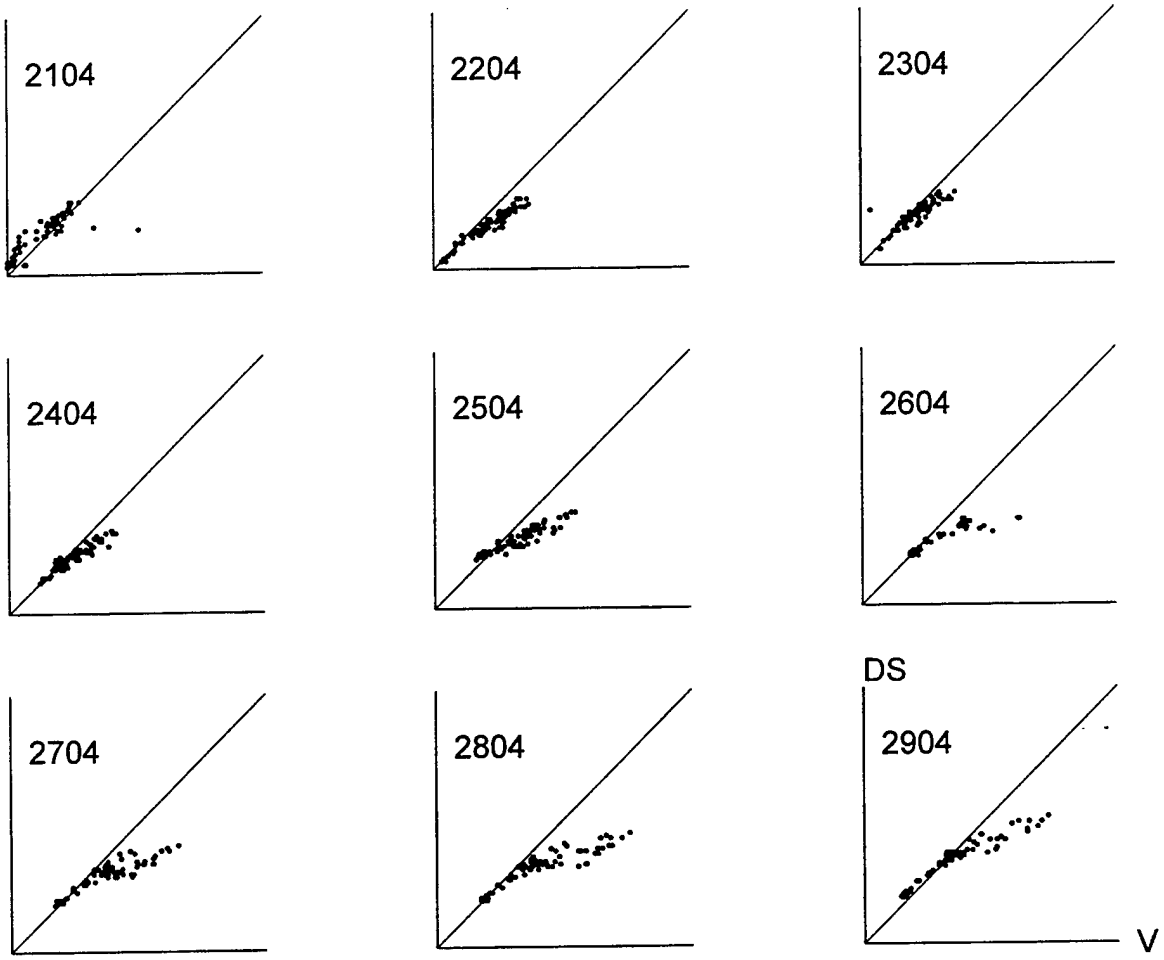

Axis Length = 7 ft

DELILAH Surf Zone Wave Height Validation 9010060400-9010161000

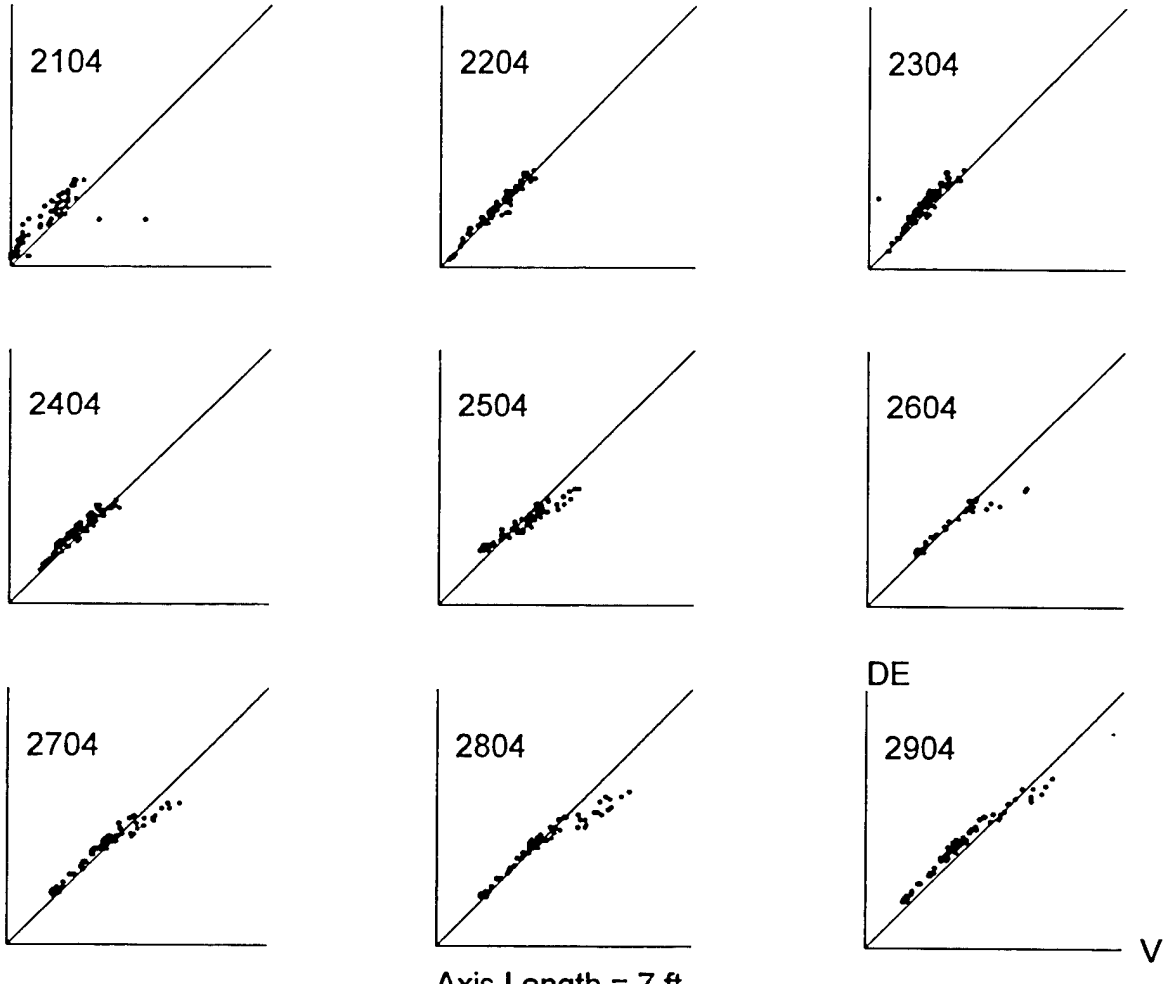

Axis Length = 7 ft

DELILAH Surf Zone Wave Height Validation 9010060400-9010161000

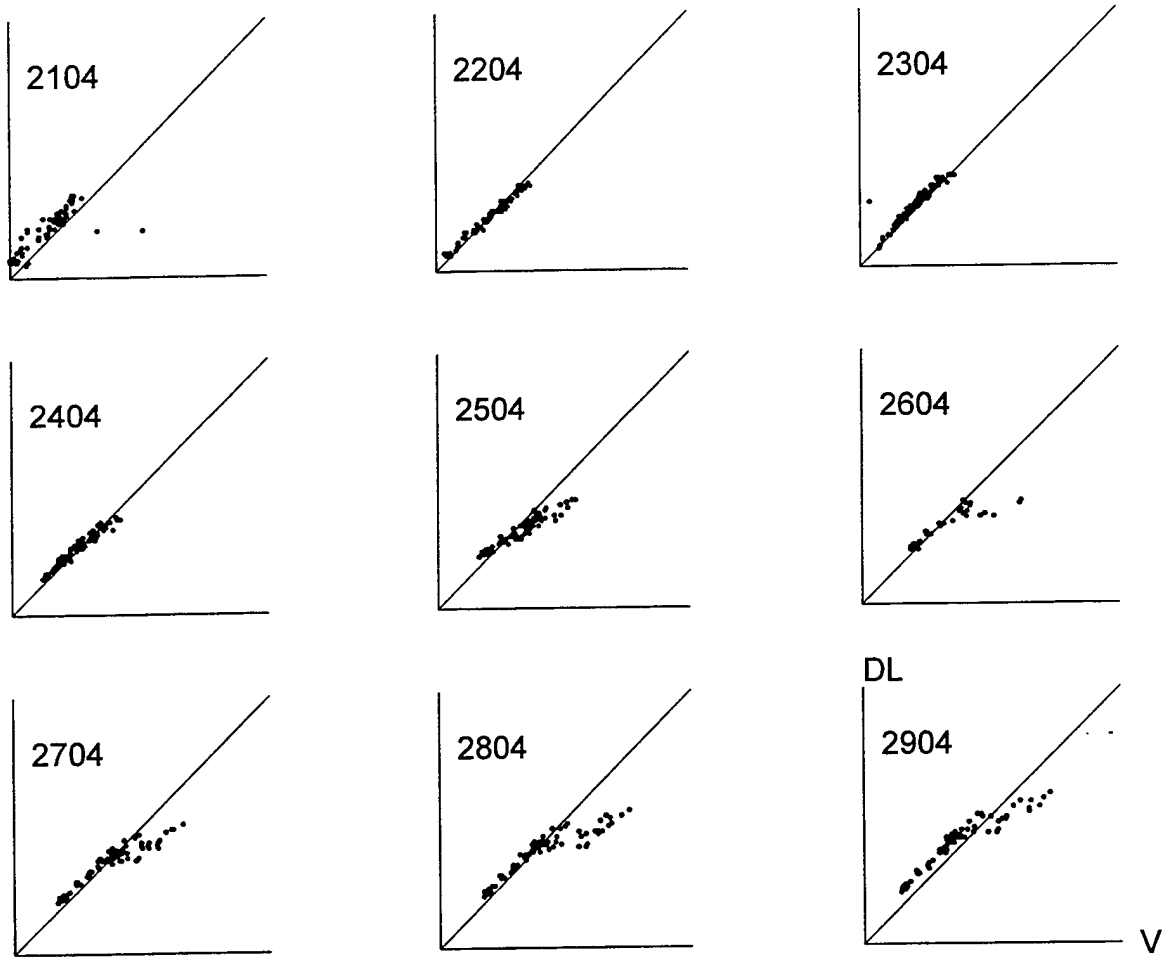

Axis Length = 7 ft

DELILAH Surf Zone Wave Height Validation 9010060400-9010161000

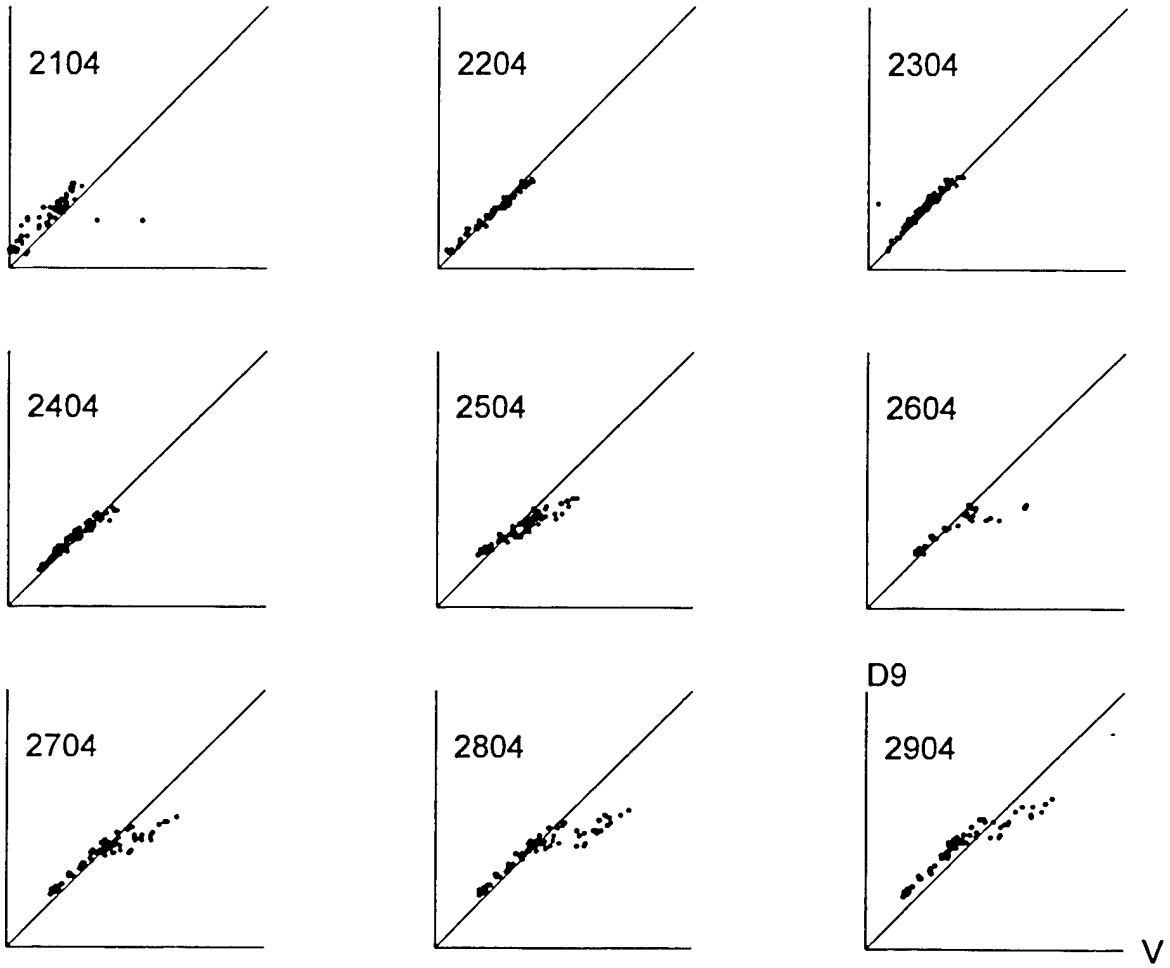

Axis Length = 7 ft

DELILAH Surf Zone Longshore Current Validation 9010060400-9010161000

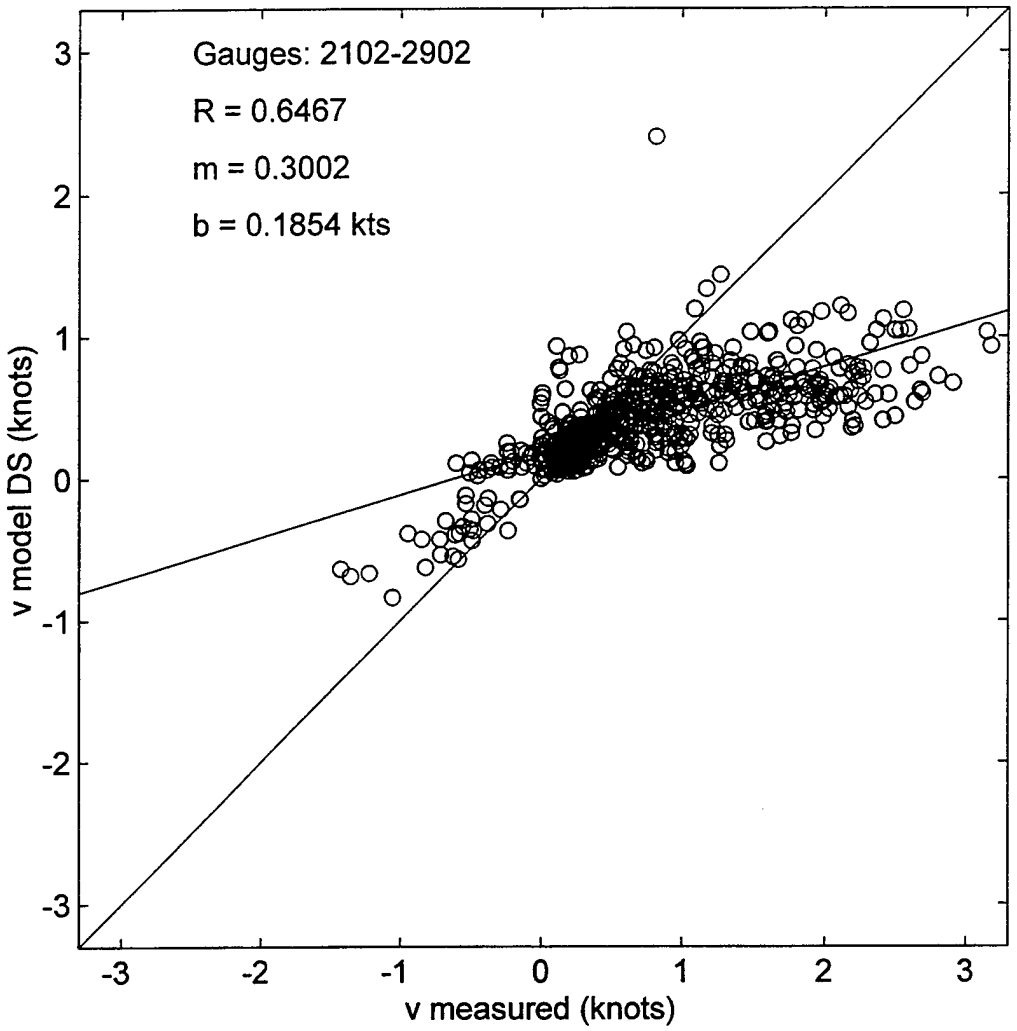

DELILAH Surf Zone Long hore Current Validation 9010060400-9010161000

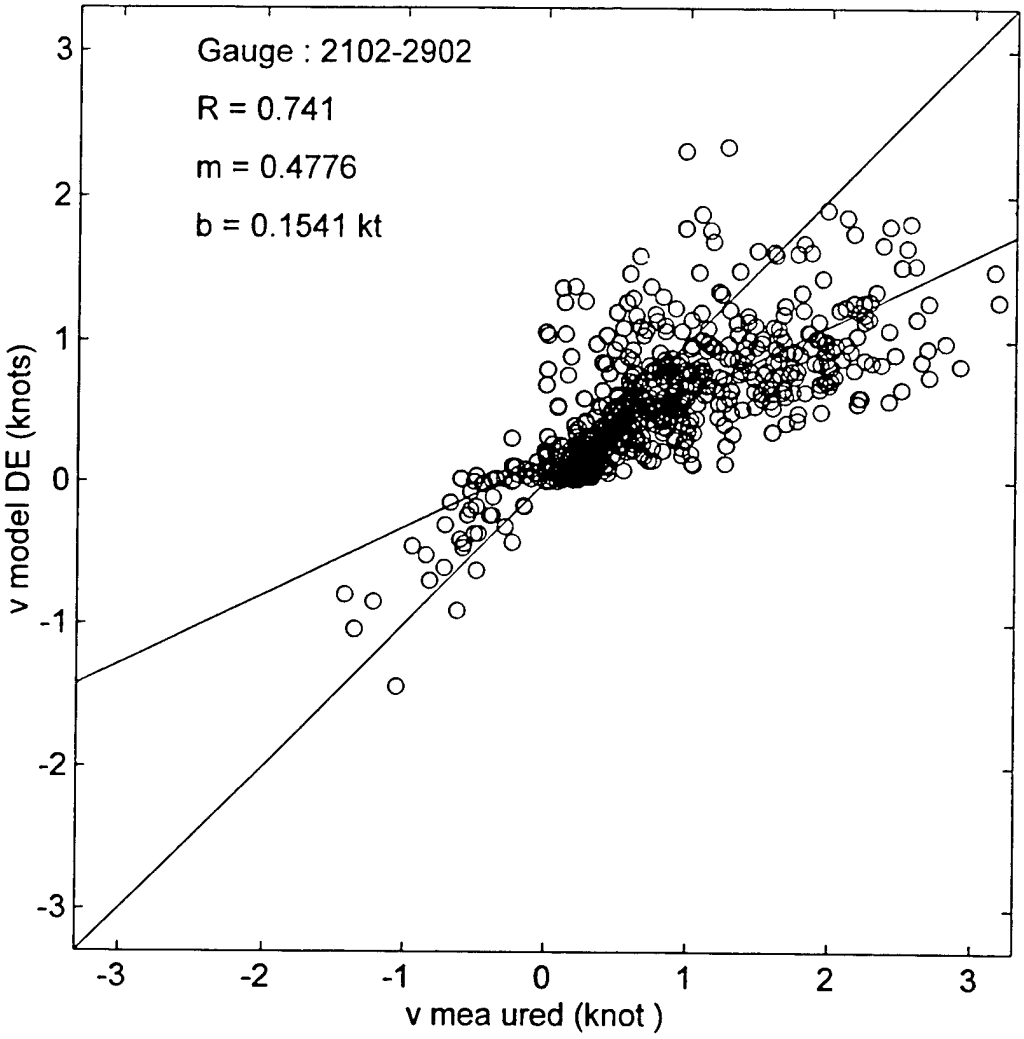

DELILAH Surf Zone Long hore Current Validation 9010060400-9010161000

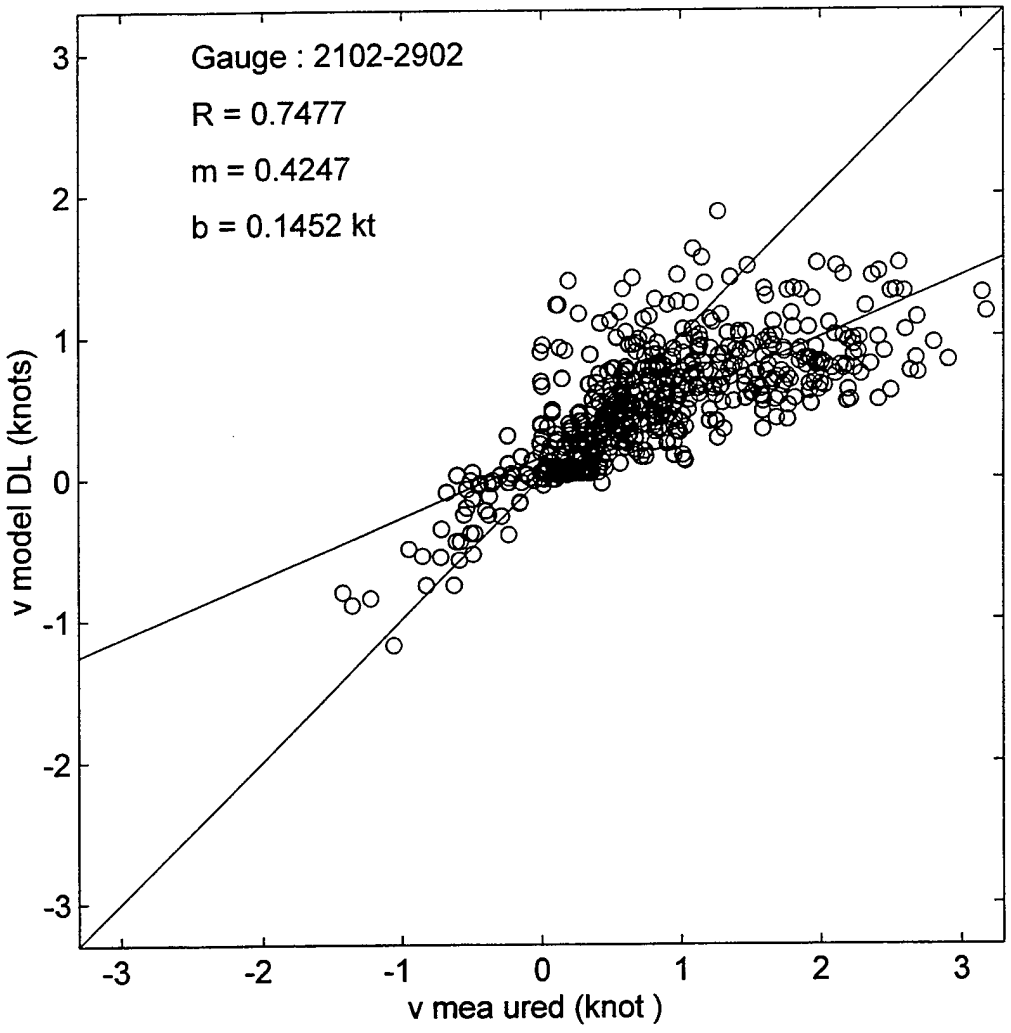

DELILAH Surf Zone Longshore Current Validation 9010060400-9010161000

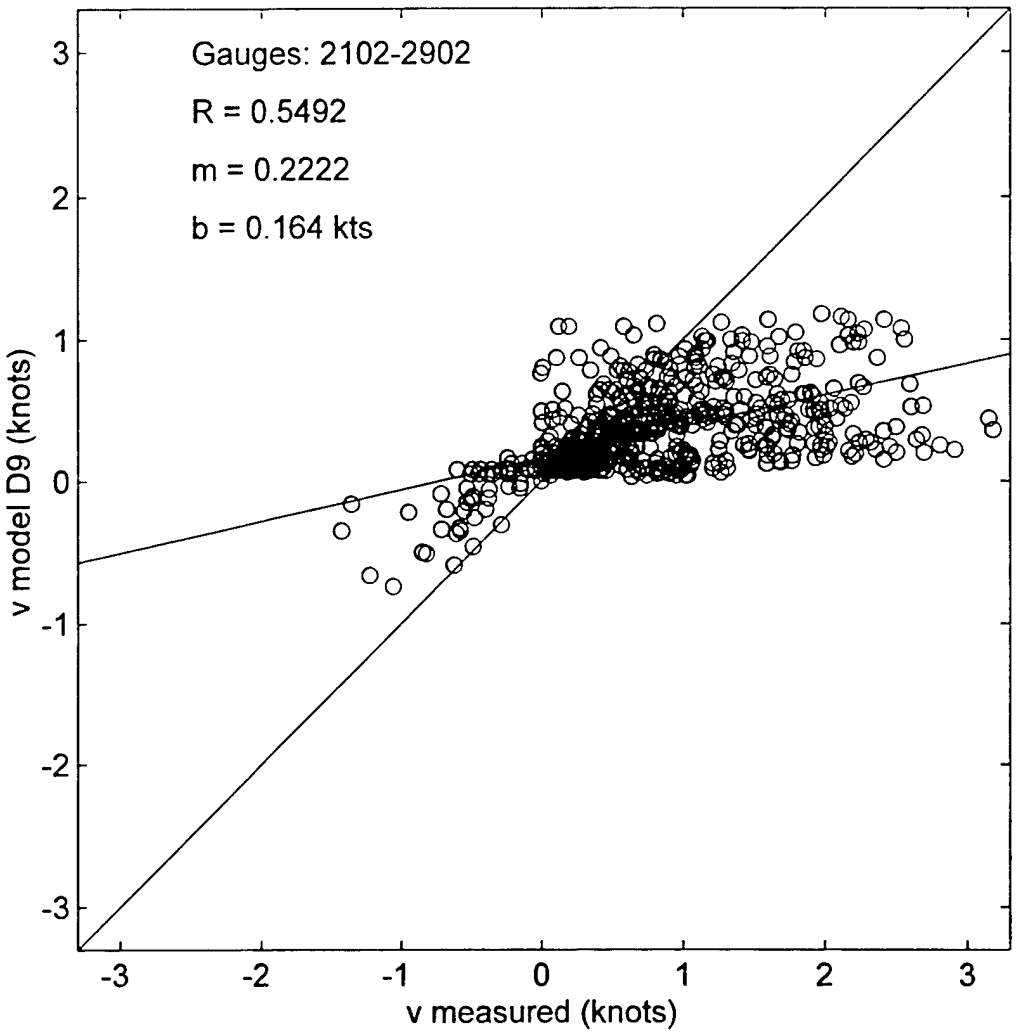

DELILAH Surf Zone Longshore Current Validation 9010060400-9010161000 DS

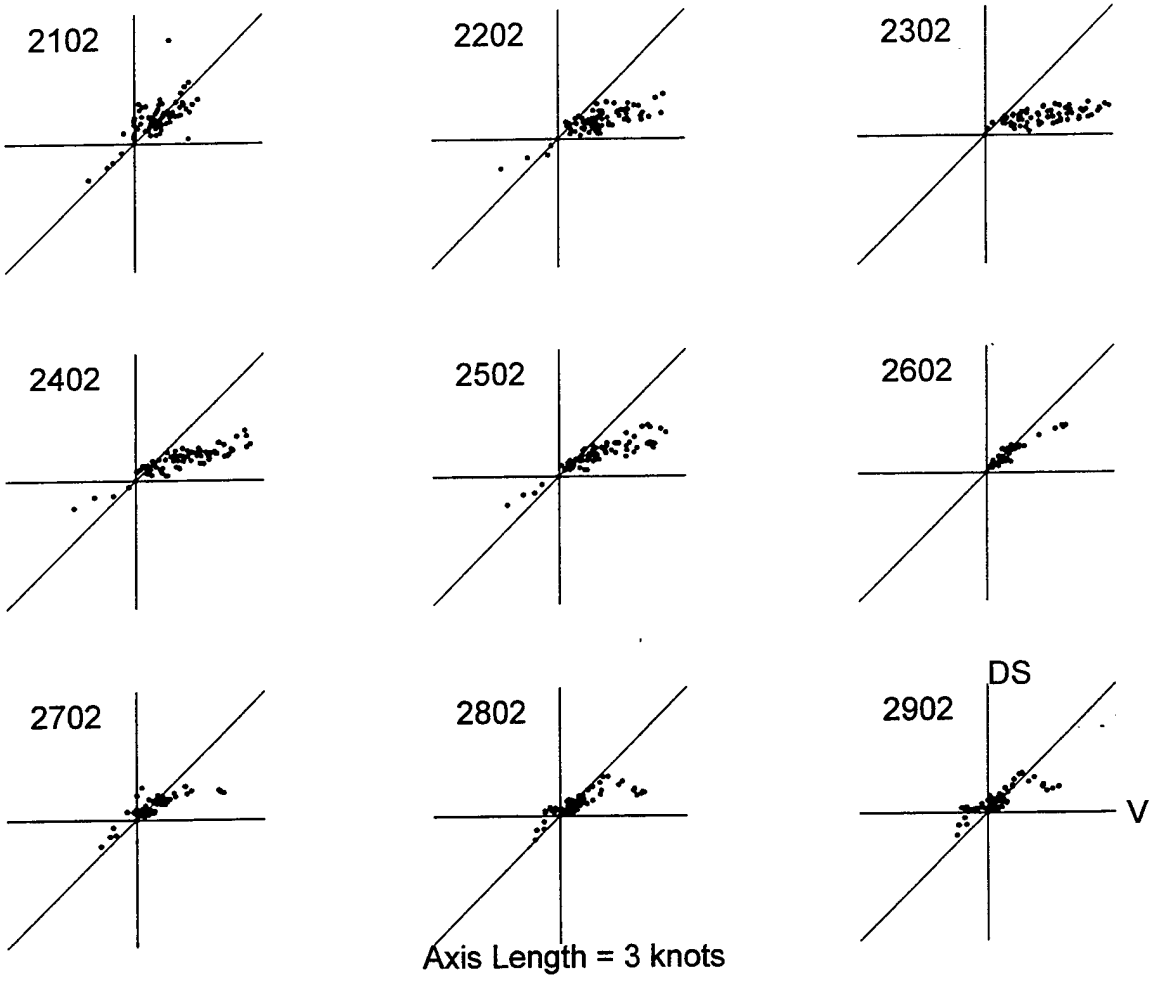

DELILAH Surf Zone Longshore Current Validation 9010060400-9010161000 DE

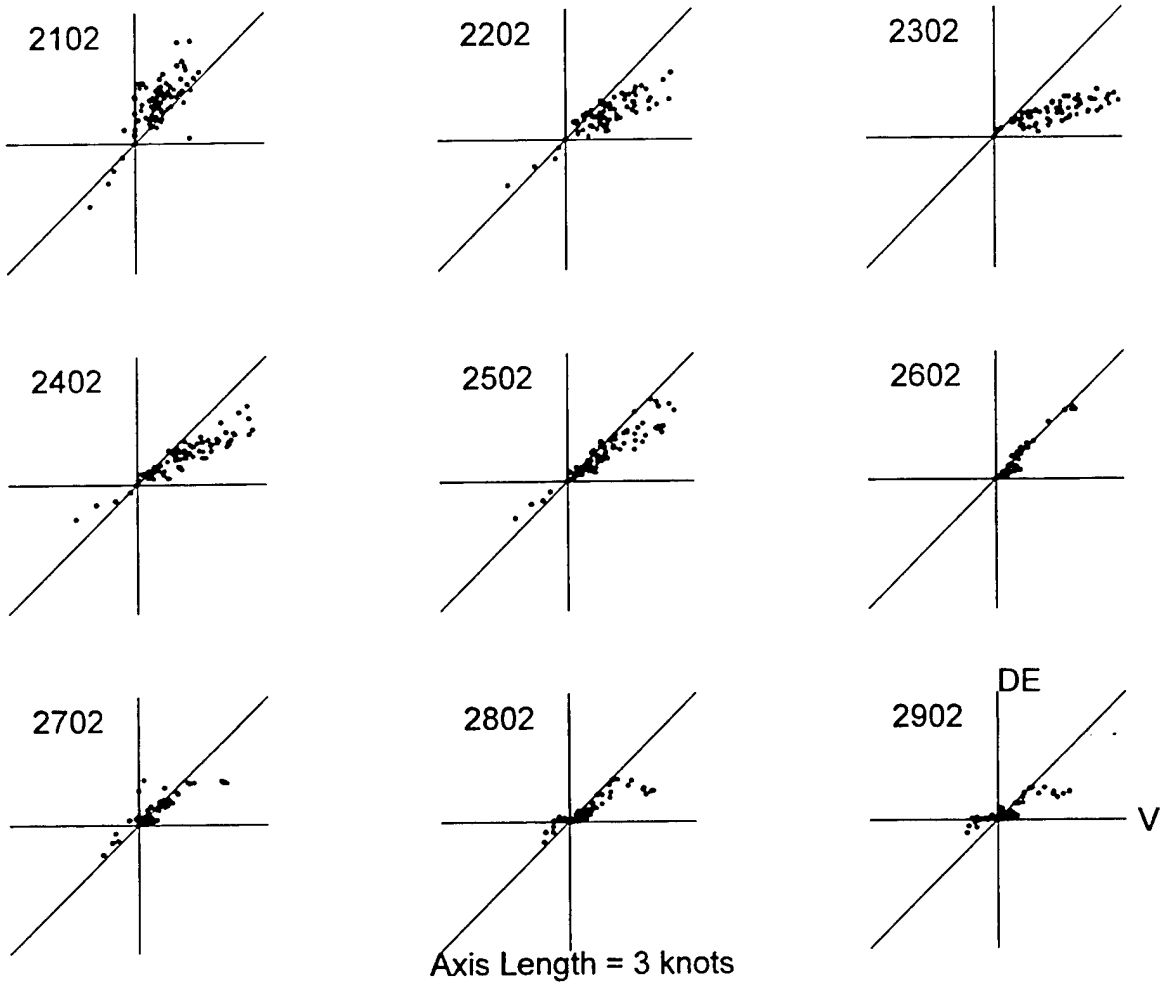

DELILAH Surf Zone Longshore Current Validation 9010060400-9010161000 DL

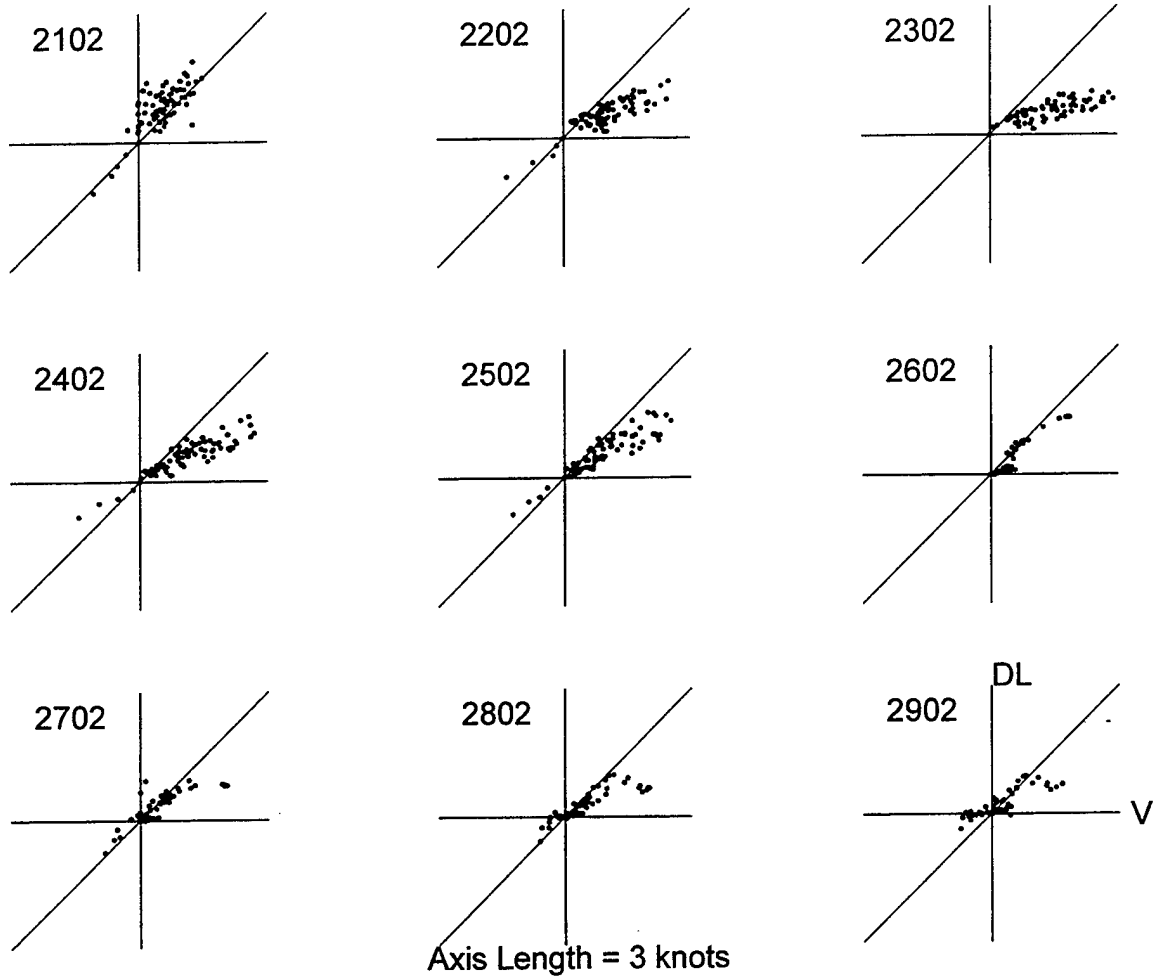

DELILAH Surf Zone Longshore Current Validation 9010060400-9010161000 D9